FLÁVIA DE TONI UCHÔA

SÍNTESE, AVALIAÇÃO DA ATIVIDADE ANTIINFLAMATÓRIA E SELETIVIDADE DE NOVAS 5-INDOL-TIAZOLIDINADIONAS FRENTE À CICLOXIGENASE-2

UFPE – RECIFE
2008

FLÁVIA DE TONI UCHÔA

SÍNTESE, AVALIAÇÃO DA ATIVIDADE ANTIINFLAMATÓRIA E SELETIVIDADE DE NOVAS 5-INDOL-TIAZOLIDINADIONAS FRENTE À CICLOXIGENASE-2

Tese apresentada à Banca Examinadora como exigência para obtenção do Título de Doutor em Ciências Biológicas, junto ao Programa de Pós-Graduação em Ciências Biológicas, na Área de Química Medicinal, Fisiologia e Farmacologia, da Universidade Federal de Pernambuco - Recife.

Orientadora: Profa. Dra. Suely Lins Galdino
Co-orientadora: Profa. Dra. Teresa Dalla Costa

UFPE - RECIFE
2008

Uchôa, Flávia De Toni

Síntese, avaliação da atividade antiinflamatória e seletividade de novas 5-indol-tiazolidinadionas frente à cicloxigenase-2/ Flávia De Toni Uchôa – Recife: O Autor, 2008.

217 folhas : il., fig., tab.

Tese (Doutorado) – Universidade Federal de Pernambuco. CCB. Ciências Biológicas, 2008.

Inclui bibliografia e anexos.

1. Ciências farmacêuticas – química medicinal - farmácia 2. Tiazolidinonas 3. Testes biológicos – atividade antiinflamatória 4.Enzimas cicloxigenases (COXs) I. Título.

615.31	**CDU (2.ed.)**	**UFPE**
615.31	**CDD (22.ed.)**	**CCB – 2008- 002**

COMISSÃO EXAMINADORA

"I Síntese, avaliação da atividade antiinflamatória e seletividade de novas 5-indol-tiazolidinadiona frente à cicloxigenase-2 "

TITULARES

Profª. Dr.ª **Suely Lins Galdino** - (Orientador/UFPE)

Prof. Dr. **Ivan da Rocha Pitta** – (UFPE)

Prof. Dr. **Marcelo Zaldini Hernandes** - (UFPE)

Prof. Dr. **Isac Almeida de Medeiros** (UFPB)

Profª. Dr.ª **Teresa Cristina Tavares Dalla Costa** (UFRGS)

Recife, 14 de Fevereiro de 2008.

AGRADECIMENTOS

A Profa. Dra. Suely Lins Galdino, minha orientadora e meu exemplo, são muitos os motivos que me fazem admirá-la: seu excelente trabalho como líder, como professora e como orientadora. Muito obrigada por tudo!

A Profa. Dra. Teresa Dalla Costa, minha orientadora no sanduíche, pela acolhida em Porto Alegre e por ter me dado a oportunidade de conhecer a Farmacocinética, mais do que isso, por ter-me feito gostar de Farmacocinética, pelos ensinamentos e confiança.

Ao Prof. Dr. Ivan da Rocha Pitta, pelo grande exemplo e por compartilhar sua imensa sabedoria.

A Profa. Dra. Maria do Carmo Alves de Lima, pela disponibilidade no Laboratório Planejamento e Síntese de Fármacos, mas também pelos lanches, almoços, brincadeiras e agradáveis conversas.

A Profa. Dra. Teresinha Gonçalves da Silva, pela agradável convivência, auxílio na execução dos ensaios biológicos, discussões científicas e amizade.

A Profa. Dra. Lúcia Fernanda Cavalcanti Costa Leite e ao Prof. Dr. Marcelo Zaldini Hernandes, pela execução dos cálculos de modelagem molecular e docking.

A Profa. Dra. Rosa Helena Veras Mourão, pelo exemplo de dedicação e pelas preciosas aulas práticas no Biotério do Departamento de Antibióticos.

A Dra. Leila Cabral dos Santos, pela agradável convivência e valorosa discussão na parte sintética e análise estrutural dos compostos sintetizados.

A Sra. Adenilda Eugenia de Lima, pela agradável convivência, saborosos cafezinhos e disposição em ajudar, o que vai deixar saudades.

Aos Professores integrantes do Grupo de Pesquisa em Inovação Terapêutica (GPIT), pelas interessantíssimas reuniões científicas, pela constante colaboração e principalmente por ser um exemplo dos bons resultados que podem ser obtidos através de um bom trabalho em equipe.

Aos Professores do Programa de Pós-Graduação em Ciências Biológicas, pelas preciosas aulas, colaborações e convivência.

Aos Professores do Departamento de Antibióticos, pela convivência e colaboração.

Aos Funcionários da Central Analítica do Departamento de Química Fundamental, pela realização dos espectros de Infravermelho e Ressonância Magnética Nuclear.

Ao alunos de iniciação científica, em especial Pedro Canuto Vieira da Costa, pela agradável convivência e pela grande ajuda nas várias etapas deste trabalho.

A todos os integrantes da grande família que forma o Laboratório de Planejamento e Síntese de Fármacos LPSF, entre eles meus colegas de doutorado: Laudelina Magalhães, Daniel Pereira, Andréia Apolinário, Ricardo Moura, Micheline Miranda, Manuela Carvalho, Sibele Oliveira, Diana Malta e Juliana Kelle, pela companhia nos estudos e na bancada; e meus companheiros de laboratório Cássia Ramos, Janaína Couto, Maria Andréia, Cleiton Barros, Francimary Guedes, Iane Vasconcelos, Larissa Cabral e Marina Galdino Pitta.

Aos amigos que circulam pelo LPSF, Maira Galdino Pitta, Janaína Versiani, Irapuan Oliveira, Bruno Monlevade, Francisco Jayme, Valderes Almeida e Ivanildo Mangueira, pelos agradáveis momentos que compartilhamos.

Aos colegas PKs, da Universidade Federal do Rio Grande do Sul: Bibiana Araújo, Leandro Tasso, Rodrigo Freddo, Sandra Hass, Vitória Berg Cattani, Daniela Conrado, Candice Felipi, Clarissa Bettoni, Moacir Kaiser, Francine Azeredo, Patrícia Severino, Laura Oliveira e Cristófer Farias, pela carinhosa recepção, ajuda e companheirismo nas longas noites de coleta de dados.

Aos amigos do Centro Bioanalítico de Medicamentos (CBIM) Eduardo Palma e Ana Lúcia Xavier Villagran, e aos amigos do Laboratória 405 da Faculdade de Farmácia da UFRGS, Karina Paesi, Nathaly Siqueira, Renata Raffin, Irene Kulkamp, Franceline Reynaud, Letícia Cruz, Manuela França, Letícia Sias, Fernanda Poletto, Alessandro Jager e Eliezer Jager, pela companhia e agradável convivência.

Aos colegas do Programa de Pós-Graduação em Ciências Biológicas, em especial Andréia Apolinário, Maria Luiza Bastos, Fabíola Lys de Medeiros, Valentina Carvalho e Cícero Carlos, pelas agradáveis horas de estudo e companheirismo.

A minha pequena grande família: Adriano, Gustavo e Guilherme, pela paciência, amor e apoio constantes.

Aos meus familiares, que infelizmente moram longe dos olhos, mas dentro do coração: Stelita, Luciana, Beto, Alessandra, Plaucídio, Cecília, Theodolinda, Atílio, Juliane, Mané, Elói, Neca, Terezinha, Suzy, José Gláucio, Maria Helena, Cristiane, Eduardo, Gabriela, Mariana, Fabiana, Rodolfo, Alzira, Vera Lúcia e Leda.

A Maria José, Cláudia e Nevinha, que ficaram cuidando dos meus filhos enquanto eu estava no laboratório, meu mais do que sincero muito obrigado. Sem o comprometimento e dedicação de vocês, nada teria sido possível.

A Deus, ser de suprema bondade, que conduziu com muita propriedade meus passos para que eu chegasse aqui.

Dedico esta tese aos meus filhos - Gustavo e Guilherme - que são a minha razão de cada dia, o meu sonho de cada noite e a expressão da minha felicidade.

RESUMO

Uma série de novas 5-indol-tiazolidinadionas bioativas foi sintetizada visando a obtenção de um novo protótipo antiinflamatório com ação simbiótica direcionada a dois diferentes alvos relevantes no processo inflamatório: as enzimas cicloxigenases (COXs) e o receptor gama ativado pelo proliferador de peroxissomo (PPAR-γ). A presença de um grupamento indol na posição 5 do anel tiazolidínico central representa uma das particularidades desses compostos, os quais são de um lado relacionados estruturalmente à indometacina, um anti-inflamatório não-esteroidal (AINE), e de outro, ao anti-diabético rosiglitazona, um agonista PPAR-γ. Este estudo conduziu à identificação de moléculas que apresentaram atividade antiinflamatória em modelo *in vivo* de inflamação, bem como a capacidade de inibir as isoformas COX-1 e COX-2 em ensaio de inibição enzimática *in vitro*. Dentre as moléculas estudadas, a 5(*Z,E*)-3-[2-(4-clorofenil)-2-oxoetil]-5-(1H-indol-3-ilmetileno)-1,3-tiazolidin-2,4-diona (PG-15) mostrou excelente atividade antiinflamatória, avaliada através da inibição de migração lucocitária nos modelos de inflamação do air pouch, com uma DE_{50} de 7,5 mg/Kg (p.o.), e de peritonite, apresentando 30,7% de inibição após administração oral na dose de 3mg/Kg. O composto PG-15, pelos promissores resultados apresentados, foi conduzido a um estudo farmacocinético, onde foram avaliadas as suas concentrações no plasma de rato durante 16 horas, após as administrações intravenosa de 3m/Kg, e oral de 3 e 6 mg/kg. Os resultados mostraram que o PG-15 é rapidamente absorvido após administração oral atingindo o pico de concentração plasmática entre 30 e 60 minutos e uma meia-vida de 5,9 ± 3,8 horas, após administração intravenosa. A quantidade de PG-15 também foi quantificada no sítio da inflamação, através do doseamento do mesmo no exsudato inflamatório do bolsão e da peritonite após a administração oral de 3mg/Kg, onde foram detectadas 83,85 ± 43,46 e 30,51 ± 7,7 ng/mL (média ± erro padrão), respectivamente.

Termos de Indexação: Tiazolidinonas, antiinflamatórios, COX-2.

ABSTRACT

A series of new 5-indol-thiazolidinones was synthesized in order to design a new prototype based on a symbiotic approach where molecules are potentially active in two different targets, both relevant to inflammatory process: cyclooxygenase-2 enzyme and peroxissome -activated receptor subtype γ (*PPAR-γ*).

An indol group attached at 5-position of thiazolidinic ring is the chemical feature of this chemical series, where compounds are structurally related to indomethacin, a potent non-steroidal anti-inflammatory drug (NSAID) and also to anti-diabetic rosiglitazone, a *PPAR-γ* agonist

This study led to molecules that presented good anti-inflammatory activity in inflammation air pouch model. They revealed to be capable to inhibit *in vitro* COX-1 and COX-2.

From this series, the 5(*Z,E*)-3-[2-(4-chlorophenyl)-2-oxoethyl]-5-(1H-indol-3-ylmethylen3)-1,3-thiazolidin-2,4-diona (PG-15) exhibited excellent anti-inflammatory activity inhibiting leukocyte migration in air pouch model, with an ED_{50} of 7,5 mg/kg (p.o.) and peritonitis, where presented 30,7% of inhibition. Promising compound PG-15 was conducted to a pharmacokinetic study, where plasma concentrations of PG-15 were followed during 16 hours after intravenous administration of 3mg/kg and oral administration of 3 and 6 mf/kg.

Results showed that PG-15 is rapidly absorbed after oral administration reaching plasma peak level between 30 and 60 minutes and a 5.9 ± 3.8h half-life after iv dosis. PG-15 was also detected at inflammatory site, by dosing air pouch and peritonitis exudates after 3mg/kg oral administration, where 83.85 ± 43.46 and 30.51 ± 7.7 ng/mL were detected (average ± se), respectively.

Index terms: thiazolidinones, anti-inflammatory, COX-2.

LISTA DE FIGURAS E TABELAS

LISTA DE ABREVIATURAS

Abreviatura	*Descrição*
5-ASA	Ácido 5-amino-salicílico
AchE	Acetilcolinesterase
AINE	Fármaco antiinflamatório não-estóide
AP-1	Activator protein 1, em português: Proteín ativadora 1
Arg	Arginina
COX	Cicloxigenase
DE 50	Dose Eficaz 50%
eNOS	Óxido Nítrico sintase endotelial
ESI	Eletrospray ionization, em português: Ionização por eletrospray
Glu	Glutamina
His	Histidina
HTS	High Throughput Screening, em português: Varredura de alto rendimento
IC 50	Inhbitory concentration 50%, em português: Concentração Inibitória 50%
IL	Interleucina
Ile	Isoleucina
iNOS	Óxido Nítrico Sintase Inducível
IV	Infravermelho
LC	Liquid chromatography, em português: Cromatografia Líquida
Leu	Leucina
L-NMMA	N-(G)-monometil-L-arginina
LOX	Lipoxigenase
LPS	Lipopolissacarídeo
LT	Leucotrieno
MS	Mass spectrometry, em português: Espectrometria de Massas
MRP-1	Multiple resistence protein, em português: Proteína de múltipla resistência à drogas
NFAT	Nuclear factor activator T cells, em português: Fator nuclear de células T ativadas
NO	Nitric Oxide, em português: Òxido Nítrico
NOS	Óxido Nítrico Sintase
AO	Osteoartrite
PAF	Fator de ativação plaquetária
PG	Prostaglandina
Phe	Fenilalanina
PPAR	Peroxissome -activated receptor, em português: Receptor ativador de peroxissomos
RMN	Ressonância Magnética Nuclear
SAR	Structure-activity relationship, em português: Relação estrutura-atividade
Ser	Serina
SERT	Transportador de serotonina
STAT-1	Signal transducers and activators of transcription, em português: Sinal trasdutor e ativador de trascrição-1
TNF-α	Tumoral Necrosis Factor, em português: Fator de necrose tumoral
Tyr	Tirosina
TZD	Tiazolidinona
Val	Valina

SUMÁRIO

1 INTRODUÇÃO

O processo inflamatório é uma resposta complexa, não-específica e coordenada dos tecidos a um dano, o qual envolve, em linhas gerais, permeabilidade vascular, migração de células sanguíneas e passagem de plasma para os tecidos danificados. As moléculas que medeiam os eventos iniciais da inflamação são as moléculas de adesão, as quais são fundamentais para a migração dos leucócitos até a superfície dos vasos sanguíneos. Esta migração inicia as complexas reações que são controladas por inúmeros mensageiros intracelulares chamados mediadores (MASLINSKA e GAJEWSKI, 1998). A magnitude da resposta inflamatória é crítica para os organismos, pois uma resposta deficiente pode resultar em infecções secundárias, enquanto uma resposta excessiva pode ser mais prejudicial do que o dano inicial (CZURA, FRIEDMAN e TRACEY, 2003).

Os prostanóides estão amplamente envolvidos no processo de comunicação entre as células. Estes mediadores são produtos do metabolismo do ácido araquidônico na rota da cicloxigenase, uma enzima que se apresenta em pelo menos duas isoformas (COX-1 e COX-2), as quais exercem diferentes funções fisiológicas devido aos diferentes locais de expressão e regulação dessa expressão (VANE, 1998).

Atualmente, o direcionamento das terapias para doenças que passam por alguma fase inflamatória inclui os inibidores da COX-2 e a regulação do processo apoptótico em algumas células (DOAN E MASSAROTTI, 2005).

Dentre as doenças inflamatórias crônicas merece ser destacada a osteoartrite (OA), uma das mais comuns e que, de acordo com a Organização

Mundial de Saúde, mais de 14 milhões de casos são diagnosticados anulamente (WHO, 2003). O único tratamento oral reconhecido para a OA é sintomático, utilizando agentes analgésicos ou antiinflamatórios, como o paracetamol ou inibidores da COX (WEILAND *et al.,* 2005).

A partir de fins da década de 1990, os inibidores seletivos da COX-2 foram os fármacos de escolha nesses casos. Estes fármacos foram desenvolvidos baseados na hipótese de que a inibição seletiva da isoforma COX-2 reduziria a dor e a inflamação sem os efeitos gastrintestinais e sangramentos comuns aos inibidores não-seletivos. Entretanto, em setembro de 2004, o rofecoxib (Vioxx®), um desses fármacos, foi retirado do mercado farmacêutico pelo alto risco cardiovascular que apresentava, e, em abril de 2005, o valdecoxib (Bextra®), pelos mesmos motivos, teve o mesmo destino (BROPHY, 2005).

Após pouco mais de oito anos de tratamento com relativo sucesso utilizando inibidores seletivos da COX-2, tornou-se evidente que existe a necessidade de se aprimorar o tratamento das doenças inflamatórias de forma que os efeitos benéficos sejam preservados, mas que os riscos cardiovasculares sejam reduzidos. Neste contexto, a comunidade científica volta seus esforços, mais uma vez, na busca por um tratamento eficaz das doenças inflamatórias, que afligem grande parte da população mundial.

Atualmente, com uma abordagem multidisciplinar, o planejamento racional de fármacos representa uma excelente e indispensável ferramenta que agrega conhecimentos da patologia, alvos biológicos, estruturais e físico-químicos que podem conduzir à estratégias de desenho, síntese e testes biológicos de novas

moléculas que tenham, potencialmente, as características de resposta biológica que são desejadas.

Na busca por fármacos que atuem em mais de uma via da resposta inflamatória, que apresentem melhores características que os atuais e que sejam farmacodinamicamente mais eficazes mantendo uma boa biodisponibilidade e reduzidos efeitos colaterais, o presente trabalho foi desenvolvido abrangendo duas áreas de conhecimento: a Química Orgânica e a Biologia.

No âmbito da Química Orgânica Medicinal, observamos o desenho estrutural e o estabelecimento dos métodos para síntese e purificação, seguida da comprovação estrutural e determinação de características físico-químicas. Na grande área das Ciências Biológicas, foram apropriados conhecimentos fundamentais de bioquímica, farmacologia e fisiologia, inclusive para realização de ensaios *in vitro* e *in vivo* da atividade antiinflamatória das novas moléculas sintetizadas. Por fim, a interdisciplinaridade desses conhecimentos nos auxiliam na estratégia de modificações estruturais visando fármacos mais potentes, seguros e com maior aceitabilidade.

No escopo deste trabalho temos inicialmente uma revisão da literatura, que aborda os principais aspectos da inflamação e em quais momentos deste complexo processo existem possibilidades de intervenção, bem como uma breve revisão dos trabalhos apresentados pela comunidade científica focando a relação entre a estrutura química e a atividade biológica de compostos ativos na inflamação.

Sequencialmente, tem-se a apresentação dos objetivos deste trabalho e posteriormente uma breve explanação sobre o planejamento das moléculas que formam o alvo deste trabalho.

Em atendimento às normas estabelecidas pelo Programa de Pós-Graduação em Ciências Biológicas, os resultados obtidos neste trabalho estão apresentados na forma de artigos científicos para divulgação internacional.

Por fim, apresentamos nossas considerações finais, como fechamento do trabalho realizado durante o doutoramento. Nossas perspectivas futuras também estão elencadas, pois tendo a pesquisa um caráter naturalmente dinâmico, a sua continuidade é fundamental.

2 Revisão da Literatura

No campo do descobrimento de novas moléculas biologicamente ativas, cada vez mais tem sido apreciada a abordagem fisiológica de que resultados mais robustos são obtidos a partir dos resultados das ações de fármacos em diferentes partes do organismo, o qual, por constituir um complexo sistema biológico, é composto por células e tecidos interligados com vias sinalizadoras redundantes, convergentes e divergentes (BORYSI et al., 2003). Segundo Csermelin, Agoston e Pongron (2005) a inibição parcial de dois ou mais alvos biológicos é mais eficiente na resolução da patologia do que a inibição total de um único alvo. Baseado nessa primissa está o conceito de fármacos com ação em múltiplos alvos moleculares, também chamados duais ou simbióticos (MORPHY e ZORAN, 2005).

Em relação ao alvo molecular, a ação das moléculas simbióticas pode ser dividida em três categorias. A primeira configura àquelas moléculas que atuam em alvos separados para criarem um efeito combinado, seja pela inibição de diferentes alvos na mesma rota metabólica, diferentes alvos em diferentes rotas na mesma célula ou em diferentes tecidos. Numa segunda categoria estão as moléculas que atuando em diferentes alvos, a modulação da resposta do primeiro alvo facilita a ação do segundo alvo. Na terceira, a molécula atua em diferentes sítios dentro de um mesmo alvo (ZIMMERNANN, LEHA e KIETHM, 2007).

Exemplos bem sucedidos de fármacos racionalmente planejados com ação em alvos distintos incluem a duloxetina, um antidepressivo que atua na recaptação tanto da serotonina quanto da norepinefrina (TURCOTTE et al., 2001).

No tratamento da inflamação o conceito de multi-alvos é muito importante e precisa ser tratado criteriosamente, pois a resposta inflamatória é complexa, não-específica e coordenada dos tecidos como consequência a um ou mais danos. O processo inflamatório envolve uma série de eventos, os quais podem ser agrupados em permeabilidade vascular, migração de células sanguíneas e passagem de plasma para os tecidos danificados. As moléculas que medeiam os eventos iniciais da inflamação são as moléculas de adesão que são críticas para a migração dos leucócitos até a superfície dos vasos sanguíneos. Esta migração inicia as complexas reações que são controladas por inúmeros mensageiros intracelulares chamados mediadores (MASLINSKA e GAJEWSKI, 1998). A magnitude da resposta inflamatória é crítica aos organismos, pois uma resposta deficiente pode resultar em infecções secundárias, enquanto uma resposta excessiva pode ser mais prejudicial que o dano inicial (CZURA, FRIEDMAN e TRACEY, 2003).

2.1 Resposta Inflamatória

A resposta inflamatória é uma resposta complexa e coordenada dos tecidos a uma agressão (MASLINSKA e GAJEWSKI, et al*.,* 1998), destacando-se que o grau com que estas ações ocorrem é proporcional à severidade da agressão e à sua extensão (STVRTINOVÁ, JAKUBOVSKÝ e HULÍN, 1995).

A inflamação pode ser dividida em diversas fases. A primeira, um evento imediato, é uma vasoconstrição temporária causada pelos mediadores bradicinina e serotonina, seguida por fases que ocorrem posteriormente em minutos, horas ou dias, os quais são: a resposta vascular aguda, a resposta celular aguda, a

resposta celular crônica e a resolução (STVRTINOVÁ, JAKUBOVSKÝ e HULÍN, 1995).

A resposta vascular aguda é iniciada segundos após o dano e dura alguns minutos, caracterizando-se por vasodilatação, aumento da permeabilidade vascular, aumento do fluxo sanguíneo (hiperemia e eritema) e entrada de fluído nos tecidos (edema). Na situação onde o dano tecidual foi relevante ou quando ocorre infecção, a resposta celular aguda inicia nas próximas horas, cuja principal característica é o surgimento de granulócitos, particularmente neutrófilos, que se aproximam das células endoteliais dos vasos sanguíneos (marginação) e a seguir atravessam para os tecidos circundantes (diapedese) (SANCHEZ-MADRID e DEL POZO, 1999). Também faz parte desta fase a formação de coágulos, os quais impedem o sangramento, bem como o início da formação de pus, composto por uma mistura de exsudato inflamatório, leucócitos polimorfonucleares vivos e mortos, e bactérias vivas e mortas (STVRTINOVÁ, JAKUBOVSKÝ e HULÍN, 1995).

Na seqüência, surge uma resposta celular crônica onde ocorre a infiltração de células mononucleares: os macrófagos e os linfócitos (FUJIWARA e KOBAYASHI, 2005). Em seguida deverá ocorrer a resolução, ou seja, a volta a normalidade dos tecidos. Os coágulos são removidos por fibrinólise ou então ocorre a formação de uma ferida (MODARAI et al., 2005) e a infecção é debelada, ou forma-se um granuloma com os macrófagos e linfócitos circundantes ao material que não foi eliminado (FUJIWARA e KOBAYASHI, 2005).

As moléculas que são responsáveis pelo comando e que medeiam a resposta inflamatória são chamadas mediadores inflamatórios (Figura 1).

Quimicamente esses mediadores pertencem à diversas classes e são liberados em momentos específicos dessa resposta. Primeiramente, são liberadas aminas vasoativas e mediadores lipídicos que promovem exsudação e edema, seguidos pela expressão de citocinas e quimioquinas que ativam o endotélio e medeiam a migração leucocitária. Finalmente, mediadores antiinflamatórios atenuam a migração celular e promovem a apoptose e a retirada dos leucócitos do sítio inflamatório (STVRTINOVÁ, JAKUBOVSKÝ e HULÍN, 1995).

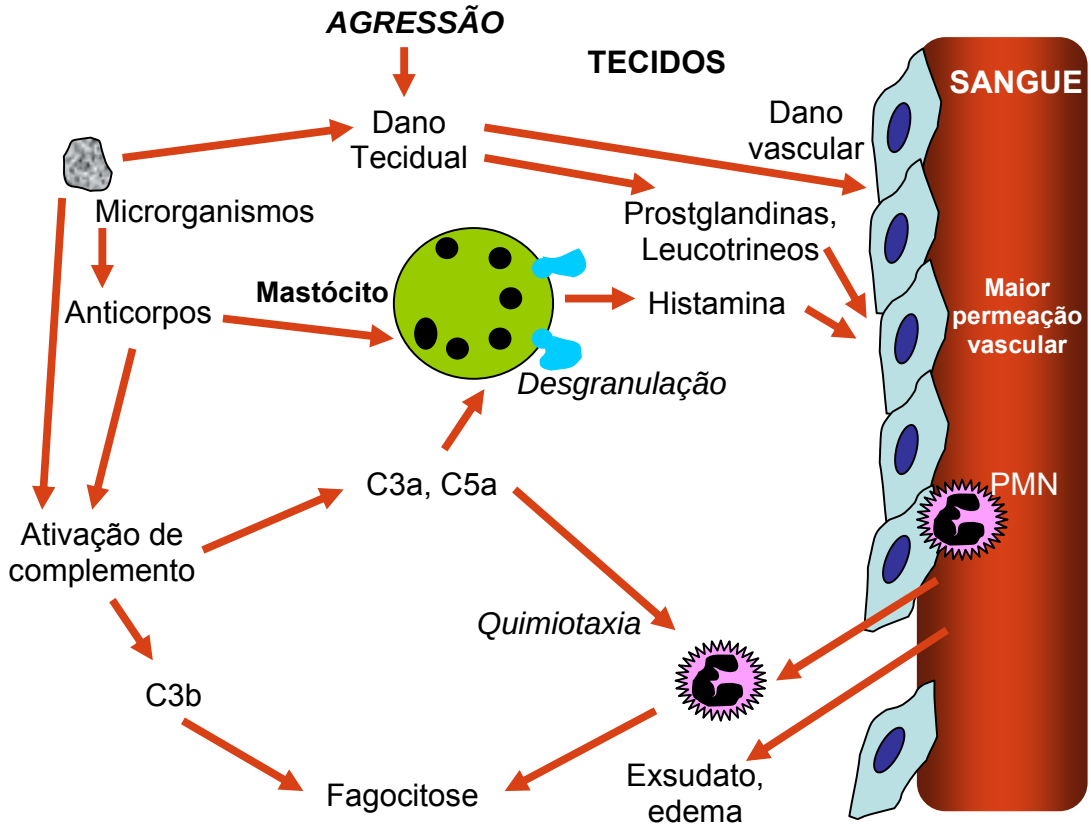

Figura 1: Representação esquemática dos eventos desencadeados por uma agressão tecidual, alguns dos mediadores liberados e suas principais ações (PMN= leucócito) (Adaptado de http://www-micro.msb.le.ac.uk/ MBChB/1b.html)

De acordo com Feghali e Wrigth (1997), os mediadores inflamatório podem ser classificaods em quatro principais categorias:

1. metabólitos lipídicos como o Fator de Ativação Plaquetária (PAF) e os derivados do ácido araquidônico, que incluem as prostaglandinas (PGs), prostaciclinas e os leucotrienos (LTs), formados a partir dos fosfolipídios celulares;

2. três cascatas de proteases e substratos solúveis (coagulação, complemento), que geram numerosos peptídeos pró-inflamatórios;

3. óxido nítrico (NO), um potente vasodilatador endógeno; e

4. um grupo de polipeptídeos celulares chamados citocinas (FEGHALI e WRIGTH, 1997).

As respostas fisiológicas desencadeadas por cada mediador pode ser observada na Tabela 1.

Tabela 1: Mediadores envolvidos em ações específicas da resposta inflamatória

Aumento da permeabilidade vascular	***Quimiotaxia e ativação leucocitária***	***Vasodilatação***	***Febre***	***Dor***	***Dano tecidual***
-Aminas vasoativas -C3a e C5a -Bradicinina -LTs C_4, D_4, E_4 -PAF	-C5a -LTB_4 -Produtos bacterianos-- IL-8	-PGs -Óxido nítrico	-IL-1 -IL-6 -TNF -PGs	-PGs -Bradicinina	-Enzimas lisossomais de Neutrófilos e macrófagos -Espécies reativas de oxigênio -Óxido nítrico

A inflamação é um processo protetor essencial na preservação da integridade do organismo contra agressões, sejam das químicas, físicas ou biológicas. Sob esse ponto de vista, a inflamação desempenha um papel chave na resposta imune inata. Entretanto, não raro, a resposta inflamatória leva a danos

nos tecidos normais e seus efeitos fisológicos são desagradáveis (FIRNK, 2002; HABASHY et al., 2004). Adicionalmente, esses eventos podem levar o indivíduos à morte, como no choque anafilático, ou ainda conduzir à doenças crônicas debilitantes, como nas doenças reumáticas geradas por falhas na fase de resolução da inflamação (STVRTINOVÁ, JAKUBOVSKÝ e HULÍN, 1995).

Nesse contexto, torna-se necessária a utilização de fármacos que possam interferir na inflamação de modo a encerrá-la apropriadamente, minimizando os efeitos dolorosos e desconfortáveis e ainda evitando reações exacerbadas.

A interferência na inflamação pode ser feita em diversas etapas e em diferentes vias do processo inflamatório, entre as quais se destacam, pela utilização terapêutica eficaz, a inibição na liberação de óxido nítrico, a inibição da atividade das citocinas, a inibição da produção dos leucotrienos, assim como a inibição da produção ou interação das prostaglandinas, onde se encontram os fármacos antiinflamatórios não esteróides (AINEs), os fármacos mais utilizados na terapêutica atual com esse propósito (DANNHARDT e KIEFER, 2001).

2.1.1 Óxido Nítrico

Sob condições fisiológicas, em todo organismo, as concentrações de óxido nítrico (NO) são flutuantes em níveis relativamente baixos. Estes níveis são controlados por dois tipos de enzimas, as chamadas óxido nítrico sintases (NOSs), expressas constitutivamente: a neuronal (nNOS) e a endotelial (eNOS). Ambas são distribuídas por todo organismo humano. Entretanto, nos estados inflamatórios, o NO é liberado em grandes quantidades e ocorre uma massiva expressão da NOS inducível (iNOS) que leva a produção de grandes quantidades

de NO, colocando-o como um subproduto tóxico da inflamação, que pode ser inibido através da inibição da iNOS, restabelecendo a homeostase (MOLLACE et al., 2005).

Adicionalmente, em 1993, uma importante relação entre a NOS e a COX foi descrita por Salvermini e colaborados (Apud: MOLLACE et al., 2005) (Figura 2). A interação entre a geração de NO e do sistema enzimático gerador das PGs ocorre em diversos níveis:

1º O NO interfere diretamente na expressão da COX;

2º O NO liberado pelos macrófagos exerce uma ação estimulatória da atividade da COX-2, uma vez que a molécula sinalizadora •NO pode iniciar a síntese de prostaglandinas pela reação com o aniôn superóxido (O2•-) para produzir peroxinitrila, que oxida o ferro do grupo heme por transferência de elétrons do aminoácido tirosina do sítio catalítico da COX (POLI, 2002).

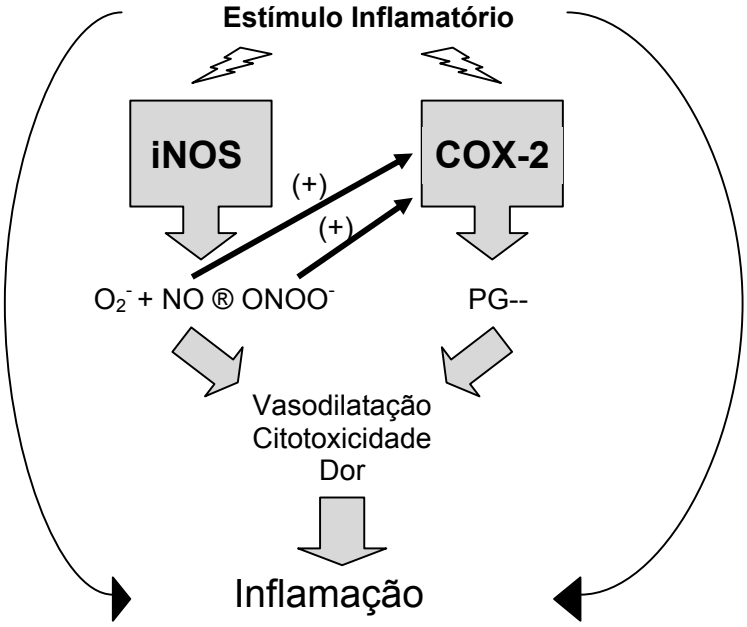

Figura 2: Interação entre iNOS e COX-2. A formação de NO ocorre após um estímulo inflamatório, potencializando a atividade da COX-2 (MOLLACE et al., 2005)

As NOS geram NO a partir da arginina e um número considerável de inibidores estruturalmente relacionados ao substrato L-arginina tem sido desenvolvidos, a exemplo do conhecido N-(G)-monometil-L-arginina (L-NMMA). Entretanto, nenhuma dessas substâncias atua de forma seletiva para cada uma das isoformas. Como a inibição da isoforma endotelial (eNOS) produz hipertensão, o desenvolvimento farmacêutico de inibidores altamente seletivos da iNOS é bastante desejável (STRUB et al., 2005).

Um derivado estrutural da imidazopiridina, o composto BYK191023 (Figura 3), foi sintetizado recentemente e demonstrou potência e seletividade frente à iNOS, sendo uma molécula promissora não somente como ferramenta de pesquisas pré-clínicas envolvendo as NOS, mas como um forte candidato a medicamento (STRUB et al., 2005).

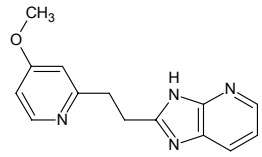

BYK191023

Figura 3: Estrutura química do composto BYK191023 (2-[2-(4-metóxi-piridin-2-il)-etil]-3H-imidazo[4,5-b]piridina), um inibidor seletivo da iNOS

Adicionalmente, substâncias que são doadores de NO combinados com AINEs (NO-AINEs), têm sido sintetizadas e utilizadas no tratamento de doenças inflamatórias, sugerindo um possível efeito benéfico pela ação simultânea do NO e de PGs. Estas drogas liberam NO a partir de grupos liberadores em suas estruturas químicas exercendo efeitos protetores no estômago e mediando diversos componentes envolvidos na defesa da mucosa gastrintestinal. A atividade antiinflamatória e analgésica dos NO-AINEs são, no mínimo, equivalentes àquelas

apresentadas pelo AINE que estes contém isoladamente, dentre as quais as NO-aspirinas, como o composto NCX4016 (Figura 4a e 4b), são as que tem despertado maior interesse, pois exercem efeitos antitrombóticos, antiinflamatórios iguais ou maiores do que aqueles produzidos pela aspirina, mas não causam danos gastrintestinais (WALLACE, IGNARRO e FIORUCCI, 2002).

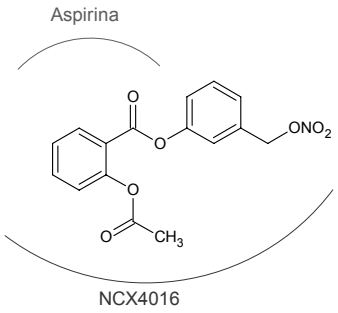

Figura 4a: Estruturas da aspirina e do NCX4016. O NCX4016 consiste da aspirina ligada por uma ligação éster a um grupo espaçador. O grupo liberador de NO, o ONO_2 está ligado ao espaçador (WALLACE, IGNARRO e FIORUCCI, 2002)

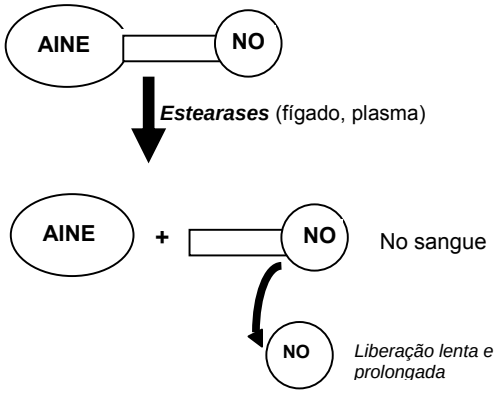

Figura 4b: Metabolismo dos NO-AINEs por estearases (primeiramente no fígado e no plasma) liberando a fármaco-mãe (aspirina) mais o grupamento espaçador acoplado ao grupo liberador de NO. Metabolismo subseqüente leva a liberação de NO, que pode acontecer horas após a liberação da droga (WALLACE, IGNARRO e FIORUCCI, 2002)

2.1.2 Citocinas

A inflamação é regulada, em parte, pelas citocinas, que são pequenas proteínas, glicosiladas de forma características e que interagem com receptores de membrana com o propósito de regular processos celulares tais como proliferação, diferenciação e secreção. Existem muitas citocinas conhecidas que têm ações estimulantes e supressoras sobre as células linfáticas e a resposta imune. Algumas das mais conhecidas são: o fator de necrose tumoral (TNF-α), a

interleucina-1 (IL-1) e a interleucina-6 (IL-6) (DRISCOL et al., 1997). A interação entre as citocinas na resposta inflamatória pode ser vista na Figura 5.

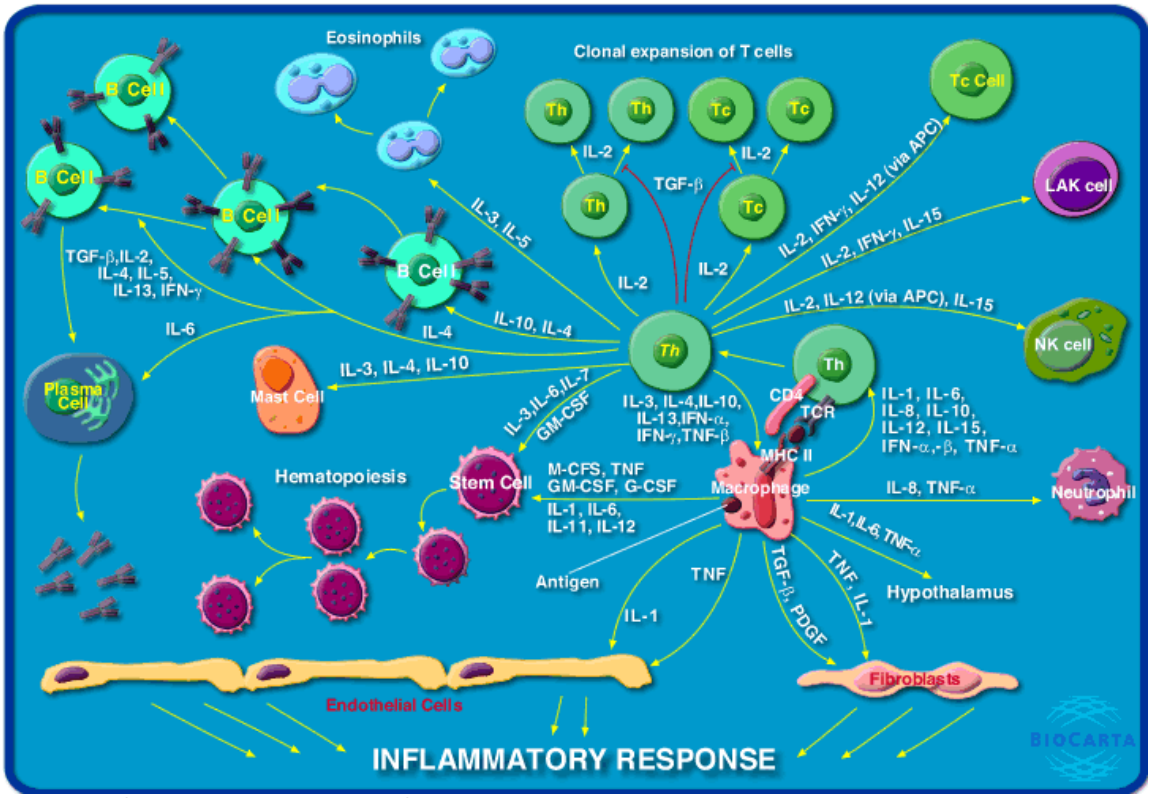

Figura 5: Citocinas na resposta inflamatória: as citocinas secretadas realizam a sinalização entre as células imunes a fim de coordenar a reposta inflamatória. Algumas citocinas, como IL-1, IL-6 e TNF atuam amplamente para provocar a resposta inflamatória, enquanto outras atuam em tipos específicos de células imunes. Macrófagos e outras células fagocíticas formam a primeira linha de defesa contra infecções bacterianas. Os macrófagos estimulam a resposta inflamatória de neutrófilos, fibroblastos e células endoteliais em resposta a uma infecção pela secreção de IL-1 e TNF. IL-1 e TNF causam febre através da alteração da temperatura corporal no ponto de controle do hipotálamo. Fibroblastos e células endoteliais respondem a IL-1 e ao TNF com um recrutamento de mais células imunes ao sítio da inflamação. A IL-8 secretada é uma quimiocina que atrai neutrófilos aos locais infectados. Macrófagos também apresentam antígenos às células T auxiliares ($T\text{-}_{aux}$) que tem um papel importante na coordenação da resposta imune. As $T\text{-}_{aux}$ induzem expansão clonal das células $T\text{-}_{aux}$ que responderam ao antígeno, com IL-2 como mediador chave da proliferação e ativação das $T\text{-}_{aux}$. A atividade citotóxica das células natural killer (NK) e células NK-linfocina-ativadas (LAK) é estimulada por IL-2 e outras citocinas na presença de infecções virais ou células tumorais. As $T_{\text{-aux}}$ secretam IL-3 e IL-5 para estimular a proliferação e ativação de eosinófilos. Os eosinófilos estão envolvidos na resposta imune às infecções parasitárias. As $T\text{-}_{aux}$, IL-10, IL-4 e outras citocinas são requeridas para estimular a resposta das células B. Além da ativação e proliferação de células imune especificamente diferenciadas, as citocinas atuam sobre as células-tronco hematopoéticas, causando sua proliferação e diferenciação nas diferentes células do sistema imune (SHIH, 2001). Fonte: http:// biocarta.com

Com finalidade terapêutica, as pesquisas têm-se direcionado para o TNF-α, que tem um papel na iniciação da resposta inflamatória e atua pelas vias parácrina e autócrina estimulando as células a liberarem outras citocinas, chamadas quimioquinas, as quais são quimioatratoras diretas de leucócitos e outras células que participam da resposta inflamatória (DRISCOL et al., 1997). Alguns inibidores do TNF-α são clinicamente utilizados no tratamento das doenças reumáticas. Entre eles têm-se o infliximab, um anticorpo monoclonal, e o etanercept, um receptor p75 TNF-α (MIOSSEC, 2004).

2.1.3 Leucotrienos

Os leucotrienos (LTs), derivados lipídicos do ácido araquidônico, são sintetizados através de uma rota biossintética que envolve a enzima lipoxigenase (LOX), chamada via da LOX. Os LTs estão envolvidos na produção e manutenção da inflamação e, portanto, são considerados mediadores da inflamação. Entretanto, moléculas capazes de bloquear a via da LOX, inibidores da LOX ou antagonistas dos receptores dos LTs são insuficientes no tratamento da inflamação, embora sejam potencialmente efetivos no tratamento da asma. Moléculas capazes de inibir as vias da COX e da LOX (duais) têm sido desenvolvidas e investigadas farmacologicamente (LEVAL et al., 2002).

2.1.4 Prostaglandinas

As prostaglandinas (PGs) são uma família de moléculas lipossolúveis tipo-hormônio produzidas por diferentes tipos de células no organismo. Ao contrário de

mediadores amínicos, como histamina e a serotonina, as prostaglandinas não existem livremente nos tecidos, mas têm de ser sintetizadas e liberadas em resposta a um estímulo apropriado. Entre as PGs, a PGE_2 é a responsável pelo aumento da permeabilidade vascular, é pirogênica, aumenta a sensibilidade à dor e estimula o AMP cíclico leucocitário, que tem um importante efeito supressivo na liberação de mediadores por mastócitos, linfócitos e fagócitos (STVRTINOVÁ, JAKUBOVSKÝ e HULÍN, 1995).

Na década de 1990, a busca pela compreensão do processo inflamatório possibilitou a descoberta de que a enzima cicloxigenase é encontrada em pelo menos duas isoformas: a cicloxigenase-1 (COX-1) e a cicloxigenase-2 (COX-2), as quais são responsáveis por uma etapa chave na biossíntese das prostaglandinas (SIMMONS, BOTTING e HLA, 2004).

Recentemente, uma proteína variante, chamada COX-3 foi identificada. Esta proteína possui uma produção de prostaglandinas reduzida, se comparada à COX-1. Mas fármacos analgésicos/antipiréticos, como o acetaminofeno e a dipirona inibem preferencialmente esta atividade (CHANDRASEKHARAN et al., 2002).

Ações fisiológicas e patológicas das prostaglandinas incluem àquelas associadas à inflamação, citoproteção da mucosa gastrintestinal e controle das funções renais. Altos níveis de COX-1 são expressos nas plaquetas, células do endotélio vascular, estômago e tubos coletores renais. Prostanóides derivados da COX-1 desempenham um papel importante na tromobogênese e na homeostase dos tratos gastrintestinal e renal (LEVAL et al., 2002).

Em contraste, a COX-2 é praticamente indetectácel em condições fisiológicas, mas sua expressão é inducível por uma gama de estímulos, tais como: forbol ésteres, interleuicna-1 (IL-1) ou lipopolissacarídeo (LPS). Altos níveis de COX-2 são detectados nos exsudatos e na medula espinhal em diferentes modelos animais de inflamação. Além disso, destaca-se que inibidores seletivos da COX-2 apresentam atividade antiinflamatória, antipirética e propriedades analgésicas em diversos modelos animais e humanos de inflamação (LEVAL et al., 2002).

Há indícios de que as prostaglandinas também estejam envolvidas em outras condições patológicas. De fato, por afetarem a mitogênese, a adesão celular, a apoptose e a angiogênese (LEAHY, KOKI e MASFERRER, 2000), as PGs podem ter um papel importante na patogênese de diversos tipos de cânceres. Superprodução de PGs e super-expressão da COX-2 são encontradas em cânceres de cabeça e pescoço, mama, pulmão, cólon e pâncreas, sugerindo o envolvimento da COX-2 na carcinogênese. Tais dados são corroborados por diversos estudos epidemiológicos que sugerem que a utilização regular de AINEs é eficiente na prevenção de câncer colorretal (LEVAL et al., 2002).

Longos períodos de tratamentos com AINEs têm demonstrado serem responsáveis por um decréscimo na incidência da Doença de Alzheimer, fato que sugere o envolvimento das prostaglandinas e da COX nesta enfermidade (HOOZEMANS E O'BANION, 2005).

Envolvidos em mecanismos de modulação da resposta inflamatória, os ácidos 13-hidroxioctadecadienóico e 15-hidroxieicosatetraenóico, assim como a prostaglandina 15-desoxi-$\Delta^{12,14}$-prostaglandina J_2, tem sido identificados como

ligantes endógenos ativadores dos receptores ativadores da proliferação de peroxissomos (PPARs). Os PPARs são receptores nucleares que promovem a transcrição de diversos fatores envolvidos em inúmeras funções fisiológicas (ROGLER, 2006).

Muitos estudos têm confirmado as propriedades antiinflamatórias dos PPARs *in vitro* e *in vivo*. A administração de fibratos em pacientes com lipidemia moderada leva a um decréscimo nas concentrações plasmáticas de IL-6, TNF-α, interferon, fibrinogênio e proteína C reativa, enquanto o tratamento do Diabete Tipo 2 com rosiglitazona (ativador do PPAR-γ) resulta em diminuição nas concentrações plasmáticas de MMP-9 (gelatinase-B) e proteína C-reativa (BLANQUART et al., 2003).

A ativação do PPAR-α resulta na repressão da sinalização do Fator Nuclear Kappa-B (NFκB), fator de transcrição para sobrevivência celular) e da produção de citocinas em diferentes tipos de células, entre elas a proteína ativadora (AP-1), que é um fator de transcrição implicado na indução da apoptose em resposta a estresse ou retirada do fator de crescimento; o fator nuclear de células T ativadas (NFAT) que regula a expressão de citocinas e proteínas de membrana que modulam a resposta imune, sinal trasdutor e ativador de trascrição-1 (STAT-1), uma proteína citoplasmática sinalizante envolvida na transdução de diversas citocinas (STAELS e FRUCHART, 2005)

O papel do PPAR-γ na inflamação tem sido descrito em monócitos/macrófagos, onde ligantes deste receptor inibem a ativação de macrófagos e a produção de citocinas inflamatórias (TNF-α, IL-6 e IL-1β).

Entretanto, o mecanismo dos efeitos antiinflamatórios destes ligantes não envolve diretamente o PPAR-γ, mas sim a modulação negativa destas citocinas. A ativação do PPAR-γ também estimula a diferenciação de queratinócitos e reduz a resposta inflamatória na pele (HEIKKINEN, AUWERX e ARGMANN, 2007). Estes resultados sugerem que o papel dos PPARs no controle da resposta inflamatória poderá ter aplicações terapêuticas nas doenças inflamatórias (Figura 6) (CABRERO, LAGUNA e VAZQUEZ, 2002).

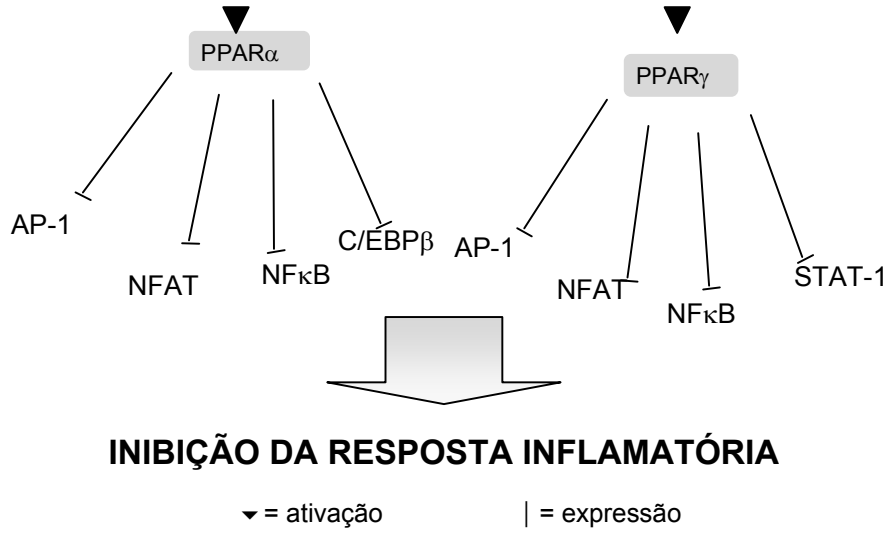

Figura 6: Inibição de diferentes via inflamatórias pelos PPARs. Por interferirem na maioria das rotas de inflamação, os PPARs apresentam funções antiinflamatórias. Estas propriedades levam a modulação da expressão de quimiocinas, receptores de quimiocinas e de moléculas de adesão, e assim, inibem a resposta inflamatória (BLANQUART et al., 2003).

2.2 Fármacos antiinflamatórios não-esteróides

Os fármacos antiinflamatórios não-esteróides, ou AINEs (Non Steroidal Antiinflammatory Drugs), são os fármacos mais utilizados na terapêutica, primariamente para o tratamento da dor e da inflamação, especialmente em artrite. Do ponto de vista histórico, o primeiro AINE com benefícios na clínica foi a

aspirina, que tem sido usada há mais de 100 anos (DANNHARDT e KIEFER, 2001).

Os AINEs bloqueiam a biossíntese de prostaglandinas (PGs) (Vane et al., 1998) e a sua utilização leva a uma diminuição global na produção de PGs. O tratamento das doenças inflamatórias com tais fármacos leva a graves efeitos colaterais, como alta incidência de irritação gástrica, conduzindo a úlceras e sangramento, também podendo gerar disfunções renais e efeito hipertensivo (PARENTE e PERRETTI, 2002).

Como a COX-1 é a isoforma que produz as PGs responsáveis pelas funções fisiológicas de citoproteção e homeostase, enquanto a COX-2 produz as PGs inflamatórias, os AINEs clássicos, por inibirem ambas isoformas, provocam efeitos colatarais relacionados à inibição da COX-1, ou seja, efeitos na citoproteção gastrintestinal e na função renal (HAWKEY, 1999). Estas informações conduziram um grande desafio à Química Medicinal: produzir fármacos seletivos para a COX-2, mas que não apresentassem tais efeitos colaterais (LEVAL et al., 2000). Em 1998, foi comercializado o primeiro fármaco antiinflamatório seletivo para a COX-2: o celecoxib (Celebra®) (HAWKEY, 1999).

2.2.1 Inibidores da cicloxigenase-2

A busca por compostos seletivos para a COX-2, ou seja, substâncias capazes de se ligarem ao sítio ativo da COX-2, mas não da COX-1, tem sido intensa, e o planejamento dessas substâncias, baseado na estrutura do sítio ativo da enzima, já conhecido, tem gerado substâncias com seletividade.

Muita controvérsia foi gerada desde setembro de 2004, quando rofecoxib foi retirado do mercado pelos riscos cardiovasculares apresentados, seguido pela retirada do análogo valdecoxib pelos mesmos motivos. Inibidores seletivos da COX-2 aumentam os riscos cardiovasculares devido à inibição da síntese de prostaciclinas no tecido endotelial (FUNK e FITGERALD, 2007). Enquanto a situação dos inibidores da COX-2 ainda não está totalmente esclarecida sabe-se que os inibidores da COX, seletivos ou não, ainda são a melhor escolha terapêutica no tratamento das doenças inflamatórias, agudas ou crônicas (MITCHEL e WARNER, 2006).

2.2.2 Propriedades estruturais das COX-1 e COX-2 responsáveis pela ligação do substrato e dos inibidores

A estrutura das COX-1 e COX-2 já foram bem definidas por cristalografia de raios-X, sendo homodímeros. Cada monômero consiste de três grandes sítios: um domínio tipo fator de crescimento epidérmico, um domínio membrana-ligante e um domínio catalítico que contem ambos os sítios ativos COX e peroxidase. Ambas as estruturas revelam um canal que se estende do centro do sítio catalítico até superfície do sítio membrana-ligante. A região membrana ligante das COX-1 e COX-2 fica incorporada no interior da membrana plasmática, permitindo que o ácido araquidônico livre tenha acesso ao sítio ativo ou canal, onde este é ciclizado à prostaglandia G_2 (PGG_2). Outra interação com o sítio ativo resulta na redução da PGG_2 em PGH_2. A maioria dos AINEs competem com o ácido araquidônico na ligação com o sítio ativo (Figura 7a) (HAWKEY, 1999).

O grupo hidroxila da serina na posição 530 (Ser-516 na COX-2) é o alvo para a acetilação e inibição irreversível da COX-1 pela aspirina (SMITH, GARAVITO e DeWITT, 1996). Análises de raios-X e experimentos envolvendo mutações nas enzimas elucidaram uma função adicional para a Ser-530. Este aminoácido polar está envolvido na ligação de inibidores que contenham um grupamento benzoíla, tais como a indometacina, ou contendo um NH, como diclofenaco e meclofenamato (VAN RYN, TRUMMLITZ e PAIRET, 2000).

Dois aspectos na estrutura da COX-2 devem ser considerados na sensibilidade da ligação de seus inibidores seletivos. O primeiro é uma susbtituição da Ile-523 na COX-1 por uma aminoácido menor, a valina na COX-2 (Val-509) permite o acesso a um bolso lateral (“side pocket”) adjacente ao canal da COX. Adicionalmente, a diferença de aminoácidos nas duas isoformas (His-513 na COX-1 e Arg-499 na COX-2) permite a formação de uma importante ligação de hidrogênio com os inibidores seletivos da COX-2. A parte estrutural da COX-2 relativa ao bolso lateral tem sido alvo da nova classe de fármacos que são inibidores seletivos desta (Figura 7b e 7c) (VAN RYN, TRUMMLITZ e PAIRET, 2000).

A segunda diferença está no topo do canal. O aminoácido Phe-503 na COX-1 é substituído por uma leucina na COX-2 (Leu-489). A presença de um resíduo menor na COX-2 leva a formação de um espaço extra no topo do sítio de ligação, permitindo que inibidores estruturalmente maiores possam se ligar (VAN RYN, TRUMMLITZ e PAIRET, 2000).

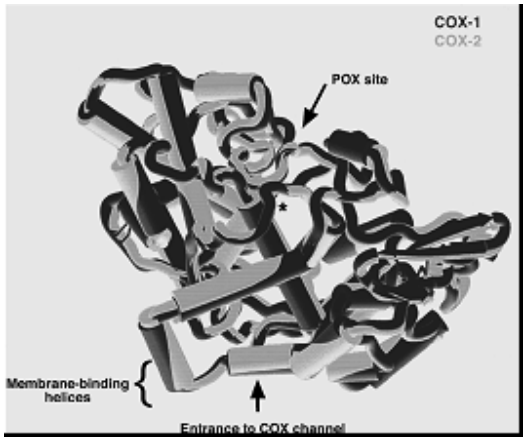

Figura 7a: As estruturas das COX-1(preto) e COX-2 (cinza) estão sobrepostas e mostram-se praticamente sobreponíveis. As hélices anfipáticas que formam o sítio membrana ligante estão destacadas. O sítio peroxidade está assinalado, e o sítio COX marcado com um asterisco (FITZGERALD e LOLL, 2001)
.

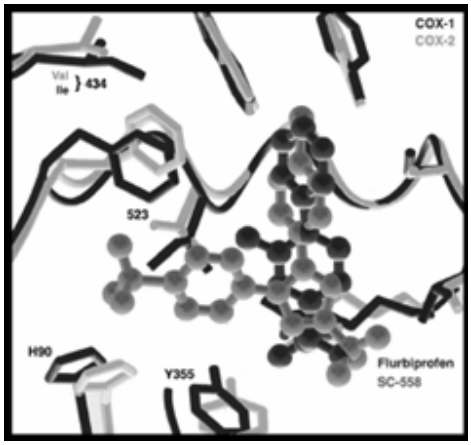

Figura 7b: Sobreposição dos sítios ativos das COX-1 (preto) e da COX-2 (cinza) ligadas a inibdores específicos: flubiprofeno (COX-1, preto) e SC-558 (COX-2, cinza). O flubiprofeno ocupa a parte superior do sítio ativo, impedindo a entrada do substrato. O inibidor seletivo da COX-2 se projeta a esquerda entrando no bolso lateral, espaço não ocupado pelo flubiprofeno.
(FITZGERALD e LOLL, 2001)

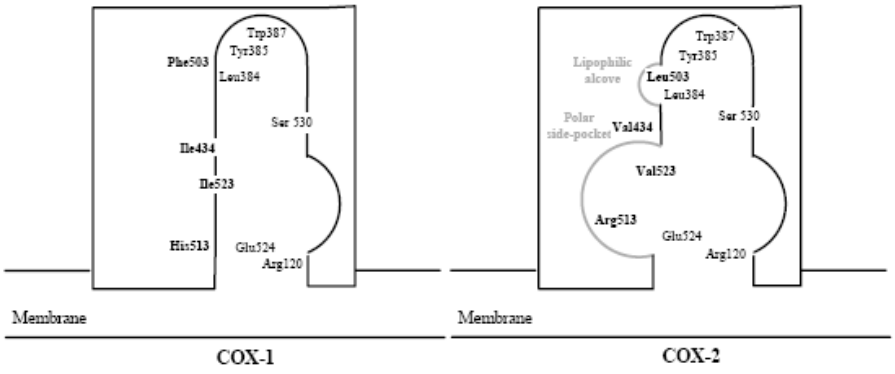

Figura 7c: Representação esquemática do sítio ativo das isoenzimas COX-1 e COX-2. A maioria dos AINEs compete com o ácido araquidônico pela ligação no sítio ativo de ambas COXs. A estrutura da COX-2 tem sido alvo de uma nova classe de fármacos mais seletivos (GAUTIER et al., 2005)

2.2.3 Modificações moleculares utilizadas no melhoramento de AINEs

Diversas modificações realizadas em AINEs clássicos os convertaram em inibidores seletivos da COX-2 ou inibidores duais COX-LOX, as quais compilam

preciosas informações no que tange à relação estrutura química e atividade biológica destes compostos antiinflamatórios. Fármacos como a indometacina e zomepirac (Figura 8) já foram manipulados com sucesso em inibidores seletivos da COX-2 (KALGUTKAR et al., 2000).

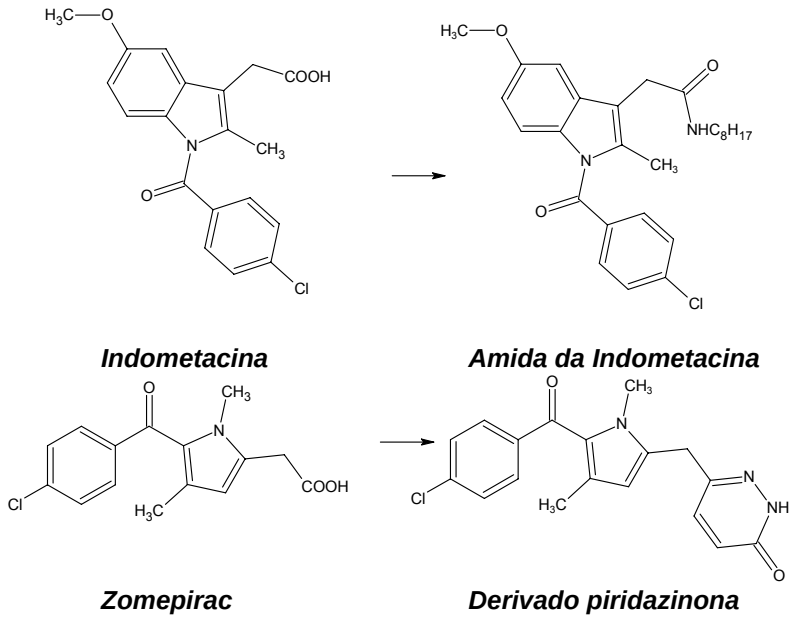

Figura 8: Fármacos inibidores da COX-2 da classe dos AINEs clássicos estruturalmente modificados. Transformação do grupamento ácido da indometacina em amida e substituição do grupo carboxílico do zomepirac por um anel piridazinona.

A substituição da função ácida de diversos fenamatos por 1,3,4-oxadiazol-2-tionas e 1,3,4-tiadiazol-2-tionas converteu estes fenamatos, inibidores das COX-1 e COX-2 em inibidores duais, atingindo ambas as COX e também a 5-LOX (Figura 9) (BOSCHELLI et al., 1992a).

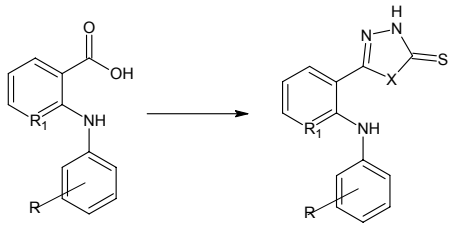

Fenamato ***Derivado oxa- ou tia-diazol***
R= Cl, F.OH, COOH X=N or S

Figura 9: Estrutura geral do fenamato e de derivados oxadiazóis e tiadiazois sintetizados por Boschelli e colaboradores (1992a)

Com o mesmo propósito de atingir as enzimas COX e LOX, Boschelli e colaboradores (1992b) prepararam derivados do tiazolidinônico do ácido meclofenâmico (Figura 10) obtendo resultados satisfatórios na atividade dual sobre as duas enzimas.

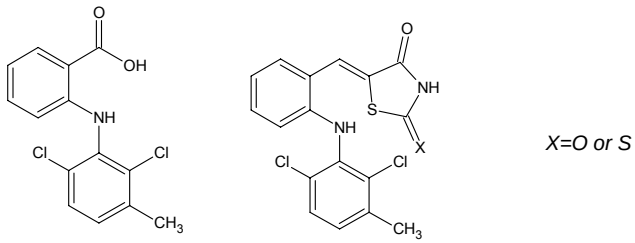

Ácido meclofenâmico ***Derivado tiazolidinônico***

Figura 10: Estruturas químicas do ácido meclofenâmico e de derivado tiazolidinônico

Derivados da indometacina tem sido modificados, formando inibidores seletivos da COX-2. O ácido 6-cloro-2-(4-clorobenzoil)-1H-indol-3-il-acético (Figura 11) foi identificado pela Pfizer Global Research e desenvolvido como inibidor seletivo da COX-2 como candidato a fármaco no tratamento da dor e doenças inflamatórias (CARON e VAZQUEZ, 2003)

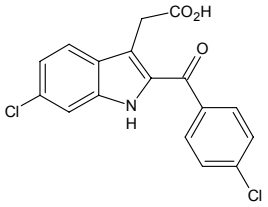

Ácido 6-cloro-2-(4-clorobenzoil)-1H-indol-3-il-acético

Figura 11: Estrutura química do derivado indólico ácido 6-cloro-2-(4-clorobenzoil)-1H-indol-3-il-acético

Com o objetivos de obter compostos duais que inibissem as enzimas COX e LOX, a substituição da função ácida carboxílica da indometacina por ácidos hidroxâmicos reversos (Figura 12) (KRAMER et al., 1992) levou a formação de compostos inibidores duais da COX e da 5-lipoxigenase (LOX).

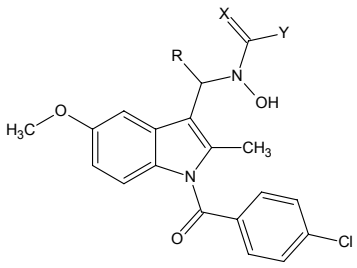

X=O or S
Y=COOH, CH_2COCH_3 or $N(CH_3)_2$

Ácido hidroxâmico reverso da indometacina

Figura 12: Estrutura geral de derivados ácido hidroxâmico reverso da indometacina (KRAMER et al., 1992).

Derivados da indometacina (Figura 13) foram estudados por Touhey e colaboradores (2002) frente às enzimas COX e também na inibição da proteína associada a múltipla resistência à drogas (MRP-1). A indometacina tem demonstrado capacidade de aumentar a citoxicidade *in vitro* de inúmeros fármacos com atividade anticâncer (incluindo doxorrubicina, daunorrubicina, epirrubicina, teniposídeo e vincristina), quando co-administrados em linhagens de células que expressam a MRP-1.

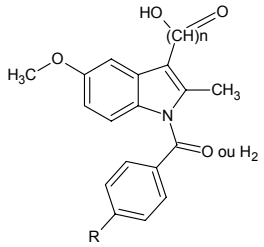

Estrutura geral de análogos da indometacina

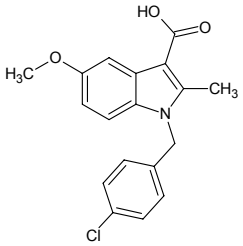

Ácido 1-(4-clorobenzil)-5-metoxi-2-metil-1H-indol-3-carboxílico

Figura 13: Estrutura geral de análogos da indometacina sintetizados por Touhey e colaboradores (2002) e composto ácido 1-(4-clorobenzil)-5-metoxi-2-metil-1H-indol-3-carboxílico, ativos gente COX-1, COX-2 e MRP-1

Frente à MRP-1, a mudança do grupamento N-benzoil por N-benzil (que permite rotação livre sobre as ligações que unem os dois sistemas arílicos) não afetaram a atividade inibitória. Para COX, os análogos N-benzoil-indometacina foram efetivos na inibição das COX-1 e COX-2, enquanto os análogos N-benzil apresentaram fraca inibição da COX-1, sugerindo que o grupo carbonila seja importante para a inibição da COX-1. Apenas o análogo ácido 1-(4-clorobenzil)-5-metoxi-2-metil-1H-indol-3-carboxílico (Figura 13) demonstrou inibição da COX-2, fraca inibição da COX-1 e forte atividade inibitória da MRP-1 (TOUHEY et al., 2002).

Utilizando a estratégia de neutralizar o grupamento ácido de AINEs com a finalidade de obter inibidores seletivos da COX-2, têm-se vários estudos com a indometacina. Kalgutkar e colaboradores (2000) obtiveram derivados ésteres e amidas da indometacina a partir da transformação do grupamento ácido da indometacina em diferentes ésteres e amidas (Figura 14) capazes de inibir a COX-2 sem inibir a COX-1. Os ésteres e amidas da indometacina inibiram a enzima COX-2 humana com concentrações de IC_{50} na faixa nanomolar (10^{-9}M), enquanto seus efeitos na COX-1 ovina foram relativamente inferiores.

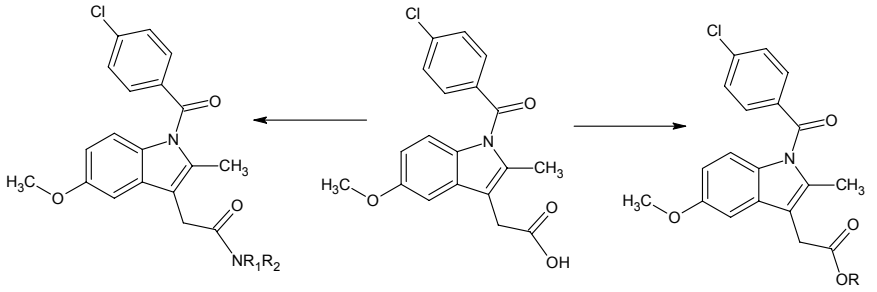

Amidas da Indometacina ***Indometacina*** ***Ésteres da Indometacina***
R= alkyl, R1= alkyl, R2= acetyl

Figura 14: Estrutura geral dos derivados amídicos e ésteres da indometacina

Compostos nos quais foram realizados a substituição do grupo 4-clorobenzoil do nitrogênio indólico por 4-bromobenzoil resultou em moléculas que mantiveram a seletividade para COX-2, assim como derivados da indometacina contendo amidas primárias e secundárias foram mais potentes na inibição da COX-2 que as amidas terciárias correspondentes (KALGUTKAR et al., 2000).

A base molecular para a seletividade apresentada por estes compostos não está esclarecida, mas parece envolver ligações de hidrogênio aos aminoácidos da região carboxilato-ligante do sítio ativo da COX. Os ésteres e amidas da indometacina não se ligam ao bolso lateral como os heterociclos diarílicos (celecoxib, p.e.) o fazem, mas poderiam romper a constrição na base do sítio ativo da COX compreendida entre os aminoácidos Arg-120, Tyr-355 e Glu-524 (Figura 15). Os grupos funcionais éster e amida projetam-se dentro de uma espaçosa cavidade no domínio membrana-liagante, chamado “lobby”. O modelo estrutural é compatível com o tamanho dos substituintes ésteres e amidas que podem ser inseridos na indometacina mantendo a seletividade para COX-2 (TIMOFEESVSKI et al., 2002).

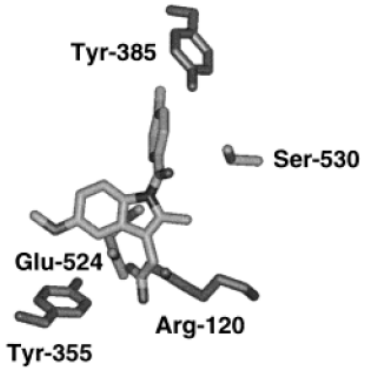

Figura 15: Estrutura da indometacina acoplada nos resíduos chave da COX-2 (KURUMBAIL et al., 1996)

A substituição do grupo carboxílico da indometacina por uma variedade de tiazóis substituídos (Figura 16), realizada por Woods e colaboradores (2001), levou a uma série de compostos potentes e inibidores seletivos da COX-2, onde tiazóis com substituintes aromáticos revelaram-se potentes inibidores da COX-2.

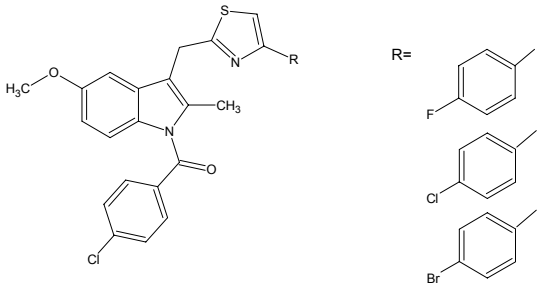

Derivado tiazol 4-substituído

Figura 16: Indometacina modificada com tiazóis substituídos

Análogos às estruturas químicas de Woods (WOODS et al*.*, 2001), derivados N-triptofil-5-arilideno-2,4-tiazolidinadionas e N-triptofil-5-arilideno-rodaninas (Figura 17) foram obtidos por Góes e colaboradores (2004) e avaliados

para atividade antiinflamatória, demonstrando-se ativos na prevenção da formação do edema de pata induzido por carragenina.

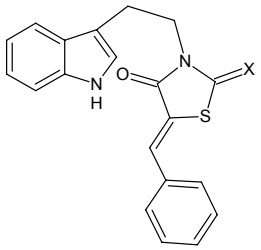

X=O : N-triptofil-5-arilideno-2,4-tiazolidinadionas
X=S : N-triptofil-5-arilideno-rodaninas

Figura 17: Estrura química dos derivados N-triptofil-5-arilideno-2,4-tiazolidinadionas e N-triptofil-5-arilideno-rodaninas

Recentemente, nosso grupo de pesquisa desenvolveu a síntese de um novo derivado indol-4-tioxotiazolinona (LPSF-LYS5) (Figura 18) com relevante atividade antiinflamatória (SANTOS et al., 2005), o qual, em estudos de docking na COX-2, apresentou favoráveis valores de energia de ligação (LEITE et al., 2005).

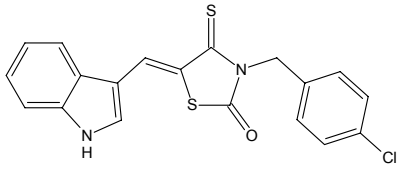

(5)-3-(4-clorobenzil)-5-(1H-indol-3-ilmetileno)-4-tioxo-tiazolidin-2-ona (LPSF-LYS5)

Figura 18: Estrutura química do (5)-3-(4-clorobenzil)-5-(1H-indol-3-ilmetileno)-4-tioxo-tiazolidin-2-ona LPSF-LYS5

2.3 Agonistas do PPAR-γ

Os ligantes endógenos já identificados do PPAR-γ incluem inúmeros ácidos graxos, eicosanóides, prostaglandinas e seus metabólitos. Considerados ligantes

de fraca afinidade, a concentração necessária dos ácidos graxos para ativação do PPAR-γ são consistentes com aquelas encontradas no soro humano, enquanto os ácidos graxos poliinsaturados apresentam uma maior afinidade. As tiazolidinadionas (TZDs) são ligantes sintéticos de alta afinidade do PPAR-γ, frequentemente chamadas de agonistas PPAR-γ. As TZDs são utilizadas como agentes sensibilizadores de insulina no tratamento do Diabete tipo 2 (WILLSON et al., 2000) e estes foram os primeiros compostos identificados como receptores de alta afinidade pelo PPAR-γ . Duas TZDs encontram-se atualmente com utilização terapêutica, a rosiglitazona e a pioglitazona (Figura 19).

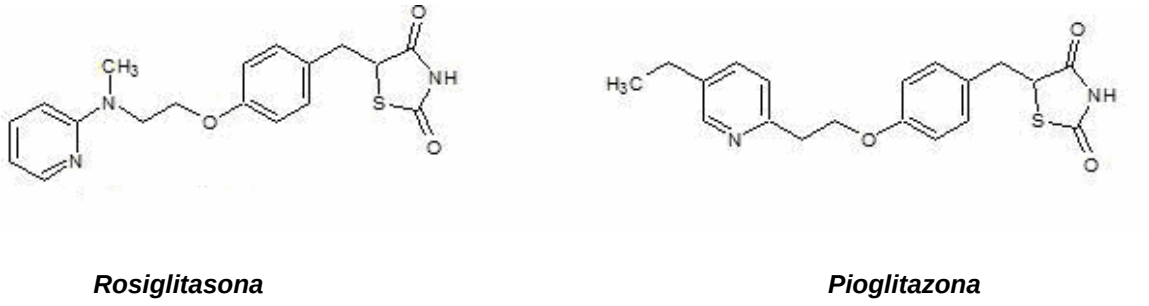

Rosiglitasona ***Pioglitazona***

Figura 19: Estrutura química dos agonistas do PPAR-γ que são comercializados: rosiglitazona e pioglitazona

2.3.1 Propriedades estruturais do PPAR-γ e modificações moleculares nos agonistas

Estruturalmente o PPAR-γ tem um grande bolso de ligação que acomoda ligantes lipofílicos pertencentes a diversas classes químicas, entre elas as TZDs (DUBUQUOY et al., 2006). Os estudos das ligações entre os agonistas dos PPARs (todos os subtipos) revelam que os agonistas, tais como TZDs, fibratos e ácidos graxos formam o mesmo tipo de ligação, no qual a cabeça acídica participa

de uma rede de ligações de hidrogênios no bolso de ligação, o qual inclui um resíduo de tirosina essencial, que fica localiza na porção C-terminal da hélice AF-2 (Figura 20) (NOLTE et al., 1998).

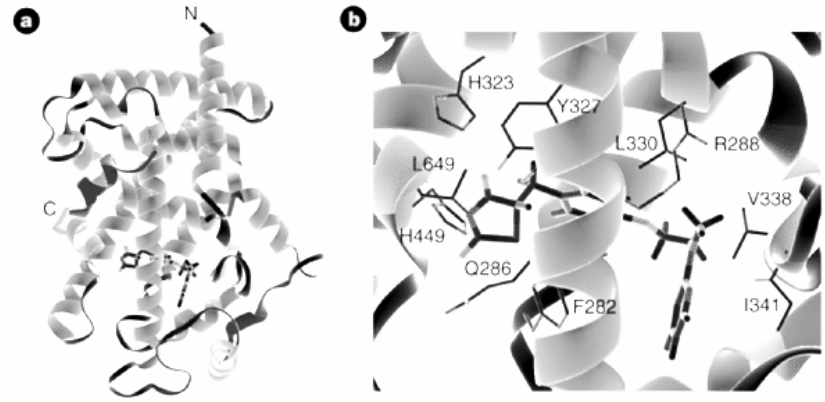

Figura 20 : **a)** Representação esquemática da estrutura terciária do PPAR-γ (fitas). Em vermelho, os resíduos que formam o "charged clamp". A rosiglitazona (palitos) aparece ligada por uma rede de interações polares na cavidade do domínio AF-2. **b**) Estrura secundária, enfocando os aminoácidos envolvidos na ligação com a rosiglitazona. Os átomos estão assim representados: carbono (verde), oxigênio (vermelho), nitrogênio (azul) e enxofre (amarelo) (NOLTE et al., 1998).

Tem sido demonstrado que estes agonistas podem ser divididos em três partes (Figura 21). A parte A, é uma cabeça lipofílica, a parte C é uma cauda hidrofóbica, e a parte B é a porção da molécula que faz a ligação entre A e C. A parte A revela a necessidade da formação de ligações de hidrogênio, conseguida através de grupamentos hidrofílicos como a porção tiazolidinônica das TZDs. Os ligantes da parte C contém um anel aromático hidrofóbico, que pode possuir uma diversidade muito grande de substituintes sem perder a capacidade de ligação. De acordo com a estrutura de raio-X do PPAR-γ, a parte C fica localizada na entrada do sítio de ligação e como esta entrada é bastante flexível, é compreensível que esta porção da molécula comporte tamanha diversidade estrutural (CHEN et al, 2005).

A estrutura cristalográfica do PPAR-γ mostra que o sítio ocupado pela parte B é um canal plano. Desse modo, fragmentos planares rígidos são seus melhores ligantes. De fato, a otimização de ligantes nesta porção do receptor mostra preferência por anéis planares de cinco ou seis membros (CHEN et al., 2005).

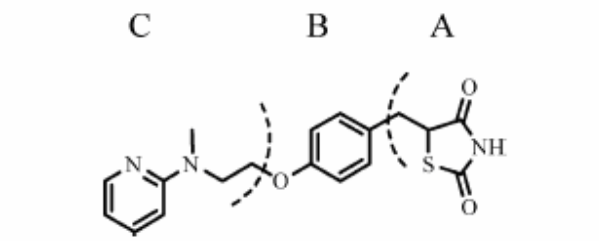

Figura 21: Estrutura comum aos agonistas do PPAR-γ e divisão em parte A (cabeça hidrofílica), B (linker) e C (cauda lipofílica) (CHEN et al., 2005).

Enquanto está claro como as TZDs se ligam ao PPAR-γ , ainda não está esclarecido se os efeitos adversos dessa classe de moléculas são causados pelo mecanismo de ação dessas, ou se são oriundos da estrutura química tiazodolidônica que é comum a essa classe (CHEN et al., 2005).

Visando evitar a recemização que ocorre com derivados TZDs em condições fisiológicas, uma série de ácidos α-alcóxi-β-fenilpropanóico, tais como o derivado carbazólico, foi sintetizada (Figura 22). Nestes compostos foram combinados elementos estruturais da rosiglitazona com a classe dos ácidos alcóxipropanóicos, que são sensibilizadores de insulina que possuem tendência reduzida à racemização. Estudos de SAR realizados nessas estruturas concluíram que uma grande cauda lipofílica confere melhor resultado, uma vez que habilita ao composto a capacidade de inibir dualmente o PPAR-γ e o PPAR-α (MORPHY e RANKOVICK, 2005).

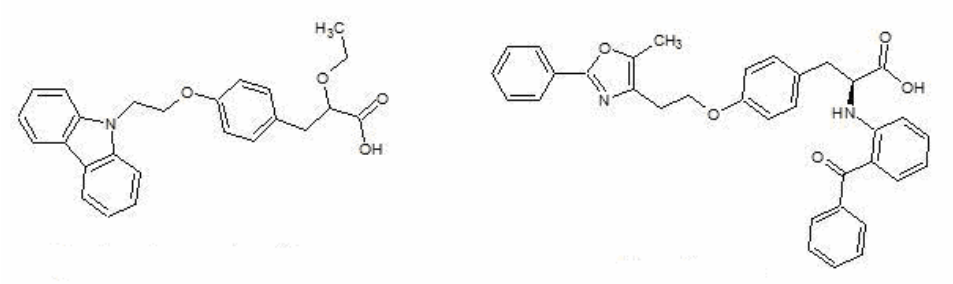

Ácido 3-((9H-carbazol-il)-4-(etóxifenil))-propanóico ***Farglitazar***

Figura 22: Estruturas químicas do derivado alcóxi-propanóico e do farglitazar

Utlizando a tirosina como base de suas estruturas, compostos como farglitazar (Figura 22) estão em fase de desenvolvimento. O farglitazar é até o momento o agonista mais potente já encontrado, apresentando potente redução de gllicemia, redução de triglicerídeos e elevação do colesterol HDL em pacientes portadores de Diabetes (FIEDOREK et al., 2000). Sua estrutura já foi docada no PPAR-γ, e esta ligação se dá no mesmo sítio onde as TZDs ocupam (Figura 23) (MARSHAL, LEE e MARSHAL, 2006).

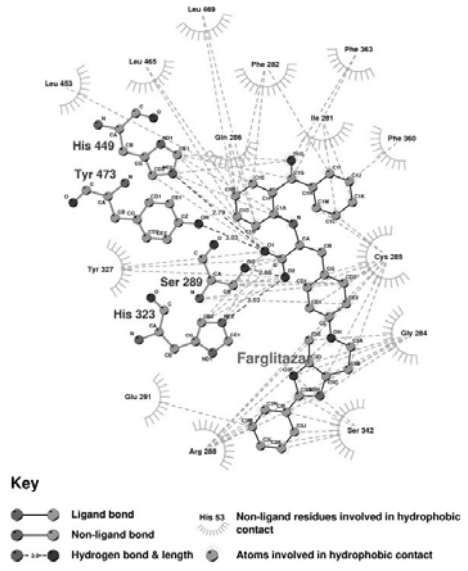

Figura 23: Farglitazar ancorado no domínio ligante do PPAR-γ . Os resíduos envolvidos nas ligações de hidrogênio estão detalhados (MARSHAL, LEE e MASRSHAL, 2006.).

Lehman e colaboradores (1997) demonstraram que AINEs, como indometacina, ácido flufenâmico e fenoprofeno são agonistas ativadores dos PPAR-γ e PPARα, sendo a indometacina o mais potente ativador do PPAR-γ .

Recentemente, foram publicados estudos demonstrando as evidências químicas, biológicas e farmacológicas de que aminosalicilatos são ligantes sintéticos do PPAR-γ em células epiteliais do cólon. O ácido 5-amino salicílico (5-ASA) (Figura 24) é um dos antiinflamatórios mais antigos utilizados na doença inflamatória intestinal crônica, mas seu mecanismo de ação permanece desconhecido. Simulações do docking do 5-ASA no PPAR-γ revelaram que o modo de ligação é similar à orientação da cabeça tiazolidinônica (parte A) da rosiglitazona. O 5-ASA encaixa-se no domínio de ligação via ligações de hidrogênio com os resíduos His-323, His-449, Tyr-473, e Ser-289, considerados pontos determinantes para o reconhecimento molecular e ativação do PPAR-γ (Figura 24) (DUBOQOUY et al., 2006).

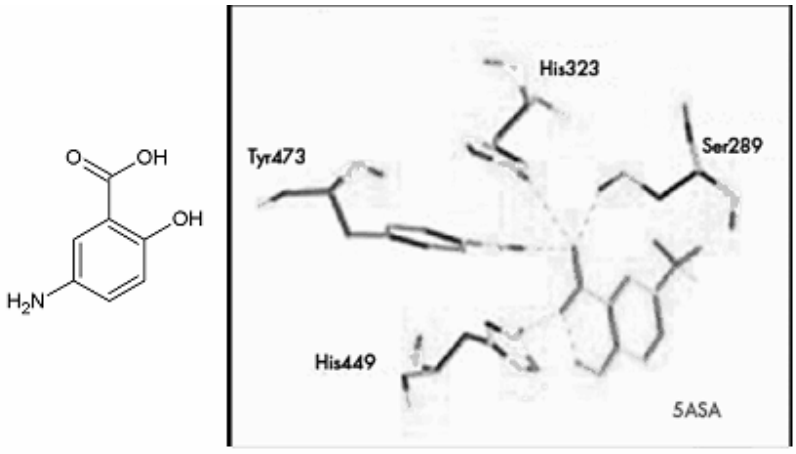

Figura 24: Estrutura química do ácido 5-amino salicílico (5-ASA) e representação esquemática da sua ligação (verde) no domínio ligante do PPAR-γ , formando ligações de hidrogênio com os resíduos His-323, His-449, Tyr-473 e Ser-289, de forma análoga às TZDs (DUBOQOUY et al., 2006).

2.4 Estratégias para o design de ligantes múltiplos

Existem duas estratégias principais através das quais podem ser iniciados os estudos de compostos com capacidade de ligação múltipla. Uma delas se baseia no “screening” através de “high-troughpout screening” (HTS), e a outra no conhecimento prévio. No HTS de grandes bibliotecas de compostos, aqueles que apresentaram qualquer atividade frente ao primeiro alvo, serão testados frente ao segundo. O conhecimento prévio utiliza dados anteriormente obtidos para fármacos, ou outros compostos químicos já conhecidos, seja na literatura ou em banco de dados (MORPHY e RANKOVIC, 2005).

Neste cenário, dois compostos que são ativos nos seus respectivos alvos são utilizados como ponto de partida (Figura 25). Para incorporar em uma única molécula os requisitos estruturais que resultem em atividade nos dois alvos, elementos estruturais particulares de cada um dos ligantes são combinados.

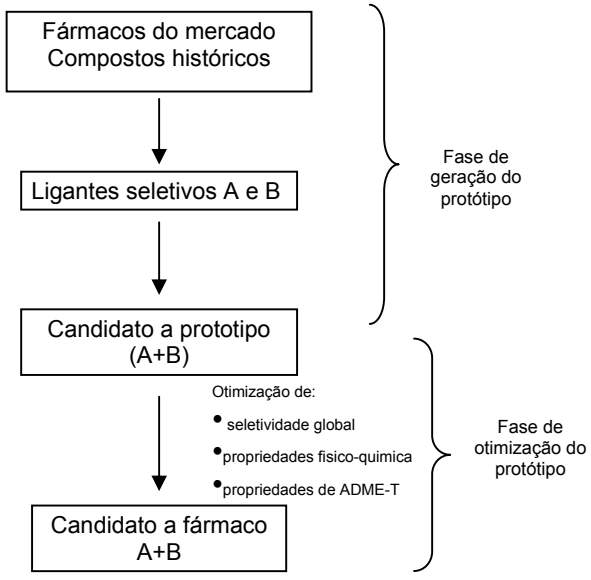

Figura 25: Etapas no desenho de ligantes em dois alvos (adaptado de MORPHY e RANKOVIC, 2005).

O sucesso quando se objetiva alcançar dois alvos que pertencem filogeneticamente a diferentes superfamílias é reconhecidamente mais difícil. Entretanto, moléculas que acomodam grupamentos farmacofóricos múltiplos vêm sendo descritas. Um exemplo foi descrito por Kogen e colaboradores (2003) onde foi obtida a combinação para inibir a acetilcolinestarase (AChE) e o transportador de serotonina (SERT) para o tratamento da Doença de Alzheimer. A hibridização de dois inibidores, a rivastigmina (AChE) e a fluoxetina (SERT), seguida por otimização dos substituintes dos grupamentos carbamato e fenóxi, levou a um inibidor dual (Figura 26).

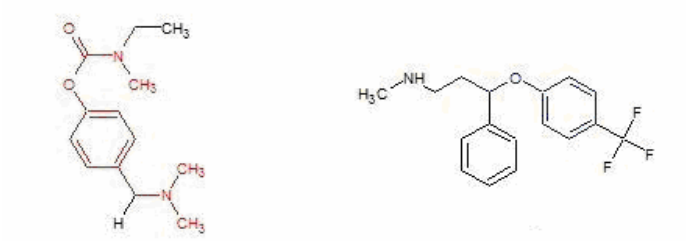

Rivastigmina ***Fluoxetina***

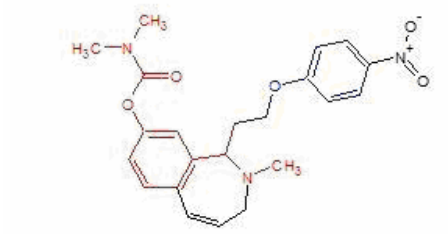

Inibidor Dual

Figura 26: Desenho de um ligante múltiplo que inibe a ACeH e o SERT, realizado a partir da revistagmina e fluoxetina

O combinatório destas informações apresentado nesta revisão nos permitiu o desenho das moléculas que será apresentado no item 4 desta tese, através da incorporação de elementos estruturais que permitam atingir as enzimas COX 2 e e também o PPAR-γ.

3 OBJETIVOS

A procura de novos e melhores fármacos antiinflamatórios, como também o melhoramento dos já existentes é essencial para o tratamento e prevenção das doenças inflamatórias, especialmente às crônicas.

Baseadas no conhecimento do papel desempenhado pelas enzimas COXs, bem como do PPAR-γ no processo inflamatório, com suas respectivas conformações espaciais singulares e regiões com características químicas particulares em seus sítios ativos, a estratégia de integração de elementos estruturais que acessem estes dois alvos envolvem a incorporação de propriedades estruturais específicas em porções distintas das moléculas de modo que as habilitem a promover interações químicas tanto com a enzima COX quanto com o PPAR-γ e, em conseqüência, desencadear os processos que conduzem a resposta biológica desejada.

A observância dos resultados experimentais e teóricos obtidos em moléculas derivadas da indometacina, somado ao conhecimento e estudo da estrutura da enzima COX-2 e de seu sítio ativo, além do sítio de ligação do PPAR, subsidiaram o desenho de novas moléculas 5-indol-tiazolidinadionas que sejam potencialmente mais ativas e seguras, o que constitui objeto deste trabalho.

3.1 Geral

- Contribuir na descoberta e desenvolvimento de novos agentes antiinflamatórios mais eficazes, menos tóxicos e com maior aceitabilidade.

3.2 Específicos

- Preparar, por síntese orgânica, novos derivados bioisostéricos 5-indol-tiazolidinônicos antiinflamatórios.
- Elucidar as estruturas químicas dos compostos sintetizados pelos métodos espectroscópicos de infravermelho, ressonância magnética nuclear de hidrogênio e espectrometria de massas.
- Avaliar a atividade antiinflamatória de moléculas 5-indol-tiazolidinadionas em modelos animais.
- Avaliar a seletividade de moléculas 5-indol-tiazolidinônicas para a enzima COX-2 dos novos derivados 5-indol-tiazolidinônicos sintetizados.
- Estudar o perfil farmacocinético da molécula mais promissora da série tiazolidinônica estudada.
- Investigar as características moleculares relacionadas à potência e seletividade por meio de estudos de docking.

4 Desenho de 5-indol tiazolidInonas visando multi-alvos no tratamento da inflamação

O desenho estrutural de novas moléculas potencialmente antiinflamatórias partiu da indometacina, uma molécula capaz de inibir as enzimas COX-1 e COX-2, e também o PPARγ, alvos pretendidos neste estudo. Foram observadas as diversas modificações realizadas em NSAIDs clássicos, assim como as estruturas de ligantes do PPARγ.

Numa primeira etapa foi analisada a inserção de grupamento tiazol na indometacina realizado por Woods e colaboradores (2001) e foi proposta a substituição do tiazol pelo núcleo tiazolidinônico, presente nas TZDs, como a rosiglitazona.

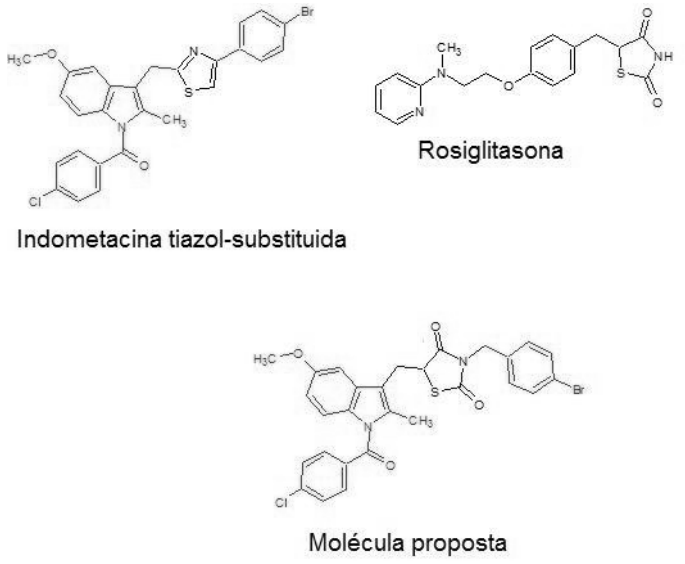

Figura 27: Hipótese para pesquisa e desenvolvimento de moléculas com atividade dual: incorporação na estrutura base da indometacina o anel tiazolidinadiônico da rosiglitazona

Considerando o sucesso obtido anteriormente por nosso grupo de pesquisa com moléculas similares, propôs-se a retirada do grupamento N-benzoil, e dos substituintes metil e metóxi da indometacina, chegando-se na molécula básica. Por conveniência de metodologia sintética, uma vez que o custo do processo sintético também deve ser avaliado no processo de descoberta de novos fármacos, a ligação entre o grupamento indol e a tiazolidina-2,4-diona foi adequadamente substituída por uma ligação dupla.

A molécula matriz aqui representada foi dividida nas porções A, B e C, recebendo modificações moleculares que se construíram *(i)* de inserções de átomos volumosos, como bromo, na porção A, e a substituição do NH indólico por um N-acetil; *(ii)* de um aumento no espaçamento entre B e C, introduzindo-se uma carbonila, a qual também confere à molécula uma maior hidrofilicidade na porção B; e *(iii)* finalmente, foram testadas na porção C diversas substituições em diferentes posições com grupamentos tanto retiradores como doadores de elétrons (Figura 28).

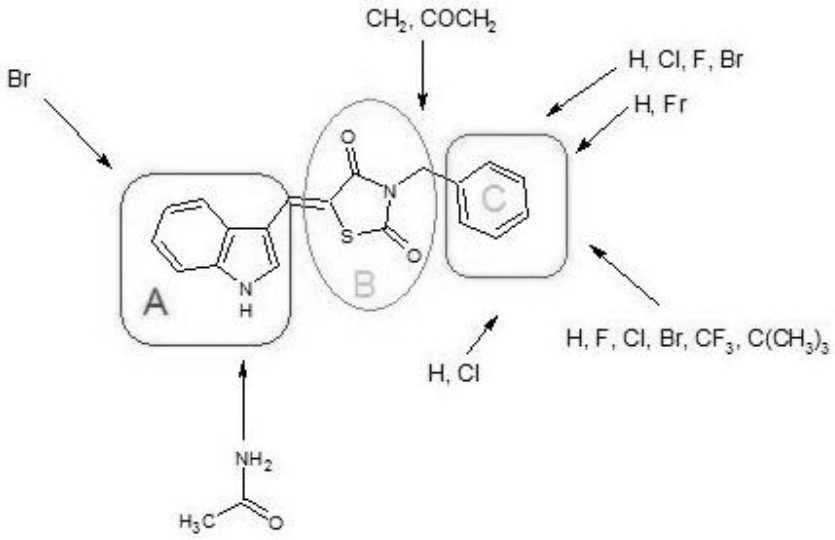

Figura 28: Hipótese para a descoberta e desenvolvimento de moléculas antiinflamatórias: posições das modificações moleculares propostas para série 5-indol-tiazolidinadiônicas

Artigo 1

Novel 5-indol-thiazolidinedinones: synthesis and anti-inflammatory evaluation

O artigo encontra-se no formato para submissão do Journal of Enzymatic Inhibition and Medicinal Chemistry (ISSN: 1475-6366; Fator de Impacto 2006: 1,636).

Novel 5-indol-thiazolidinedinones: synthesis and anti-inflammatory evaluation

Flávia De Toni Uchôa, Pedro Canuto Vieira da Costa, Leila Cabral dos Santos, Teresinha Gonçalves da Silva, Maria do Carmo Alves de Lima, Suely Lins Galdino, Ivan da Rocha Pitta*

Departamento de Antibióticos – Universidade Federal de Pernambuco

Av. Prof. Moraes do Rego, S/N - Recife-PE. CEP 50.670-901

*ivan.pitta@pesquisador.cnpq.br

Novel 5-indol-thiazolidinedinones: synthesis and anti-inflammatory evaluation

A series of new 5-indol-thiazolidinones **13a-z'** was synthesized in order to obtain a new prototype of anti-inflammatory drugs, designed with hybrid features to bind cyclooxygenase (COX) and also activate peroxisome proliferator-activated receptor sub-type gamma (PPAR-γ). The anti-inflammatory activity was evaluated by inhibition of leukocyte migration in mice air pouch model and *in vitro* enzymatic inhibition studies were also performed. This study has led to molecules with interesting anti-inflammatory activity that were evaluated in terms of structure-activity relationship.

Keywords: thiazolidinones, anti-inflammatory, COX-2.

1. Introduction

In drug discovery, it has been considered the idea that treatment is applied to human as a complex biological system, composed by cells and tissues, networked by redundant, converging and diverging signalizing pathways. Thus, better results are obtained when responses are evocated by multipoint intervention, in more than one mechanism and in different targets [1]. According to Csermelin, Agoston e Pongron [2] , partial inhibition of two or more targets is more efficient in pathology resolution than total inhibition of a single target. In this field, it is situated the concept of multi-target drugs, also known as dual or symbiotic [3].

Symbiotic compounds can be classified by its action on molecular target. The first classified group is for those molecules that act on separate targets to generate combined effect, by inhibition on different target in same pathway; by different target in different pathways within the same cell, or in different target in different tissues. On the second classified group, modulation on first target facilitates action of the second target. On the third, compound acts in different sites into the same target [4].

Successful multitarget drugs have already been obtained, as duloxetine, an antidepressant that acts in serotonin and norepinephrin uptake [5].

In inflammation treatment, the multitarget concept is well applicable. Inflammation is a complex, non-specific and coordinated response to an injury. This process involves vascular permeability, blood cell migration and plasma extravasations to damaged tissues. First inflammatory mediators are adhesion molecules, which are determinant to leukocyte migration to vessel lumen.

Leukocyte migration initiates complex reactions which are controlled by intracellular messengers [6].

Important and well described messengers are the prostaglandins, which are araquidonic acid metabolites from cyclooxygenase, an enzyme presented in at least two isoforms (COX-1 and COX-2). COX-1 and COX-2 have distinct expression, regulation and physiologic function. COX-1 is present in most tissues and is responsible for physiological function as gastric mucosal maintenance, and COX-2 is present mainly in inflammed tissues. Non-steroidal anti-inflammatory drugs (NSAIDs) act in both isoforms and anti-inflammatory effects are attributed to COX-2 inhibition, while gastrointestinal undesired effects are attributed to COX-1 inhibition [7].

From 1990 anti-inflammatory therapy started to use COX-2 inhibitors, but after 2005 some of these compounds were retrieved from market due to cardiovascular risks [8]. Now, they are carefully prescribed but non selective inhibitors, as NSAIDS, remains as first choice therapy to inflammatory conditions [9].

Indomethacin, a classical NSAIDs has been described as capable to bind besides COX enzymes, the nuclear peroxisome proliferator-activated receptors (PPARs) [10], which are involved in several cell functions that includes inflammatory response regulation. Pro-inflammatory proteins, such as chemokines, chemokines receptors and adhesion molecules are inhibited by PPARs agonists, as rosiglitazone **1** (Figure 1) [11].

Indomethacin **2** (Figure 2) is considered a prototype to COX-2 selective inhibitors, due to chemical structure flexibility by functional groups manipulations [12]. 6-choloro-2-(4-chlorobenzoyl)-1*H*-indol-acetic acid **3** (Figure

2) was identified by Pfizer Global Research as COX-2 selective inhibitor [13]. By NSAIDs acid function neutralization, Kalgutkar and co-workers [14], obtained indomethacin esthers **4** and amides **5** (Figure 2) capable to inhibit COX-2 without inhibiting COX-1, with a COX-2 IC_{50} in namomolar range.

SAR studies from these indomethacin derivatives demonstrated that when 4-chlorobenzoyl group at indolic nitrogen was replaced by a 4-bromobenzoyl group, COX-2 selectivity was conserved and derivates containing primary and secondary amides were more potent in COX-2 inhibition than corresponding tertiary amides [14].

Aromatic-thiazoles were replaced in carboxylic moiety from indomethacin **6** (Figure 2) by Woods and co-workers [15], and compounds from this series were COX-2 potent and selective inhibitors. Similar to those, N-trypyofil-5-arylidene-2,4-thiazolidinediones **7** and N-tryptofil-5-arylidene-rhodanine **8** (Figure 2) were obtained and evaluated to anti-inflammatory activity, exhibiting activity in carrageenin induced rat paw edema [16].

Our group recently published the synthesis of (5)-3-(4-chlorobenzyl)-5-(1*H*-indol-3-ylmethylene)-4-thioxo-thiazolidin-2-one (LYS5) **9** (Figure 2) which exhibited interesting anti-inflammatory activity [17]. The chemical structure of LYS5 has hybridization chemical features, in which same molecule, indolic moiety from indomethacin **2** is attached to a central thiazolidinonic ring, the PPAR-gamma activator pharmacophoric group in agonists as rosiglitasone **1** (Figure 3).

Optimizing this promising compound, a chemical series of 27 new indol-2,3-thaizolidinones compounds were synthesized **13a-z'.**

2. Results and Discussion

2.1 Chemistry

New 5-indolthiazolidinones were obtained by synthetic route presented at Figure 4. Starting reagent was thiazolidin-2,4-dione **10** which was reacted with aryl halides in basic medium to obtain N-benzylated intermediates **11a-n** (Table 1). Laterally, ethyl-2-cyane-3-indol-acrylates **12a-c** (Table 1) were synthesized by Knoavenagel condensation between different indol-3-carbaldheydes and ethyl cyaneacetate. As a final step, a Michel type addition was performed reacting N-benzyl intermediates **11a-n** with ethyl-2-cyane-3-indol-acrylates **12a-c**, forming final 5-indol-3-benzyl-2,4-thiazolidinediones compounds **13a-z'** (Table1). ^{1}H NMR analysis revealed that 5-indol-thiazolidinediones were isolated in a single isomer form. X-ray crystallographic studies and ^{13}C NMR have demonstrated preference to Z configuration for 5-arylidene-thiazolidinones [17]. Compound **13x** was analyzed by LC/MS/MS and presented both isomers in a 77:23 ratio. Preference to Z configuration was confirmed by configurational analysis of **13x** by AM1 method [18] available in the BioMedCache software [BioMedCAChe version 6.1, Copyright ©2000-2003 Fujitsu Limited, Copyright©1989-2000, Oxford Molecular Ltd.,http:///www.CACheSoftware.com], using internal default settings for convergence criteria. Chemical shifts listed in experimental part are those of the Z isomer, which is the prevalent isomer. MS data, by ESI method, fully agree with proposed structures, having M-H, M+H or M+22 ion peak.

2.2 Air pouch model

Compounds **13e, 13f, 13j, 13i, 13q** and **13y** were tested for anti-inflammatory activity by air pouch model, as previously described by Klemm, Harris e Parretti

[19] using carrageenin as inflammatory stimulus [20] where leukocyte migration is proportionally related with inflammatory response. Results obtained are described in Table 2. Compounds **13e** and **13q** did not present expressive anti-inflammatory activity in tested doses. At highest tested dose (50mg/kg), they presented only 14,0 ± 5,34 e 36,7± 10,0 % inhibition, respectively. Compound **13i** was tested only with 3mg/kg dosis and revealed more then 50% of leukocyte migration inhibition, which could be considered a promising result. At the same dose, **13j** exhibited 52,0 ± 7,6% anti-inflammatory activity, and at higher doses, lead to diminished activity. This particular behaviour could be result of compound low solubility in physiological fluids, leading to poor absorption when higher concentrations of **13j** were presented.

Best results were obtained with **13f** and **13y.** At all tested doses they presented results about 60-70%, without activity increment when doses were raised, suggesting that maximum effect could have been already reached. Poor absorption due low solubility, as suggested to **13j,** also should be considered.

Comparing 5-indol-thazolidone compounds with standard anti-inflammatory drugs, we observed that some, as **13f** and **13y** performed similar results, showing series interesting potential.

2.3 COX-1 and COX-2 *in vitro* inhibition

COX-1 and COX-2 inhibition by **13e, 13t, 13u, 13z, 13f, 13y, 13j, 13g, 13i** and **13k** at 0,01, 1, and 10 μM was evaluated *in vitro* by an indirect method where the oxidation of the peroxidase co-substrate N,N,N',N'-tetramethyl-*p*-phenylenediamine (TMPD) forms a blue compound that reflects the rate of

conversion of arachidonic acid to PGH_2, firstly described by Kulmacz and Lands [21]. Results are reported in Table 3.

COX inhibition revealed that **13f, 13g, 13i** and **13j** were weak COX-1 and COX-2 inhibitors, exhibiting slightly preference to COX-1. Thiazolidinone **13y** was also a weak inhibitor to both COXs, but it was the only tested compound that inhibited slightly preference to COX-2. Compounds **13k, 13t, 13u** and **13z** inhibited only COX-1 isoform, and **13e** did not inhibit both COXs in tested doses, which is compatible with *in vivo* results, where **13e** exhibited weak anti-inflammatory properties.

In vitro results confirm anti-inflammatory results obtained *in vivo*, where higher COXs inhibitions rates were presented by **13f** and **13y,** same compounds that presented higher leukocyte migration inhibition. But it is important to note that maximum inhibition results obtained, with higher concentration (10μM), was not so expressive as *in vivo* results. As inflammatory response is a process derived from several different mediators pathways, there is a strong suggestion that *in vivo* results were reached by compounds action not only in COX pathway, and this possibility should be further investigated.

Structurally **13f,** the most active and potent tested compound in air pouch model, presented a replacement by an hydrogen to a bromo in indolic ring, and this is the only difference between **13f** and **13e.** Thiazolidinone **13e** were not COXs inhibitor and also didn't show expressive *in vivo* results. This structural feature provides and increased hydrophobicity and it could be responsible for the increased activity.

Comparing **13f** with **13y,** another compound with expressive results, the only structural difference is the distance between thiazolidinic and bezylic ring, which

is enlarged by a carbonyl group in **[13y]** structure. The presence of a carbonyl group results in larger distance between rings, additional hydrogen bond site and additional rotation possibility. However, these features did not change inflammatory activity between **13f** and **13y**. Analysing all tested compounds, difference in benzylic group led to some difference in activity, but data obtained didn't reveal a relationship and more studies should be done to establish that.

3. Conclusions

A 5-indol-thiazolidinone series was successfully obtained and, from this series, **13f** and **13y** compounds were the most active ones. The weak COXs inhibition from series compounds but strong suppression in inflammatory response, indicate that those molecules could be acting in more than one inflammatory mechanism, which should be investigated. Compounds optimization aiming better solubility in physiological fluids should be done.

4. Experimental

4.1 Chemistry

Chemical reagents were purchased from Merck (Germany) and Sigma-Aldrich (USA), and solvents from Vetec (Brazil). Reactions were monitored with analytical thin layer chromatography (TLC) in EM silica gel 60 F254 plates and visualized under UV (254 nm). Flash column chromatography was performed using Merck silica gel 60 (230-400 mesh). Melting points were determined on a Quimis 340 capillary melting point apparatus and were not corrected. The infrared spectra were recorded as KBr discs using a BRUKER (IFS 66) infrared spectrophotometer. 1H NMR spectra were recorded on a UNITYplus – 300 MHz – VARIAN spectrometer at 20 °C. Chemical shifts (δ ppm) were assigned

according to the internal standard signal of tetramethylsilane in $DMSOd_6$ (δ = 0 ppm). Coupling constants (J) are reported in Hz. Splitting patterns are described by using the following abbreviations: s, singlet; d, doublet; t, triplet; q, quartet; m, multiplet. ^1H NMR spectra are reported in this order: chemical shift; multiplicity; number(s) and type of proton and coupling constant(s). Mass spectra with ESI mass spectra were obtained on a Waters/Micromass. (Manchester, UK) ZQ mass spectrometer. The molecular masses of the compounds were estimated from the m/z ratio of the protonated molecular ions of the formula (M+H)+ in positive ionisation mode, and deprotonated molecular ions of the formula (M-H)- in negative ionisation mode. LC/MS/MS were performed in a Shimadzu® HPLC system coupled to a mass spectrometer Micromass®, equiped with a double quadrupole and an electrospray ionization interface, operated in a negative mode using a C18 Waters Novapack®.column. Thiazolidine-2,4-dione **10** [22] and intermediates **11a** [22], **11b** [23] , **11c** [24], **11d** [25] , **11g** [23] , **11j** [26] , **11k** [27] , **11m** [28], **11n** [25] and **12a** [29] were synthesized according to the literature.

4.2 Intermediates 11a-n

Thiazolidin-2,4-dione was solubilizated in absolute ethanol and while stirred a potassium hydroxide solution was added drop by drop. Few minutes later, aryl halide was added and mixture heated at 70ºC for 4-48 hours, depending on reagent consumption velocity. Mixture was then cooled and solid formed was separated by filtration. When necessary, purification was done by recristalyzation with hot ethanol.

4.2.1 *3-(4-trifluoromethylbenzyl)-thiazolidine-2,4-dione* **11e**

MF: $C_{11}H_8F_3NO_2S$; MW: 275.24; MP: 89-90°C; Yied: 35%; IR (ν,cm^{-1}.KBr): 3417 cm^{-1}, 3007 cm^{-1}, 1753cm^{-1}, 1671 cm^{-}1; 1385 cm^{-}1; NMR^{1}H (300 MHZ, $DMSOd_6$): d(2H, benzylic) 7,733-7,705 J=8,4; d(2H, benzylic) 7,530-7,481 J=8,4; s(2H NCH_2) 4,767; s(2H, cyclic CH_2) 4,290; MS (m/z; relative intensity): 274,2 ([M-H]$^-$, 100), 143,2 (5), 116,1 (9).

4.2.2 *3-(4-tertbutylbenzyl)-thiazolidine-2,4-dione* **11f**

MF: $C_{14}H_{17}NO_2S$; MW: 263.35; MP: 110-112 °C; Yied: 86%; IR (ν,cm^{-1}.KBr): 3395 cm^{-1}, 2951 cm^{-1}, 1713 cm^{-1}, 1376 cm^{-}1; 1150 cm^{-}1; NMR^{1}H (300 MHZ, $DMSOd_6$): d(2H, benzylic) 7,367-7,339 J=8,4; d(2H, benzylic) 7,207-7,179 J=8,4; s(2H NCH_2) 4,625; s(2H, cyclic CH_2) 4,268; s(9H, *tert*-butyl) 1,251; MS (m/z; relative intensity): 286,2 ([M+Na]$^+$, 50), 281,3 (100), 264,3 (8), 147,3 (20), 117,2 (13).

4.2.3 *3-(2-chloro-6-fluorobenzyl)-thiazolidine-2,4-dione* **11h**

MF: $C_{10}H_7ClFNO_2S$; MW: 259.68; MP: 90°C; Yied: 11% IR (ν,cm^{-1}.KBr): 1681,62 cm^{-1}, 1380,72 cm^{-1}, 1337,07cm^{-1}, 970,66 cm^{-}1; NMR^{1}H (300 MHZ, $DMSOd_6$): m(2H, benzylic) 7,429-7,307; dt(1H, benzylic) 7,253-7,192; s(2H, NCH_2) 4,807; s(2H cyclic CH_2) 4,215; MS (m/z; relative intensity): 282,1 ([M+Na]$^+$, 30), 277,1 (27), 117,1 (15), 112,9 (100).

4.2.4 *3-(3-fluorobenzyl)-thiazolidine-2,4-dione* **11i**

MF: $C_{10}H_8FNO_2S$; MW: 225.23; MP: 59-60 °C; Yied:: 92%; IR (ν,cm^{-1}.KBr): 3075 cm^{-1}, 2982 cm^{-1}, 1744 cm^{-1}, 1682 cm^{-}1; 1379 cm^{-}1NMR^{1}H (300 MHZ, $DMSOd_6$): dd(2H, benzylic) 7,342-7,294 J=5,4; t(2H, benzylic) 7,197-7,137 J=9; s(2H N CH_2) 4,651; s(2H cyclic CH_2) 4,264. MS (m/z; relative intensity): 246 ([M+Na]$^+$, 10), 214 (100)

4.3 Indol-cyane acrylates **12a-c**

Aldheydes 1-H-indol-3-carbaldheyde, 5-bromo 1-H-indol-3-carbaldheyde, or 1-acetyl-indol-3-carbaldheyde and ethyl cyaneacetate were reacted using benzene as solvent and piperidin as catalyzer. Reaction mixture was heated to 110ºC during 2-24 hours. After that, reaction back to room temperature and formed solid was filtrated. **12c** was purified by column chromatography on flash silica gel (hexane / ethyl acetate = 8:2).

4.3.1 *Ethyl (2Z)-3-(5-bromo-1H-indol-3-yl)-2-cyanoacrylate* **12b**

MF: C_{14} H_{11} Br N_2 $O_{2;}$ MW: 319.15; MP: 201-204 ^{o}C; Yied: 91%; IR (ν,cm^{-1}.KBr): 3366,21 cm^{-1}, 2213,35 cm^{-1}, 1683,00 cm^{-1}, 1288,80 cm^{-}1; NMR1H (300 MHZ, $DMSOd_6$): s(1H, indol) 12,681; s(1H, indol) 8,588; d(1H, indol) 7,551-7,520 J=8,7; dd(1H, indol) 7,433-7,398 J= 8,7 e J=1,8; d(1H, indol) 7,259-7,280 J=1,8; s(1H, =CH), 8,598; q(2H, ethyl) 4,323-4,252 J=7,2; t(3H, ethyl) 1,329-1,282 J= 7,2; MS (m/z; relative intensity): 319,1 ($[M-H]^{-}$, 100), 245,1 (17), 163,2 (51), 112,0 (18).

4.3.2 *(2Z)-3-(1-acetyl-2,3-dihydro-1H-indol-3-yl)-2-cyanoacrylate* **12c**

MF: $C_{16}H_{16}N_2O_{3;}$ MW: 284.30; MP: 110-112 ^{o}C; Yied: 35%; IR (ν,cm^{-1}.KBr): 2983,00 cm^{-1}, 2216,35 cm^{-1}, 1723,62 cm^{-1}, 1238,78 cm^{-}1; NMR1H (300 MHZ, $DMSOd_6$): s(1H, indol) 8,592; d(1H, indol) 8,381-8,356 J=7,5; d(1H, indol) 8,080-8,057 J= 6,9; m(2H, indol) 7,519-7,412; s(3H, N-acetyl) 2,760; s(1H, =CH), 8,821; q(2H, ehtyl) 4,378-4,307 J=7,2; t(3H, ehtyl) 1,355-1,308 J= 7,2

4.4 5-indol-thiazolidnones **13a-z**

Equimolar amounts of N-benzylated thaizolidin-2,4-dione **11a-n** and cyaneacrylates **12a-c** were reacted using absolute ethanol as solvent and piperidin as catalyzer. Mixture was heated to 50ºC during a variable time from 15 minutes to 72 hours, depending on reagents consumption velocity. After that, solid formed was filtrated and washed with ethanol and *n*-hexane. *N*-acetyl derivatives were purified by column chromatography.

4.4.1 *(5Z)-3-benzyl-5-(1H-indol-3-ylmethylene)-thiazolidin-2,4-dione* **13a**

MF: C_{19} H_{14} N_2 O_2 S; MW: 334.39; MP: 237 ^oC; Yied: 46%, IR (ν, cm^{-1}; KBr): 3418,49 cm^{-1}, 1723,62 cm^{-1};1661,56 cm^{-1};1594,98 cm^{-1}; NMR^{1}H (300 MHZ, $DMSOd_6$): s (1H, indol) 12,196; m (2H, indol) 7,289-7,182; d (1H, indol) 7,929-7,905 J= 7,2; d (1H, indol) 7,523-7,499 J= 7,2; s (1H, indol) 7,827; s (1H, =CH) 8,223; s (2H, NCH_2) 4,840; m (5H, benzylic) 7,387-7,285;

4.4.2 *(5Z)-3-benzyl-5-[(5-bromo-1H-indol-3-ylmethylene)-thiazolidin-2,4-dione* **13b**

MF: C_{19} H_{13} Br N_2 O_2 S; MW: 413.28; MP: 224-226 ^oC; Yied: 40 %; IR (ν, cm^{-1}; KBr):: 3316,56 cm^{-1}, 1728,51 cm^{-1}, 1671,34 cm^{-1}, 1607,02 cm^{-1}, NMR^{1}H (300 MHZ, $DMSOd_6$): s (1H, indol) 12,345; dd (1H, indol) 7,388-7,353 J= 8,7 e 1,8; d(1H, indol) 7,486-7,458 J= 8,4; d (1H, indol) 8,217-8,121 J= 1,5; s (1H, indol) 7,864; s (1H, =CH) 8,250; s (2H, NCH_2) 4,843; m (5H, benzylic) 7,359-7,299; MS (m/z; relative intensity): 413,0 ($[M-H]^-$, 100), 317,1 (4), 143,2 (5), 115,2 (7).

4.4.3 *(5Z)-5-[(1-acetyl-1H-indol-3-il)methylene]-3-benzyl-thiazolidin-2,4-dione* **13c**

MF: $C_{21}H_{16}N_2O_3S$; MW: 376.42; MP: 221-222 ^oC; Yied: 4%;; NMR^{1}H (300 MHZ, $DMSOd_6$): s(3H, N-acetyl) 2,789; m (2H, indol) 7,477-7,410; d (1H, indol) 8,027-8,002 J= 8,7; d (1H, indol) 8,391-8,362 J=8,7; s (1H, indol) 7,975; s (1H, =CH) 8,165; s (2H, NCH_2) 4,870; m(5H, benzylic) 7,373-7,315; MS (m/z; relative intensity): 413,0 ($[M+Na]^+$, 100), 377,1 (21), 335,2 (21), 152,2 (32), 129,1 (76), 115,1 (62).

4.4.4 *(5Z)-3-(4-fluorbenzyl)-5-(1H-indol-3-ylmethylene)-thiazolidin-2,4-dione* **13d**

MF: $C_{19}H_{13}FN_2O_2S$; MW: 352.38; MP: 240-241 ^oC; Yied: 32,32%; IR (ν, cm^{-1}; KBr):: 3278,19 cm^{-1}; 1723,62 cm^{-1}; 1666,45 cm^{-1}; 1599,87 cm^{-1}; NMR^{1}H (300 MHZ, $DMSOd_6$): s (1H, indol) 12,227;m (2H, indol) 7,160-7,286; d (1H, indol) 7,932-7,908 J= 7,2; d (1H, indol) 7,252-7,498 J=8,1; s (1H, indol) 7,826; s (1H, =CH) 8,222; s (2H, NCH_2) 4,826; dd (2H, benzylic) 7,402-7,335 J= 8,7 e 5,7; t (2H, benzylic) 7,160-7,218 J= 9; MS (m/z; relative intensity): 351,1 ($[M-H]^-$, 100), 309,3 (5), 265,3 (10), 239,3 (9), 172,2 (9).

4.4.5 *(5EZ)-3-(4-chlorobenzyl)-5-(1H-indol-3-ylmethylene)-thiazolidin-2,4-dione* **13e**

MF: $C_{19}H_{13}ClN_2O_2S$; MW: 368.83; MP: 239-241 ^oC; Yied: 58%; IR (ν,cm^{-1}, KBr): 3259,38 cm^{-1}; 1723,62 cm^{-1}; 1666,45 cm^{-1}; 1599,87 cm^{-1}; NMR^{1}H (300 MHZ, $DMSOd_6$): s (1H, indol) 12,32;1; m (2H, indol) 7,181-7,288 J= 7,2; d (1H, indol) 7,931-7,907 J= 7,2; d (1H, indol) 7,529-7,505 J= 7,2; s (1H, indol) 7,828; s (1H, =CH) 8,223; s (2H, NCH_2) 4,830; dd (4H, benzylic) 7,443-7,330

4.4.6 *(5E)-5-[(5-bromo-1H-indol-3-il)methylene]-3-(4-chlorobenzyl)-thiazolidin-2,4-dione* **13f**

MF: $C_{19}H_{12}BrClN_2O_2S$; MW: 447.73; MP: 265 ^oC; Yied: 60 %; IR (ν,cm^{-1}, Kbr): 3389,90 cm^{-1}, 1730,77 cm^{-1}, 1671,34 cm^{-1}, 1607,02 cm^{-1}; NMR^{1}H (300

MHZ, $DMSOd_6$): d (1H, indol) 12,368-12,358 J=3; dd (1H, indol) 7,417-7,382 J= 1,8 e 8,7; d (1H, indol) 7-486-7,457 J= 8,7; d (1H, indol) 8,224-8,218 J= 1,8; s (1H, indol) 7,874-7,864 J=3; s (1H, =CH) 8,252; s (2H, NCH_2) 4,830; m (4H, benzylic) 7,45-7,329; MS (m/z; relative intensity): 447,0 ($[M-H]^-$, 100), 317,1 (15), 265,3 (7), 240,2 (7), 161,0 (9).

4.4.7 (*5Z)-5-[(1-acetyl-1H-indol-3-yl)methylene]-3-(4-chlorobenzyl)-thiazolidin-2,4-dione* **13g**

MF: $C_{21}H_{15}ClN_2O_3S$; MW: 410.87; MP: 215 ^oC; Yied: 11%; NMR^1H (300 MHZ, $DMSOd_6$): s(3H, N-acetyl) 2,790; m (2H, indol) 7,526-7,459; d (1H, indol) 8,026-8,002 J= 7,2; d (1H, indol) 8,386-8,361 J=7,5; s (1H, indol) 7,969; s (1H, =CH) 8,161; s (2H, NCH_2) 4,858; m(4H, benzylic) 7,451-7,295

4.4.8 *(5Z)-3-(4-bromobenzyl)-5-(1H-indol-3-ylmethylene)-thiazolidin-2,4-dione* **13h**

MF: C_{19} H_{13} Br N_2 O_2 S; MW: 413.28; MP: 245 ^oC; Yied: 63 %; IR (ν,cm^{-1}, KBr): 3264,27 cm^{-1}; 1721,36 cm^{-1}, 1664,19 cm^{-1}, 1599,87 cm^{-1}; NMR^1H (300 MHZ, $DMSOd_6$): s (1H, indol) 12,207; m (2H; indol) 7,240-7,178; d (1H, indol) 7,928-7,904 J= 7,2; d (1H, indol) 7,524-7,5499 J= 7,5; s (1H, indol) 7,829; s (1H, =CH) 8,220; s (2H, NCH_2) 4,810 ;d (2H, benzylic) 7,572-7,544 J= 8,4; d (2H, benzylic) 7,294-7,266 J= 8,4; MS (m/z; relative intensity): 413,0 ($[M-H]^-$, 100), 265,3 (9), 239,3 (33), 198,0 (23), 161 (11), 128,1 (52).

4.4.9 *(5Z)-3-(4-bromobenzyl)-5-[(5-bromo-1H-indol-3-ylmethylene)-thiazolidin-2,4-dione* **13i**

MF: C_{19} H_{12} Br_2 N_2 O_2 S; MW: 492.18; MP: 270 ^oC; Yied: 54 %; IR (ν,cm^{-1}, KBr): 3395,17 cm^{-1}, 1730,77 cm^{-1}, 1673,59 cm^{-1}, 1609,65 cm^{-1}; NMR^1H ($DMSOd_6$): s (1H, indol) 12,364; dd (2H, indol) 7,387-7,352 J= 8,7 e 1,8; d (1H, indol) 7,486-

7,457 J= 8,7; d (1H, indol) 8,216-8,211 J= 1,5; s (1H, indol) 7,864; s (1H, =CH) 8,247; s (2H, NCH_2) 4,812; d (2H, benzylic) 7,575-7,330 J= 8,1; d (2H, benzylic) 7,294-7,267 J= 8,1

4.4.10 *(5Z)-5-(1H-indol-3-ylmethylene)-3-[4-(trifluoromethyl)benzyl]-thiazolidin-2,4-dione* **13j**

MF: $C_{20}H_{13}F_3N_2O_2S$; MW: 402.38; MP: 232-234 ^oC; Yied: 32 %; IR (ν, cm^{-1} , KBr): 3316,56 cm^{-1}1723,62 cm-1; 1657,04 $cm^{-1;}$ 1592,72 cm^{-1}; NMR^{1}H (300 MHZ, 300 MHZ, $DMSOd_6$): s(1H, indol) 12,229; d(1H, indol) 7,506-7,531; m(2H, indol) 7,189-7,290; d(1H, indol) 7,939-7,915; s(1H, indol) 7,852; s (1H, =CH) 8,239, s (2H, NCH_2) 4,942, d (2H, benzylic) 7,755-7,728; d (2H, benzylic) 7,557-7,531; MS (m/z; relative intensity): 401,1 ($[M-H]^-$, 100), 265,3 (8), 172,2 (70), 140,2 (15).

4.4.11 *(5Z)-5-[(5-bromo-1H-indol-3-il)methylene]-3-[4-(trifluoromethyl)benzyl]-thiazolidin-2,4-dione* **13k**

MF: $C_{20}H_{12}BrF_3N_2O_2S$; MW: 481.28; MP: 230 ^oC; Yied: 47,76%; IR (ν, cm^{-1}, KBr): 3421,12 cm^{-1} ;1730,67 cm^{-1} ;1673,97 cm^{-1} ;1607,39 cm^{-1} ;NMR^{1}H (300 MHZ, $DMSOd_6$): s (1H, indol) 12,300; d(1H, indol) 7,494-7,465 J= 8,7; dd (1H, indol) 7,358-7,393 J= 8,7 e 1,8; d(1H, indol) 8,227-8,221 J= 1,8; s(1H, indol) 7,887; s (1H, =CH) 8,268; s (2H, NCH_2) 4,943; d (2H, benzylic) 7,757-7,729; d (2H, benzylic) 7,555-7,529;

4.4.12 *(5Z)-5-[(1-acetyl-1H-indol-3-yl)methylene]-3-[4-(trifluoromethyl)benzyl]-thiazolidin-2,4-dione* **13l**

MF: $C_{22}H_{15}F_3N_2O_3S$; MW: 444.42; MP: 208 ^oC; Yied: 6%; IR (ν, cm^{-1}, KBr): 1711,96 cm^{-1} ;1735,65 cm^{-1} ;1680,74 cm^{-1} ; NMR^{1}H (300 MHZ, $DMSOd_6$): m (2H, indol) 7,477-7,416, d (1H, indol) 8,031-8,007 J= 7,2, d (1H, indol) 8,388-

8,362 J= 7,8, s (2H, N-acetyl) 2,794, s (1H, indol) 7,978; s (1H, =CH) 8,174; s (2H, NCH_2) 4,966; d (2H, benzylic) 7,578-7,739 J= 7,8, d (2H, benzylic) 7,765-7,739

4.4.13 *(5Z)-3-(4-tert-butylbenzyl)-5-(1H-indol-3-ylmethylene)-thiazolidin-2,4-dione* **13m**

MF: $C_{23}H_{22}N_2O_2S$; MW: 390.49; MP: 210-213 ^oC;Yied: 15 %; IR (ν, cm^{-1}, KBr): 3297,37 cm^{-1} ;;1728,51 cm^{-1} ;1666,45 cm^{-1} ;1597,61 cm^{-1} ; NMR^{1}H (300 MHZ, $DMSOd_6$): s (1H, indol) 12,225; d (1H, indol) 7,501-7,526; m (2H, indol) 7,182-7,288; d (1H, indol) 7,909-7,933; s (1H, indol) 7,829; s (1H, =CH) 8,218; s (2H, NCH_2) 4,800; d (2H, benzylic) 7,392-7,364 J=8,4; d (2H, benzylic) 7,261-7,233 J= 8,4; s (9H, *tert*-butyl) 1,254; MS (m/z; relative intensity): 389,2 ($[M-H]^-$, 100), 172,1 (65), 140,1 (12), 138,2 (8).

4.4.14 *(5Z)-3-(2,4-dichlorobenzyl)-5-(1H-indol-3-ylmethylene)-thiazolidin-2,4-dione* **13n**

MF: $C_{19}H_{12}Cl_2N_2O_2S$; MW: 403.28; MP: 200 ^oC; Yied: 22,7%; IR (ν, cm^{-1}, KBr): 3356,80 cm^{-1} ;1728,51 cm^{-1} ;1669,08 cm^{-1} ;1595,36 cm^{-1} ; e 1569,03 cm^{-1} ;NMR^{1}H (300 MHZ, $DMSOd_6$): s (1H, indol) 10,231; d (1H, indol) 7,538-7,513; m (2H, indol) 7,211-7,277; d (1H, indol) 7,952-7,925; s (1H, indol) 7,865; s (1H, =CH) 8,238; s (2H, NCH_2) 4,896; d (2H, benzylic) 7,621-7,627 J=1,8; d (1H, benzylic) 7,343-7,315 J= 8,4; dd (1H, benzylic) 7,455-7,418 J= 2,1 e 8,7

4.4.15 *(5Z)-5-[(5-bromo-1H-indol-3-il)methylene]-3-(2,4-dichlorobenzyl)-thiazolidin-2,4-dione* **13o**

MF: $C_{19}H_{11}BrCl_2N_2O_2S$; MW: 482.17; MP: 240 ^oC; Yied: 15%; IR (ν, cm^{-1}, KBr): 3359,06 cm^{-1} ;1725,88 cm^{-1} ;1678,48 cm^{-1} ;1602,50 cm^{-1} ; NMR^{1}H (300 MHZ, $DMSOd_6$): s (1H, indol) 10,229; d (1H, indol) 7,695-7,688 J=2,1; dd (1H, indol)

7,395-7,361 J= 8,4 e 21; d (1H, indol) 7,499-7,470 J= 8,7; s(1H, indol) 7,895; s (1H, =CH) 8,265; s (2H, NCH_2) 4,892; d (1H, benzylic) 7,361-7,312 J= 8,7; dd (1H, benzylic) 7,452-7,417 J= 8,4 e 2,1; d (1H, benzylic) 7,626-7,619 J=2,1

4.4.16 *(5Z)-3-(2-chloro-6-fluorbenzyl)-5-(1H-indol-3-ylmethylene)-thiazolidin-2,4-dione* **13p**

MF: $C_{19}H_{12}ClFN_2O_2S$; MW: 386.82; MP: 220-222 ^oC;; Yied: 8,4%; IR (ν, cm^{-1}, KBr): 3244,59 cm^{-1} ;1729,49 cm^{-1} ;1668,80 cm^{-1} ;1596,83 cm^{-1} ; NMR^1H (300 MHZ, $DMSOd^6$): s (1H, indol) 9,007; d (1H, indol) 7,515-7,491 J= 7,2; m (2H, indol) 7,250-7,192 (overlaped with benzylic); d (1H, indolic) 7,912-7,888 J= 7,2; s (1H, =CH) 8,170; s (2H, NCH_2) 4,983; m (2H, benzylic) 7,450-7,329 (overlapped with indolic); m (1H, benzylic) 7,227-7,244 (overlapped with indolic); MS (m/z; relative intensity): 385,1 ($[M-H]^-$, 57), 239,2 (100), 172,2 (5), 143,2 (13), 115,1 (12).

4.4.17 *(5Z)-3-(3-fluorbenzyl)-5-(1H-indol-3-ilmethylen)-thiazolidin-2,4-dione* **13q**

MF: $C_{19}H_{13}FN_2O_2S$; MW: 352.38; MP: 218-219 ^oC; Yied: 18%; IR (ν, cm^{-1}, KBr): 3394,29 cm^{-1} ;1721,53 cm^{-1} ;1658,84 cm^{-1} ;1593,60 cm^{-1} ; NMR^1H (300 MHZ, $DMSOd_6$): s (1H, indol) 12,100; m (2H, indol) 7,182-7,129; d (1H, indol) 7,528-7,501; d (1H, indol) 7,931-7,907; s (1H, indol) 7,835; s (1H, =CH) 8,229; s (2H, NCH_2) 4,855; m (1H, benzylic) 7,447-7,372; m (3H, benzylic) 7,289-7,202; MS (m/z; relative intensity): 351,1 ($[M-H]^-$, 52), 195,1 (12), 172,2 (100), 165,2 (7), 116,1 (8).

4.4.18 : *(5Z)-5-[(5-bromo-1H-indol-3-il)methylen]-3-(3-fluorbenzyl)-thiazolidin-2,4-dione* **13r**

MF: $C_{19}H_{12}BrFN_2O_2S$; MW: 431.27; MP: 234-237 ^oC; Yied: 18%; IR (ν, cm^{-1}, KBr): 3354,29 cm^{-1} ;1729,49 cm^{-1} ;1668,75 cm^{-1} ;1605,83 cm^{-1} ; NMR^1H (300

MHZ, $DMSOd_6$): s (1H, indol) 12,200; d(1H, indol) 7,460-7,458; d(1H, indol) 7,489-7,787; s(1H, indol) 7,874; s (1H, =CH) 8,255; s (2H, NCH_2) 4,857; d (1H, benzylic) 7,354-7,360; t (1H, benzylic) 7,129-7,173; d (1H, benzylic) 7,382-7,388

4.4.19 (*5Z)-3-(2-bromobenzyl)-5-(1H-indol-3-ylmethylene)-thiazolidin-2,4-dione* **13s**

MF: C_{19} H_{13} Br N_2 O_2 S; MW: 413.28; MP: 259-260 ^oC; Yied: 60%; IR (ν, cm^{-1}, KBr): 3385,10 cm^{-1} ;1712,47 cm^{-1} ;1663,62 cm^{-1} ;1587,77 cm^{-1} ; NMR^{1}H (300 MHZ, $DMSOd^6$): s (1H, indol) 12,235 / m(2H, indol) 7,287-7,241; d (1H, indol) 7,953-7,929 J= 7,2; d (1H, indol) 7,540-7,515 J= 7,5; s (1H, indol) 7,878; s (1H, =CH) 8,251; s (2H, NCH_2) 4,579; d (1H, benzylic) 7,698-7,667 J= 8,1; t (1H, benzylic) 7,407-7,297 J= 7,5; t (1H, benzylic) 7,248-7,d(1H) 7,161-7,136 J=7,5; MS (m/z; relative intensity): 413,0 ($[M-H]^-$, 100), 265,3 (28), 255,4 (20), 172,1 (36).

4.4.20 *(5Z)-5-(1H-indol-3-ylmethylene)-3-(2-oxo-2-phenylethyl)-thiazolidin-2,4-dione* **13t**

MF: C_{20} H_{14} N_2 O_3 S; MW: 362.40; MP: 258 ^oC; Yied: 26%; IR (ν, cm^{-1}, KBr): 3382,76 cm^{-1} ;1730,77 cm^{-1} ;1699,92 cm^{-1} ;1661,9 cm^{-1} ;1595,36 cm^{-1} ; NMR^{1}H (300 MHZ, $DMSOd_6$): s (1H, indol) 12,095 / m(2H, indol) 7,302-7,192; d (1H, indol) 7,959-7,935 J= 7,2; d (1H, indol) 7,544-7,517 J= 7,2; s (1H, indol) 7,889; s (1H, =CH) 8,252; s (2H, NCH_2) 5,309; d (2H, phenylic) 8,113-8,089 J= 7,5; t (2H, phenylic) 7,639-7,588 J= 7,5; t (1H, phenylic) 7,799-7,730 J=7,5; MS (m/z; relative intensity): 361,2 ($[M-H]^-$, 30), 171,1 (100), 140,2 (50).

4.4.21 *(5Z)-5-[(5-bromo-1H-indol-3-il)methylene]-3-(2-oxo-2-phenylethyl)-thiazolidin-2,4-dione* **13u**

MF: C_{20} H_{13} Br N_2 O_3 S; MW: 441.29; MP: 248 °C; Yied: 15%; IR (ν, cm^{-1}, KBr): 3361,69 cm^{-1} ;1726,25 cm^{-1} ;1692,13 cm^{-1} ;1666,82 cm^{-1} ;1588,21 cm^{-1} ; NMR^{1}H (300 MHZ, $DMSOd_6$): s (1H, indol) 12,400; d (1H, indol) 7,400 J=8,7; d (1H, indol) 7,503-7,474 J= 8,7; s (1H, indol) 8,254; s (1H, indol) 7,927; s (1H, =CH) 8,285; s (2H, NCH_2) 5,316; d (2H, phenylic) 8,115-8,090 J= 7,5, t (2H, phenylic) 7,640-7,590 J= 7,5, t (1H, phenylic) 7,757-7,732 J= 7,5

4.4.22 *(5Z)-3-[2-(4-fluorphenyl)-2-oxoethyl]-5-(1H-indol-3-ylmethylene)-thiazolidin-2,4-dione* **13v**

MF: C_{20} H_{13} F N_2 O_3 S; MW: 380.39 ; MP: 249-250 °C; Yied: 21%; IR (ν, cm^{-1}, KBr): 3363,95 cm^{-1} ;1730,00 cm^{-1} ;1702,18 cm^{-1} ;1664,19 cm^{-1} ;1597,61 cm^{-1} ; NMR^{1}H (300 MHZ, $DMSOd_6$): s (1H, indol) 12,278; m(2H, indol) 7,298-7,190; d (1H, indol) 7,957-7,932 J= 7,5; d (1H, indol) 7,541-7,515 J= 7,8; s (1H, indol) 7,887; s (1H, =CH) 8,248; s (2H, NCH_2) 5,310; dd (2H, phenylic) 8,219-8,171 J= 8,7; t (2H, phenylic) 7,480-7,422 J= 8,7; MS (m/z; relative intensity): 379,2 ([M-H]$^-$, 100), 195,1 (81), 172,2 (41), 110,0 (8).

4.4.23 *(5Z)-5-[(5-bromo-1H-indol-3-il) methylene]-3-[2-(4-fluorphenyl)-2-oxoethyl]-thiazolidin-2,4-dione* **13w**

MF: C_{20} H_{12} Br F N_2 O_3 S; MW: 459.28 ;MP: 232 ; °C; Yied: 26%; IR (ν, cm^{-1}, KBr): 3318,81 cm^{-1} ;1728,51 cm^{-1} ;1676,23 cm^{-1} ;1592,72 cm^{-1} ; NMR^{1}H (300 MHZ, $DMSOd_6$): s(1H, indol) 12,140; dd(1H, indol) 7,365-7,400 J= 1,8 e 8,7; d (1H, indol) 7,504-7,475 J= 8,7; d (1H, indol) 8,251-8,245 J=1,8; s (1H, indol) 7,921; s (1H, =CH) 8,282; s (2H, NCH_2) 5,315; dd (2H, phenylic) 8,220-8,172 J= 5,4 e 8,7, t (2H, phenylic) 7,482-7,423 J= 8,7

4.4.24 *(5ZE)-3-[2-(4-chlorophenyl)-2-oxoethyl]-5-(1H-indol-3-ylmethylene)-thiazolidin-2,4-dione* **13x**

MF: C_{20} H_{13} Cl N_2 O_3 S; MW: 396.84 ; MP: 240 °C; Yied: 13 %; IR (ν, cm^{-1}, KBr): 3397,42 cm^{-1} ;1733,02 cm^{-1} ;1697,29 cm^{-1} ;1666,45 cm^{-1} ;1595,36 cm^{-1} ; NMR^{1}H (300 MHZ, $DMSOd_6$): s (1H, indol) 12,273; m (2H, indol) 7,301-7,187; d (1H, indol) 7,955-7,937 J= 7,2; d (1H, indol) 7,543-7,516 J= 7,5; s (1H, indol) 7,887; s (1H, =CH) 8,248; s (2H, NCH_2) 5,312; d (2H, phenylic) 8,130-8,100 J= 9; d (2H, phenylic) 7,705-7,675 J= 9; MS (m/z; relative intensity): 395,1 ($[M-H]^-$, 100), 200,2 (12), 172,2 (67).

4.4.25 : *(5Z)-5-[(5-bromo-1H-indol-3-il)methylene]-3-[2-(4-chlorophenyl)-2-oxoethyl]-thiazolidin-2,4-dione* **13y**

MF: C_{20} H_{12} Br Cl N_2 O_3 S; MW: 475.74 ; MP: 222 °C; Yied: 20% ; IR (ν, cm^{-1}, KBr): 3321,45 cm^{-1} ;1720,99 cm^{-1} ;1675,85 cm^{-1} ;1590,47 cm^{-1} ; NMR^{1}H (300 MHZ, $DMSOd_6$): s (1H, indol) 12,370; dd (1H, indol) 7,400-7,365 J= 8,7 e 1,8; d (1H, indol) 7,502-7,473 J= 8,7; d (1H, indol) 8,253-8,246 J= 2,1; s (1H, indol) 7,921; s (1H, =CH) 8,281; s (2H, NCH_2) 5,319, dd (2H, phenylic) 8,132-8,103 J= 8,7 e 1,8; d (2H, phenylic) 7,707-7,678 J= 8,7 e 1,8; MS (m/z; relative intensity): 475,0 ($[M-H]^-$, 100), 319 (6), 198,0 (19), 161,0 (18), 111,0 (19).

4.4.26 *(5Z)-3-[2-(4-bromofenyl)-2-oxoethyl]-5-(1H-indol-3-ilmethylene)-thiazolidin-2,4-dione* **13z**

MF: C_{20} H_{13} Br N_2 O_3 S; MW: 441.29 ; MP: 260 °C; Yied: 18% ; IR (ν, cm^{-1}, KBr): 3351,91 cm^{-1} ;1733,40 cm^{-1} ;1695,03 cm^{-1} ;1673,97 cm^{-1} ;1585,95 cm^{-1} ; NMR^{1}H (300 MHZ, $DMSOd_6$): s (1H, indol) 12,272; m (2H, indol) 7,258-7,152; d (1H, indol) 7,910-7,887 J= 7,2; d (1H, indol) 7,502-7,476 J= 7,5; s (1H, indol) 7,777; s (1H, =CH) 8,205; s (2H, NCH_2) 5,259; d (2H, phenylic) 8,003-7,975 J= 8,4; d (2H, phenylic) 7,845-7,806 J= 11,7; MS (m/z; relative intensity): 441,1 ($[M-H]^-$, 49), 200,2 (13), 172,2 (100), 161,0 (7).

4.4.27 : *(5Z)-5-[(5-bromo-1H-indol-3-il)methylene]-3-[2-(4-bromophenyl)-2-oxoethyl]-thiazolidin-2,4-dione* **13z'**

MF: $C_{20}H_{12}Br_2N_2O_3S$; MW: 520.19 ; MP: 226-230 ^oC; Yied: 47% ; IR (ν, cm^{-1}, KBr): 3316,56 cm^{-1} ;1728,13 cm^{-1} ;1675,85 cm^{-1} ;1587,83 cm^{-1} ; NMR^{1}H (300 MHZ, $DMSOd_6$): dd(1H, indol) 7,399-7,371 J= 1,8 e 8,4; d (1H, indol) 7,504-7,475 J= 8,7; d (1H, indol) 8,251-8,244 J=2,1; s (1H, indol) 7,920; s (1H, =CH) 8,281; s (2H, NCH_2) 5,311; d (2H, phenylic) 8,047-8,019 J= 8,4, d (2H, phenylic) 7,849-7,821 J= 8,4; MS (m/z; relative intensity): 519,0 ($[M-H]^-$, 100), 353,2 (18), 317,1 (51), 265,3 (61), 198,1 (26), 161,1 (23).

4.5 Biological

Swiss mice, male and female (30-35g) were acquired from Departamento de Antibióticos bioterium and animal experiments were conducted according to international agreements to care and use of laboratory animals and were approved by Universidade Federal de Pernambuco Animal Ethics Committe (#23076.011488/2005-35). Carrageenin was purchased by Sigma-Aldrich, Celecoxib® from Pfizer, Dexamethasone, Indomethacin e Nimesulide from DEG (Brasil), Aspirin® from Bayer, Heparin 5000 UI/mL from Roche, Ovine COX-1 and COX-2 colorimetric kit from Caymann Chemicals (Ann Arbor) and Tween® 80 from Merck (Germany).

4.6 Air pouch model

Air pouch model was done as previously described by Klemm, Harris e Parretti [18] using carrageenin as inflammatory stimulus [19]. Mice (n=10) had pouch formed in back by a sterile air injection (2.5mL), which was repeated 3 days

later. On day 6, fasted (8 hours) animals received orally test compounds **13e, 13f, 13j, 13i, 13q,** and **13y** or standard drugs one hour before carrageenin injection (1mL, 1% physiologic solution, w/v) directly into air pouch. Six hours later, animals were killed by cervical dislocation and exudate from pouchs was harvested with 3mL of phosphate buffer solution heparinizated (50 UI/mL). Exudate was diluted with Turk solution and leukocyte counted in a Newbauer chamber with optical microscope. As leukocyte migration is proportionally related with inflammatory response, animals that didn't receive treatment were considered control group in whom inflammation was established as 100%. Cell counting was statistically analyzed by variance analyse (ANOVA) with 95% confidence interval.

4.7 COX-1 and COX-2 *in vitro* inhibition

COX-1 and COX-2 inhibition by 5-indol-thiazolidinones was evaluated *in vitro* by an indirect method where the oxidation of the peroxidase co-substrate N,N,N',N'-tetramethyl-*p*-phenylenediamine (TMPD) forms a blue compound that reflects the rate of conversion of arachidonic acid to PGH_2 [20].

The test was performed using a COX inhibitor screening assay (Cayman Chemical) according to the manufacturer's protocol. Celecoxib and Indomethacin at 0,01, 1, and 10 μM were used as positive controls for COX-1 and COX-2 isoenzyme inhibition, respectively. COX-1 and COX-2 isoenzymes treated with vehicle only (DMSO) served as the negative controls (100% activity). The concentrations of **13e, 13t, 13u, 13z, 13f, 13y, 13j, 13g, 13i** and **13k** tested were 0,01, 1, and 10 μM. The 96-well plate was read in an automated microplate reader at 590 nm.

5. Acknowledgments

The authors would like to acknowledge the financial support by CNPq- Brazil. Flávia De Toni Uchôa thanks CNPq-Brazil for the individual grant.

6. References

1. BORISY, A. A., ELLIOTT, P. J., HURST, N. W., LEE, M. S., LEHAR, J., PRICE, E. R., SERBEDZIJA, G., ZIMMERMANN, G.R., FOLEY, M.A., STOCKWELL, B.R., KEITH, C.T. Systematic discovery of multicomponent therapeutics PNAS, vol. 100, p. 7977–7982, 2003

2. CSERMELIN, P., AGOSTON, V., PONGO, S. The efficiency of multi-target drugs: the network approach might help drug design TRENDS in Pharmacological Sciences, V..26, p.4, 2005.

3. MORPHY, R., RANKOVIC, Z. Designed Multiple Ligands. An Emerging Drug Discovery Paradigm, Journal of Medicinal Chemistry, V. 48, p. 21, 2005

4. ZIMMERMANN, G. R., LEHAR, J., KEITH, C.T. Multi-target therapeutics: when thewhole is greater than the sum of the parts, Drug Discovery Today, V. 12, 2007.

5. TRUCOTTE, J.E.; DEBONNEL, G.; MONTIGNY, C.; HEBERT, C.; BLIER, P.. Assessment of the Serotonin and Norepinephrine Reuptake Blocking Properties of Duloxetine in Healthy Subjects Neuropsychopharmacology, v.24, p. 511-521, 2001.

6. MASLINSKA, D., GAJEWSKI, M., “Some aspects of the inflammatory process”, Folia Neurophatologyca, v.36, p. 199-204, 1998.Vane

7. VANE JR, BAKHLE YS, BOTTING RM. Annu. Ver. Pharmacol. Toxicol. 38:97-120. 1998.

8. BROHPY, J.M., “Celecoxib and cardiovascular risks”, Expert Opinion on Drug Safety, v. 4, p-1005-1015, 2005.

9. WEILAND, H.A., MICHAELIS, M., KIRSCHBAUM, B. J., RUDOLPHI, K.A. “Osteoarthritis: na untreatable disease” Nature Reviews – Drug Dicovery, v. 4, p. 331-344, 2005.

10. LEHMANN, J.M., LENHARD, J.M., OLIVER, B.B., RINGOLD, G.M., KLIEWER, S.A., Peroxisome Proliferator-activated Receptors a and g Are Activated by Indomethacin and Other Non-steroidal Anti-inflammatory Drugs, The Journal Of Biological Chemistry, V. 272, pp. 3406–3410, 1997.

11. BLANQUART, C., BARBIER, O., FRUCHART, J.C, STAELS, B., GLINEUR, C. “Peroxisome proliferators-activate receptors: regulation of transcriptational activities and roles in inflammation” Journal of Steroid Biochemistry & Molecular Biology, v. 85, p. 267-273, 2003.

12. KALGUTKAR, A.S., CREWS, B., ROWLINSON, S.W., GARNER, C., SEIBERT, K., MARNETT, L.J. “Aspirin-like molecules that covalently inactivate cyclooxygenase-2” Science, v. 280, p. 1268-1270, 1998

13. CARON, S., VAZQUEZ, E., STEVENS, R.W., NAKAO,K., KOIKE, H., MURATA, Y. “Efficient synthesis of 6-Chloro-2-(4-chlorobenzoyl)-1H-indol-3-ylacetic acid, a novel COX-2 inhibitor” Journal of Organic Chemistry, v. 68, p. 4104-4107, 2003

14.. KALGUTKAR AS, CREWS BC, ROWLINSON SW, MARNETT AB, KOZAK KR, REMMEL RP, MARNETT, L.J. Proc. Natl. Acad. Sci. USA. 97 (2): 925-930, 2000.

15. WOODS KW, McCROSKEY RW, MICHAELIDES MR, WADA CK, HULKOWER KI, BELL RL, Bioorganic & Medicinal Chemistry Letters.. 11: 1325-1328. 2001

16. GÓES, A.J.S., ALVES, A.J., FARIA, A.R., LIMA, J.G., MAIA, M.B.S., " Síntese e atividade antiedematogênica de derivados N-triptofil-benzylideno-2,4-thiazolidinadione e N-triptofil-5-benzylideno-rodanina" Química Nova, v. 27, p. 905-910, 2004

17. SANTOS, L.C.; UCHOA, F.T.; CANAS, A.R.P.A.; SOUSA, I.A.; MOURA, R.O.; LIMA, M.C.A.; GALDINO, S.L. ; PITTA, I.R.; BARBE, J. "Synthesis and anti-inflammatory activity of new thiazolidine-2,4-diones, 4-thioxothiazolidinones and 2-thioxoimidazolidinones" Heterocyclic Communications, 11 (2): 121-128 2005.

18 DEWAR,M.J.S. ZOEBISCH,E.G. HEALY, E.F. STEWART,J.J.P. J. Amer. Chem. Soc. 107 (1985) 3902-
3909.

19. KLEMM, P., HARRIS, H.J.; PERRETI, M. "Effect of rolipram in a murine model of acute inflammation: comparison with the corticoid dexamethasone" European Journal of Pharmacology, v. 281, p. 69-74, 1995.

20. ROMANO, M., FAGGIONI, R., SIRONI, M., SACCO, S., ECHTENACHER, B., DI SANTO, E., SALMONA, M., GHEZZI, P. "Carrageenan-induced acute inflammation in the mouse air pouch model. Role of tumor necrosis factor" Mediators of Inflammation, v. 6, p.32-38, 1997.

21. KULMACZ RJ, LANDS WEM. Prostaglandins 25: 531-540, 1983.

22. AMORIM, E. L. CAVALCANTI; BRANDAO, S. S. FERREIRA; CAVALCANTI, C. O. MORAIS; GALDINO, S. LINS; PITTA, I. ROCHA; LUU

DUC, C. “Synthesis and structural study of substituted bromo- and nitrobenzyl (benzylidene) imidazolidinediones and thiazolidinediones” Annales Pharmaceutiques Francaises (1992), 50(2), 103-11.

23. BOZDAG-DUNDAR O., OZGEN O., MENTESE A., ALTANLAR N., ATLI O., KENDIB E., ERTAN R. “Synthesis and antimicrobial activity of some new thiazolyl thiazolidine-2,4-dione derivatives” Bioorganic & Medicinal Chemistry 15 (2007) 6012–6017

24. GOES, A. J. SILVA; ALVES DE LIMA, M. C.; GALDINO, S. LINS; PITTA, I. DA ROCHA; LUU-DUC, C. “Synthesis and antifungal activity of chlorobenzyl (benzylidene) thiazolidinediones and imidazolidinediones” Annales Pharmaceutiques Francaises (1991), 49(2), 92-8.

25. ALBUQUERQUE, J.F., AZEVEDO, L.C., GALDINO, S.L., CHANTEGREL, J., PITTA, I.R., LUU-DUC, C. Annales Pharmaceutiques Francaises, 1995, 53, 209.

26. BOZDAG-DUNDAR, OYA; CEYLAN-UNLUSOY, MELTEM; VERSPOHL, EUGEN J.; ERTAN, RAHMIYE, “Synthesis and antidiabetic activity of novel 2,4-thiazolidinedione derivatives containing a thiazole ring” Arzneimittel Forschung (2006), 56(9), 621-625.

27. SALAMA, HASSAN M.; LABOUTA, IBRAHIM M.; MOUSTAFA, MOHAMED A Synthesis and in vitro antimicrobial evaluation of some 5-substituted-3-phenacylthiazolidine-2,4-diones Journal of Pharmaceutical Sciences (1990), 4(1), 44-6

28. DE LIMA, J. G.; PERRISSIN, M.; CHANTEGREL, J.; LUU-DUC, C.; ROUSSEAU, A.; NARCISSE, G. Arzneim.-Forsch. Drug Res. 1994, 44, 831.

29. BRANDAO, S. S. F.; ANDRADE, A. M. C.; PEREIRA, D. T. M.; BARBOSA FILHO, J. M.; LIMA, M. C. A.; GALDINO, S. L.; PITTA, I. R.; BARBE, J. A novel way of synthesis of 1,3,5-trisubstituted-2-thioxoimidazolidinones Heterocyclic Communications (2004), 10(1), 9-14.

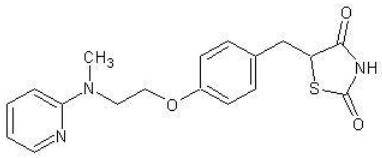

[1]

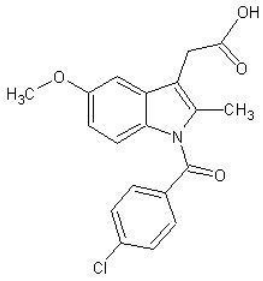

[2]

Figure 1: Rosiglitasone **1** and Indometacin **2.**

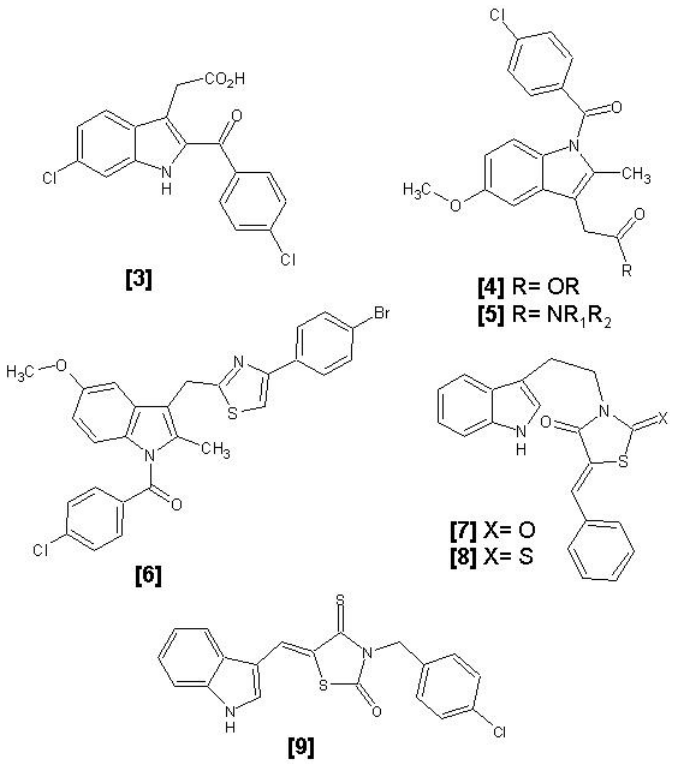

Figura 2: Chemical structure of indolic derivatives: 6-Chloro-2-(4-chlorobenzoyl)-1H-indol-3-yl-acetic acid **3**, indomethacin estheres **4**, indomethacin amides **5** aryl-thiazolic Indometacin derivatives. **6;** N-tryptofil-5-arylidene-2,4-thiazolidinadiones **7** N-tryptofil-5-arylidene-rhodanin **8** and (5)-3-(4-clorobenzyl)-5-(1H-indol-3-ylmethylene)-4-thioxo-thiazolidin-2-one (LYS5) **9.**

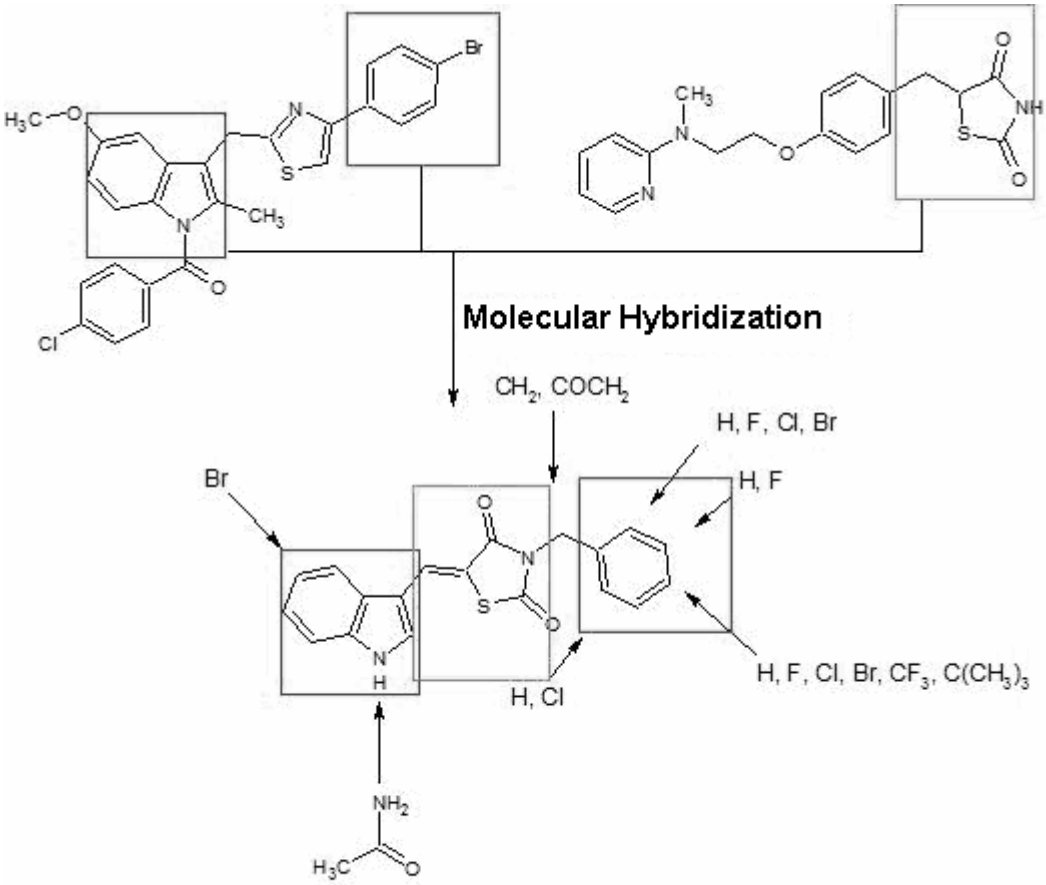

Figura 3: Molecular hybridization approach from thiazol-indomethacin and rosiglitazone that was the scaffold to 5-indolthiazolidinones **13a-z'**

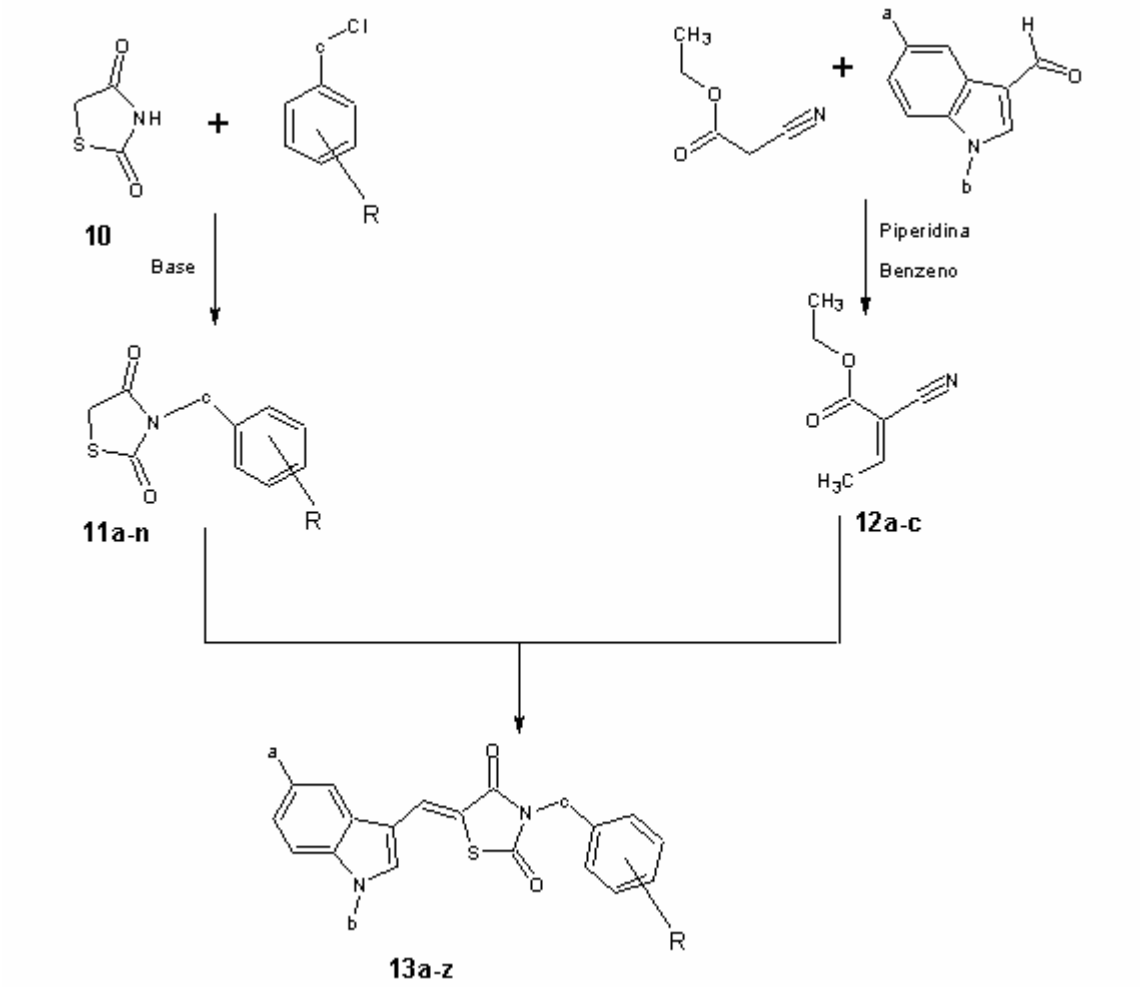

Figure 4: Synthetic route to compounds **13a-z'**. Aromatic substituted halide and thiazolidin-2,4-dione **10** reacted in basic medium to form **11a-n** that react with ethyl 2-cyano-3-indol – acrylate **12a-c** formed by substituted indol-3-carbahldeyde and ethyl cyaneacetate.

Table 1: Chemical structure of **11a-n**, **12a-c** e **13a-z'**

	Compound	a	b	c	d	e	f	g
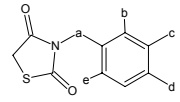 **11**	**11a**	CH_2	H	H	H	H	-	-
	11b	CH_2	H	H	F	H	-	-
	11c	CH_2	H	H	Cl	H	-	-
	11d	CH_2	H	H	Br	H	-	-
	11e	CH_2	H	H	CF_3	H	-	-
	11f	CH_2	H	H	$C(CH_3)_3$	H	-	-
	11g	CH_2	Cl	H	Cl	H	-	-
	11h	CH_2	Cl	H	H	F	-	-
	11i	CH_2	H	F	H	H	-	-
	11j	CH_2	Br	H	H	H	-	-
	11k	$COCH_2$	H	H	H	H	-	-
	11l	$COCH_2$	H	H	F	H	-	-
	11m	$COCH_2$	H	H	Cl	H	-	-
	11n	$COCH_2$	H	H	Br	H	-	-
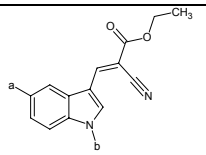 **12**	**12a**	H	H	-	-	-	-	-
	12b	Br	H	-	-	-	-	-
	12c	H	$COCH_3$	-	-	-	-	-
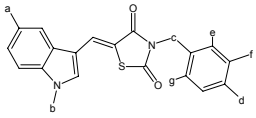 **13**	**13a**	H	H	CH_2	H	H	H	H
	13b	Br	H	CH_2	H	H	H	H
	13c	H	$COCH_3$	CH_2	H	H	H	H
	13d	H	H	CH_2	F	H	H	H
	13e	H	H	CH_2	Cl	H	H	H
	13f	Br	H	CH_2	Cl	H	H	H
	13g	H	$COCH_3$	CH_2	Cl	H	H	H
	13h	H	H	CH_2	Br	H	H	H
	13i	Br	H	CH_2	Br	H	H	H
	13j	H	H	CH_2	CF_3	H	H	H
	13k	Br	H	CH_2	CF_3	H	H	H
	13l	H	$COCH_3$	CH_2	CF_3	H	H	H
	13m	H	H	CH_2	$C(CH)_3$	H	H	H
	13n	H	H	CH_2	Cl	Cl	H	H
	13o	Br	H	CH_2	Cl	Cl	H	H
	13p	H	H	CH_2	H	F	H	Cl
	13q	H	H	CH_2	H	H	F	H
	13r	Br	H	CH_2	H	H	F	H
	13s	H	H	CH_2	H	Br	H	H
	13t	H	H	$COCH_2$	H	H	H	H
	13u	Br	H	$COCH_2$	H	H	H	H
	13v	H	H	$COCH_2$	F	H	H	H
	13w	Br	H	$COCH_2$	F	H	H	H
	13x	H	H	$COCH_2$	Cl	H	H	H
	13y	Br	H	$COCH_2$	Cl	H	H	H
	13z	H	H	$COCH_2$	Br	H	H	H
	13z'	Br	H	$COCH_2$	Br	H	H	H

Table 2: Anti-inflammatory activity of **13e, 13f, 13i, 13j, 13q** and **13y**. Values are presented as average (± SE) and are significant to a 95% confidence interval (ANOVA).

Compound	Dose (mg/kg)	Leukocyte counting/mL	Antiinflammatory activity (%)
13e	0.	$3.17 \pm 0.75 \times 10^6$	0
	2.0	$2.12 \pm 0.17 \times 10^6$	0
	3	$1.28 \pm 0.27 \times 10^6$	25.1 ± 16.0*
	12.5	$1.44 \pm 0.3 \times 10^6$	15.8 ± 17.1 *
	50	$1.47 \pm 0.09 \times 10^6$	14.0 ± 5.34*
13f	0.8	$0.56 \pm 0.08 \times 10^6$	67.1 ± 4.7
	3	$0.56 \pm 0.13 \times 10^6$	66.8 ± 7.7
	12.5	$0.58 \pm 0.1 \times 10^6$	66.1± 6.3
	50	$0.51 \pm 0.07 \times 10^6$	70.2 ± 4.4
13j	0.8	$1.21 \pm 0.16 \times 10^6$	29.2 ± 16.4
	3	$0.82 \pm 0.13 \times 10^6$	52.0 ± 7.6
	12.5	$1.66 \pm 0.04 \times 10^6$	2.9 ± 2.5 *
	50	$1.52 \pm 0.15 \times 10^6$	10.8 ± 8.7*
13q	0.8	$1.49 \pm 0.28 \times 10^6$	12.3± 16.48
	3	$1.86 \pm 0.35 \times 10^6$	0
	12.5	$1.47 \pm 0.24 \times 10^6$	13.9 ± 14.2*
	50	$1.03 \pm 0.17 \times 10^6$	36.7± 10.0
13y	0.8	$0.84 \square 0.12 \times 10^6$	50.7± 7.5
	3	$0.60 \square 0.09 \times 10^6$	64.9± 8.9
	12.5	$0.69 \square 0.20 \times 10^6$	59± 11.9
	50	$0.47 \square 0.08 \times 10^6$	73± 4.9
13i	3	$0.79 \pm 0.02 \times 10^6$	54.7± 1.16
Aspirin	200	$0.45 \pm 0.03 \times 10^6$	73.7± 2.04
Indomehtacin	10	$0.76 \pm 0.07 \times 10^6$	55.5 ± 4.3
Dexamethasone	1	$0.40 \pm 0.1 \times 10^6$	76.6± 6.2
Nimesulide	5	$1.16 \pm 0.1 \times 10^6$	32.2± 5.86
Celecoxib	10	$0.27 \pm 0.06 \times 10^6$	84.2± 3.9
	CONTROL	$1.71 \pm 0.12 \times 10^6$	

*= not significant

Table 3: *in vitro* inhibition of COX-1 and COX-2 enzymes by **13e, 13f, 13g, 13l, 13j, 13k, 13t, 13u, 13y e 13z.**

Compound	Concentration	COX-1 Inhibition (%)	COX-2 Inhibition (%)
Celecoxib	10μM	0	54.7
	1 μM	0	47.5
	0.01 μM	0	11.6
Indomethacin	10μM	100	44.8
	1 μM	100	0
	0.01 μM	41.3	0
13e	10μM	0	0
	1 μM	0	0
	0.01 μM	0	0
13f	1 μM	38.5	16.5
	0.01 μM	35.3	23.1
	0.01 μM	30.3	13.9
13g	1 μM	27.8	14.7
	0.01 μM	26.6	7.9
13i	1 μM	22.7	10
	0.01 μM	22.4	10
13j	1 μM	23.4	25.8
	0.01 μM	10.5	NT
13k	1 μM	20.9	0
	0.01 μM	16.3	NT
13t	10μM	41.6	0
	1 μM	6.6	0
	0.01 μM	0	0
13u	10μM	46.6	0
	1 μM	0	0
	0.01 μM	0	0
13y	1 μM	30.0	39.6
	0.01 μM	0	NT
13z	10μM	8.3	0
	1 μM	0	0
	0.01 μM	0	0

NT= not tested

6. Artigo 2

Development and Validation of LC-UV Method for the Quantification of the Anti-inflammatory thiazolidinone PG15 in Rat Plasma

O artigo encontra-se no formato de submissão ao Journal of Brazilian Chemical Society (ISSN: 0103-5053; Fator de Impacto: 1,003).

Development and Validation of LC-UV Method for the Quantification of the Anti-inflammatory thiazolidinone PG15 in Rat Plasma

Flávia De Toni Uchôa[1], Vitória Berg Cattani[2], Maria Do Carmo Alves de Lima[1], Suely Lins Galdino[1], Ivan da Rocha Pitta[1], Teresa Dalla Costa[2*].

[1]Universidade Federal de Pernambuco, Departamento de Antibióticos, Recife - PE, Brazil

[2]Universidade Federal do Rio Grande do Sul, Programa de Pós-Graduação em Ciências Farmacêuticas, Porto Alegre – RS, Brazil

Corresponding address

Teresa Dalla Costa

Universidade Federal do Rio Grande do Sul

Programa de Pós-Graduação em Ciências Farmacêuticas

Av. Ipiranga, 2752 - Porto Alegre – RS – 90.610-000 – Brazil

Phone (+55 51) 3308 5418

Fax (+55 51) 3308 5437

E-mail:teresadc@farmacia.ufrgs.br

ABSTRACT

A simple and rapid liquid chromatography–ultraviolet detection (LC–UV) method has been developed and validated for quantifying (5*Z*,*E*)-3-[2-(4-chlorophenyl)-2-oxoethyl]-5-(1*H*-indol-3-ylmethylene)-thiazolidine-2,4-dione (PG15) in rat plasma. A C18 reversed phase column provided chromatographic separation of the analyte which was followed by UV detection at 385 nm. The method involves precipitation of PG15 from plasma and isocratic elution with methanol:water (90:10 v/v). Total elution time was as low as 7.5 min. The proposed method was validated and showed linear correlation in the range of 62.5 to 4000 ng/mL. The within- and between-day precision, expressed as the relative standard error, were found to be less than 15 and 10 %, respectively, for all the concentrations investigated. Accuracy, measurement using the quality control (QC) samples, was in the range of 86.1-114.9 %. The applicability of the validated method was tested in the preclinical pharmacokinetic study of thiazolidinone PG15.

KEYWORDS: PG15; LC–UV; rat plasma; pharmacokinetics

RESUMO

Um método rápido e simples de cromatografia líquida com detecção em ultravioleta foi desenvolvido e validado para quantificação, em plasma de rato, do composto (5*Z*,*E*)-3-[2-(4-clorofenil)-2-oxoetil]-5-(1*H*-indol-3-ilmetileno)-tiazolidina-2,4-diona (PG15). Uma coluna em fase reversa C18 foi utilizada para separação do analito, seguida por detecção em UV (385nm). O método utilizou a precipitação do PG15 a partir do plasma e uma eluição isocrática com metanol:água (90:10 v/v). O tempo total da corrida foi 7.5 minutos. O método proposto foi validado e mostrou-se linear entre 62.5 e 4000 ng/mL. A precisão intra- e inter dia, expressa como desvio padrão relativo, foi menor que 15 e 10%, respectivamente, para todas as concentrações investigadas. A exatidão, medida através dos controles de qualidade (QC), ficou entre 86.1-114.9 %. A aplicabilidade do método validado foi testado no estudo farmacocinético pré-clínico do PG15.

KEYWORDS: PG15; LC–UV; plasma; farmacocinética

1. INTRODUCTION

Anti-inflammatory drugs are widely used to treat pain, fever, and inflammatory acute and chronic conditions. Clinical use of non-steroidal anti-inflammatory drugs (NSAIDs) is associated with significant toxicity particularly in the gastrointestinal tract and kidney.[1] In the past 15 years cyclooxygenase-2 (COX-2) inhibitors have been used to relieve inflammatory diseases symptoms without exhibiting the classical side effects of regular NSAIDs, especially the gastric complications.[2] In contrast, some COX-2 inhibitors expose patients to an increased risk of cardiovascular adverse effects.[3] As far as synthesis of new effective and safer anti-inflammatory drugs is concerned, new molecules have been synthesized aiming to bind COX enzymes or reach anti-inflammatory activity by others mechanisms.

Novel 5-indol-thiazolidinones and 3-benzyl thiazolidinones have been synthesized and exhibited anti-inflammatory activity.[4, 5, 6] Besides anti-inflammatory activity by COX pathway, some thiazolidines has been described as peroxisome proliferator-activated receptor ligands (PPAR) which are capable of suppressing inflammatory process.[7] A 5-indol substitution on the central thiazolidinic ring and the absence of a sulfonyl moiety are the two structural features of this chemical series, which is chemical related to the potent NSAID indomethacin as well as to the anti-diabetic PPAR-activator thiazolidinones, as roziglitazone. Previously docking studies in our laboratory showed that indol-thiazolidinones are capable of binding COX-2.[8] These results were confirmed by *in vitro* inhibition of purified ovine COX-1 and COX-2 measured using a colorimetric assay.[9] One of the compounds of this series, the drug candidate (5*Z*,*E*)-3-[2-(4-chlorophenyl)-2-oxoethyl]-5-(1*H*-indol-3-ylmethylene)-thiazolidine-2,4-dione (PG15) (Fig. 1), demonstrated an important activity in leukocyte migration evaluated by carragenin-induced inflammation in the murine air pouch model. PG15 given orally (3 mg/kg) exhibited a 67.2 ± 4.6% inhibition of the leukocyte migration to the inflammation site 6 hours after the beginning of the experiment compared to the control

group.[9] This result could be due to the drug's inhibition of COX-2 isoenzymes present in the air pouch tissue or to PPAR activation which is associated to a reduced leukocyte migration. [10; 11]

The success of PG15 in animal models such as carragenin-induced inflammation in air pouch and peritonitis, using very low doses, lead to the need of investigating its pharmacokinetics in rodents.[9]

Because PG15 is a original compound, no analytical method has been previously reported in literature for monitoring its plasma levels. In this context, the aim of this work was to develop and validate a rapid, specific and sensitive LC-UV analytical method to quantify PG15 in rat plasma viewing to investigate its pharmacokinetics.

2. METHODS

2.1 Chemicals

PG15 was obtained by synthesis as described by Uchoa[9]. High purity water was prepared in-house using a Milli-Q water purification system. HPLC grade methanol and acetonitrile was purchased from Tedia (Brazil). Ethyl acetate, dichloromethane and ammonium phosphate monobasic were of analytical grade, purchased form Merck (Germany).

2.2 Standard Solutions Preparation

The PG15 solutions were prepared in methanol:ethyl acetate (80:20, v/v) at concentration of 400 μg/mL. Sequentially standard solutions were prepared from this mother-

solution by dilution with water:methanol (50:50, v/v). These diluted working standard solutions were used to prepare the calibration curve or quality control samples. The calibration curve concentrations ranged from 6.25 to 4000 ng/mL. Quality control samples were prepared at three concentration levels: low concentration (LCQ) (8 ng/mL), intermediate (IQC) (400 ng/mL) and high (HQC) (3200 ng/mL).

2.3 Sample Preparation

The standard curve of PG15 and the QC samples were prepared by spiking 100 μL of blank rat plasma with 10 μL of each standard curve solution. These spiked plasma samples were vortexed for 10 sec and 200 μL of ice-cold methanol was added in each sample. The samples were vortexed for 30 sec and centrifuged at 6800g for 10 min. The supernatants were separated and 50 μL were injected into the LC-UV system. Blank plasma samples were prepared as described, without the drug, and 50 μL were injected.

2.4 LC-UV System

Chromatographic separation was carried out in Waters Alliance® 2695 LC separation module with a 2487 UV-detector. A Novapack® C18 column (4 μm, 150 x 3.9 mm) preceded by a Phenomenex® C18 guard column (5 μm, 3.0 x 4.0 mm) was used. The mobile phase consisted of methanol:water (90:10, v/v) and it was used with a flow rate of 1 mL/min. The auto-injector temperature was kept at 15 ^{o}C and the column was kept at room temperature. PG15 was detected at 385 nm.

2.5 Validation Procedure

The validation was performed in two consecutive days by injecting 3 calibration curves and 3 sets of quality controls each day, according to FDA guidelines. [12] The method was validated for selectivity, sensitivity, linearity, precision, and accuracy. Selectivity was evaluated by comparing the chromatograms obtained from the samples containing PG15 with those obtained from blank plasma samples. Furthermore, the chromatograms of the experimental samples obtained after intravenous administration of PG15 to Wistar rats were compared to the calibration curve standards chromatograms in order to detect interfering peaks. The sensitivity was determined by the lower limit of quantification (LLOQ). The response to the LLOQ was at least three times greater than the response of any interference at the retention time. Linearity of calibration curves based on peak-area weighted (1/y) as function of the nominal concentration was assessed by least square regression using the computer program Scientist for Windows ™ (MicroMath®). Slopes, intercepts and determination coefficients were calculated. Intra- and inter-day precision and accuracy of the analytical method were shown by triplicate processing and following analysis of QC samples. Precision was calculated as relative standard deviation (RSD) of the experimental concentrations and accuracy as the comparison between the experimental and nominal samples concentration. The criteria for acceptability of the data included accuracy within ± 15% deviation from the nominal values and precision within ± 15% RSD, except for the lower limit of quantification (LLOQ), where it should not exceed 20% of RSD[12]. Recovery experiments (extraction efficiency) were performed by comparing the analytical results for CQ extracted samples (n = 3) with un-extracted standard solutions that represent 100% recovery. Recovery experiments (extraction efficiency) were performed by comparing the analytical results for LCQ and HCQ extracted samples (n = 6/each) with unextracted standard solutions that represent 100% recovery.

2.6 Preliminary Stability Study

Short and a long-term PG15 stability in plasma were evaluated, as well as stability after freeze-thaw cycles and stability of the processed sample. Spiked quality control samples of 80 ng/mL (LQC) and 3200 ng/mL (HQC) were used to assess stability. The short-term stability was performed by keeping the PG15 CQ plasma samples at room temperature for 3 and 6 h, before processing for protein precipitation. The long-term stability study was carried by storing the plasma QC samples at -20 ºC for 4 or 8 days before analysis. The freeze-thaw stability study was conducted by analysis the QC samples after 3 cycles (- 20 ºC and room temperature). Processed samples stability was conducted by analyzing recently prepared CQ samples and samples kept on the auto-injector for 3 and 6 h before injection.

2.7 Pharmacokinetic Study

The applicability of the LC-UV method developed for pharmacokinetic studies was tested using plasma samples obtained after intravenous administration of PG15 to Wistar rats. The animals study protocol was approved by the Ethics in Research Committee of the Universidade Federal do Rio Grande do Sul (#2006608, UFRGS, Porto Alegre–RS). The animals were kept under controlled 12 h light-dark cycle during the acclimation period and had access to water and food *ad libitum*.

Male Wistar rats (n = 3) purchased from FEPPS (Fundação Estadual de Produção e Pesquisa em Saúde, Porto Alegre-RS) received a single dose of 15 mg/kg of PG15. The drug suspension for administration was prepared in 5% glucose solution with 10% of polysorbate 80. Blood samples (0.25 mL each), collected into heparinized tubes, were obtained from lateral tail vein sequentially at 0.083, 0,17, 0.25, 0.5, 1, 2, 4, 6, 8, 10 and 12 h post-dosing. Plasma (100 μL) was immediately separated by centrifugation (4º C, 6800g, 10 min) and

stored at -20 ºC until analysis. The individual and average profiles were evaluated by non-compartmental and compartmental approaches viewing to estimate the pharmacokinetic parameters using Excel® 2007 (Microsoft®) and Scientist® v 2.01 (MicroMath®) software, respectively.

3. RESULTS AND DISCUSSION

3.1 Method Development

Aiming to develop a simple, rapid and sensitive method for the quantification of PG15 in biological matrix, suitable for pre-clinical pharmacokinetics investigation, different conditions were evaluated to optimize sample extraction and chromatographic parameters during method development, based on PG15 physico-chemical properties (MW = 396; LogP 4.05, calculated by Tekto's method[13]; UV_{max} = 256 and 392 nm in acetonitrile, and 256 and 388 nm in methanol:water). PG15 is insoluble in water; partially soluble in methanol, ethanol and diethyl ether and soluble in ethyl acetate and acetone.

Optimization of the chromatographic conditions were conducted to obtain better peak resolution, shorter runtime, higher sensitivity and peak symmetry with accuracy, according to FDA requirements for an LC method for drug quantification in biological fluids.

Different mobile phases, consisting of acetonitrile or methanol in different proportions with aqueous phase or ammonium phosphate monobasic buffer, with diverse pH, were investigated with flow rate from 0.6 to 1.2 mL/min. Initially, acetonitrile was used due to its good UV transmittance, low viscosity and better capability of PG15 solubilization than methanol. All mobile phases testes with acetonitrile, independently of its proportion or pH investigated, resulted in chromatograms with double peaks due two PG15 *E/Z* configurations.

Because an isomeric separation is not intended at this stage of drug development, the organic solvent was switched to methanol, which produced a symmetrical single peak. A mobile phase consisting of water:methanol (30:70, v:v) in a flow rate of 1ml/min was selected. When methanol proportions higher then 70% were used, PG15 peak's eluted close to plasma interferents. A mobile phase with more than 30% of water resulted in better peak symmetry, but longer retention times and higher operating pressures. Ammonium phosphate monobasic (20 to 40%, v/v) did not result in better chromatograms. Flow rate gradients were also tested with higher water contests in the mobile phase viewing to reduce the retention time without significant improvement.

The wavelength selected for PG15 quantification in plasma, 385 nm, resulted in a higher sensitivity than the other maximum of absorbance investigate, 256 nm, with no interference from endogenous substances from rat plasma at the drug retention time.

Sample preparation such as protein precipitation with acetonitrile or methanol at room temperature or ice-cold as well as liquid-liquid extraction using dichloromethane and ethyl-acetate were tested No difference in recovery and in peak symmetry were observed between precipitation or liquid-liquid extraction. Precipitation with acetonitrile (1:2 ratio) was acceptable; however lead to an unstable baseline due to the composition of mobile phase. Due the simplicity and efficacy of sample preparation, precipitation with ice-cold methanol (1:2 ratio) was chosen.

The search for internal standard was performed testing compounds that absorbed well at 385 nm. From all compounds tested, best results were obtained with nefidipine (UV_{max} 340 nm). However, nifedipine peak was too close to plasma front leading to interference is some chromatograms. Due to difficulties to find a molecule with good absorption at 385 nm and retention time higher then 4 minutes, the validation was conducted without internal standard.

3.2. Method Validation

3.2.1 Selectivity and recovery

The selectivity of the analytical method developed can be observed in Fig. 2 by comparing representative chromatograms of independent blank plasma and blank plasma spiked with PG15 (3200 ng/mL). No additional peaks due to endogenous substances were observed that would interfere with the detection of the compound of interest. In addition, the experimental chromatograms obtained after intravenous administration of PG15 (15 mg/kg) to Wistar rats (Fig. 2C) did not show interfering metabolites. The retention time of PG15 was approximately 6.8 min. The extraction recovery of PG15 was, in average, 73.9 ± 12.8% for the concentrations investigated (8 and 32 μg/mL).

3.2.2 Linearity

The linearity of the method was observed in the investigated concentration range (62.5 to 4000 ng/mL). PG15 calibration curve parameters determined in two consecutive validation days are shown in Table 1. The mean calibration curve is presented in Figure 3. Calibration curves of weighted (1/y) peak area as function of nominal concentration were linear presenting a determination coefficient greater than or equal to 0.996 for all curves. The ANOVA evaluation showed no significant intra- or inter-day variability for the slopes and intercepts ($\alpha = 0.05$).

3.2.3 Lower limit of quantification (LLOQ)

The lower limit of quantification (LLOQ) was 62.5 ng/mL, which was accepted as the lowest level on the calibration curve that could be determined with appropriate precision and accuracy under the experimental conditions of this analytical method (Tables 2 and 3). [12]

3.2.4 Precision and accuracy

The intra- e inter-day relative standard deviation for PG15 are shown in Table 2. The intra-assay and inter-assay precision (RSD) values for QC samples were less than or equal to 14.58% and 7.37%, respectively. The method showed an accuracy within 15%, which can be observed in Table 3. The results obtained for PG15 LC-UV quantification method were within the acceptable limits stated for bioanalytical methods validation. [12]

3.2.5 Preliminary Stability Study

Preliminary studies showed that PG15 is not a very stable compound. Short-term stability test performed at room temperature showed that low and high QC samples were stable for up to 6 h with recoveries of 97.7 ± 2.8% at 3 hours and 93.1 ± 8.3% at 6 hours after spiking, without significant difference from time zero samples.

The long- term stability results indicated that PG15 samples were stable at -20 ºC up to 8 days, with an average recovery of 99.0% in 4 days and 96.2% after 8 days.

Significant decrease of PG15 concentration in plasma was detected after exposing samples to three freeze/thaw cycles and mean recovery was found to be 90.9% for the HQC and 83.0% for the LQC. Stability of the processed sample ready to injection in the auto-

sampler was also determined. Result showed that QC samples were stable for at least 4 h at 15 ºC, with loss no higher than 6%.

Considering the preliminary stability results plasma samples were processed and analyzed within 8 days after animal experiments, the samples were froze/thaw only once, samples were processed immediately after thawing and processed samples were injected no longer than 4 hours after processing.

3.2.6 Applicability of the analytical method

To investigate the suitability of the analytical method developed and validated it was applied to determine PG15 plasma profile after intravenous administration of 15 mg/kg dose in a pilot pharmacokinetic study (n = 3). The mean plasma profile obtained is shown in Fig. 4. The average profile shows a rapid plasma decline in concentrations after dosing, a prolonged period of constant concentration followed by an elimination phase after 10 h, consistent with a profile of saturation of elimination. The estimated half-life was found to be 9.5 ± 4.3 h although a compartmental fitting of the profile would be more adequate to describe the elimination process because non-compartmental analysis are not appropriate to describe non-linear pharmacokinetic profiles. A compartmental fitting of the data using models that assume *Michaelis-Menten* elimination after distribution to one, two or three compartments were unsuccessfully tested. Because the elimination phase was not completely characterized, it was not possible to estimate the pharmacokinetic parameters by non-compartmental or compartmental approaches. These results indicated that the analytical method is suitable to measure plasma concentrations of the compound in pre-clinical studies when high doses of the drug are administered. For low doses, a more sensitive method has to be developed.

4. CONCLUSION

A simple, specific and rapid analytical method for the determination of (5*Z*,*E*)-3-[2-(4-chlorophenyl)-2-oxoethyl]-5-(1*H*-indol-3-ylmethylene)-thiazolidine-2,4-dione (PG15) in rat plasma has been developed and validated according FDA guidelines. The method provided excellent specificity and linearity with a concentrations range of 62.5 to 4000 ng/mL. The method showed to be appropriate to investigate plasma levels of the drug when high doses are used, however, for a proper characterization of smaller doses, a more sensitive assay has to be developed.

5. ACKNOWLEDGMENTS

This work was supported by INOFAR/CNPq-Brazil (Process 420.015/05-1). Flávia De Toni Uchôa thanks CNPq-Brazil for the individual grant.

6. REFERENCES

1. HAWKEY CJ. *The Lancet*.**1999,** 353: 307.

2. MITCHELL, J.A.; WARNER, T.D. *Nature Rev. Drug Disc*., **2006**, 5, 75.

3. ZHANG J, DING EL, SONG Y. *J. Am. Med. Ass*. **2006,** 296, 1619.

4. MURTHY, N. S., SRINIVASA, V. *Indian J. Pharmacol.* **2003**; 35: 61.

5. GÓES, A.J.S., ALVES, A.J., FARIA, A.R., LIMA, J.G., MAIA, M.B.S. *Química Nova,* **2004**, 27, 905.

6. SANTOS, L.C.; UCHOA, F.T.; CANAS, A.R.P.A.; SOUSA, I.A.; MOURA, R.O.; LIMA, M.C.A.; GALDINO, S.L. ; PITTA, I.R.; BARBE, J. *Heterocyclic Comm.*, **2005,** 11, 121.

7. CHO MC, LEE WS, HONG JT, PARK SW, MOON DC, PAIK SG, YOON DY; *Mol Cell Endocrinol*; **2005**, 20, 96.

8. LEITE, L. F. C. C.; UCHOA, F. D.T, LIMA, M. C. A., GALDINO, S. L., PITTA, I. R., HERNANDES, M. Z; *Resumos do XII Simpósio Brasileiro de Química Teórica*, São Pedro, Brasil, 2005.

9. UCHOA, F.D.T. *Tese de doutorado*, Universidade Federal de Pernambuco, Brasil, 2008.

10. SEIBERT, K., ZHANG, Y., LEAHY, K., HAUSER, S., MASFERRERJ., PERKINS, W., LEN, L., ISAKSON, P. *PNAS*, **1994**, 91, 12013.

11. TANAKA T, FUKUNAGA Y, ITOH H, DOI K, YAMASHITA J, CHUN TH, INOUE M, MASATSUGU K, SAITO T, SAWADA N, SAKAGUCHI S, ARAI H, NAKAO K., *Eur J Pharmacol.* **2005,** 31, 255.

12. FDA. *Guidance for Industry. Bioanalytical Method Validation*. **2001** (http://www.fda.gov/cder/guidance/index.htm).

13. TETKO IV; BRUNEAU P, *J Pharm Sci*, **2004**, 93, 3103.

Table 1. Calibration curve parameters and statistics for thiazolidinone PG15 in rat plasma

Curve	*Slope*	*y-Intercept*	*Determination coefficient*
Day 1			
1	32218	-99,76	0.999
2	44119	-1946,92	0.996
3	42106	-1826,80	0.998
Day 2			
1	42905	-783,43	0.998
2	33074	-588,67	0.998
3	42810	-303,15	0.998
Mean (n = 6)	42458	-686.05	
S.D. [a]	5384.95	-782.05	
R.S.D. (%)[b]	12.68		

[a]S.D., standard deviation; [b]R.S.D., relative standard deviation

Table 2. Intra and inter-day variation of thiazolidinone PG15 in rat plasma.

Nominal concentration		Day	Experimental concentrations[a]		
			Mean (ng/mL)	S.D.	R.S.D.
Intra-day variation					
LLOQ	62.5 ng/mL	1	68.42	5.41	7.91
		2	68.38	5.24	7.67
QC	3200 ng/mL	1	3013.10	279.38	9.27
		2	3132.14	177.75	5.67
	400 ng/mL	1	376.86	8.39	2.22
		2	413.57	60.32	14.58
	80 ng/mL	1	88.87	4.81	5.41
		2	80.07	5.19	6.48
Inter-day variation					
LLOQ	62.5 ng/mL		68.40	0.29	3.93
QC	3200 ng/mL		3072.62	84.17	2.74
	400 ng/mL		395.21	25.96	6.57
	80 ng/mL		84.47	6.23	7.37

[a] Values (mean and S.D.) represent n = 3 observations.

Table 3. Accuracy for the analysis of thiazolidinone PG15 in rat plasma

Concentration (ng/mL)		Range (ng/mL)	Accuracy (%)[a]
LLOQ	62.5 ng/mL	62.1-72.03	99.5-115.2
QC	3200 ng/mL	2836.0-3335.1	88.62-104.2
	400 ng/mL	344.4-455.3	86.1-113.8
	80 ng/mL	74.5-91.9	93.2-114.9

[a]n = 6 observations**.**

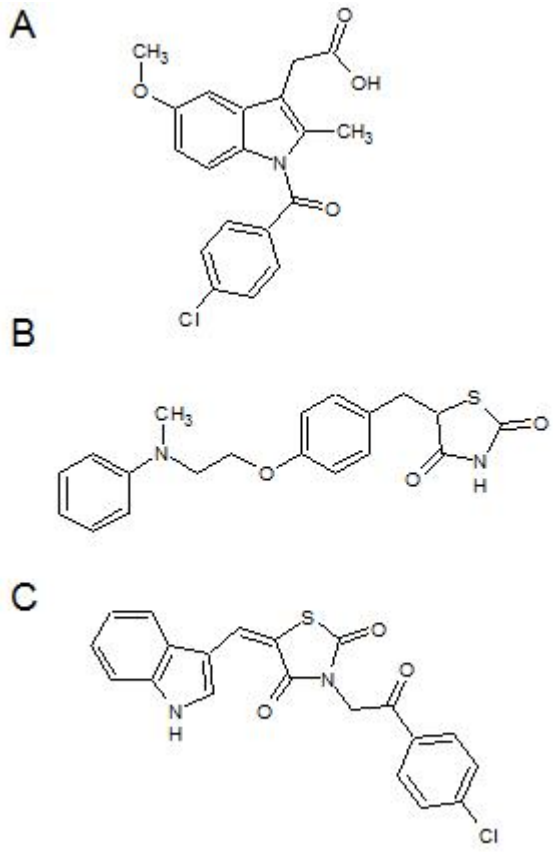

Figure 1. Chemical structure of indomethacin (A), rosiglitazone (B) and (5*Z*,*E*)-3-[2-(4-chlorophenyl)-2-oxoethyl]-5-(1*H*-indol-3-ylmethylene)-thiazolidine-2,4-dione (PG15)(C)

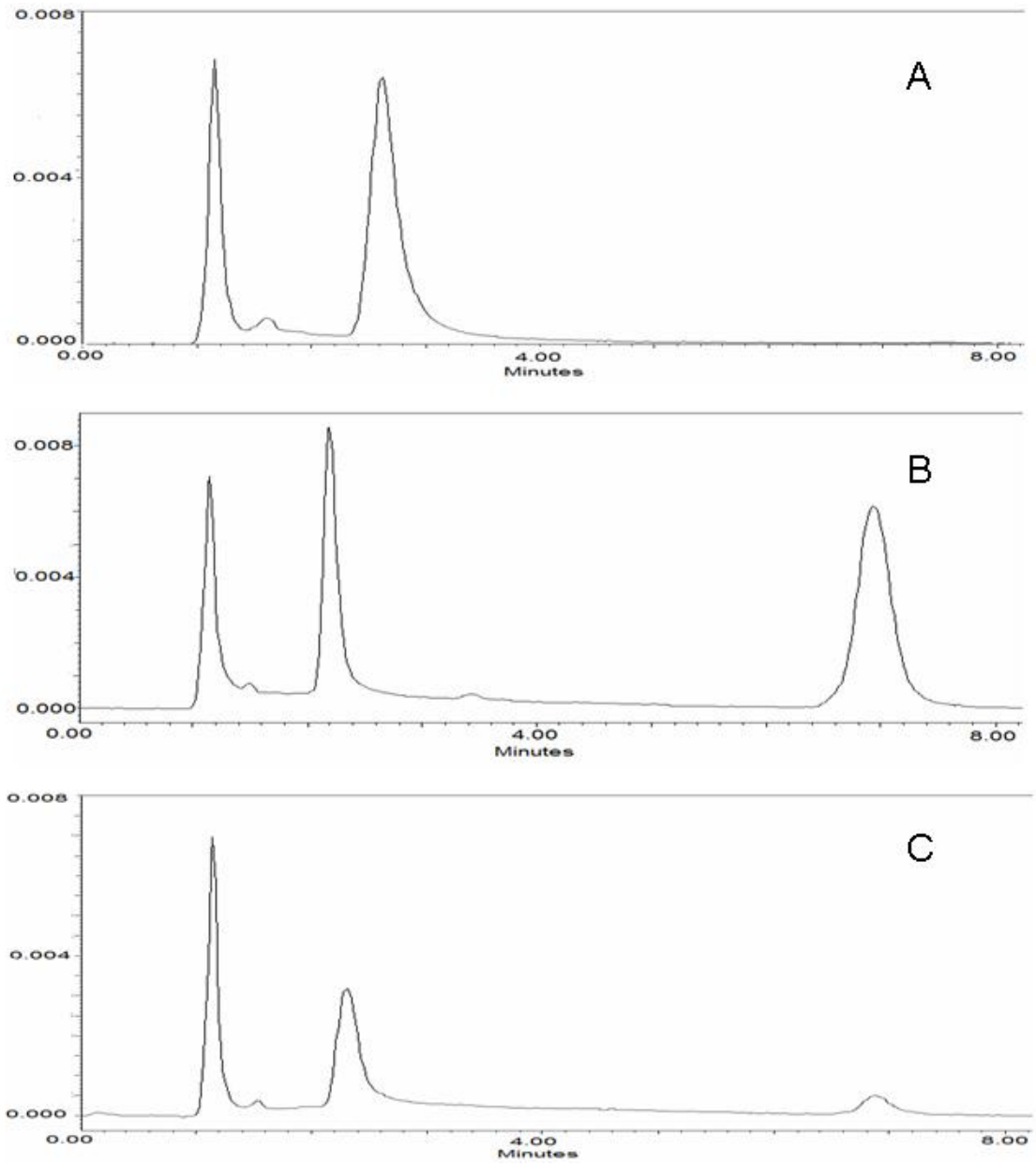

Figure 2. Representative chromatogram of blank plasma (A), plasma spiked with PG15 3200 ng/mL (B) and plasma sample 4 h post-administration of PG15 15 mg/kg i.v. (plasma concentration 156 ng/mL). PG15 retention time was around 6.8 min. Peaks of plasma and heparin were observed up to 3.5 min. No interference was observed at PG15 retention time.

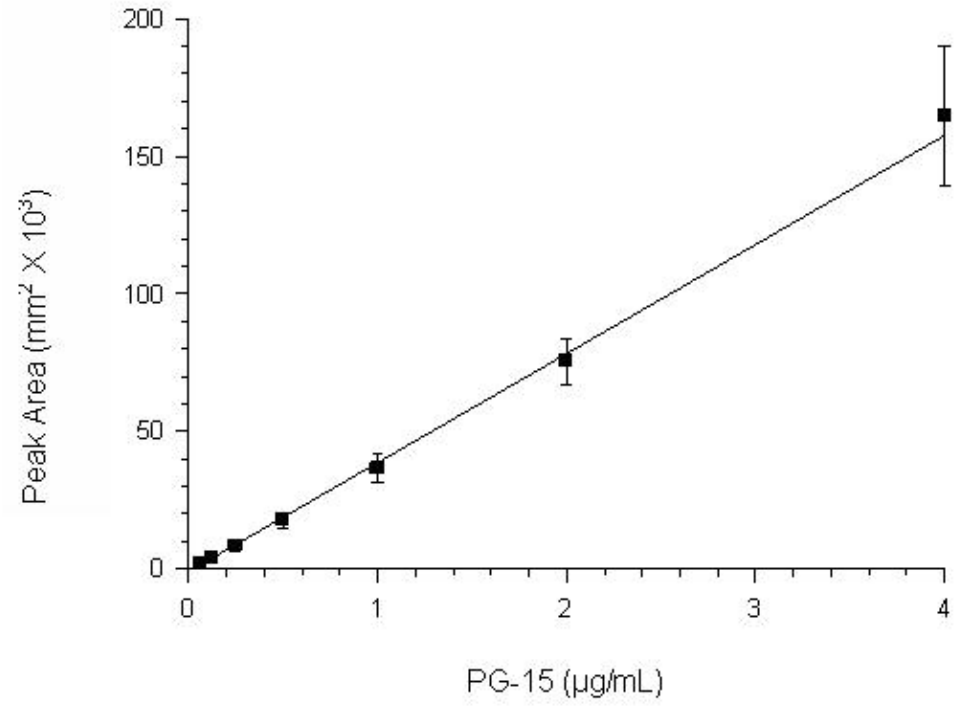

Figure 3: Mean calibration curve of 6 determinations. Mean calibration curve equation was y = 39.634x – 958.937

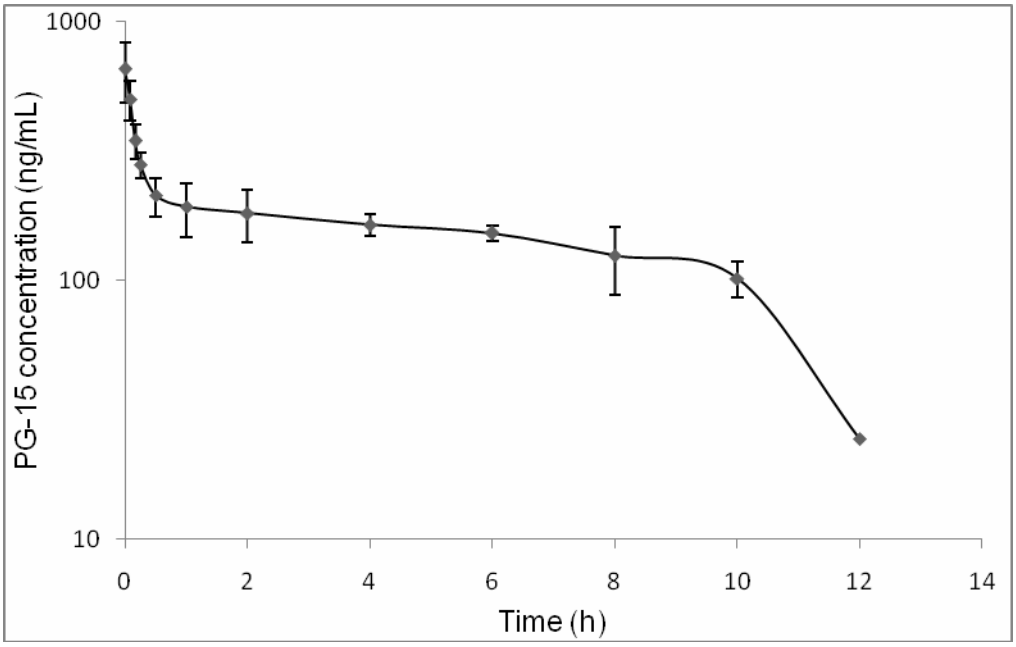

Figure 4. Mean plasma profile of thiazolidinone PG15 after a single 15 mg/kg i.v. dose to Wistar rats (Average ± SD) (n = 3).

Artigo 3

Development and validation of a LC/MS/MS method for analyzing thiazolidinone PG15 in rat plasma

O artigo encontra-se no formato para submissão no Journal of Pharmaceutical and Biomedical Analysis (ISSN: 0731-7085; Fator de impacto 2006: 2,032.

Development and validation of a LC/MS/MS method for analyzing thiazolidinone PG15 in rat plasma

Flávia De Toni Uchôa[1], Eduardo C. Palma[2], Natalia Freitas de Souza[1], Maria do Carmo Alves de Lima[1], Suely Lins Galdino[1], Ivan da Rocha Pitta[1], Teresa Dalla Costa[2,3].

[1]Departamento de Antibióticos, Universidade Federal de Pernambuco, Recife, Brazil; [2]Centro Bioanalítico de Medicamentos, Faculdade de Farmácia, Universidade Federal do Rio Grande do Sul, Porto Alegre, Brazil; [3]Programa de Pós-Graduação em Ciências Farmacêuticas, Universidade Federal do Rio Grande do Sul, Porto Alegre, Brazil

Corresponding address:
Teresa Dalla Costa
Universidade Federal do Rio Grande do Sul
Programa de Pós-Graduação em Ciências Farmacêuticas
Av. Ipiranga, 2752 - Porto Alegre – RS – 90.610-000 – Brazil
Phone (+55 51) 3308 5418
Fax (+55 51) 3308 5437
E-mail: teresadc@farmacia.ufrgs.br

Development and validation of a LC/MS/MS method for analyzing thiazolidinone PG15 in rat plasma

Abstract

A rapid, sensitive and simple LC–MS/MS analytical method was developed and validated for the determination of (5*Z*,*E*)-3-[2-(4-chlorophenyl)-2-oxoethyl]-5-(1*H*-indol-3-ylmethylene)-thiazolidine-2,4-dione (PG15) in rat plasma using chlortalidone as internal standard (IS). Analysis were performed on a Shimadzu® HPLC system using a Shimadzu® C18 Waters Symmetry® column and isocratic elution with 10 mM ammonium hydroxide in acetonitrile: water (90:10, v/v) as mobile phase at a flow of 0.3 mL/min and a mass spectrometer Micromass®, equiped with a double quadrupole and an electrospray ionization interface, operated in a negative mode. Plasma sample were prepared by deproteinizing 100 µl aliquot of rat plasma with ice-cold acetonitrile (3:1). The analysis was performed by monitoring the decay of mass-to-charge (m/z) ratio 395.1>171.9 for PG15 and 337.3 >189.9.5 for the IS. The retention times of PG15 and IS were approximately 3.4 and 2.4 min, respectively. Calibration curves in spiked plasma were linear over the concentration range of 10–1000 ng/mL with determination coefficient >0.99. The intra and inter-day precision, expressed as the relative error, were found to be less than 1222 and 11.3%, respectively. The accuracy of the method was within 13%. The applicability of the LC–MS/MS method for pharmacokinetic studies was tested using plasma samples obtained after oral administration of PG15 (3 mg/kg) to male Wistar rats. The reported method provided the necessary sensitivity, linearity, precision, accuracy, and specificity to allow the determination of PG15 in pre-clinical pharmacokinetic studies.

KEYWORDS: thiazolidinone PG15; LC-MS/MS; biological fluid; validation; pharmacokinetics.

1. Introduction

Non-steroid anti-inflammatory drugs (NSAID) are the most widely used in clinical practice for the treatment of acute and chronic inflammatory conditions. Their mechanism of action is based on the inhibition of cyclooxygenase(COX), an enzyme which catalyzes the generation of prostaglandins from arachidonic acid [1]. COX exists in two isoforms, COX-1 is constitutively expressed, generating prostaglandins responsible for protecting the gastric mucosa, and maintaining renal homeostatic and platelet aggregation; whereas COX-2 is inducible expressed by inflammatory stimulus, as a lesion, mediating responses to pathologic processes such as pain, fever and inflammation [2].

Recently, it has been shown that certain NSAIDs besides binding to COX enzymes, are also capable to activate peroxisome proliferator-activated receptor (PPAR)-γ which plays an interesting role in regulating the inflammatory response, because 15-deoxy-12,14-prostaglandin J2 and other PPAR-γ agonists inhibit the expression of a variety of proteins with pro-inflammatory properties, including COX-2, inducible nitric-oxide synthase (iNOS), and several cytokines [3,4]. Recent studies suggest that the thiazolidinedione (TZD) class of PPAR-γ ligands may be clinically beneficial in several inflammatory diseases, even if the molecular mechanisms responsible for these activities have not yet been clarified [3].

The thiazolidinone (5*Z*,*E*)-3-[2-(4-chlorophenyl)-2-oxoethyl]-5-(1*H*-indol-3-ylmethylene)-thiazolidine-2,4-dione (PG15) (Figure 1A)is one new 5-indolthiazolidinonic derivative designed to be COX-enzymes inhibitor and a PPAR-γ activator. The chemical structure of this anti-inflammatory candidate has similarities to indomethacin (Figure

1B), aiming to bind COX enzymes and has a thiazolidinonic ring, that are the pharmacophoric group that activate PPAR-γ for TZDs such as rosiglitazone (Figure 1C).

Previously studies in our laboratory show that PG15 has an important activity inhibiting leukocyte migration in the mouse air pouch model, exhibiting an ED_{50} of 7.49 mg/kg p.o. when inflammation was induced by carragenin and leukocyte were counted 6 hours after inflammation induction [5]. PG15 also inhibits 30% of leukocyte migration in carragenin-induced peritonitis in mice model, after a 3mg/kg oral dosing. Docking studies performed by Leite and co-workers [6] reveled that similar indol-thiazolidinones are capable of binding COX-2, which was confirmed for PG15 by *in vitro* inhibition of purified ovine COX-1 and COX-2 measured using a colorimetric assay [5]. The promising results of PG15 in these animal models lead to the need of investigating PG15 pharmacokinetics in pre-clinical studies.

A LC-UV method was previously published for analyzing PG15 in rat plasma but the method was unable to properly characterize the drug's elimination phase after administration of low doses [5]. So there is still a need for a sensitive method for analyzing the drug in plasma. This paper describes a method to quantify PG15 in rat plasma using mass spectrometer detector. The method was validated according to FDA guidelines [6] for bioanalytical methods and tested in a PG15 pharmacokinetic preliminary study after oral dosing.

2. Materials and methods

2.1 Chemicals

Thiazolidinone PG15 was obtained by synthesis under form of two *E*/*Z* configurations of PG15 isomers as described by Uchoa [5]. Acetonitrile (Tedia, Brazil) and water for the mobile phase were of chromatographic grade. Chlortalidone was purchased by DEG (Brazil). Ammonium hydroxide, ethanol and polysorbate 80 were from Merck (Germany).

2.2. Preparation of solutions and quality control samples

Stock solutions of PG15 and chlortalidone (internal standard) were prepared in acetonitrile:water (50:50, v/v) as 200 µg/mL and 100 µg/ml, respectively. Working solutions were prepared by diluting the stock solutions. For calibration curve seven different concentrations of PG15 (10, 20, 50, 100, 250, 500 and 1000 ng/mL) in plasma were prepared by adding required volume of working solution of PG15 blank plasma. Internal standard final concentration in plasma was 10 µg/mL. Quality controls samples were prepared in the same way at three concentration levels: low concentrations (30 ng/mL - LQC), intermediate concentration (300 ng/mL - IQC) and high concentration (800 ng/mL - HQC).

2.3 Sample preparation

An aliquot of 100 µL of plasma was spiked with 10 µL of PG15 and 10 µL of IS. To this sample, 300 µL of ice-cold acetonitrile was added and vortexed. The mixture

was centrifuged for 10 min at 6800 g. The resulting supernatant (20 µL) was injected into LC-MS/Ms for analysis. All plasma samples, including calibration curve, QC and samples from pharmacokinetic experiments were processed in the same manner.

2.4 Chromatographic and mass spectrometer conditions

The LC-MS/MS apparatus was composed of a Shimadzu® HPLC system consisting of a SCL-10A controller, LC-10AD pump, SIL-10AD injector and CTO-10A oven, which were coupled with a mass spectrometer Quattro LC Micromass®, controlled by MassLynx® 2000 software. The analysis were performed at 40 ºC using a C18 Waters Symmetry® (75×4.6 mm, 3.55 µm particle size) column with a security-guard column Phenomenex® (3.0 x 4.0 mm, 5 µm particle size). The mobile phase consisted of acetonitrile:water (90:10, v/v) with 10mM of ammonium hydroxide used in a flow rate of 0.3 ml/min. The analyte and internal standard (IS) were monitored using mass spectrometer equipped with a double quadrupole and an electrospray ionization interface operating in a negative mode (ESI). Samples were introduced into the interface through a heated nebulizer probe set at 280 ◦C. Nitrogen was the nebulizer and desolvation gas, and argon was used as collision gas. The other operating conditions were: nebulizer gas flow= 50 L/h; desolvation gas flow = 350 L/h; ion spray voltage = 1.0 kV; cone voltage = 50 V; ion source temperature = 130 ◦C; entrance potential = −5 V; collision energy = 31 V; collision cell exit potential =31 V. The spectrometer was programmed in multiple reaction monitoring (MRM) mode to allow the specific transition of precursor ion to fragment for each compound. The detection of ion species was performed by monitoring the decay of the mass-to-charge (m/z) ratio

395.1, corresponding to the parent molecular ion of PG15, to the m/z 171.9 product ion, which correspond to the indolic moiety from the parent molecule. Chlortalidone was detected by the decay of the 337.30 m/z precursor ion to the 189.9.5 m/z daughter ion, corresponding to benzyl sulphonamidic moiety, as seen in Table 1.

2.5 Method validation

Six replicates of calibration curve and quality control were prepared and analyzed in two consecutive days, three by day. Linearity of calibration curves based on peak area ratio (area of analyte/area of IS) as function of the nominal concentration was assessed by weighted (1/y) least square regression. Slopes, intercepts and determination coefficients were calculated and compared by ANOVA (α = 0.05). The selectivity of the method was investigated for potential interferences of endogenous substances by comparing chromatograms of the experimental samples obtained after i.v. administration of VRC to Wistar rats to the calibration curve standards chromatograms in order to detect interfering peaks. The limit of quantification (LLOQ) was determined from the peak signal to noise level as ten times the baseline noise. Intra- and inter-day precision and accuracy of the analytical method were shown by triplicate processing and following analysis of QC samples. Precision was calculated as relative standard deviation (R.S.D.) of the experimental concentrations and accuracy as the comparison between the experimental and nominal samples concentration. The criteria for acceptability of the data included accuracy within ±15% deviation from the nominal values and precision within ±15% R.S.D., except for the LLOQ, where it should not exceed 20% of R.S.D [7]. Recovery experiments (extraction efficiency) was

performed by comparing the analytical results for extracted samples (n = 3) with unextracted standards that represent 100% recovery.

2.6 Pharmacokinetic study

The LC-MS/MS method was used in a pre-clinical pharmacokinetic study of PG15. The study protocol was approved by the Universidade Federal do Rio Grande do Sul Ethics in Research Committee (#2006608). Male Wistar rats purchased from Fundação Estadual de Produção e Pesquisa em Saúde (Porto Alegre-RS, Brazil) received a single oral dose of PG15 3 mg/kg (n = 3) PG15 suspension was prepared in 5% glucose solution with 10% polysorbate 80 and 10% ethanol. Blood samples (0.25 mL) were harvested from the lateral tail vein sequentially at 0.25, 0.5, 0.75, 1, 3, 6, 9 and 16 h post-dose. The plasma (100 µL) was immediately separated by centrifugation (4º C, 6800g, 10 min) and stored at –20 ^{o}C until analysis. From the individual profiles, the following pharmacokinetic parameters were determined by non-compartmental approach using Excel® 2007 software (Microsoft®, USA): area under the plasma-concentration-time curve from time zero to the last measurable PG15 sampling time and to infinity (AUC_{0-t} and AUC_{0-inf}), maximum concentration (C_{max}), time to maximum concentration (T_{max}), elimination rate constant (Ke) and elimination half-life ($t_{1/2}$).

3. Results and Discussion

3.1 Selectivity and Recovery

Representative chromatogram of blank plasma and plasma spiked with PG15 and internal standard are shown in Figure 2. Retention time for the PG15 and internal

standard were 3.4 min and 2.4 min, respectively. The chromatographic run time was 4 minutes. No interfering peaks were found in the chromatogram obtained from blank plasma. Good separation and baselines with low background noise were observed. No additional peaks due to endogenous substances were observed that would interfere with the detection of the target compounds. The extraction recovery of PG15, 86.7 ± 10.7%, was PG15 concentration independent.

3.2 Linearity

The standard curves of PG15 in rat plasma were linear over the range of 10 to 1000 ng/ml. The linearity of the calibration curve was evaluated by determination coefficient of determination, never smaller than 0.991 and the variability of the slopes and intercepts which were determined automatically by the MassLynx® software. The results indicated no significant intra- or inter-day variability of slopes and intercepts over concentration range investigated (α = 0.05) as exhibited in Table 2.

3.3 Precision and Accuracy

Intra- and inter-day precision and accuracy of the method were assed by analyzing the LLOQ and QC samples spiked with known amount of PG15. Results are shown in Tables 3 and Table 4, respectively. The accuracy of the bioanalytical method was higher than 86% for all investigate concentrations. The intra- and inter day precision ranged from 3.68 to 12.24% and from 0.52 to 11.33%, respectively.

The data obtained for PG15 validation was within acceptable limits stated for FDA for bioanalytical methods [7].

3.4 Applicability of the analytical method

The bioanalytical method was used in the pre-clinical study of PG15. Figure 3 shows the mean plasma level of PG15 after the oral administration of a single dose of PG15 3mg/kg to rats. Table 4 shows the pharmacokinetic parameters estimated by non-compartmental analysis of individual profiles. PG15 was rapidly absorbed after oral administration reaching peak concentration (214.5 ± 121.3 ng/ml) before one hour post-dosing. Compatible with the compound high lipophilicity (LogP 4.05, calculated by Tekto's method) [8] after absorption plasma levels decrease 3.5 times in 45 minutes, probably due to distribution to peripheral compartments. Elimination was slow with an estimated half life of 8.1 ± 3.5 h. The method adequately characterized the drug's elimination, which can be observed by the extrapolated AUC, which in average was smaller than 28%.

4. Conclusions

A LC–MS/MS bioanalytical method for the determination of (5*Z*,*E*)-3-[2-(4-chlorophenyl)-2-oxoethyl]-5-(1*H*-indol-3-ylmethylene)-thiazolidine-2,4-dione (PG15) in rat plasma using chlortalidone as IS was developed and validated. This method showed adequate sensitivity, linearity, precision and accuracy and it has been successfully applied to determine the concentration–time profile of the drug in pharmacokinetic preliminary studies in rat. The method proved to be reliable to pursue further pre-clinical pharmacokinetic investigations of PG15.

5. Acknowledgements

This work was supported by INOFAR/CNPq-Brazil (Process 420.015/05-1). Flávia De Toni Uchôa thanks CNPq-Brazil for the individual grant.

6. References

1. J.R. Vane, R.M. Botting, Thromb Res. 15 (2003) 255.

2. C.J. Hawkey, Lancet 353 (1999) 307.

3. A. Ialenti, G. Grassia, P. Di Meglio, M. Pasquale, M. Di Rosa, A. Ianaro, Mol Pharmacol, 67 (2005) 1620.

4. M.C. Cho, W.S. Lee, J.T. Hong, S.W. Park, D.C. Moon, S.G. Paik, D.Y. Yoon; Mol Cell Endocrinol, 20 (2005) 96.

5. F.D.T. Uchoa, PhD Thesis, Universidade Federal de Pernambuco, Brasil (2008).

6. L.F.C.C. Leite, F.D.T Uchoa, M.C.A Lima, S.L.Galdino, I.R.Pitta, M.Z Hernandes, Resumos do XII Simpósio Brasileiro de Química Teórica, São Pedro, Brasil (2005).

7. FDA. Guidance for Industry. Bioanalytical Method Validation. (2001) (http://www.fda.gov/cder/guidance/index.htm).

8. I.V. Tetko, P. Bruneau; J Pharm Sci, 93 (2004) 3103.

Table 1. Chemical structure of thiazolidinone PG15 and the internal standard chlortalidone parent and daughter ion formed during LC-MS/MS analysis as well cone voltage and collision energy applied to each compound.

Compound	**Parent ion (m/z)**	**Daughter ion (m/z)**	**Cone voltage (V)**	**Collision energy (eV)**
PG15	395.10 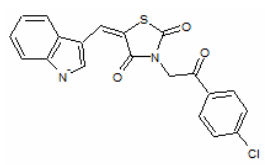	171.90 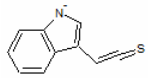	50	31
Chlortalidone (IS)	337.30 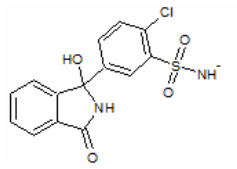	189.9 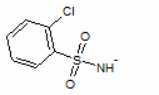	52	15

Table 2. Calibration curve parameters and statistics for thiazolidinone PG15 in rat plasma

Curve	*Slope*	*y-Intercept*	*Determination coefficient*
Day 1			
1	0.00343	0.0250	0.999
2	0.00293	0.0179	0.996
3	0.00310	0.0042	0.998
Day 2			
1	0.00288	0.0113	0.991
2	0.00259	0.0176	0.999
3	0.00305	0.0141	0.997
Mean (n = 6)	0.00300		
S.D. [a]	0.00028		
R.S.D. (%)[b]	9.2		

[a] S.D., standard deviation; [b] R.S.D., relative standard deviation

Table 3. Intra and inter-day variation of thiazolidinone PG15 in rat plasma.

Nominal concentration		***Day***	***Experimental concentrations***[a]		
			Mean (ng/mL)	S.D.	R.S.D.
Intra-day variation					
LLOQ	10 ng/mL	1	10.23	1.04	10.16
		2	9.60	1.17	12.24
QC	800 ng/mL	1	823.09	55.49	6.74
		2	817.06	71.62	8.77
	300 ng/mL	1	281.88	30.12	10.68
		2	331.00	12.18	3.68
	30 ng/mL	1	31.57	2.01	6.35
		2	28.84	2.04	7.08
Inter-day variation					
LLOQ	10 ng/mL		9.92	0.45	4.49
QC	800 ng/mL		820.07	4.27	0.52
	300 ng/mL		306.44	34.44	11.33
	30 ng/mL		30.21	1.93	6.39

[a] Values (mean and S.D.) represent n = 3 observations for intra-day and n = 6 observations for inter-day variation.

Table 4: Accuracy for the analysis of thiazolidinone PG15 in rat plasma.

Nominal Concentration		**Range (ng/mL)**	**Accuracy (%)**
LLOQ	10 ng/mL	8.59-11.43	85.9-114.4
QCs	800 ng/mL	764.05-889.53	95.5-112.3
	300 ng/mL	260.85-339.25	86.9-113.1
	30 ng/mL	26.62-33.22	88.7-110.7

[a] n = 6 observations**.**

Table 5: Pharmacokinetic parameters of thiazolidinone PG15 following a single oral dosing of 3 mg/kg to Wistar rats (n = 3)

Pharmacokinetic Parameters	Average ± SD
T_{max} (h)	0.83 ± 0.14
C_{max} (ng/mL)	214.5 ± 121.3
K_e (h^{-1})	0.09 ± 0.03
t½ (h)	8.1 ± 3.5
AUC $_{0-t}$ (ng·h/mL)	704 ± 223
AUC $_{0-\infty}$ (ng·h/mL)	1113 ± 724

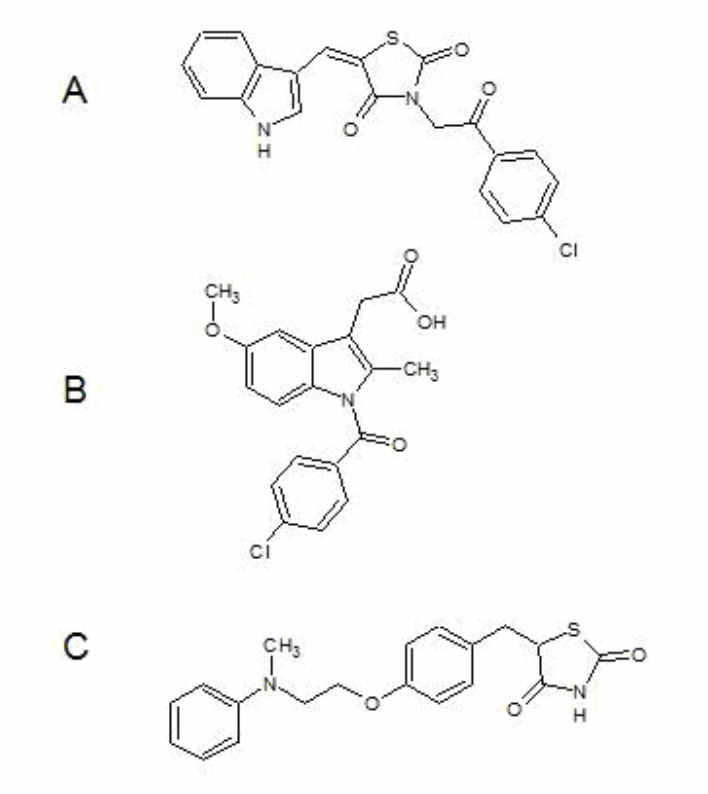

Figure 1. Chemical structure of (5*Z*,*E*)-3-[2-(4-chlorophenyl)-2-oxoethyl]-5-(1*H*-indol-3-ylmethylene)-thiazolidine-2,4-dione (PG15) (A), indomethacin (B) and rosiglitazone (C).

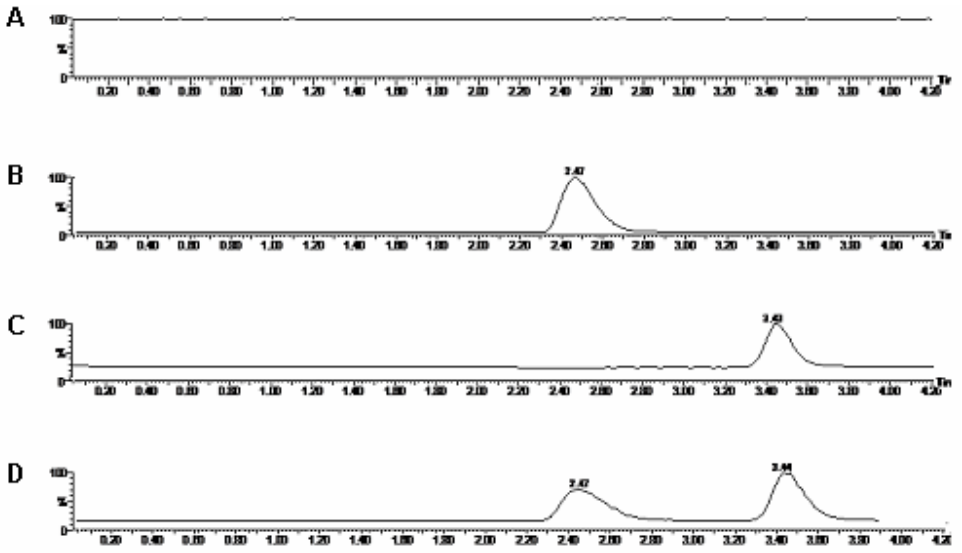

Figure 2. Representative total ion chromatograms in MRM-ESI- mode in rat plasma: (A) blank plasma, (B) plasma spiked with IS (10 µg/mL), (C) plasma spiked with PG15 (250 ng/mL), (D) plasma sample 0.5 h post-administration of PG15 3mg/kg p.o. corresponding to 67.9 ng/mL. The retention times were 2.4 min for the I.S. and 3.4 min for PG15.

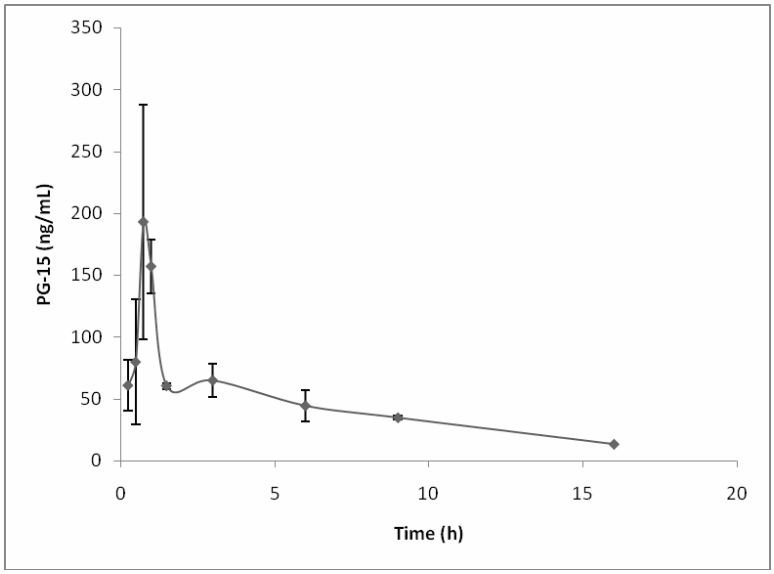

Figure 3: Mean plasma profile of thiazolidinone PG15 after a single 3 mg/kg p.o. dose to Wistar rats (n = 3) (Average ± SE).

Artigo 4

Preclinical Pharmacokinetic and Pharmacodynamic Evaluation of thiazolidinone PG-15: an Anti-inflammatory Candidate

O artigo encontra-se no formato para submissão ao Journal of Pharmacy and Pharmacology (ISSN: 0022-3573; Fator de impacto 2006: 1,533), uma publicação mensal da Pharmaceutical Press.

Preclinical Pharmacokinetic and Pharmacodynamic Evaluation of Thiazolidinone PG15: an Anti-inflammatory Candidate

Flávia De Toni Uchôa [1,3], Teresinha Gonçalves da Silva[2], Maria do Carmo Alves de Lima[2], Suely Lins Galdino[1,2], Ivan da Rocha Pitta[1,2], Teresa Dalla Costa[3].

[1]Programa de Pós-Graduação em Ciências Biológicas, Universidade Federal de Pernambuco, Brazil; [2]Departamento de Antibióticos, Universidade Federal de Pernambuco, Brazil; [3]Programa de Pós-Graduação em Ciências Farmacêuticas, Universidade Federal do Rio Grande do Sul, Brazil.

Corresponding Author:
Teresa Dalla Costa
Universidade Federal do Rio Grande do Sul,
Programa de Pós-Graduação em Ciências Farmacêuticas
Av. Ipiranga, 2752, Porto Alegre – RS – Brazil – 90.610-000
Phone: (55 51) 33085418
Fax: (55 51) 33085437
E-mail: teresadc@farmacia.ufrgs.br

Abstract

Inflammation is associated with a wide range of human diseases, pre-diseases, and conditions which are often treated with anti-inflammatory drugs. Novel 5-benzilidene thiazolidinones have been synthesized and exhibited anti-inflammatory activity (Santos et al. 2005). In this work one of the thiazolidinone chemical series, the (5*Z*,*E*)-3-[2-(4-chlorophenyl)-2-oxoethyl]-5-(1*H*-indol-3-ylmethylene)-thiazolidine-2,4-dione (PG15), was synthesized by a short and easy synthetic pathway (Uchoa et al. 2008). The aim of this study was to investigate the anti-inflammatory potential of PG-15 in pre-clinical studies including the *in vitro* inhibition of COX-1 and COX-2, the *in vivo* evaluation of anti-inflammatory activity by the air pouch (0.8, 3, 12.5 and 50mg/kg p.o.) and peritonitis (3mg/kg p.o.) models and the pharmacokinetic investigation after intravenous (3 mg/kg) and oral (3 and 6 mg/kg) administration to Wistar rats. Results showed that PG-15 was rapidly absorbed following oral administration to rats with peak plasma levels between 0.5 - 1 h and half-life of 5.9 ± 3.8h after i.v. dosing. PG-15 inhibited, *in vitro*, more then 30% and 13% of purified COX-1 and COX-2, respectively, in a concentration of 0.1 μM. The drug inhibited leukocyte migration in the carragenin-induced (1% saline solution, 1 mL,) mouse air pouch with an ED_{50} of 7.5 mg/kg and a 30.7% in peritonitis model. The activity of PG-15 in mouse in the carragenin-induced air pouch model was not dose-dependent and it leukocyte migration was similar that obtained using the standard drug indomethacin.

Key-words: PG-15, anti-inflammatory drug, pharmacodynamics, pharmacokinetics.

1. **Introduction**

Prostaglandins are the major mediators in both physiological and inflammatory processes, regulating platelet aggregation, vascular tone and inflammatory signals as edema, cellular migration, fever and pain (Vane & Botting 2003). Prostaglandins are synthesized by a pathway that depends on the activity of cyclooxygenase (COX), which exists in two isoforms: COX-1 and COX-2 (Xie et al. 1995). The isoforms are highly homologous in DNA sequence and differ only in one amino acid at their COX catalytic sites (Van Ryn et al. 2000). The expression of COX-1 is constitutive in most tissues throughout the body; in contrast, COX-2 has a restricted tissue distribution under normal physiological conditions but is highly induced at sites of inflammation and cell proliferation (Hawkey 1999).

As a result of these different expression and consequent pathophysiological roles, COX-2 selective inhibitors have been used in clinical setting aiming to achieve anti-inflammatory activity, while COX-1-dependent physiological functions such as gastrointestinal cytoprotection and platelet aggregation are preserved. Clinical trials with COX-2 inhibitors have been reported to cause a lower incidence of gastrointestinal side effects than nonselective COX inhibitors (Farkouh et al. 2004; Hawkey et al. 1998). Recently, COX-2 selective inhibitors have been associated with an increased cardiovascular risk due the inhibition of prostacyclin synthesis in endothelial tissue (Funk & Fitgerald 2007). While the selective COX-2 inhibitors situation in therapeutics remain unclear, it is known that COX selective or non-selective inhibitors stay as the best therapeutic choice to treat acute and chronic inflammatory diseases (Mitchel & Warner 2006).

Peroxisome proliferator-activated receptor gamma (PPAR-γ) is a member of the nuclear hormone receptor superfamily that includes the estrogen, thyroid hormone and glucocorticoid receptors. Recent data showed that PPAR-γ ligands modulate inflammatory responses (Fahmi et al. 2002). The role of PPAR-γ in regulating the inflammatory response involves 15-deoxy-$\Delta^{12,14}$-prostaglandin J_2 and other PPAR-γ agonists inhibit the expression of a variety of proteins with pro-inflammatory properties,

including COX-2, inducible nitric-oxide synthase (iNOS)(Ialenti et al. 2005), and several cytokines implicated in the inflammatory response via negative modulation, such as nuclear factor-kappa B (NFκB,), activator protein (AP-1), CCAAT/enhancer-binding protein beta (C/EBPβ), signal transducer and activator of transcription 1 (STAT-1) and nuclear factor of activated T-cells (NFAT) (Blanquart et al. 2003). This receptor is the molecular target of fatty acid derivatives, the thiazolidinedione (TZD) class of anti-diabetic drugs, which includes rosiglitazone and ciglitazone and certain non-steroidal anti-inflammatory drugs (Ialenti et al. 2005). So, if PPAR-γ ligands could modulate inflammatory response, design of this kind of ligands could lead to efficient novel drugs.

From TZD group of molecules, several compounds have been synthesized and tested presenting anti-inflammatory activity. From a group of thiazolidine derivatives with pyrazolone-5 substituent synthesized and tested *in vivo* for anti-inflammatory activity some molecules presented very important results (Lesyk et al. 1998). Related to those thiazolidines, 3-benzyl thiazolidinones have also been prepared and tested, exhibiting anti-inflammatory activity (Murthy & Srinivasa 2003).

A series of 5-arylidene-2-imino-4-thiazolidinones were obtained by Ottaná and co-workers (2005) and all derivatives exhibited significant activity levels in models of acute inflammation such as carragenin-induced paw and pleurisy edema in rats. From this series, 5-(3-methoxyphenylidene)-2-phenylimino-3-propyl-4-thiazolidinone displayed high levels of carragenin-induced paw edema inhibition, comparable to indomethacin. Similar structurally, 2-(4'-oxo-2'-phenyl-thiazolidin-3'-ylaminomethyl)- 3-[4''-(*p*-chlorophenyl)-thiazol-2''-yl]-6-bromoquinazolin-4-ones derivatives were prepared and screened for anti-inflammatory and analgesic activities at the dose of 50 mg/kg po. The compound with the best results in the series showed maximum anti-inflammatory (38.35%) and analgesic (37.36%) activities and ulcerogenic activity presented an UD_{50} (ulcerogenic dose) of 195.6 mg/kg po (Kumar et al. 2007).

The lead compound CGP52608 (1-(3-allyl-4-oxothiazolidine-2-ylidene)-4-methylthiosemicarbazone) of a class of 4-oxo-thiazolidinediones with high potency in experimental model of chronic inflammation suppression and joint destruction exhibits

antiarthritic activity at daily oral doses between 0.01 and 1 mg/kg (Missbach et al. 1996).

Woods and co-workers (2001) synthesized a series of potent COX-2 selective compounds presenting indol group attached to a thiazol moiety (Figure 1A). Our group (2005) published the synthesis of thiazolidinones and activity in carragenin induced rat paw edema of a 3-(4-chlorobenzyl)-5-(1*H*-indol-3-ylmethylene)-4-thioxo-thiazolidin-2-one (LYS5) (Figure 1B), which exhibited 77.5% inhibition of an inflammatory stimulus 240 min after dosing (Santos et al. 2005). This compound, that has indol group attached to thazolidine central ring, was docked in the COX-2 channel using the FlexX program interfaced with Sybyl 7.2 (Leite et al. 2005) with good bonding, exhibiting a free energy of -13,254 kcal·mol^{-1}. Silva and co-workers (2003) synthesized *N*-tryptophyl-5-(3,5-di-*tert*-butyl-4-hydroxybenzylidene)-2,4-thiazolidinedione (GS28) (Figure 1C) which exhibited in the carragenin induced paw edema an average inhibition of 28.36% after a 100 mg/kg oral doses and did not show ulcerogenic activity on gastric mucous.

A 5-indol substitution on the central thiazolidinic ring and the absence of a sulfonyl moiety are the two structural features of this chemical series that is chemically related to indomethacin (Figure 1D), a potent NSAID, and also to the anti-diabetic PPAR-activator thiazolidinones, as roziglitazone (Figure 1E). One compound from this series is 5(*Z,E*)-3-[2-(4-chlorophenyl)-2-oxoethyl]-5-(1*H*-indol-3-ylmethylene)-1,3-thiazolidine-2,4-dione (PG-15) (Figure 1F), which is a symbiotic leading-candidate, designed to be effective in two different target, COX and PPAR-γ, both relevant to inflammatory process but belonging to distinct biochemical pathways (Uchoa, 2008).

In this context, the aim of this work was to investigate the anti-inflammatory potential of PG-15 in pre-clinical studies including the *in vitro* inhibition of COX-1 and COX-2, the *in vivo* evaluation of anti-inflammatory activity by the air pouch and peritonitis model as well as to conduct a preliminary pharmacokinetic investigation of the drug after systemic and non-systemic dosing to rats.

2. Material and Methods

2.1. Chemicals

PG-15 was obtained by synthesis as described previously by Uchôa (2008), and was authenticated using mass and NMR spectroscopy. Carrageenin was acquired from Sigma (USA). Chlortalidone, nimesulide and dexamethasone were purchased from Galena (Brazil) and indomethacin and aspirin from Deg (Brazil). Celecoxib was acquired as commercial Celebra® (Pfizer, Brazil). COX inhibition reagents were supplied from Cayman Chemical Company (USA.) Acetonitrile HPLC grade, ammonium hydroxide and polysorbate 80 were purchased from Merck (Germany). HPLC water from Millipore's Milli-Q System was used throughout the analysis. Saline sterile solution was purcheased from B Braun (Brazil). All other chemicals used in this study were of analytical grade.

2.2. Inhibition of purified COX-1 and COX-2

COX-1 and COX-2 assays were performed using the colorimetric Ovine Cyclooxygenase (COX) assay kit (Cayman Chemical Company, USA). Inhibition of enzyme activity was determined by a colorimetric assay as previously described by Kulmacz and Lands (1983). The assay measures the peroxidase component of cyclooxygenases which is assayed colorimetrically by monitoring the appearance of oxidized N,N,N',N'-tetramethyl-p-phenylenediamine (TMPD) at to form a blue compound (610 nm) wich reflect the rate of conversion of arachidonic acid to PGH_2.

Different dilutions of PG-15 were prepared in dimethyl sulfoxide (DMSO) and diluted further to derive the appropriate concentrations for testing. The assay was then performed as described in the assay kit booklet (Cayman Chemeicals, 2005).

2.3. *In vivo* procedure

All *in vivo* procedures were approved by the Universidade Federal do Rio Grande do Sul Ethics in Research Comittee (protocol #2006/608) or the Universidade Federal de Pernambuco Ethics in Animal Experimentation Committee (protocol #23076.011488/2005-35). Male Wistar rats were purchased from Fundação para

Produção e Pesquisa em Saúde - FEPPS (Porto Alegre, RS, Brazil). Male and female albino Swiss mice were purchased from Aggeu Magalhães Biotério (Recife, PE, Brazil). All animals were housed in accredited facilities under standard conditions for rodents. Animals were acclimatized for at least 3 days prior to use.

2.4. Carrageenan-induced air pouch inflammation

To induce air pouches, male and female swiss mice (n=10) were injected subcutaneously on the back with 2.5 ml of air. After 3 days, the pouches were reinflated with 2.5 ml of air. On day 6, animals received orally PG-15 (0,8; 3; 12,5 and 50 mg/kg) or vehicle and one hour later inflammation was induced by injecting 1 ml of a suspension of carragenin (1% weight/volume in saline solution) into the air pouch, as described by Klemm, Harris and Parretti (1995) adapted by Romano and co-workers. (1997). After 6 hours, the mice were euthanized and the pouches were flushed with 3 ml of phosphate buffered saline (PBS) with heparine (10UI/mL). Aliquots were diluted with Turk Solution, and leukocytes were counted in a Newbauer chamber. From 3 mg/kg group, exudate aliquots were freeze until analysis by Liquid Chromatography/Mass Spectrometry/Mass Spectrometry (LC-MS/MS) to quantify PG-15 in inflammatory site, as describe in 2.6.

2.5. Carragenin-induced Peritonitis

Carragenin-induced peritonitis experiment was conduced in Male Swiss mice (n = 6) as describe by Oliani, Damazo and Perretti (2002). Animals were injected intraperitoneally with 0.25 ml of carrageenan (1% weight/volume in saline solution) one hour after received orally 3mg/kg dose of PG-15 or vehicle to control group, then euthanized after 4 hours. The peritoneal exudate was flushed with 2 mL of heparinizated PBS (10UI/mL) collected and the total count of leukocytes determined. To quantify PG-15 in peritonite exudates, aliquots were freeze until analysis by LC-MS/MS as describe in 2.6.

2.6. Pharmacokinetics

To determined PG-15 pharmacokinetics, the drug was administered to male Wistar rats (290–325 g) intravenously (3 mg/kg, n = 5) or orally by gavage [3 mg/kg (n = 3) or 6 mg/kg (n = 7)]. PG-15 was administrated as a 4mg/mL suspension prepared with 10% ethanol, 10% polisorbate 80 in a 5% glucose solution. For i.v. administration, the maximum volume administrated was 250 µL and for oral administration, 500 µL.

After dosing, blood samples were collected into heparinized tubes by venopucturing the lateral tail vein at scheduled time points up to 16 hours. Plasma was separated by centrifugation (10 min, 6800g, 4 ºC) and 100 µL samples were stored at -20 ºC until analysis. On the analysis day, samples were thaw, spiked with 10 µL of internal standard (IS) (chlortalidone 100 µg/mL); deproteinized by addition of acetonitrile (300 µL) and centrifuged (10 min, 15000 rpm, 4 ºC). 20 µL of the supernatant was used to quantify PG-15 using an LC-MS/MS method previously validated according to Food and Drug Administration (FDA) guidelines (Uchôa et al. 2008). Briefly, a reversed phase C18 Symmetry® Waters column (75×4.6 mm, 3.55 µm particle size) preceded by a C18 pre-column and kept at 40 ^{o}C was eluted with a mobile phase consisting of acetonitrile:10 mM ammonium hydroxide (90:10%, v/v) with a flow rate of 0.3 mL/min using. The LC-MS/MS consisted of a Shimadzu® LC coupled to a Micromass® mass spectrometer with electrospray ionisation in the negative mode. Detected fragments were 395.1>171.9 and 337.3>189.9 to PG-15 and IS, respectively. The calibration curve were linear in the range of 10 and 1000 ng/mL, the lower limit of quantification was 10 ng/mL. The intra and inter-day precision expressed as the relative error were found to be less than 12.2 and 11.3%, respectively for all the concentrations investigated. Accuracy in the measurement of quality control (QC) samples was in the range of 86.9-113.1%.

From individual rats plasma profiles analysis after i.v. and oral dosing, pharmacokinetic parameters were derived by non-compartmental and compartmental approaches. Non-compartmental analysis was conducted in Microsoft Office Excel 2007® using classical pharmacokinetic equations (Shargel et al. 2005). For compartmental analysis, plasma curve fitting was performed using Scientist® v. 2.01 (MicroMath®). The criteria employed to select the appropriate model to describe the

profiles, given by the computer program Scientist®, were: the model selection criterion (MSC), a modified Akaike Information Criterion (AIC) given by the program, the visual fitting of the model to the experimental data and the mathematical coherence between the pharmacokinetic parameters determined by modeling and phenomena experimentally observed.

2.7. Statistics

Statistical comparisons between the vehicle-treated control and compound-treated groups were made by ANOVA followed by Tukey's test. P-values less than 0.05 were considered statistically significant. Pharmacokinetics parameters ere compared with Students t-test assuming equal variances (α = 0.05).

3. Results and Discussion

3.1. Inhibition of purified COX-1 and COX-2

PG-15 inhibited COX-1 and COX-2 with micro molar affinity (Table 1) with no significant difference between 100 times increase in concentration, showing that possibly this is the higher inhibition that PG-15 could reach. The results show that PG-15 is capable to inhibit both COXs at tested concentrations, exhibiting slightly preference to COX-1.Comparing with the COX-1 inhibitor indomethacin we observed that indomethacin exhibited a higher affinity to COX-1 then PG-15, reaching 100% of enzymatic activity inhibition at 1μM, but to COX-2, PG-15 presented more affinity in tested doses. Although, the COX-2 inhibitor Celecoxib exhibited more affinity to COX-2 then PG-15.

3.2. Inhibition of leukocyte migration in carrageenan mice air pouch

The injections of air into mice back forms an in vivo chamber which is a highly reactive lining tissue composed primarily of fibroblast-like cells (Sedgwick et al. 1983). When carragenin is injected into this produced tissue, it rapidly induces the inflammatory processes and leukocyte migration starts. Results obtained evaluating leukocyte migration inhibition is expressed as anti-inflammatory activity of PG-15, orally from 0.8 mg/kg to 50 mg/kg, and are listed on Table 2. The effective dose for inhibition on leukocyte migration by 50% (ED_{50}) was 7.5 mg/kg, calculated using linear regression analysis, plotting probit of percent activity vs log dose (mg/kg).

Increasing doses of PG-15 did not result in increased activity at the range of doses tested; revealing that the effect was not dose-dependent and probably highest effect was reached with 3 mg/kg.

Leukocyte migration to inflammatory sites is a gradual process, which is dominated in its early phases by chemokine- and cytokine-mediated neutrophil recruitment (Ferrandi et al. 2007). After a time lag of about 2 h, neutrophils steadily accumulated in the carrageenin/air-pouch until 8 h. Similarly, the interleukin 8 level of exudate increased after about a 2 h lag, and reached a maximum at 8 h (Nagakawa et al. 1992). It´s also known that tumour necrosis factor (TNF) is a mediator of inflammation in the carrageenan-induced mouse air pouch model (Romano et al. 1997).These facts suggests that PG-15 could be active by interfering in chemokine- and cytokine-mediated leukocyte recruitment.

But its important to note that in the air pouch model, production of PGE_2 is induced, a process which is largely derived from COX-2 originating in the lining tissue (Seibert et al., 1994). Another prostaglandin derived form COX-2, PGF_2, is responsible to stimulated leukocyte migration to inflammation site (Menezes et al. 2005), so, there is good relationship between COX-2 inhibition and reduction on leukocyte count in exudate from pouches and *in vitro* COX inhibition by PG-15 results showed that PG-15 is capable to bind COX enzymes.

We observed that PG-15 exhibited a very important activity, comparable to reference NSAIDs, as indomethacin. Based on model features, we can suggest that

PG-15 activity is from COX inhibition, but not only from this inhibition. *In vivo* inflammatory processes it's a sum of several mediators effects. As PG-15 inhibition *in vivo* was practically twice then was observed in *in vitro* COX inhibition, we can suggest that PG-15 is acting in more then one mechanism of inflammation.

From the group that received 3 mg/kg dose, exudates aliquots were analyzed to quantify PG-15 at the inflammation site. Seven hours after dosing it was possible to determine a mean concentration of 84.85 ± 43 ng/mL (n = 6) of PG-15 in the exudates, showing that indeed the drug penetrates into the inflammation and it is present in high concentrations at the inflammatory site.

3.3. Carragenin-induced peritonitis

Changes in a number of peritoneal leukocytes 4 h after carragenin-induced peritoneal inflammation are shown in Table 2. PG-15 inhibited 30.7% of leukocyte migration in peritonitis model. Exudates analyzed to quantify PG-15 in inflamed peritoneal fluid 5 hours after dosing exhibiting average drug concentration of 30.51 ± 7.7 ng/mL (n = 3).

The lower anti-inflammatory activity observed in this inflammation model compared to the air pouch model may be a reflection of the differences in mediators presents in this timepoint of inflammation. Air-pouch exudates were collected six hours after inflammation, whereas in peritonitis model exudates were collected four hours after. We also observed that lower levels of PG-15 were determined in the peritonitis site compared to the air pouch exudates, this difference is probably related with PG-15 affinity to these inflammations sites, that are not equals. According to Sedgwick and co-workers (1983), air pouch model induces the proliferation of cells that stratify on the surface of the cavity to form a structure similar to the synovia. In peritonitis model, inflammatory site correspond to cells of regular peritoneal cavity and recruited cells.

3.4. Pharmacokinetics in rats

PG-15 pharmacokinetics was evaluated in Wistar rats after 3mg/kg iv dosing and 3 and 6 mg/kg oral dosing. After 3 mg/kg iv dosing, PG-15 exhibited a rapidly distribution, with plasma levels falling from 9 000 ng/mL, 5 min after administration, to 300 ng/mL in last then 30 min, as shown in Figure 2. After distribution, PG-15 elimination was slow, characterizing drug body disposition as a two-compartment model.

Pharmacokinetic parameters determined from individual plasma profile analysis after intravenous dosing are presented in Table 4. No significant difference was observed between parameters estimated by compartmental and non-compartmental approaches, showing the appropriateness of the model selected to fit the experimental data. The goodness of fit, determined by MSC, was in the range of range 2.93 to 4.98, also confirming the model selected. PG-15 presented an average half-life around 5 h, with an average volume of distribution of 2 L/kg and a clearance of 0.9 L/h/kg.

Although PG-15 after 3 mg/kg i.v. dosing showed a plasma profiles compatible with first order elimination, data from a 15 mg/kg i.v. dose showed that the drug presents a saturable elimination at higher doses (Uchôa et al., 2008).

After PG-15 3 mg/kg oral dosing the drug was rapidly absorbed showing peak plasma levels between 0.5 and 1 h, as it can be seen in Figure 3. Even though the first hour after dosing was not well-characterized, the one-compartment model more adequately fit the experimental data, with an MSC in the range of 0.11 to 0.56. The pharmacokinetic parameters determined for this dose are presented in Table 5. No significant differences were observed between parameters determined by compartmental and non-compartmental analysis, confirming the adequability of the choose model.

Although the half-life, the elimination rate constant and the total clearance following oral and i.v. administration of a 3 mg/kg were statistically similar (α = 0.05) (Tables 3 and 4), the volume of distribution after iv dosing was almost 5 times higher than after oral dosing. One hypothesis to explain this difference only on Vd_{ss} can be that the sampling scheduled used did not allow for the characterization of PG-15 distribution

adequately and, instead of a one-compartment model used, a two-compartment would better characterize the drug disposition in the body. This hypothesis is supported by the fact that it was not possible to fit the higher PG-15 levels observed in plasma after oral dosing (Figure 3) although different models were used. To better characterize the drug distribution; at least another 4 blood samples would have to be withdrawn up to 5 hours after dosing.

PG-15 plasma levels after i.v. dosing were extremely high in first 15 min after administration and they declined very quickly. These high concentrations resulted in a greater overall body exposure to PG-15 after systemic administration, expressed by an area under the curve (AUC) of 3949 ± 2068 ng·h/mL that compared to the AUC observed after the same dose was administered orally (1113 ± 724 ng·h/mL) lead to an bioavailability of 28%.

Aiming to evaluate whether PG-15 exhibits a linearity pharmacokinetics in the dose range investigated in the pharmacodynamic studies, an oral dose of 6 mg/kg was evaluated. Plasma profiles obtained after this dose were very erratic and variable. The profiles could be split into two distinct groups (Figure 4). One profile was similar to those obtained after 3 m/kg p.o. dosing (sub-group A). In the other, plasma concentrations reach high levels 15 min post-dosing and were kept high for almost 16 h, suggesting a saturation of drug elimination (sub-group B).

No pharmacokinetic model was capable of fitting both sub-groups, alone or simultaneously. A non-compartmental analysis was performed for the sub-groups separately (Table 6). Elimination phase could not be properly characterized for sub-group B because the AUC extrapolated was around 70%. Blood sampling was collected after 16 hours in order to better characterize the elimination phase but the concentrations were bellow the limit of quantification of the analytical method used to quantify PG-15 in plasma. Due to the high inter-individual variation, a statistical analysis proved to be pointless.

Comparing the profile of sub-group A (6 mg/kg) with that obtained after oral dosing of 3 mg/kg one can observe that doubling the dose did not reflect in overall

increase in body exposure to the drug. The AUC for both groups were statistically similar (α = 0.05). Furthermore, the AUC of both sub-groups A and B, that received 6 mg/kg orally, was no statistically difference besides the differences in the shape of the profiles.

An erratic absorption of PG-15 after oral administration can be observed in the profiles (Figures 3 and 4), by the elevated variability of the pharmacokinetic parameters determined as well as by the fact the higher dose administered by this route showed two distinct patter than could not be modeled. Furthermore, some individual profiles after the higher oral dose showed multiple peaks. Similar variability was not observed after intravenous administration. PG-15 erratic absorption can be attributed to its poor solubility at the site of absorption due to its high lipophilicity (LogP = 4.05, calculated by Tekto's method) (Tekto and Bruneau, 2004). The low solubility of the drug to in aqueous media, even in different pHs, probably render the drug to be poorly and non-homogenously absorbed along the gastrointestinal tract.

Another explanation for the erratic absorption observed after oral dosing could also be absorption due to active transport which was saturated at the higher dose used. This hypothesis could explained why increasing doses it was not possible to observe an increase in the AUC. It's also possible to associate the lack of difference in overall exposure between the two doses investigated by an active efflux mechanism, such as glycoprotein P (PgP), which could lead to high variability in drug plasma levels due to genetic individual variability in PgP expression (Urquhart et al. 2007).

Erratic absorption behavior, similar to what was observed for PG-15, has been reported for drug like 5-flourouracil and cannabinoids in clinical trials. Oral administration of 5-fluorouracil give rise to erratic plasma values due to greater variability in absorption, whereas 96 h i.v. infusions showed constant levels of the drug in plasma (Fraile et al. 1980). After oral administration of the highly lipophilic cannabinoid drugs dronabinol and nabilone Guzman (2003) reported that the absorption was slow and erratic probably due to degradation in the acid pH of the stomach and variable individual rates of first-pass metabolism in the liver. Some patients showed more than one plasma peak after oral dosing which made it more difficult to control the

drugs effects. Other routes of cannabinoid administration such as intravenous, rectal and sublingual circumvent the aforementioned problems of oral administration by producing single, rapid and high drug-plasma peaks, confirming that the oral route is the source of profiles and not the drug *per se*.

The results of the pharmacokinetic lack of linearity and erratic profiles after oral dosing are in accordance with the anti-inflammatory results obtained in the air pouch model, where no significant difference in activity was observed by increasing the dose from 0.8 mg/kg to 3 mg/kg. Moreover, when doses increased from 3 mg/kg to 12.5 or 50 mg/kg, the activity was reduced, probably as result of absorption difficulties.

It is also important to notice PG-15 concentration present at the inflammatory site of the air pouch model measured 7 h after a 3 mg/kg oral dose was in the same order of magnitude (83.85 ± 43.46 ng/mL) that it was observed in plasma at the same time (approximately 42 ng/mL), demonstrating that the drug in plasma equilibrates with drug in the inflammatory exudates and plasma levels can be used as surrogate for inflammatory tissue concentrations.

Thus, pharmacokinetic evaluation of PG-15 in rat plasma reveals an interesting profile for a COX inhibitor. After oral dose of 3mg/kg, PG-15 has a volume of distribution of approximately 11 L, was absorbed rapidly (T_{max} 0.62 h), demonstrated a rapid plasma elimination (t1/2 5.2 h). After oral dosing, PG-15 exhibits a low and erratic absorption, probably due to its low solubility in water associated to first-pass metabolism, efflux by pg-P, saturation of active mechanism of absorption or saturable metabolization. All hypotheses should be further investigated.

Plasma levels detected in pharmacokinetic study were coherent with pharmacodynamic results and contributed to explain the lack of dose-effect relationship. To deal with PG-15 absorption problem the use of pharmaceutical technology knowledge can be applied. Preparation of co-crystals, metastable polymorphs, high-energy amorphous forms or ultrafine particles (Blagden et al. 2007); preparation of microparticles (Wong et al. 2006); incorporation into micro or nanoparticles (Gonalez et al. 1999) or even incorporation into carrier systems as cyclodextrin clusters, which are

successful strategies that were previously employed in similar situations, should be pursued.

4. Conclusions

PG-15 was found to be effective in two mice models used to establish anti-inflammatory activity. The efficacy of PG-15 was similar to indomethacin, and the potency was generally comparable. *In vitro* COX inhibition showed that PG-15 is not COX-selective, leading to classify the drug as nonselective NSAID. Pharmacokinetic profile of PG-15 revealed oral absorption problems when dose is increased and further studies viewing to improve drug absorption should be conducted. Combination of results described in this manuscript allowed to indicate PG-15 as a potential leading compound for anti-inflammatory candidate that can be further optimized.

Acknowledgements

The authors would like to acknowledge the financial support by IM-IMOFAR/CNPq-Brazil (Process # 420015/05-1). Flávia De Toni Uchôa thanks CNPq-Brazil for the individual grant.

References

Blagden N, De Matas M, Gavan PT, York P (2007), Crystal engineering of active pharmaceutical ingredients to improve solubility and dissolution rates *Adv Drug Deliv Rev*. **30**: 617-630

Blanquart C, Barbier O, Fruchart JC, Staels B, Glineur C, (2003), Molecules with dissociated effects could be useful for the treatment of lipid disorders or inflammation *J Steroid Biochem Mol Biol* **85**: 267–273

Brandao SSF, Andrade AMC, Pereira DTM, Barbosa Filho JM, Lima MCA, Galdino SL, Pitta IR, Barbe J, (2004), Synthesis of new 1,3,5-trisubstituted-2-thioxoimidazolidinones *Heterocyclic Communications*, **10**: 9-14

Cayman Chemical Company Colorimetric (2005), *COX (ovine) Inhibitor Screening Assay, Booklet*, Cayman Chemicals, Ann Arbor.

Fahmi H., Pelletier J-P, Mineau F, Martel-Pelletier J, (2002), 15d-PGJ2 is acting as a 'dual agent' on the regulation of COX-2 expression in human osteoarthritic chondrocytes *Osteoarthr. Cartil*., **10**: 845–848

FDA. *Guidance for Industry. Bioanalytical Method Validation*. (2001), <http://www.fda.gov/cder/guidance/index.htm>

Farkouh ME, Kirshner H, Harrington RA, Ruland S, Verheugt Fw, Schnitzer TJ, Burmester Gr, Mysler E, Hochberg Mc, Doherty M, Ehrsam E, Gitton X, Krammer G, Mellein B, Gimona A, Matchaba P, Hawkey CJ, Chesebro JH; (2004), Study group.comparison of lumiracoxib with naproxen and ibuprofen in the Therapeutic Arthritis Research and Gastrointestinal Event Trial (TARGET), cardiovascular outcomes: randomised controlled trial'. *Lancet*. **21-27**: 675-684

Ferrandi C, Ardissone V, Ferro P, Rückle T, Zaratin P, Ammannati E, Hauben E, Rommel C, Cirillo R, (2007), Phosphoinositide 3-kinase gamma inhibition plays a crucial role in early steps of inflammation by blocking neutrophil recruitment. *J Pharmacol Exp Ther.* **322**: 923-930

Fraile RJ, Baker LH, Buroker TR, Horwitz J, Vaitkevicius VK, (1980) Pharmacokinetics of 5-fluorouracil administered orally by rapid Intravenous and by slow Infusion *Cancer Res*. **40**: 2223-2228

Funk CD, Fitzgerald GA, (2007) COX-2 Inhibitors and cardiovascular risk. *J Cardiovasc Pharmacol*. **50**: 470-479

Gonález LJ, Palma-García AJ, Arreola R, Brizuela V, Nava RJ, Morán-Lira S, Vela-Ojeda J, Castañeda-Hernández, G, Florres-Murrieta FJ, (1999) Comparative

bioavailability evaluation of two cyclosporine oral formulations in healthy mexican volunteers *Arch. Med. Res* **30**: 315-319

Guzman M, (2003) Cannabinoids: Potential Anticancer Agents *Nature Rev. Cancer* **3:** 745-755

Hawkey C, Kahan A, Steinbrück K, Alegre C, Baumelou E, Bégaud B, Dequeker J, Isomäki H, Littlejohn G, Mau J, Papazoglou, (1998) Gastrointestinal tolerability of meloxicam compared to diclofenac in osteoarthritis patients. International MELISSA Study Group. Meloxicam large-scale international study safety assessment. *S.Br J Rheumatol*. **37**: 937-45

Hawkey CJ. (1999) COX-2 Inhibitors *Lancet*. **353**: 307-314

Ialenti A, Grassia G, Di Meglio P, Pasquale M, Di Rosa M, Ianaro A, Mol Pharmacol,(2005) Mechanism of the Anti-Inflammatory Effect of Thiazolidinediones: Relationship with the Glucocorticoid Pathway **67**: 1620-1628

Klemm P, Harris HJ, Perreti M, (1995) Effect of rolipram in a murine model os acute inflammation: comparision with the corticoid dexamethasone *Eur J Pharmacol*, **281**: 69-74

Kulmacz, RJ., Lands, WEM. (1983) Requirements for hydroperoxide by the cyclooxygenase and peroxidase activities of prostaglandin H synthase*. Prostaglandins* **25**: 531-540

Kumar A, Rajput CS, Bhati SK (2007) Synthesis of 3-[4'-(*p*-chlorophenyl)-thiazol-2'-yl]-2-[(substituted azetidinone/thiazolidinone)-aminomethyl]-6-bromoquinazolin-4-ones as anti-inflammatory agent. *Bioorg Med Chem*. **15**: 3089-3096

Leite LFCC, Uchoa FDT, Lima MCA, Galdino SL, Pitta IR, Hernandes MZ, (2005) Docking studies of heterocyclic derivatives with potential COX-2 inhibition activities using Autodock In: *XII Simpósio Brasileiro de Química Teórica*, São Pedro pp.263.

Lesyk R, Vladzimirska O, Zimenkovsky B, Horishny V, Nektegayev I, Solyanyk V, Vovk O. (1998) New thiazolidones-4 with pyrazolone-5 substituent as the potential NSAIDs *Boll Chim Farm*. **137**: 210-7

Menezes, GB, Reis WG, Santos JMM, Duarte IDG, Francischi JN, (2005) Inhibition of prostaglandin F2 by selective cyclooxygenase 2 inhibitors accounts for reduced rat leukocyte migration', *Inflammation* **29**: 163-169

Missbach M, Jagher B, Sigg I, Nayeri S, Carlberg C, Wiesenberg I. (1996) Thiazolidine diones, specific ligands of the nuclear receptor retinoid Z receptor/retinoid acid receptor-related orphan receptor alpha with potent antiarthritic activity. *J Biol Chem*. **7**: 13515-13522

Mitchell JA, Warner TD, (2006) COX isoforms in the cardiovascular system: understanding the activities of non-steroidal anti-inflammatory drugs *Nature Reviews Drug Discovery*, **5**: 75-86

Murthy NS, Srinivasa V, (2003) Screening of new synthetic thiazolidine-4-ones for antiinflammatory activity in albino rats *Ind. J.Pharmacol.,* **35**: 61-62.

Nakagawa HI, Kato A, Debuchi H, Watanabe H, Tsurufuji K, Naganawa S, Mitamura M, (1992) Changes in the levels of rat interleukin 8/CINC and gelatinase in the exudate of carrageenin-induced inflammation in rats *J Pharmacobiodyn* **15**: 461-466

Oliani S, Damazo A, Perretti M, (2002) Annexin 1 localisation in tissue eosinophils as detected by electron microscopy *Mediators of Inflamm.*, **11**: 287–292

Ottanà R, Maccari R, Barreca Ml, Bruno G, Rotondo A, Rossi A, Chiricosta G, Di Paola R, Sautebin L, Cuzzocrea S, Vigorita MG, (2005) 5-Arylidene-2-imino-4-thiazolidinones: design and synthesis of novel anti-inflammatory agents. *Bioorg Med Chem*. **13**: 4243-52

Romano M, Faggioni R, Sironi M, Sacco S, Echtenacher B, Di Santo E, Salmona M, Ghezzi P, (1997) Carrageenan-induced acute inflammation in the mouse air pouch model. Role of tumour necrosis factor *Mediators of Inflamm*, **6**: 32-38.

Santos LC, Uchoa FDT, Cañas ARPA, Sousa IA, Moura RO, Lima MCA, Galdino SL, Pitta IR, Barbe J, (2005) Synthesis and anti-inflammatory activity of new thiazolidine-2,4-dione, 4-thioxothazolidinones and 2-thioxoimazolidinones *Heterocyclic Communications*, **11**: 121-128

Sedgwick AD, Sin YM, Edwards JC, Willoughby DA, (1983) Increased Inflammatory reactivity in newly formed lining tissue *J. Pathol.*, **141**: 483-495

Seibert K, Zhang Y, Leahy K, Hauser S, Masferrerj-Perkins W, Len L, Isakson P, (1994) Pharmacological and biochemical demonstration of the role of cyclooxygenase 2 in inflammation and pain *PNAS*, **91**: 12013-12017

Shargel L, Yu ABC, Wu-Pong S. (2005), *Applied Biopharmaceutics & Pharmacokinetics* McGraw-Hill, New York.

Silva AAR, Goes AJS, Lima WT, Maia MBS, (2003) Antiedematogenic activity of two Thiazolidine Derivatives: N-tryptophyl-5-(3,5-di-*tert*-butyl-4-hydroxybenzylidene) rhodanine (GS26) and N-tryptophyl-5-(3,5-di-*tert*-butyl-4-hydroxybenzylidene)-2,4-thiazolidinedione (GS28) *Chem. Pharm. Bull*. **51**: 1351-1355

Tetko IV; Bruneau P, (2004) Application of ALOGPS to predict 1-octanol/water distribution coefficients, logP, and logD, of AstraZeneca in-house database *J Pharm Sci*, **93**: 3103-10

Uchoa FDT, PhD Thesis, Universidade Federal de Pernambuco, Brazil, 2008.

Uchoa, F.D.T.; Cattani, V.B.; Lima MCA, Galdino SL, Pitta IR, Barbe J, Dalla Costa, T Development and Validation of LC-UV Method for the Quantification of the Anti-inflammatory Thiazolidinone PG15 in Rat Plasma; *J. Braz. Chem. Soc*. To submit.

Urquhart BL, Tirona RG, Kim RB. (2007) Nuclear receptors and the regulation of drug-metabolizing enzymes and drug transporters: implications for interindividual variability in response to drugs. *J Clin Pharmacol*. **47**: 566-578

Van Ryn J, Trummlitz G, Pairet M, (2000) Cox-2 selectivity and inflammatory processes *Curr. Med. Chem.*, **7**: 1145-1161

Vane JR, Botting RM, (2003) The mechanism of action of aspirin. *Thromb Res*. **15**: 255-258

Xie W, Reed D, Bradshaw WS, Simmons DI, (1995) Nonsteroidal antiinflammatory drugs cause apoptosis and induce cyclooxygenases in chicken embryo fibroblasts *PNAS*, **15**: 7961-7965

Wong SM, Kellaway IW, Murdan S, (2006) Enhancement of the dissolution rate and oral absorption of a poorly water soluble drug by formation of surfactant-containing microparticles. *Int J Pharm*. **317**: 61-68

Woods KW, Mccroskey RW, Michaelides MR, Wada CK, Hulkower KI, Bell RI, (2001) Thiazole analogues of the NSAID indomethacin as selective COX-2 Inhibitors *Bioorg. & Med. Chem. Let*. **11**:1325-1328

Table 1 COX-1 and COX-2 (ovines) inhibition by thiazolidinone PG15, celecoxib and indomethacin at 1 μM and 0,01 μM (average ± standard error (SE).

Compound	Concentration	COX-1 Inhibition % (mean ± SE)	COX-2 Inhibition % (mean ± SE)
PG-15	1 μM	39.1 ± 3.6	10.1 ± 3.0
	0.01 μM	30.0 ± 0.7	13.9 ± 3.7
Celecoxib	1 μM	0	47.5 ± 1.0
	0.01 μM	0	11.6 ± 1.0
Indomethacin	1 μM	100 ± 0.1	0
	0.01 μM	41.6 ± 0.1	0

Table 2 Anti-inflammatory activity exhibited to thiazolidinone PG-15 and standard drugs (aspirin, dexamethazone, nimesulide, indomethacin, celecoxib) given orally at respective doses. PMNL count is expressed as total cell number by exudate mL. Activity (%) is calculated considering control group cell counting as 100% and values are significant to an α =0.05 (ANOVA. Tukey's test).

Compound	Dose	PMNL/mL	Anti-inflamatory activity (average ± S.E.)
PG-15	0.8 mg/kg	$0.70 \pm 0.06 \times 10^6$	59.1± 3.5
	3 mg/kg	$0.56 \pm 0.08 \times 10^6$	67.2 ± 4.6
	12.5 mg/kg	$0.83 \pm 0.08 \times 10^6$	51.5± 4.6
	50 mg/kg	$1.04\ 0.05 \pm \times 10^6$	39.2± 2.9
Aspirin	200 mg/kg	$0.45 \pm 0.03 \times 10^6$	73.7± 2.04
Indomethacin	10 mg/kg	$0.76 \pm 0.07 \times 10^6$	55.5 ± 4.3
Dexamethazone	1 mg/kg	$0.40 \pm 0.1 \times 10^6$	76.6± 6.2
Nimesulide	5 mg/Kg	$1.16 \pm 0.1 \times 10^6$	32.2± 5.86
Celecoxib	10 mg/Kg	$0.27 \pm 0.06 \times 10^6$	84.2± 3.9
	CONTROL	$1.71 \pm 0.12 \times 10^6$	-

Table 3 Anti-inflammatory activity exhibited to thiazolidinone PG-15 given orally at 3 mg/kg and indomethacin given orally at 10mg/kg. Leukocyte count is expressed as total cell number by peritoneal exudate mL. Activity (average $\pm$ SE) is calculated considering control group cell counting as 100%. Values are significant to α =0.05 (ANOVA)

Compound	Leukocyte/mL	Anti-inflamatory activity (%)
PG-15 (3 mg/kg)	6.79×10^6	30.7 ± 4.2
CONTROL	9.80×10^6	-

Table 4 Pharmacokinetic parameters of thiazolidinone PG-15 following single i.v. dosing of 3 mg/kg to Wistar rats (n = 5).[c]

Parameters[b]	Compartmental Analysis[a]	Non-compartmental Analysis[a]
A (µg/mL)	71.3 ± 67.5	
B (ng/mL)	162.2 ± 98.2	
α (h^{-1})	21.28 ± 10.63	
β (h^{-1}) or ke (h^{-1})	0.16 ± 0.09	0.17 ± 0.08
$AUC_{0-\infty}$ (ng·h/mL)	3949 ± 2068	4025 ± 1496
Vc (L/kg)	0.11 ± 0.12	
Vd_{ss} (L/kg)	2.4 ± 1.8	1.9 ± 0.9
Vd_{area} (L/kg)	7.4 ± 4.2	
CL_{tot} (L/h/kg)	0.9 ± 0.5	0.9 ± 0.3
t½α (h)	0.04 ± 0.03	
t½β (h)	5.9 ± 3.8	4.7 ± 1.9
MSC range	2.93-4.98	

[a]Values represent average ± SD; [b]A = intercept of the distribution phase; B = intercept of the elimination phase; α = distribution rate constant; β = elimination rate constant; Vc = volume of the central compartment, Vd_{ss} = volume of distribution at steady sate, CL_{tot} = total clearance, k_e= elimination rate constant, t½α = distribution half-life; t½β = elimination half-life, MSC = model selection criteria. [c]No statistically difference were observed between the parameters estimated by both approaches (α = 0.05).

Table 5 Pharmacokinetic parameters of thiazolidinone PG-15 following oral dosing of 3 mg/kg to Wistar rats (n = 3) (Average ± SD)

Parameters	Compartmental analysis	Non-compartmental analysis
Vd (L/h)	9.7 ± 4.5	8.6 ± 2.0
CL_{tot} (L/h/kg)	1.4 ± 0.7	0.9 ± 0.5
$AUC_{0-\infty}$ (ng*h/mL)	692 ± 280	1113 ± 724
ka (h^{-1})	6.82 ± 3.08	
ke (h^{-1})	0.16 ± 0.07	0.09 ± 0.03
t½ (h)	5.2 ± 3.2	8.1 ± 3.5
C_{max} (ng/mL)	95.7 ± 54.6	214.5 ± 121.3
t_{max} (h)	0.6 ± 0.2	0.8 ± 0.1
Bioavailability	-	0.28
MSC range	0.11 to 0.56	-

Table 6 Pharmacokinetic parameters of thiazolidinone PG-15 following oral dose of mg/kg to Wistar rats. (Average ± SD)

Parameters	Sub-Group A (n = 3)	Sub-Group B (n = 4)
ke (h^{-1})	0.19 ± 0.11*	0.020 ± 0.015
t½ (h)	4.5 ± 2.2	69.5 ± 64.4
$AUC_{0-\infty}$(ng·h/mL)	465 ± 72,0	6506 ± 4842
% $AUC_{extrapolated}$	20.8 ± 13.0*	75.2 ± 18.6
CL_{tot} (L/h/kg)	0.8 ± 0.1	-
C_{max} (ng/mL)	150.8 ± 103.4	-
t_{max} (h)	0.42 ± 0.14	-
Bioavailability	0.06	-

*statistical difference (α = 0.05)

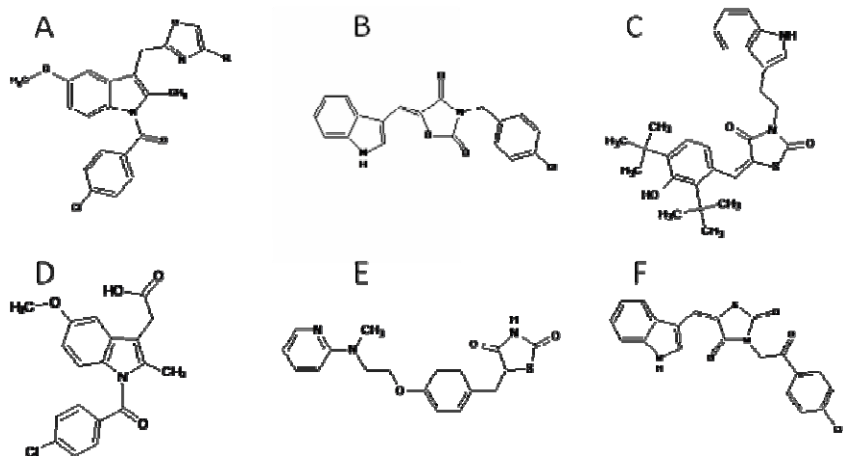

Figure 1 Chemical strucuture of (**A**) Indomethacin attached to thiazol group (R=Aromatic group); (**B**) 3-(4-Chlorobenzyl)-5-(1*H*-indol-3-ylmethylene)-4-thioxo-thiazolidin-2-one (LYS-5); (**C**) *N*-Triptofil-5-substituted-2,4-thiazolidinedione (GS28); (**D**) Indomethacin; (**E**) Rosiglitazone and (**F**) 5-(*Z,E*)-3-[2-(4-chlorophenyl)-2-oxoethyl]-5-(1*H*-indol-3-ylmethylene)-thiazolidine-2,4-dione (PG-15).

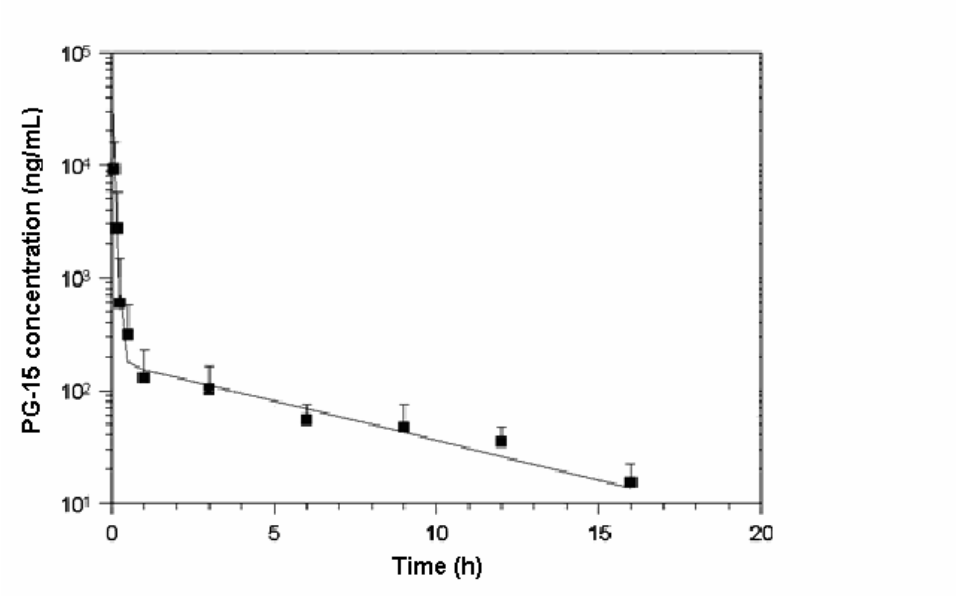

Figure 2 Mean plasma profile of thiazolidinone PG-15 after a single 3 mg/kg i.v. dose (n = 5) (Average ± S.D).

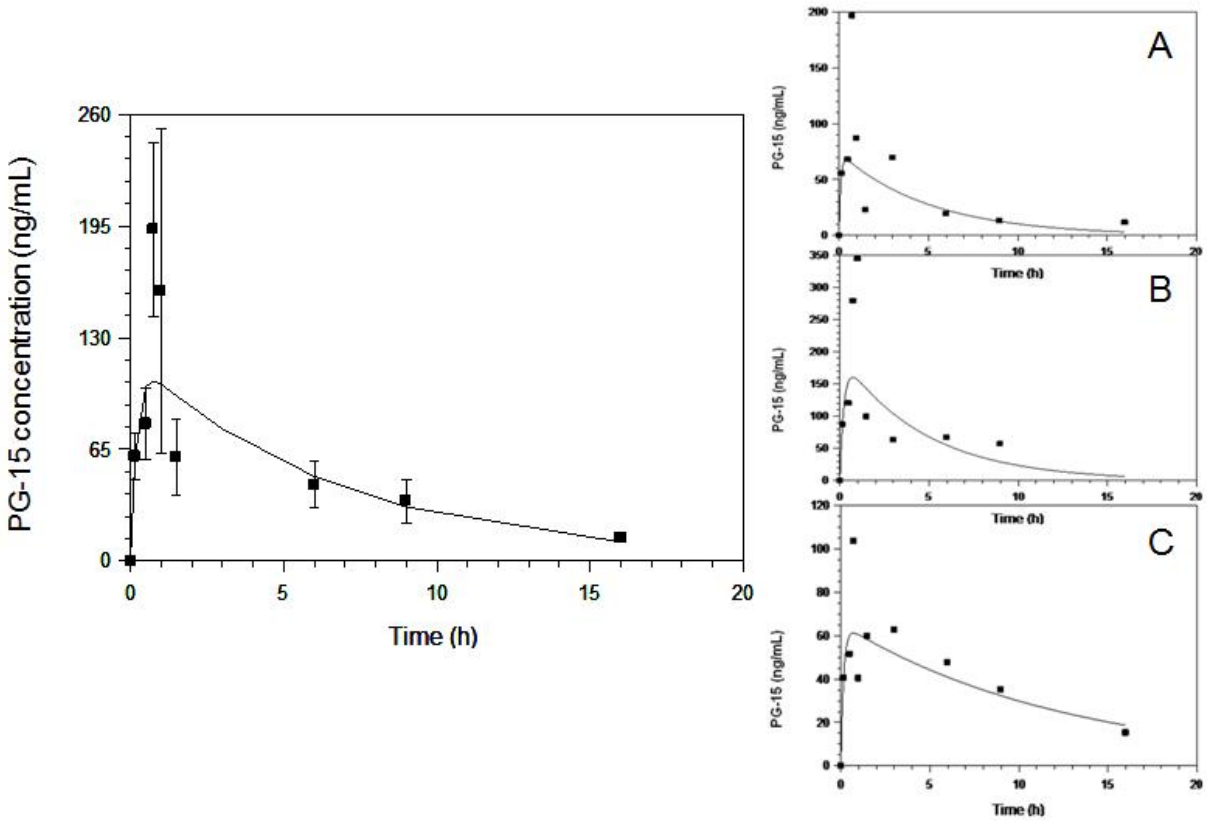

Figure 3 Mean (A) and individual (B, C, D) plasma profiles of thiazolidinone PG-15 after a single 3 mg/kg oral dose (Mean ± SD) (n = 3). (Average ± SE).

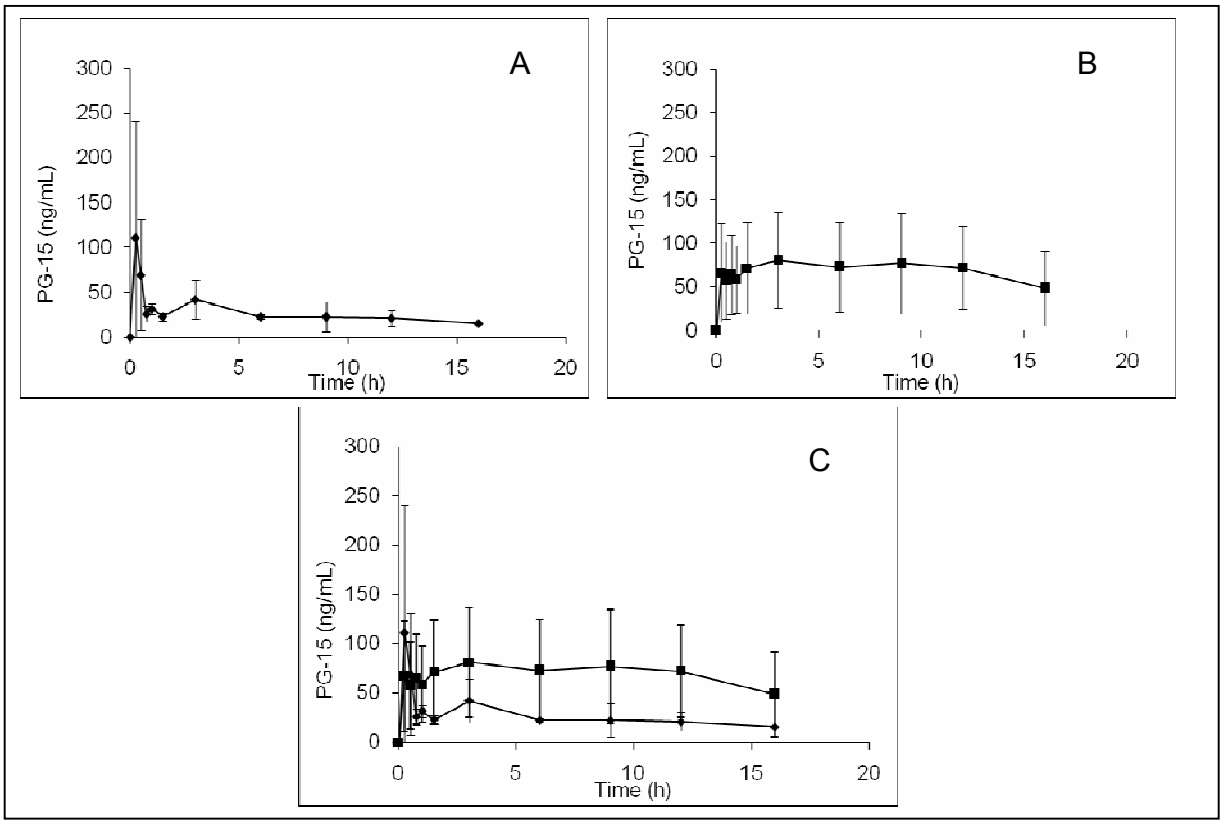

Figure 4 Mean plasma profile of thiazolidinone PG-15 after a 6 mg/kg oral dosing. Distinct profiles can be observed: (A) Sub-group A - profile similar to that obtained after 3 mg/kg oral dosing (n = 3); (B) Sub-group B – Maintenance of plasma levels for 16 hours post-dosing (n = 4); (C) superposition of profiles of sub-groups A (◆) and B (■) profiles (Average ± SE).

Artigo 5

Synthesis, receptor docking studies and anti-inflammatory activity of new 3,5-imadozilines and thiazolidines derivatives

O artigo encontra-se no formato para submissão no Bioorganic and Medicinal Chemistry (ISSN: 0968-0896; Fator de Impacto 2006: 2,624)

Synthesis, receptor docking studies and anti-inflammatory activity of new 3,5-imadozilines and thiazolidines derivatives

Graphical abstract

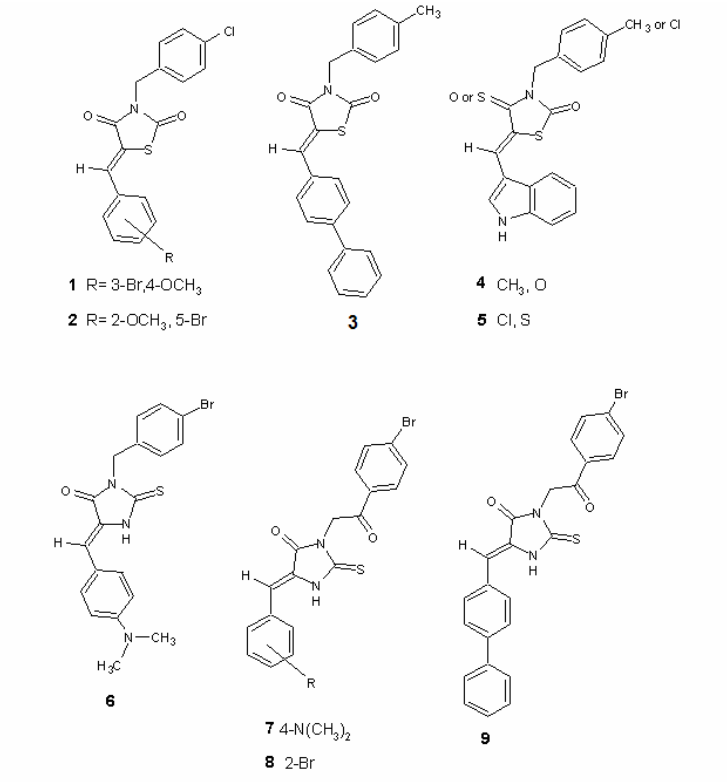

Synthesis, receptor docking studies and anti-inflammatory activity of new 3,5-imadozilines and thiazolidines derivatives

Flávia De Toni Uchôa[1], Lúcia Fernanda C. da Costa Leite[2], Diana Jussara Nascimento Malta[1], Daniel Tarciso Pereira[1], Marcelo Zaldini Hernandez[3], Maria do Carmo Alves de Lima[1], Ivan da Rocha Pitta[1]*, Suely Lins Galdino[1]

[1]Departamento de Antibióticos, [3]Departamento de Ciências Farmacêuticas - Universidade Federal de Pernambuco, Brazil

[2]Departamento de Química - Universidade Católica de Pernambuco, Brazil

Av. Prof. Moraes do Rego, S/N - Recife-PE. CEP 50.670-901

*ivan.pitta@pesquisador.cnpq.br

Abstract

In order to seek for new anti-inflammatory candidates, a series of 3,5-disubstituted-thiazolidines and imidazolidines derivatives was prepared by a simple synthetic pathway comprising three steps. Proof of the structure and configuration was obtained through ^{1}H NMR, IR, and MSA. All derivatives exhibited significant activity levels in carrageenin induced rat paw edema model. Some compounds were also tested to COX-2 inhibition *in vitro*. In addition, a docking study was performed in order to determine differences in binding modes of compounds in the cyclooxygenase channel. The results showed that only 5-(4-dimethylamine-benzilidene)-3-(4-bromine–phenacyl)-2-thioxo-imidazolin-4-one (**7**) had similar orientation of SC-558, a specific COX-2 inhibitor.

docking / imadazoline / thiazolidine / COX-2

1. Introduction

Cyclooxygenase (COX) is an endogenous enzyme that catalyses the first step of arachidonic acid conversion into prostaglandins and thromboxanes. COX is competitively inhibited by a group of drugs known as non-steroidal anti-inflammatory drugs (NSAIDs). It was discovered in 1971[1] that COX is the molecular targets for NSAIDs. Non-steroidal anti-inflammatory drugs NSAIDs[2,3] are of immense benefit in the treatment of inflammatory diseases. Their action results in anti-inflammatory, analgesic, antipyretic and antithrombotic activity exhibited by this group of molecules[4]. Members of this group include well known therapeutic agents like aspirin, diclofenac, ibuprofen, indomethacin or naproxen[5]. Despite their beneficial action, their activity is associated with deleterious side effects, and continuous administration of these drugs leads to renal toxicity and gastric ulcerations. Consequently, new NSAIDs without side effects are necessary for safer treatments.

In early 1990s, COX was demonstrated to exist as two distinct isoforms. COX-1 is expressed constitutively as housekeeping enzyme in nearly all tissues, and mediates physiological response (e.g., stomach cytoprotection, platelet aggregation)[6]. COX-2 is an inducible form that is presented only in inflammatory states[7], releasing metabolites that are used to induce inflammation and pain[8]. Drugs selectivity in their inhibition of COX-2 act by binding to a pocket in the enzyme that is presented in COX-2 but not in COX-1, as SC-558, a vicinal di-arylic compound with a central pyrazole ring (Figure 1). The therapeutic anti-inflammatory action of NSAIDs is produced by inhibition of COX-2, while the unwanted side effects arise from inhibition of COX-1 activity (Vane, 1996).

Clinical trials with COX-2 inhibitors have been reported to cause less incidence of gastrointestinal side effects than nonselective COX inhibitors[9,10]. Recently, COX-2 selective inhibitors have been associated with an increased cardiovascular risk due the inhibition of prostacyclin synthesis in endothelial tissue[11]. While the selective COX-2 inhibitors situation in therapeutics remain unclear, it is known that selective COX or non-selective inhibitors remains the best therapeutic choice to treat acute and chronic inflammatory diseases[12].

Figure 1

Several new molecules have been synthesized exhibiting anti-inflammatory activity. Heterocyclic compounds such as thiadizoles[13,14], pyrimidines[15,16], imidazole[17,18,19], triazole[20], thiazolidine[21], indazole[22] and phthalimide[23,24] have been tested successfully.

Aiming COX-2 inhibition, Ali and co-workers[25] synthesized new 2,4-thiazolidinedione derivatives which exhibited good anti-inflammatory activity and were docked into COX-1 and COX-2 X-ray structures, using DOCK6 program revealing a significant preference for COX-2. Related compounds, 5-arylidene-2-imino-4-thiazolidinones, were synthesized by Ottaná and co-workers[26]. From this serie, the compound 5-(4-methoxyphenylidene)-2-phenylimino-3-propyl-4-thiazolidinone exhibited significant activity in models of acute inflammation such as carrageenin-induced paw and pleurisy edema in rats and was docked in the known active site of COX-2 protein showing that its 4-methoxyarylidene moiety can easily occupy the COX-2 secondary pocket considered as the critical interaction for COX-2 selectivity.

With an imidazolidinic central ring, the compound 5-phenyl-3-(4-CF_3-phenyl)-2-thioxoimidazolidin-4-one was design as new COX-2 inhibitor and presented complete inhibition of human recombinant COX-2 at 50 mM, but failed in inhibition of COX-2 in human blood, due to its poor aqueous stability[27].

With the thiazolidinic and imidazolinic as central ring, we showed the synthesis of promising anti-inflammatory molecules, their evaluation in paw edema model and docking studies of thiazolidinic and imidazolidinic derivatives substituted in 3 and 5 position (1-9) (Table 1).

Table 1

2. Chemistry

The synthetic route used to obtain thiazolidinic and imidazolidinic derivatives (1-9) (Figure 2) starts with thiazolidine-2,4-dione and imidazolidin-2-thioxo-4-one.

The general method used to prepare the thiazolidinic final compounds (1-5) is shown in Figure 2. They were synthesized with thiazolidne-2,4-dione as starting material, followed by a *N*-alkylation reaction at *N*-3 position of the thiazolidine ring followed or not by the thionation in position 4 in presence of phosphorous pentasulfide. The final step was done by a Michael addition with appropriate ethyl 2-cyano-3-phenylacrylate.

Synthesis of appropriate acrylate was carried out by the Knoevenagel's condensation of substituted aromatic aldehydes and ethyl cyanoacetate in alkaline medium to obtain the 2-cyano-3-substituted-ethyl acrylate esters.

Figure 2

The method used to prepare compounds 6-9 is shown in Figure 3, which was synthesized with 2-cyano-3-substituted-ethyl acrylate esters that reacts by a Michael addition with 2-thioxo-imidizazoline-4-one, followed by a *N*-alquilation reaction at N-3 position of the imidazolidine ring. The structure of the compounds was confirmed by IR, ^{1}H-NMR and Mass spectral data.

Figure 3

3. Biological

The *in vivo* anti-inflammatory activity of synthesized compounds was determined using carrageenin induced rat paw edema[28]. Compounds 1-9 were given intraperitoneally (50mg/kg) one hour before the edema induction. Control group received only vehicle. Preliminary results revealed that tested compounds exhibited good biological activity. The results are presented in Table 2 and are discussed in terms of structural characteristics.

Compound 2 (50mg/kg, p.o.) was also evaluated to anti-inflammatory activity by air pouch model. Air pouches were formed by a subcutaneous injection of air, as described by Klemm, Harris and Parretti[29] and inflammation was induced by

carrageenin injected into the pouches[30]. After experiment, leukocytes presented in exudates fluid were counted. Treated and control groups were compared in terms of leukocyte counting. Results are listed in Table 3.

Compounds 2, 6, and 7 were tested for *in vitro* COX-2 inhibition, using the colorimetric Ovine Cyclooxygenase assay kit (Cayman Chemical Company, USA) where inhibition of enzyme activity was determined calorimetrically as described by Kulmacz and Lands[31]. Inhibition results are presented in Table 4.

4. Docking Study

The FlexX® is an automated docking program that considers ligand conformational flexibility by an incremental fragment placing technique[32] The crystal structure of COX-2 in complex with SC-558 (Figure 1), a selective COX-2 inhibitor, was recovered from RCSB Protein Data Bank (http://www.rcsb.org/pdb) (6COX – PDB code). Conformation and space orientation of SC-558 (Figure 1) extracted from the X-ray crystallographic inhibitor–enzyme complex were used as a template for the construction of the 3,5-disubstituted-thiazolidines and imidazolidines derivatives at the enzyme active site level. The active site was defined by all atoms within 6.5 A° radius of the co-crystallized ligand. The proposed interaction mode of the ligands in the active site of 6COX was determined as the highest scored conformation (best-fit ligand) among 30 conformational and binding modes generated according to FlexX® scoring function. The initial structures of heterocyclics derivatives were generated by the application of AM1[33] method available in BioMedCache® software [BioMedCAChe version 6.1, Copyright ©2000-2003 Fujitsu Limited, Copyright©1989-2000, Oxford

Molecular Ltd., http:///www.CACheSoftware.com], using internal default settings for convergence criteria. Compounds' geometries were subsequently optimized using the Tripos force field with Gasteiger-Hückel charges (Sybyl, Version 7.2. Tripos Associates: St. Louis, MO, 2006). The most stable docking solutions for the thiazolidinic and imidazolidinic compounds (1-9) complexed with the COX-2 are presented in table 2, with the score of binding values.

5. Results and discussion

A modeling study using FlexX® program was performed to dock the compounds (1-9) into the active site of the enzyme viewing to investigate the molecular characteristic of heterocyclic derivatives possibly associated with the inhibition of COX-2. In order to find possible correlations between experimental and theoretical data, the score of binding (kJ), used for distinguishing good from bad placements, and percent edema inhibition, presented in Table 1, was plotted against each other. No linear correlation between anti-inflammatory effect and score of binding was observed. Interestingly, when score of binding was plotted against LogP of the compounds (calculated by Tekto's method[34]), a correlation was observed suggesting that 3,5-imadazolidines and thiazolidines lipophilicity and COX-2 affinity had a direct relationship, as seen in Figure 4. In the same way, when edema inhibition was plotted against LogP of the compounds, a linear relationship was detected, when better anti-inflammatory activity was related with lower LogP, as seen in Figure 4. Analysing data from this point of view, compounds appeared to exhibit a reversal relationship between activity and capability to bind COX-2 (Figure 5), showing that molecules with more stable or negative energies are less active.

Table 2 and Figure 4 and 5

When score of binding results were compared with COX-2 *in vitro* inhibition, we observed that compound 7, which exhibited best binding from series, comparable to standard inhibitor SC-588, was also the best inhibitor in *in vitro* study, again comparable to standard drug celecoxib. Other tested compounds did not exhibited COX-2 inhibition in tested dosis.

Table 4

This finding could be possibly related to how 3,5-imadozolidines and thiazolidines are binding to COX-2. Only compound 7 fitted enzyme in exactly the same position of standard inhibitor SC-588, as seen in Figure 6a. Compounds 1, 3, 4, 5, 6 and 9 were occupying same site (Figure 6b), which was a different spot that was reported as “alcove mode” by Gauthier and co-workers[27] to similar imidazolidine compounds. Apparently, they occupied a secondary space between lipophilic alcove created by aminoacids Leu-384 and Leu-503 and polar side-pocket, where they bonded with Gln-192, making only a partial steric inhibition on active site channel. Besides, within these 6 compounds, structures in best fitting mode were not superimposed. We observed that all compounds that fit in this “left mode” formed hydrogen bonds between carbonyl group of central ring and Gln-192, but 1, 4, 5 and 9 fitted with arylidenic moiety oriented to internal side of the enzyme, while 3 and 6 were oriented with benzilic part more inside and arylidenic moiety were placed almost outside of enzyme channel, binding His-90 and Ser-354, respectively. So for this group of molecules, it was reasonable to suppose that there was no influence on the mechanism of araquidonic acid catalyzing.

For compounds 2 and 8, something interesting was observed. Both compounds fitted neither SC-588 nor “left mode” presented by 1, 3, 4, 5, 6 and 9. Compound 2 fitted in external position of the active site, while compound 8 occupied a space in the opposite side of “left mode” (Figure 6c and 6d). Thiazolidinic carbonyl group of compounds 2 and 8 binds with His-90 and Tyr 385, respectively. His-90 is an amino acid that takes place on active site entrance, while compound 8 bounded with Tyr-385, which is at the COX site of peroxydation, involved in abstraction of the 13-proS hydrogen from arachidonate[35].

Because a reversal relationship between docking and biological studies was observed, and *in vitro* COX-2 inhibition and docking study results suggested that compounds are not COX-2 inhibitors, we tested compound 2 in the air pouch model, aiming to verify if anti-inflammatory activity will be persistent in another model. Results presented in Table 3 shows that compound 2 exhibited anti-inflammatory activity. Comparing with controls from both assays in air pouch, compound 3 was less effective, which could be related to a difference in inflammatory response evocated by the two methods or a difference in administration route. As anti-inflammatory activity was confirmed, we can suggest that there is a strong possibility that 3,5-arylidene imadazolidin and thiazolidines acts in inflammation by a mechanism which does not involve COX-2.

As PPARs α and γ were involved in inflammation resolution[36], and earlier docking studies in PPARγ and PPARα and reduction on plasmatic levels of glucose and triglycerides were observed to similar thiazolidine compounds[37], we could infer that results in inhibition on paw edema observed for 3,5-imazolidine and thiazolidine

compounds, except compound 7, could be related to PPAR activation, instead of COX-2 inhibition.

6. Conclusion

Synthesized compounds exhibited anti-inflammatory activity in carrageenin induced paw edema. Compound 2, has anti-inflammatory activity in air pouch model. Inhibition of COX-2 in an *in vitro* assay reveals that compound 7 is a COX-2 inhibitor. Docking study was consistent with COX-2 inhibition, and only compound 7 was docked in active site as SC-588 standard inhibitor. Compounds activity is probably derived from the interference in an inflammation pathway that did not involve COX-2 enzyme.

7. Experimental methods

7.1 General Remarks

All chemicals were purchased as reagent grade and used without further purification. Reactions were monitored with analytical thin layer chromatography (TLC) in EM silica gel 60 F254 plates and visualized under UV (254 nm). Flash column chromatography was performed using Merck silica gel 60 (230-400 mesh). Melting points were determined on a Quimis 340 capillary melting point apparatus and were not corrected. The infrared spectra were recorded as KBr discs using a BRUKER (IFS 66) infrared spectrophotometer. ^{1}H NMR spectra were recorded on a UNITYplus – 300 MHz – VARIAN spectrometer at 20 °C. Chemical shifts (δ ppm) were assigned according to

the internal standard signal of tetramethylsilane in $DMSOd_6$ (δ = 0 ppm). Coupling constants (J) are reported in Hz. Splitting patterns are described by using the following abbreviations: s, singlet; d, doublet; t, triplet; q, quartet; m, multiplet. ^1H NMR spectra are reported in this order: chemical shift; multiplicity; number(s) and type of proton and coupling constant(s). Mass spectra was recorded with Varian Plus (70 eV) R-1010C Delsi-Nermag.

Intermediates were previously reported by our group[38,39,40]. Compounds 2, 3, 4 and 6 were synthesized as previously reported[21].

7.2 Typical esters-acrylate synthesis reaction

A mixture of substituted aromatic adehydes (32 mmols), ethyl cyanoacetate (32 mmols), piperidin (catalytic amount) and anhydrous benzene, used as solvent, was refluxed at 110°C in a system coupled with a Dean-Stark to separate the water formed. When no more water was formed, reaction was stopped. This time could vary from for 4 to 24hours. Mixture was kept in the refrigerator during 12-24 hours, and crystals formed separated by filtration. The obtained cyanoacrylate esters was purified by recrystalization with hot ethanol.

7.3 Typical thiazolidinic reaction procedure

A solution of thiazolidine-2,4-dione (TZD) (50mmols) an Potassium Hydroxide (50mmols) in methanol was added drop by drop of appropriated aromatic halide (55mmols). The reaction was stirred at 65°C and followed by a thin layer

chromatography until TZD was totally consumed. The mixture was filtrated while warm, liquid part was cooled, and crystals of N-alkylated-TZD (N-TZD) were filtrated and dried in vacuum desiccator. To obtain *N*-alkylated-4-thizo-thiazolidin-2-one (N-4STZ), N-TZD (8mmols) was reacted with phosphorus pentasulfide (8mmols) using dioxan as solvent under argon atmosphere. The reaction was stirred at 90°C for 24 hours. (N-4STZ) was purified by column chromatography on flash silica gel (hexane / EtOAc = 8:2). N-TZDs or N-4STZ (2mmols) was reacted with appropriated cyanoacrylate (2mmols) in ethanol with catalytic amount of piperidin at 50°C and reaction times vary from 1 hour to 2 days. Precipitated product was filtrated and dried in vacuum desiccator.

7.3.1 *(Z) 5-(3-bromine-4-metoxy-benzylidene)-3-(4-chloro-benzyl)-thiazolidine-2,4-dione* **1**.

$C_{18}H_{13}ClBrNO_3S$, yield: 83%. Mp: 190-191°C. TLC *n*-hexane: ethyl acetate (70:30) R_f: 0,75. IR cm^{-1} (KBr): υ 1.592(CH=), 1739(C=O), 1676 (C=O). H^1NMR (δ ppm, DMSO-d_6): 7,93 (s, =CH), 4,82 (s, CH2), 3,93(s,OCH3), 7,42 (d, BLH), 7,34 (d, BLH), 7,91 (d, BZH), 7,64(dd,BZH), 7,30 (d, BZH)

7.3.2 *(Z) 5-(5-bromine-2-metoxy-benzylidene)-3-(4-chloro-benzyl)-thiazolidine-2,4-dione* **2**

$C_{18}H_{13}ClBrNO_3S$, yield: 77%. Mp: 164-165°C. TLC *n*-hexane: ethyl acetate (70:30) R_f: 0,82. IR cm^{-1} (KBr): υ 1.593(CH=), 1735(C=O), 1685 (C=O). H^1NMR (δ ppm, DMSO-d_6): 7,97 (s, =CH), 4,82 (s, CH2), 3,89(s,OCH3), 7,34 (d, BLH), 7,42 (d, BLH), 7,55 (d, BZH), 7,67(dd,BZH), 7,15 (d, BZH)

7.3.3 *(Z) 5-(1-1'-biphenyl-4-il-methylene)-3-(4-chloro-benzyl)-thiazolidine-2,4-dione* **3**

$C_{23}H_{16}ClNO_2S$, yield: 81%. Mp: 191-195°C. TLC *n*-hexane: ethyl acetate (70:30) R_f: 0.95. IR cm^{-1} (KBr): υ 1.600(CH=), 1752(C=O), 1688 (C=O). H^1NMR (δ ppm, DMSO-d_6): 8,02 (s, =CH), 4,85 (s, CH2), 7,43 (d, BLH), 7,36 (d, BLH), 7,75 (d and dd overlap,BZH), 7,88 (d,BZH), 7,47 (m, BZH)

7.3.4 *5-(1-H-indol-3-il-methylene)-3-(4-methyl-benzyl)-thiazolidine-2,4-dione* **4**

$C_1H_1ClNO_2S$, yield: %. Mp: 229-231°C. TLC *n*-hexane: ethyl acetate (70:30) R_f: . IR cm^{-1} (KBr): υ 3.406 (NH), 1.595(CH=), 1727(C=O), 1664 (C=O). H^1NMR (δ ppm, DMSO-d_6): 7,82 (s, =CH), 4,78 (s, CH2), 9,09 (s, NH), 2,27 (s, CH3), 7,29-7,14 (m, INH), 7,92 (d, BLH), 7,51 (d, BLH). Ms, m/z (%):M+ 348.

7.3.5 *5-(1-H-indol-3-il-methylene)-3-(4-chloro-benzyl)-4-thioxo-thiazolidin-2-one* **5**

$C_{19}H_{13}ClN_2OS_2$, yield: 70%. Mp: 145-147°C. TLC *n*-hexane: ethyl acetate (70:30) R_f: 0.57. IR cm^{-1} (KBr): υ 3.260 (NH), 1.598 (C=C), 1.724 (C=O), 1.490 (C=S). H^1NMR (δ ppm, DMSO-d_6): 8,22 (s, =CH), 4,83 (s, CH2), 12,23 (s, NH), 7,92-24 (m, INH), 7,43 (d, BLH), 7,34 (d, BLH). Ms, m/z (%):M+ 384

7.4 Typical imidazolidinic reaction procedure

The 2-cyano-3-substituted-ethyl acrylate esters (3mmols) were reacted with 2-thioxo-imidizazoline-4-one (4TID) (3mmols) piperidin (catalytic amount) in anhydrous ethanol. Temperature rose slowly until reflux temperature and remained the same, until 4TID

was totally consumed. Reaction time varies from 1-12 hours. Mixture was filtrated and 5- substituted-4TDI was purified by washing with appropriate solvent. 5-substituted-4TDI (1,5 mmols) was solubilizated in methanol with potassium carbonate (1,5 mmols) and 1,5 mmols of appropriated aromatic halide, which was added drop by drop. Mixture was stirred at room temperature during 12-48 hours. When all reagents were consumed, final product was filtrated, washed with cold ethanol and dried in vacuum dessicator.

7.4.1 *(Z) 5-(4-dimethylamine-benzilidene)-3-(4- bromine –benzyl)-2-thioxo-imidazolin-4-one* **6**

$C_1H_1NO_2SBr$, yield: %. Mp: 220-222°C. TLC *n*-hexane: ethyl acetate (70:30) R_f: . IR cm^{-1} (KBr): υ. H^1NMR (δ ppm, DMSO-d_6): 3,00 (s, N(CH3)2), 4,50 (s, CH2), 6,66 (s,=CH), 11,50 (s, NH), 7,47 (d, BLH), 7,54 (d, BLH), 6,75 (d, BZH), 8,03 (d, BZH). Ms, m/z (%): M+2=417

7.4.2 *(Z) 5-(4-dimethylamine-benzilidene)-3-(4- bromine –phenacyl)-2-thioxo-imidazolin-4-one* **7**

$C_1H_1BrNO_2S$, yield: %. Mp: °C. TLC *n*-hexane: ethyl acetate (70:30) R_f: . IR cm^{-1} (KBr): υ 1.526 (C=C), 1.701 and 1624 (C=O), 1.589 (C=S).. H^1NMR (δ ppm, DMSO-d_6): 2,94 (s, N(CH3)2), 4,86 (s, CH2), 6,54 (s,=CH), 11,63 (s, NH), 8,11 (d, PHL)J=8,7, 7,89 (d, PHL)J=8,7, 6,22 (d, BZH)J=9, 7,60 (d, BZH)J=9. Ms, m/z (%):M+2= 445

7.4.3 *(Z) 5-(2-bromine-benzilidene)-3-(4- bromine –phenacyl)-2-thioxo-imidazolin-4-one* **8**

$C_1H_1BrNO_2S$, yield: %. Mp: °C. TLC *n*-hexane : ethyl acetate (70:30) R_f: . IR cm^{-1} (KBr): υ3060 (NH), 1.507 (C=C), 1.710 (C=O), 1.631 (C=S). H^1NMR (δ ppm, DMSO-d_6): 4,93 (s, CH2), 6,89 (s,=CH), 12,03 (s, NH), 8,11 (d, PHL)J=8,7, 7,89 (d, PHL)J=8,7, 7,63 (d, BZH)J=7,8, 7,17 (d, BZH)J=7,8, . Ms, m/z (%): M+2=480

7.4.4 *(Z) 5-(1-1'-biphenyl-3-il-metilene)-3-(4- bromine –phenacyl)-2-thioxo-imidazolin-4-one* **9**

$C_1H_1BrNO_2S$, yield: %. Mp: °C. TLC *n*-hexane: ethyl acetate (70:30) R_f: . IR cm^{-1} (KBr): υ. H^1NMR (δ ppm, DMSO-d_6):; Ms, m/z (%): M+2=478

7.5 Carrageenin induced paw edema

Experiments were performed following ethical guidelines of Brazilian Council of Animal Experimentation and were approved by Universidade Federal de Pernambuco Ethics in Animal Experimentation Committee (protocol #23076.011488/2005-35). Male Wistar rats (300-400g) were used. Hind paw volume was measured before and until 5 hours after an 1% carrageenin injection into the subplantar region of the left hind paw using a manual hydroplethysmometer. The 1-9 compounds were given intraperitoneally (50mg/kg) one hour before the edema induction. Control group received only vehicle (0,9% NaCl solution + 2% Tween 80). The volume (ml) of a hind paw of control group and treated groups were compared and reported as percent of the control paw (see

Table 1). Statistical analysis was done by T-test, with α=0,05 (table 2). Statistical significance was set at $P < 0.05$.

7,6 Air pouch model

To induce air pouches, male and female swiss mice (n=10) were injected subcutaneously on the back with 2.5 ml of air. After 3 days, the pouches were reinflated with 2.5 ml of air. On day 6, animals received orally compound 2 (50 mg/kg). One hour later, inflammation was induced by injecting 1 ml of a suspension of carrageenin (1% weight/volume in saline solution) into the air pouch, as described by Klemm, Harris and Parretti[29] adapted by Romano and co-workers[30]. After 6 hours, animals were sacrificed, the pouches were flushed with 3 ml of phosphate buffered saline (PBS) with heparin (10UI/mL), and exudates were harvested. Aliquots were diluted with Turk Solution, and leukocytes were counted in a Newbauer chamber. Leukocyte count is expressed as total cell number by exudate mL. Activity (%) is calculated considering control group cell counting as 100% and values are significant to an α =0.05 (ANOVA, Tukey's test).

7.7 COX-2 *in vitro* inhibition

COX-2 inhibition assay was performed using the colorimetric Ovine Cyclooxygenase (COX) assay kit (Cayman Chemical Company, USA). Inhibition of enzyme activity was determined by a colorimetric assay as previously described by Kulmacz and Lands[31]. The assay measures the peroxidase component of cyclooxygenases which is assayed colorimetrically by monitoring the appearance of oxidized N,N,N',N'-tetramethyl-p-phenylenediamine (TMPD) to form a blue compound

(590 nm) which reflect the rate of conversion of arachidonic acid to PGH_2. Different dilutions of 2, 6 and 7 were prepared in dimethyl sulfoxide (DMSO) and diluted further to derive the appropriate concentrations for testing. The assay was then performed as described in the assay kit booklet[41].

8. Acknowledgements

The authors would like to acknowledge the financial support by CNPq – Brazil. Flávia De Toni Uchôa thanks CNPq-Brazil for the individual grant.

9. References

1. Marnett, L.J., Kalgutkar, A.S. *Trends Pharmacol. Sci*.**1999**, *20*, 465.

2. Mantri, P., Witiak, D. *Curr. Med. Chem*.**1994** *1*, 328.

3. Vane, J.R., Botting, R. *Scand. J. Rheumatol. Suppl*.**1996**, *102*, 9.

4. Llorens, O., Perez, J.J., Palomer, A., Mauleon, D. *J. Mol. Graph. Model.*,**2002** *20*, 359.

5. Griswold, D.E., Adams, J.L. *Med. Rse. Rev*.,**1996** *16*, 181.

6. Ermondi, G., Caron, G., Lawrence R., Longo, L. *J. Comp.Aid. Mol. Des.*, **2004**, *18*, 683.

7. Price, M.L.L.P., Jorgensen, W.L. *J. Am. Chem. Soc*.,**2000** *122,* 9455.

8. Kargman, S., Chalerson, M., Cartwright, J., Frank, D., Riendeau, J., Mancini, J., .O'Neil, G. *Gastrenterol*, **1996**, *111*, 445.

9. Farkouh, M.E., Kirshner, H., Harrington, R.A., Ruland, S., Verheugt, F.W., Schnitzer, T.J., Burmester, G.R, Mysler, E., Hochberg, M.C., Doherty, M., Ehrsam, E., Gitton, X.,

Krammer, G., Mellein, B., Gimona, A., Matchaba, P., Hawkey, C., Chesebro, J.H. *Lancet*. **2004,** *21*, 675.

10. Hawkey, CJ. *The Lancet*.**1999,** 353, 307.

11. Funk, C.D., Fitzgerald, G.A., *J Cardiovasc Pharmacol*.**2007** *50*, 470.

12. Mitchell, J.A., Warner, T.D. *Nature Reviews Drug Discovery*, **2006,** *5*, 75.

13. Song, Y., Connor, D.T., Sercel, A.D., Sorenson, R.J., Doubleday, R., Unangst, P.C., Roth, B.D., Beylin, V.G., Gilbertsen, R.B, Chan, K., Schrier, D.J., Guglietta, A., Bornemeier, D.A, Dyer, R.D..*J Med Chem*. **1999** *42,* 1161.

14. Gadad, A.K., Palkar, M.B., Anand, K., Noolvi, M.N., Boreddy, T.S., Wagwade, J. *Bioorg Med Chem*. **2008,** *16,* 276.

15. Quintela, J.M., Peinador, C., González, L., Devesa, I., Ferrándiz, M.L., Alcaraz, M.J., Riguera, R. *Bioorg Med Chem.* **2003**; *11*, 863.

16. Orjales, A., Mosquera, R., López, B., Olivera, R., Labeaga, L., Núñez, M.T. *Bioorg Med Chem*. **2007** Dec 5; [Epub ahead of print]

17. Wiglenda, T., Ott, I., Kircher, B., Schumacher, P., Schuster, D., Langer, T., Gust, R. *J Med Chem*. **2005** *48,* 6516.

18. Almansa, C., Alfón, J., de Arriba, A.F., Cavalcanti, F.L., Escamilla, I., Gómez, L.A., Miralles, A., Soliva, R., Bartrolí, J., Carceller, E., Merlos, M., García-Rafanell, J. *J Med Chem.* **2003**, *46*, 3463.

19. Navidpour, L., Shadnia, H., Shafaroodi, H., Amini, M., Dehpour, A.R., Shafiee, A. *Bioorg Med Chem*. **2007,** *15*, 1976.

20. Navidpour, L., Shafaroodi, H., Abdi, K., Amini, M., Ghahremani, M.H., Dehpour, A.R., Shafiee, A. *Bioorg Med Chem*. **2006**, *14*, 2507.

21. Santos, L.C.; Uchoa, F.T.; Canas, A.R.P.A.; Sousa, I.A.; Moura, R.O.; Lima, M.C.A.; Galdino, S.L. ; Pitta, I.R.; Barbe, J. *Heterocyc. Comm.*, **2005,** *11*, 121.

22. Rosati, O., Curini, M., Marcotullio, M.C., Macchiarulo, A., Perfumi, M., Mattioli, L., Rismondo, F., Cravotto, G. *Bioorg Med Chem.* **2007,** *15*, 3463.

23. Lima, L.M., Castro, P., Machado, A.L., Fraga, C.A,. Lugnier, C., de Moraes, V.L., Barreiro, E.J. *Bioorg Med Chem.* **2002**, *10*, 3067.

24. Sano, H., Noguchi, T., Tanatani, A., Hashimoto, Y., Miyachi, H. *Bioorg Med Chem*. **2005,** *13*, 3079.

25. Ali, A.M., Saber, G.E., Mahfouz, N.M., El-Gendy, M.A., Radwan, A.A., Hamid, M.A. *Arch Pharm Res*. **2007**, *10*, 1186.

26. Ottanà, R., Maccari, R., Barreca, M.L., Bruno, G., Rotondo, A., Rossi, A., Chiricosta, G., Di Paola, R., Sautebin, L., Cuzzocrea, S., Vigorita, M.G. *Bioorg Med Chem*. **2005** *13:* 4243.

27. Gauthier, M.P., Michaux, C., Rolin, S., Vastersaegher, C., de Leval, X., Julémont, F., Pochet, L., Masereel, B. *Bioorg Med Chem.* **2006**;*14* :918.

28. Winter, C.A.; Risley, E.A.; Nuss, G.W. *Proc.Soc.Exp. Biol. Med.,***1962,** *111*, 544.

29. Klemm, P., Harris, H.J., Perreti, M, *Eur J Pharmacol*, **1995** *281*, 69.

30. Romano, M., Faggioni, R., Sironi, M., Sacco, S., Echtenacher, B., Di Santo, E., Salmona, M., Ghezzi, P. *Mediators of Inflamm*, **1997** *6*,32.

31. Kulmacz, R.J., Lands, W.E.M., *Prostaglandins* **1983**, *25*, 531.

32. Rarey, M., Kramer, B., Lengauer, T., Klebe, G..*J. Mol. Biol.* **1996,** *261*, 470.

33. Dewar, M.J.S.; Zoebisch, E.G.; Healy, E.F.; Stewart J.J.P, *J. Amer. Chem. Soc.* **1985**, *107*, 3902.

34. Tetko, I.V.; Bruneau, P., *J Pharm Sci*, **2004**, *93*, 3103.

35. Shimokawa, T.; Kulmacz, R.J.; DeWitt, D.L.; Smith, W.L. *J Biol Chem* **1990** *265,* 20073.

36 Leite, L. F.C., Mourão, R.H., Lima, M.C.A., Galdino, S.L., Hernandez, M.Z., Neves, F. A. R., Vidal, S., Barbe, J., Pitta, I.R. *Eur. J. Med. Chem*. **2007**, *42*, 1263.

37. Blanquart, C., Barbier, O., Fruchart, J.C, Staels, B., Glineur, C. *J. Steroid Biochem. Mol. Biol.*, **2003** *85*, 267.

38. Amorim, E. L. Cavalcanti; Brandao, S. S. Ferreira; Cavalcanti, C. O. Morais; Galdino, S. Lins; Pitta, I. Rocha; Luu Duc, C. *Ann. Pharmac. Fr.* **1992**, *50*, 103.

39. Goes, A. J. Silva; Alves de Lima, M. C.; Galdino, S. Lins; Pitta, I. da Rocha; Luu-Duc, C. *Ann. Pharmac. Fr,* **1991**, *49*, 92.

40. Albuquerque, J.F., Azevedo, L.C., Galdino, S.L., Chantegrel, J., Pitta, I.R., Luu-Duc, C. *Ann. Pharmac. Fr*, **1995**, *53*, 209.

41. Cayman Chemical Company Colorimetric 2005, *COX (ovine) Inhibitor Screening Assay, Booklet*, Cayman Chemicals, Ann Arbor.

Table1. 3,5-Dissubstitutes imidazolidines and thiazolidines 1-9.

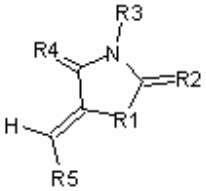

#	R_1	R_2	R_3	R_4	R_5
1	S	O	4-$ClC_6H_4CH_2$	O	3-Br,4-$CH_3OC_6H_3$
2	S	O	4-$ClC_6H_4CH_2$	O	2-CH_3O,5-BrC_6H_3
3	S	O	4-$ClC_6H_4CH_2$	O	4-$C_6H_5C_6H_4$
4	S	O	4-$CH_3C_6H_4CH_2$	O	3-indol
5	S	O	4-$ClC_6H_4CH_2$	S	3-indol
6	NH	S	4-$BrC_6H_4CH_2$	O	4-$(CH_3)_2N$-C_6H_4
7	NH	S	4-$BrC_6H_4COCH_2$	O	4-$(CH_3)_2N$-C_6H_4
8	NH	S	4-$BrC_6H_4COCH_2$	O	2-BrC_6H_4
9	NH	S	4-$BrC_6H_4COCH_2$	O	4-$C_6H_5C_6H_4$

Table 2. Percentual of Paw Edema Inhibition (average ± se) 4 hours after inflammatory stimulus (carrageenin) and Docking Results for 1-9 ligands in COX-2. Coumpounds 1-9 were given intraperitoneally at 50mg/kg, $p < 0.05$ compared to control (T-test).

Compound	% anti-inflammatory activity	Total Score FlexX
1	42.6 ± 7.4	-14.00
2	78.9 ± 2.9	-13.32
3	46.5 ± 11.3	-13.13
4	61.8 ± 5.65	-9.93
5	77.5 ± 9.2	-13.66
6	54.8 ± 12.8	-10.61
7	52.9 ± 9.3	-20.11
8	61.7 ± 18.8	-14.03
9	20.5 ± 9.7	-16.15
SC-58		-20.64

Table 3 Anti-inflammatory activity exhibited to compound 3 and standard drugs indomethacin and celecoxib given orally at respective doses. Leukocyte count is expressed as total cell number by exudate mL. Activity (%, average ± S.E.) is calculated considering control group cell counting as 100% and values are significant to an α =0.05 (ANOVA. Tukey's test).

Drug	Dose	Leukocyte/mL	Anti-inflammatory activity
Compound 2	50 mg/kg	$1.19 \pm 0.14 \times 10^6$	30.4 ± 8.2
Indomethacin	10 mg/kg	$0.76 \pm 0.07 \times 10^6$	55.5 ± 4.3
Celecoxib	10mg/Kg	$0.27 \pm 0.06 \times 10^6$	84.2± 3.9
	CONTROL	$1.71 \pm 0.12 \times 10^6$	-

Table 4 COX-2 (ovine) inhibition by compounds 2, 6 and 7 at 1 μM and 0.01 μM, and standard drugs celecoxib and indomethacin at 1 μM and 0.01 μM.

Druug	Concentration	COX-2 Inhibition %
Celecoxib	1 μM	47.5 ± 1.0
	0.01 μM	11.6 ± 1.0
Indomethacin	1 μM	0
	0.01 μM	0
Compound 2	1 μM	0
	0.01 μM	0
Compound 6	1 μM	0
	0.01 μM	0
Compound 7	1 μM	52.9 ± 1.0
	0.01 μM	2.7± 1.0*

*= not significant

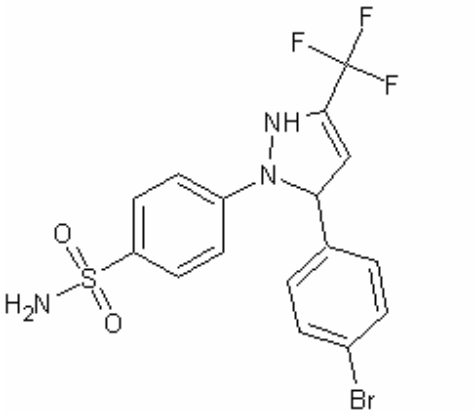

Figura 1. COX-2 inhibitor SC-558

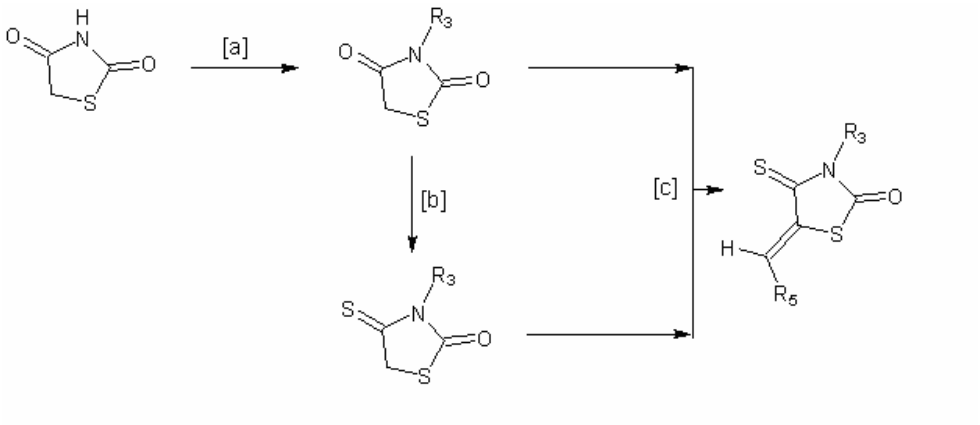

Figure 2. Synthetic route to compounds 1-5, [a] Aromatic substituted halide, KOH, MeOH, reflux, [b] P_2S_5, dioxane, reflux, [c] ethyl 2-cyano-3-substituted (R5) – acrylate, piperidin, methanol, reflux.

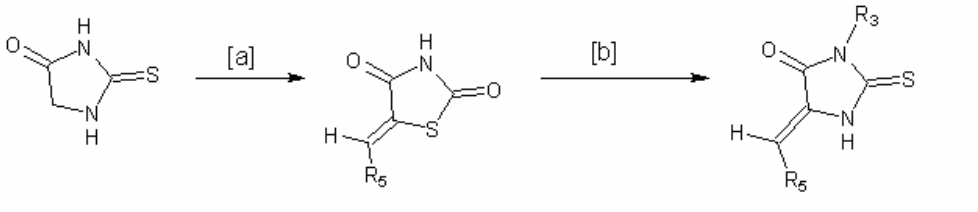

Figure 3. Synthetic route to compounds 6-9, [a] ethyl 2-cyano-3-substituted (R5) – acrylate, piperidin, methanol, reflux, [b] aromatic substituted halide, KOH/K2CO3, MeOH, reflux.

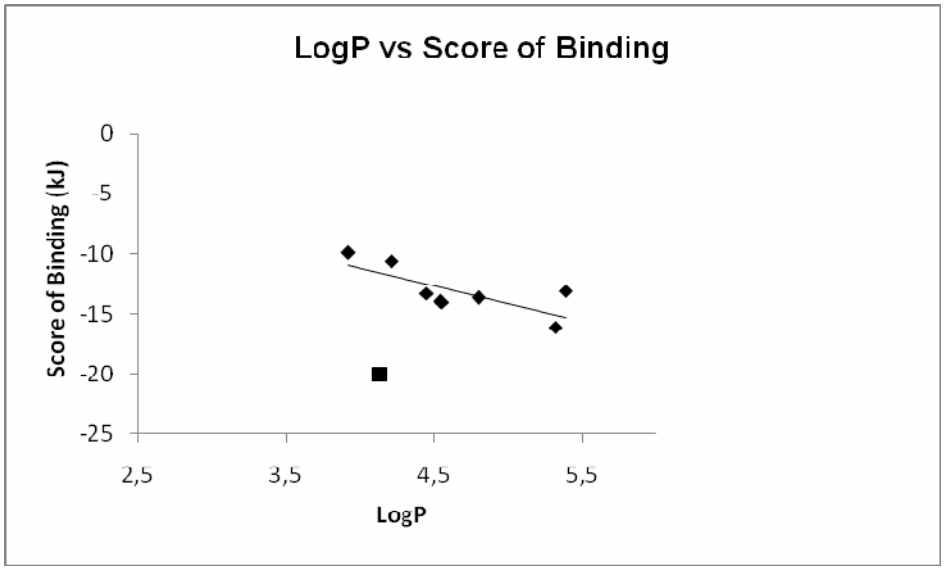

A

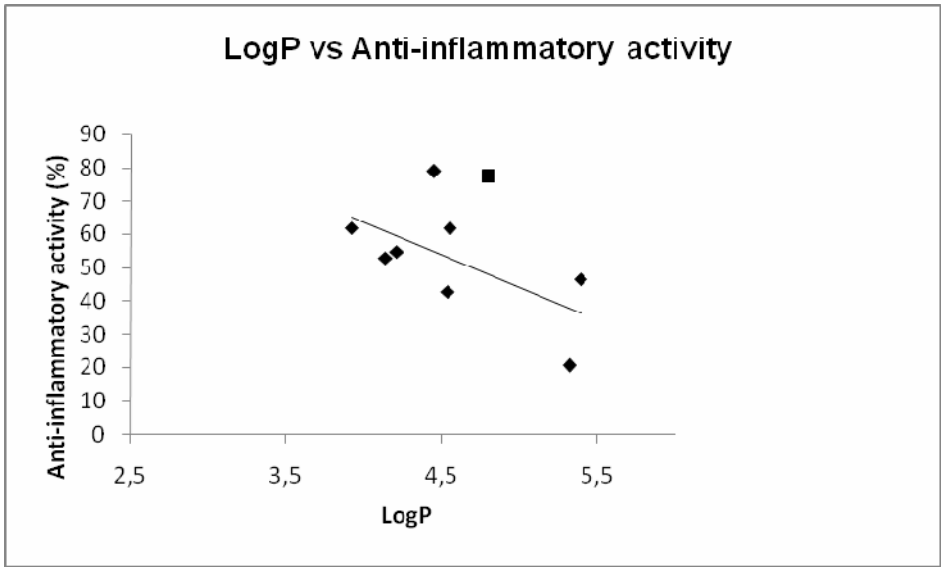

B

Figure 4. A) Correlation between the score of binding (kJ) and Compounds 1, 2, 3,4,5,6,8 and 9 LogP. Outlayer compound (7■) was removed for best fitting. B) Correlation between percent edema inhibition and Compounds 1, 2,3,4,6,7,8 and 9. Outlayer compound (5■) was removed for best fitting The stippled line at the diagonal is linear regression obtained from experimental data.

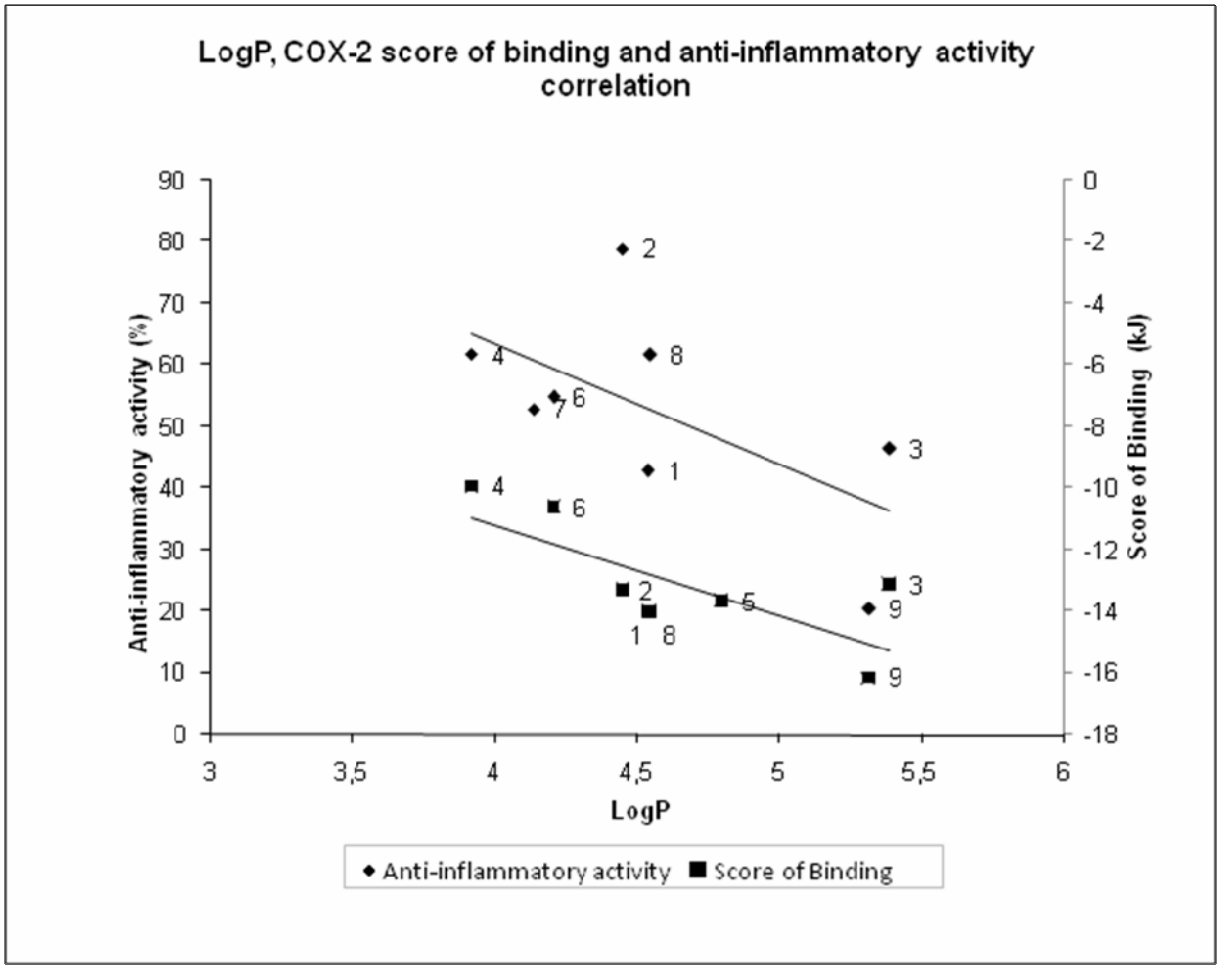

Figure 5. A) Correlation between the score of binding (kJ), percent edema inhibition (%) and Compounds 1-9 LogP. The stippled lines at the diagonal are linear regressions obtained from experimental data. Outlayers compound 7 and 5 were removed for best fitting from anti-inflammatory and score of binding regressions, respectively.

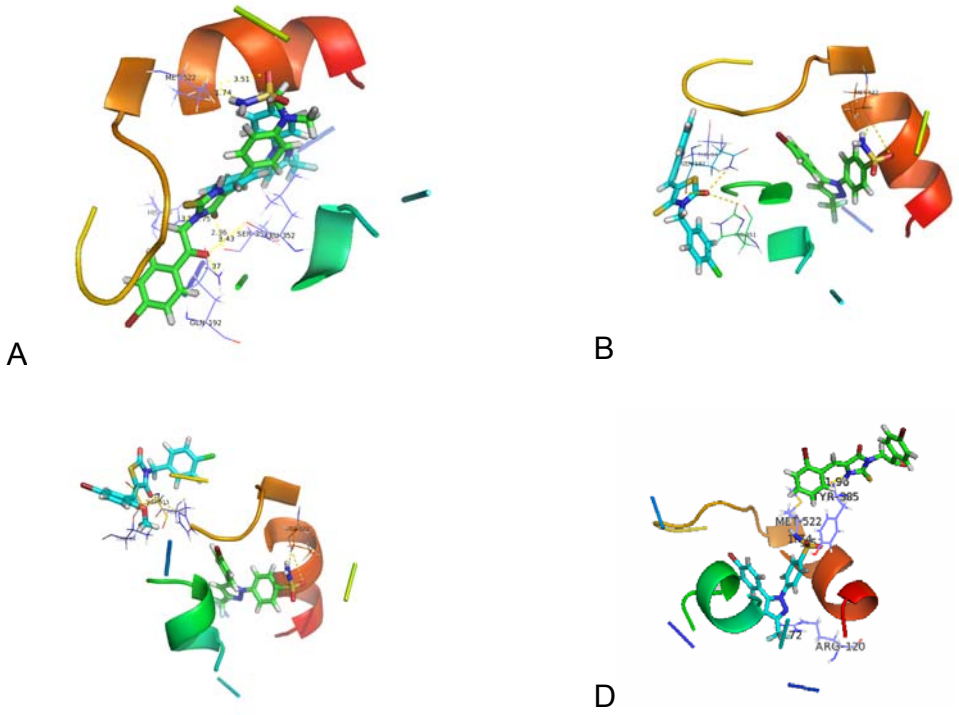

Figure 6: A) Compound 7 (green), docked into COX-2 active site, in same position of SC-588 (cyano). B) Compound 5 (cyano) docked in “left mode”, where carbonyl moiety from central ring forms Hydrogen bond with GLN-192, compound SC-588 appears in active site (green). C) Compound 2 (cyano), forming hydrogen bond with His-90, compound SC-588 appears in active site (green). D) Compound 8 (green) docked in opposite side forming hydrogen bond with Tyr-385. Compound SC-588 appears in active site (cyano).

10 CONCLUSÕES GERAIS

O objetivo principal deste estudo foi a obtenção de novas moléculas da série indol-tiazolidinadiônica com atividade antiinflamatória. Foram obtidos um total de 27 novos compostos finais. Entre os compostos que tiveram a atividade antiinflamatória avaliada, merecem destaque o LYSO-7 e o PG-15. Adicionalmente, os resultados da atividade antiinflamatória nos permitem sugerir modificações estruturais para uma otimização onde o desenho de novos compostos some as características químicas relevantes que foram levantadas sobre estes compostos.

O estudo farmacocinético do PG-15 revelou que este composto atinge o pico de concentração plasmática em aproximadamente 1 hora após a administração oral e sua presença pôde ser detectada no sítio da inflamação. A absorção oral do PG-15 mostrou-se prejudicada quando a dose foi aumentada, mostrando que o composto apresenta problemas de absorção, os quais podem estar justificando a falta de relação dose-efeito observada no estudo farmacodinâmico dos compostos desta série.

Embora a análise da seletividade para COX-2 não tenha sido realizada para todos os compostos, os resultados obtidos são úteis no direcionamento de novos estudos. Como as moléculas testadas, exceto o PG-16 mostraram-se ligeiramente inibidoras preferenciais ou seletivas da COX-1, tem-se um forte indício de que existe uma interação entre as moléculas da série com a COX e que pequenas modificações estruturais podem conduzir a compostos mais seletivos para COX-2.

A inibição da atividade antiinflamatória *in vivo* dos compostos foi maior do que 50% para a maioria dos compostos testados, em doses baixas, fato que não reflete a inibição enzimática de ambas as COX *in vitro,* onde as mesmas moléculas não ultrapassaram 30% de inibição em concentrações bastante elevadas. A conjunção destes dados sugere fortemente que, ainda que os compostos estejam atingindo as enzimas COX, a resposta inflamatória como um todo seja um resultado de um somatório desta inibição na via das prostaglandinas somada a uma interferência em algum outro mecanismo modulador da inflamação ainda não identificado.

O conjunto deste trabalho gerou cinco artigos científicos, em fase de submissão, a saber:

- Novas 5-indol-tiazolidinadionas: Síntese e avaliação da atividade antiinflamatória
- Development and Validation of LC-UV Method for the Quantification of the Anti-inflammatory Candidate PG-15 in Rat Plasma
- Development and validation of a LC/MS/MS method for analyzing PG-15 in rat plasma
- Preclinical Pharmacokinetic Pharmacodynamic Evaluation of PG-15: an Anti-inflammatory Candidate
- Synthesis, receptor docking studies and anti-inflammatory activity of new 3,5-imadozilines and thiazolidines derivatives

Este trabalho nos abre inúmeras perspectivas no que tange a continuidade deste estudo. Estudos farmacodinâmicos e de docking das moléculas no PPARγ visando o esclarecimento do mecanismo de ação seriam de grande contribuição para o estabelecimento da relação estrutura atividade com as moléculas da série.

Ainda, melhoria na solubilidade destes compostos, através da formação de sais, pode, muito possivelmente, nos levar a parâmetros farmacocinéticos diferentes daquele observado para o PG-15, uma vez que a absorção oral pode ter sido baixa e errática devido a baixa solubilidade.

Assim, mais do que modificações moleculares, a melhoria das características físico-químicas dos compostos da série, principalmente a solubilidade, mostra-se como o maior desafio no desenvolvimento destes derivados.

Fica aqui a sugestão de que o composto PG-15 é um excelente protótipo para fármacos antiinflamatórios, cujos estudos farmacológicos devem ser prosseguidos e a otimização estrutural realizada.

11 REFERÊNCIAS BIBLIOGRÁFICAS

BLANQUART, C., BARBIER, O., FRUCHART, J.C, STAELS, B., GLINEUR, C. “Peroxisome proliferators-activate resceptors: regulation of transcriptational activities and roles in inflammation” **Journal os Steroid Biochemistry & Molecular Biology,** v. 85, p. 267-273, 2003.

BORISY, A. A., ELLIOTT, P. J., HURST, N. W., LEE, M. S., LEHAR, J., PRICE, E. R., SERBEDZIJA, G., ZIMMERMANN, G.R., FOLEY, M.A., STOCKWELL, B.R., KEITH, C.T. Systematic discovery of multicomponent therapeutics **PNAS,** vol. 100, p. 7977–7982, 2003

BOSCHELLI, D.H., CONNOR, D.T., HOEFLE, M. , BORNEMEIER, D.A., DYER, R.D. “Conversion of NSAIDS into balanced dual inhibitors of cyclooxygenase and 5-lipoxygenase” **Bioorganic & Medicinal Chemistry Letters**, V. 2, P. 69-72, 1992a.

BOSCHELLI, D.H., CONNOR, D.T., KUIPERS, P.J., WRIGHT, C.D. “Synthesis and cyclooxygenase and 5-lipoxygenase inhibitory activity of some thiazolidene-4-one analogs of meclofenamica acid” **Bioorganic & Medicinal Chemistry** Letters, V. 2, P. 705-708, 1992b.

BROHPY, J.M., “Celecoxib and cardiovascular risks”, **Expert Opinion on Drug Safety**, v. 4, p-1005-1015, 2005.

CABRERO, A., LAGUNA, J.C., VAZQUEZ, M., “Peroxisome proliferator-activated receptors and the control of inflammation” **Current Drug Targets – inflammatory Allergy,** v. 1, p. 243-248, 2002.

CANN, A. (responsável) **Homepage of School of Biological Sciences, University of Leicester**, última atualização: 21.out.2004. Disponível on line em: http://www.micro.msb.le.ac.uk/ MBChB/1b.html. Acesso em 10.nov.2005.

CARON, S., VAZQUEZ, E., STEVENS, R.W., NAKAO,K., KOIKE, H., MURATA, Y. “Efficient synthesis of 6-Chloro-2-(4-chlorobenzoyl)-1H-indol-3-ylacetic acid, a novel COX-2 inhibitor” **Journal of Organic Chemistry,** v. 68, p. 4104-4107, 2003.

CHANDRASEKHARAN, N.V., DAI, H., ROOS, K.L., EVANSON, N.K., TOMSIK, J., ELTON, T.S., SIMMONS, D.L., “COX-3, a cyclooxygenase-1 variante inhibited by acetaminophen and other analgesis/antipyretic drugs: cloning, structure, and expression”, **Procedures of National Academy of Science of USA**, v. 99, p. 13926-13931, 2002.

CHEN,G., ZHENG,S., LUO,X., SHEN,J., ZHU,W., LIU,H., GUI,C., ZHANG,J., ZHENG,M., PUAH, C.M., CHEN,K., JIANG, H. Focused Combinatorial Library Design Based on Structural Diversity, Druglikeness and Binding Affinity Score. **J. Comb. Chem**.,v. 7, p. 398-406, 2005.

CSERMELIN, P., AGOSTON, V., PONGO, S. The efficiency of multi-target drugs: the network approach might help drug design **TRENDS in Pharmacological Sciences**, V..26, p.4, 2005.

CZURA C.J.; FRIEDMAN S.G.; TRACEY K.J. "Neural inhibition of inflammation: the cholinergic anti-inflammatory pathway" **Journal of Endotoxin Research**, V. 9, p. 409-413, 2003.

DANNHARDT, G., KIEFER, W. "Cyclooxygenase inhibitors--current status and future prospects" **European journal of medicinal chemistry**, v. 36(2), p.109-26, 2001.

DOAN, T., MASSARITTI, E. "Rheumatoid Arthritis: An Overview of New and Emerging Therapies" **Journal of Clinical Pharmacology**, v. 45, p. 751-762, 2005.

DRISCOLL, K.E., CERTER, J.M., HASSENBEIN, D.G., HOWARD, B. " Cytokines and particule-induces inflammatory cell recruitment" **Envoirnmental and Health Perspectives**, v. 105, p. 1159-1164, 1997.

DUBUQUOY, C., ROUSSEAUX, X., THURU, L., PEYRIN-BIROULET, O., ROMANO, P., CHAVATTE, M., CHAMAILLARD, P., DESREUMAUX, L. Pparc As A New Therapeutic Target In Inflammatory Bowel Diseases, **Gut**; v. 55, p.1341–1349, 2006.

FEGHALI, C.A., WRIGTH, T.M., "Cytokines In Acute And Chronic Inflammation" **Frontiers in Bioscience,** v. 2, p. 12-26, 1997.

FIEDOREK FT, WILSON GG, FRITH L, PATEL J, ABOU-DONIA M, Study Group-PPA20005. Monotherapy with GI262570. a tyrosine-based non-thiazolidinedione PPARγ agonist, improves metabolic control in type 2 diabetes mellitus patients. **Diabetes***.*; v.49, p.- 38, 2000.

FITZGERALD, G.A., LOLL, P., "COX in a crystal ball: current status and future promise of prostaglandin research" **The Journal of Clinical Investigation,** v. 107, p. 1335-1337, 2001.

FRINK, R. J. **Inflammatory atherosclerosis: Characteristics of the injurious agent,** Sacramento, Estados Unidos:Library of Congress Cataloging-in-Publication Data, 2002. cap 3, p. 1-5.

FUJIWARA, N., KOBAYASHI, K., "Macrophages in inflammation", **Current Drug Targets in Inflammation and Allergy,** v. 4, p. 281-286, 2005.

FUNK CD, FITZGERALD GA., COX-2 Inhibitors and Cardiovascular Risk. **J Cardiovasc Pharmacol**. vol. 50, no. 5. pp.470-479, 2007.

GAUTIER, M.P., MICHAUX, C., ROLIN, S., VASTERSAEGHER, C., LEVAL, X., JULÉMONT, F., POCHET. L., MASEREEL, B., "Synthesis, molecular modeling and enzymatic evaluation of 3,5-diphenyl-2-thioxoimidazolidin-4-ones as new potential cyclooxygenase inhibitors" **Bioorganic and Medicinal Chemistry,** in press, 2005.

GÓES, A.J.S., ALVES, A.J., FARIA, A.R., LIMA, J.G., MAIA, M.B.S., " Síntese e atividade antiedematogênica de derivados N-triptofil-benzilideno-2,4-tiazolidinadiona e N-triptofil-5-benzilideno-rodanina" **Química nova,** v. 27, p. 905-910, 2004.

HABASHY, R.R., ABDEL-NAIM, A.B., KHALIFA, A., AL-AZIZI, M.M., " Anti-inflammatory effects of jojoba liquid wax in experimental models" **Pharmacological research,** v. 51, p. 95-105, 2004.

HAWKEY CJ. **The Lancet**. 353: 307-314. 1999.

HEIKKINEN, S., AUWERX, J.; ARGMANN, C.A. PPARgamma in human and mouse physiology. **Biochim Biophys Acta**. V.1771, p.999-1013, 2007.

HOOZEMANS J.J, O'BANION M.K. "The role of COX-1 and COX-2 in Alzheimer's disease pathology and the therapeutic potentials of non-steroidal anti-inflammatory drugs" **Current drug targets. CNS and neurological disorders,** v.4(3), p.307-15, 2005.

KALGUTKAR AS, CREWS BC, ROWLINSON SW, MARNETT AB, KOZAK KR, REMMEL RP, MARNETT, L.J. **Proc. Natl. Acad. Sci.** USA. 97 (2): 925-930, 2000.

KALGUTKAR, A., CREWS, B.C., SALEH, S., PRUDHOME, D., MARNETT, L.J. "Indolyl esters and amides related to indomethacin are selective COX-2 inhibitors" **Bioorganic and Medicinal Chemistry,** v. 13, p. 6810-6822, 2005.

KALGUTKAR, A.S., CREWS, B., ROWLINSON, S.W., GARNER, C., SEIBERT, K., MARNETT, L.J. " Aspirin-like molecules that covalently inactivate cyclooxygenase-2" **Science**, v. 280, p. 1268-1270, 1998.

KOGEN, H, TODA, N.; TAGO, K.; MARUMOTO, S.; TAKAMI, K.; ORI, M.; YAMADA, N.; KOYAMA, K.; NARUTO, S.; ABE, K.; YAMAZAKI, R.; HARA, T.; AOYAGI, A.; ABE, Y.; KANEKO, T. A conformational restriction approach to the development of dual inhibitors of acetylcholinesterase and serotonin transporter as potential agents for Alzheimer's disease. **Bioorg. Med. Chem**., v. 11, p. 4389-4415, 2003.

KURUMBAIL, R.G., STEVENS, A.M., GIERSE, J.K., McDONALD, J.J., STEGMAN, R.A., PAK, J.Y., GILDEHAUS, D., MIYASHIRO, J.M., PENNING, T.D., SEIBERT, K., ISAKSON, P.C., STALLINGS, W.C., **Nature** , v.384, p.644-648, 1996.

LEAHY, K.M., KOKI, A.T., MASFERRER, J.L., "Role of cyclooxygenase in angiogenesis", **Current Medicinal Chemistry**, v. 7, p. 1163-1170, 2000.

LEHMANN, J.M., LENHARD, J.M., OLIVER, B.B., RINGOLD, G.M., KLIEWER, S.A., Peroxisome Proliferator-activated Receptors a and g Are Activated by Indomethacin and Other Non-steroidal Anti-inflammatory Drugs, **The Journal Of Biological Chemistry,** V. 272, pp. 3406–3410, 1997.

LEITE, L.F.C.C.; UCHOA, F.T.,; LIMA, M.C.A.; GALDINO, S.L.; PITTA, I.R. HERNANDES, M.Z. “Docking Studies of Heterocyclic Derivatives with Potential COX-2 Inhibition Activities using Autodock” Anais do XIII Simpósio Brasileiro de Química Teórica (SBQT), 2005, São Pedro-SP, 2005.

LEVAL X, DELARGE J, DEVEL P, NEVEN P, MICHAUX C, MASEREEL B, PIROTTE B, DAVID, L, HEROTIN Y, DOGNÉ JM. **Prostaglandins, Leukotrienes and essential fatty acids** 64: 211-216, 2001.

LEVAL, X., JULÉMONT, F., DELARGE, J., PIROTTE, B., DOGNÉ, J-M.; “New trends in dual COX-LOX inhibition”, **Current Medicinal Chemistry**, v. 9, p. 941-962, 2002.

MARSHALL, T. G., LEE, R.E., MARSHALL, F.E. Common angiotensin receptor blockers may directly modulate the immune system via VDR, PPAR and CCR2b **Theoretical Biology and Medical Modelling**, v.3, p.1-33, 2006.

MASLINSKA, D., GAJEWSKI, M., “Some aspects of the inflammatory process”, **Folia Neurophatologyca**, v.36, p. 199-204, 1998.

MIOSSEC, P., “An update on the cytokine network in rheumatoid arthritis”, **Current Opinion in Rheumatology,** v.13, p. 218-222, 2004.

MITCHELL, JA.; WARNER, TD., COX isoforms in the cardiovascular system: understanding the activities of non-steroidal anti-inflammatory drugs **Nature Reviews Drug Discovery**, vol. 5, pp. 75-86, 2006.

MODARAI, B.B, BURNAND, K.G., HUMPHREIES, J., WALTHAM, M., SMITH, A. “The role of neovascularisation in the resolution of venus thrombus” **Thrombosis and Homeostasis**, v. 93, p. 801-809, 2005.

MOLLACE, V., MUSCOLI, C., MASINI, E., CUZZOCREA, S., SALVEMINI, D. “Modulation of Prostaglandin Biosynthesis by Nitric Oxide and Nitric Oxide Donors”, **Pharmacological Reviews**, v. 57, p. 217-252, 2005.

MORPHY, R., RANKOVIC, Z. Designed Multiple Ligands. An Emerging Drug Discovery Paradigm, **Journal of Medicinal Chemistry**, V. 48, p. 21, 2005

NOLTE, R. T. WISELY, G.B., WESTIN, S., COBB, J.E., LAMBERT, M.H., KUROKAWA, R., ROSENFELD, M.G., WILLSON, T.M., GLASS, C.K., MILBURN, M.V. **Nature** v. 395, p. 137-143, 1998.

PARENTE L, PERRETTI M. **Biochemical Pharmacology**. 65: 153-159. 2003.

POLI, G. “Special review: reactive oxygen and nitrogen in inflammation” **Free Radical biology & Medicine,** v. 33, p. 301-302, 2002.

ROGLER, G Significance of anti-inflammatoryeffects of PPARc agonists? **Gut**; v. 55, p.1067–1069. 2006

SANCHEZ-MADRID, F., DEL POZO, M.A., “Leukocyte polarization in cell migration and immune interactions” **The EMBO Journal,** v. 18, p. 501-5011, 1999.

SANTOS, L.C.; UCHOA, F.T.; CANAS, A.R.P.A.; SOUSA, I.A.; MOURA, R.O.; LIMA, M.C.A.; GALDINO, S.L. ; PITTA, I.R.; BARBE, J. “Synthesis and anti-inflammatory activity of new thiazolidine-2,4-diones, 4-thioxothiazolidinones and 2-thioxoimidazolidinones” **Heterocyclic Communications**, 11 (2): 121-128 2005.

SHIH, M. (submittor), “Pahtways:cytokines and inflammatory response” **Homepage of BioCarta Pathways,** disponível on line em : http:// biocarta.com

SIMMONS, D.L., BOTTING, R.M., HLA, T. “Cyclooxygenase isozymes: the biology of prostaglandin synthesis and inhibition”, **Pharmacological Reviews,** v. 56, p. 387-437, 2004.

SMITH, W.L., GARAVITO, R.M., DeWITT, D.L. “Prostaglandin edoperoxide synthases (cyclooxygenases)-1 and -2” **The Journal of Biological Chemistry**, v. 271, p. 33157-33160, 1996.

STAELS, B.; FRUCHART, J.C. Therapeutic Roles of Peroxisome Proliferator–Activated Receptor Agonists. **Diabetes**, v. 54, p.2460-2470, 2005.

STRUB, A., ULRICH, W.T., HESSLINGER, C., ELTZE, M., FUCHUSS, T., STRASSNER, J., STRAND, S., LEHNER, M., BOER, R. “The novel imidazopyridine BYK191023 is a highly selective inhibitor of the inducible nitric oxid synthase” **Molecular Phamacology,** in press, 2005.

STVRTINOVA, V., JAKUBOVSKY, J., HULIN, I. **“Inflammation and Fever *in*: Pathophysiolgy: principles of deseases – Textbook for medical students”** Slovakia: Academic Eletronic Press, 1995.

TIMOFEEVSKI, S.L., PRUSAKIEWICZ, J.J., ROUZER, C.A., MARNETT, L.J. “Isoform-selective interation of cyclooxygenase-2 with indomethacin amides studied by real-time fluorescence, inhibition kinetics, and site-directed mutagenesis”, **Biochemistry,** v.41, p. 9654-9662, 2002.

TOUHEY, S., O’CONNOR, R., PLUNKETT, S., MAGUIRE, A., CLYNES, M., “ Structure-activity relashionship of indomethacine analougues for MRP-1, COX-1 and COX-2 inhibition: identification of novel chemotherapeutic drug resistance modulators” **European Journal of Cancer,** v. 38, p. 1661-1670, 2002.

TRUCOTTE, J.E.; DEBONNEL, G.; MONTIGNY, C.; HEBERT, C.; BLIER, P.. Assessment of the Serotonin and Norepinephrine Reuptake Blocking Properties of Duloxetine in Healthy Subjects **Neuropsychopharmacology**, v.24, p. 511-521, 2001.

VAN RYN, J., TRUMMLITZ, G., PAIRET, M. “Cox-2 selectivity and inflammatory processes” **Current Medicinal Chemistry**, v. 7, p. 1145-1161, 2000.

VANE JR, BAKHLE YS, BOTTING RM. **Annu. Ver. Pharmacol. Toxicol**. 38:97-120. 1998.

WALLACE, J.L., IGNARRO, L.J, FIORUCCI, S., “Potential cardioprotective actions of NO-releasing aspirin” **Nature Reviews- Drug Dircovery,** v.1, p. 375,-382, 2002.

WEILAND, H.A., MICHAELIS, M., KIRSCHBAUM, B. J., RUDOLPHI, K.A. “Osteoarthritis: na untreatable disease” **Nature Reviews – Drug Dicovery**, v. 4, p. 331-344, 2005.

WHO SCIENTIFIC GROUP. SYMMONS, D.; MATHERS, C, PFLEGER, B. Global Burden Of Osteoarthritis In The Year 2000 **Bulletin Of World Health**. 919, 1–26, 2003.

WILLSON, T.M.,BROWN, P.J., STERNBACH, D.D., HENKE, B.R. The PPARs: From Orphan Receptors to Drug Discovery J**. Med. Chem**., v.43p. 527 -550, 2000.

WOODS KW, McCROSKEY RW, MICHAELIDES MR, WADA CK, HULKOWER KI, BELL RL, **Bioorganic & Medicinal Chemistry Letters**.. 11: 1325-1328. 2001

ZIMMERMANN, G. R., LEHAR, J., KEITH, C.T. Multi-target therapeutics: when thewhole is greater than the sum of the parts, **Drug Discovery Today,** V. 12, 2007.

Anexo:
Espectros de RMN ^{1}H, IV e Massas dos Compostos sintetizados

[11 e] GQ-47
RMN ^{1}H, $DMSOd_6$

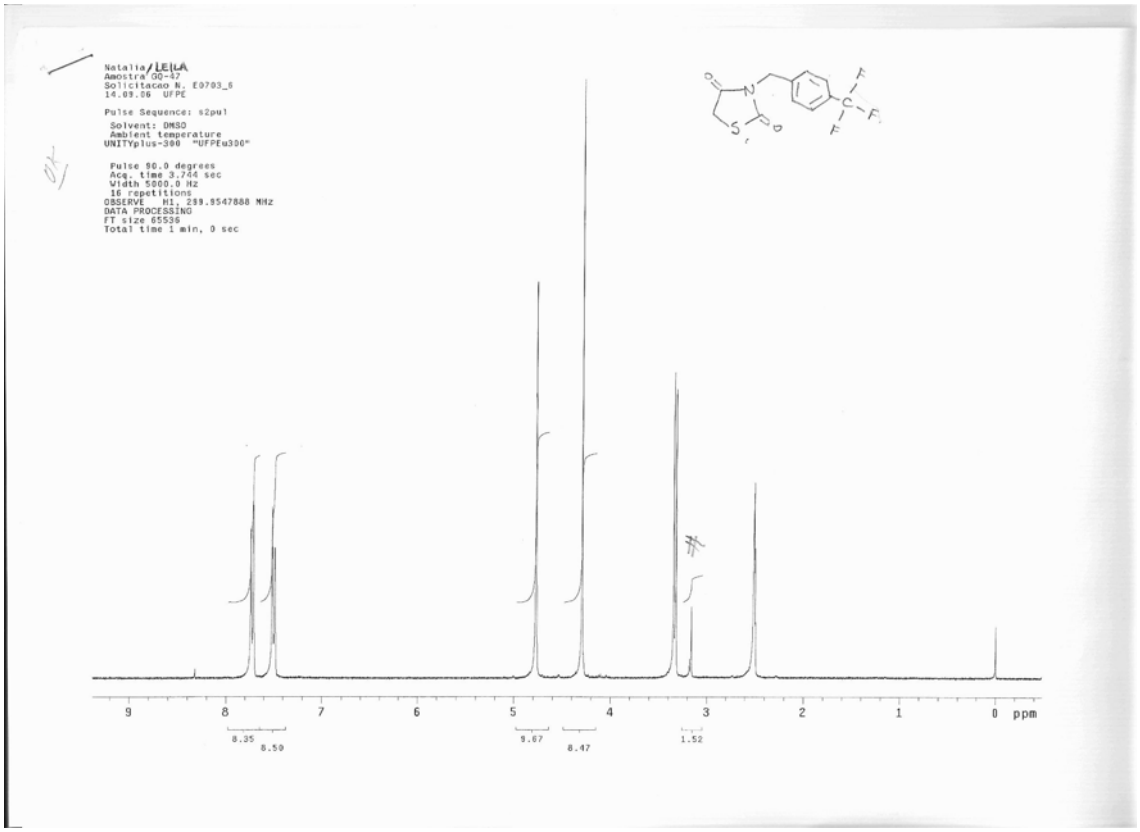

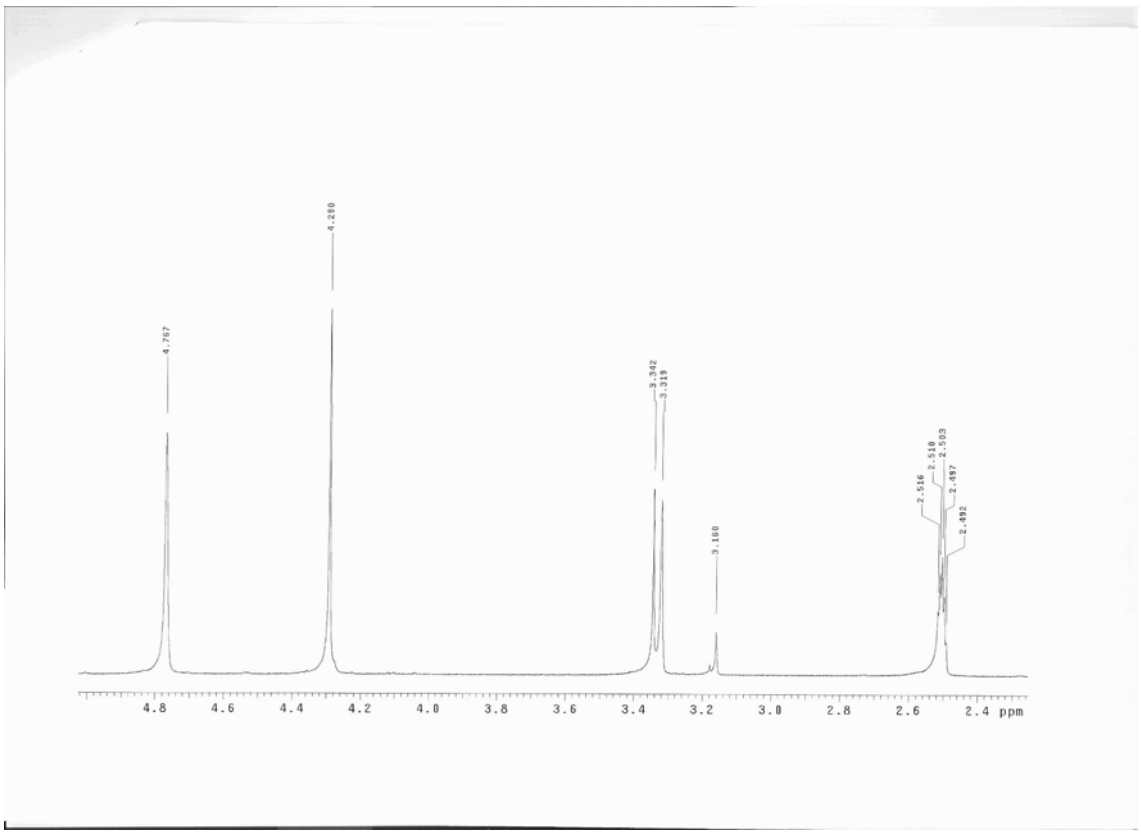

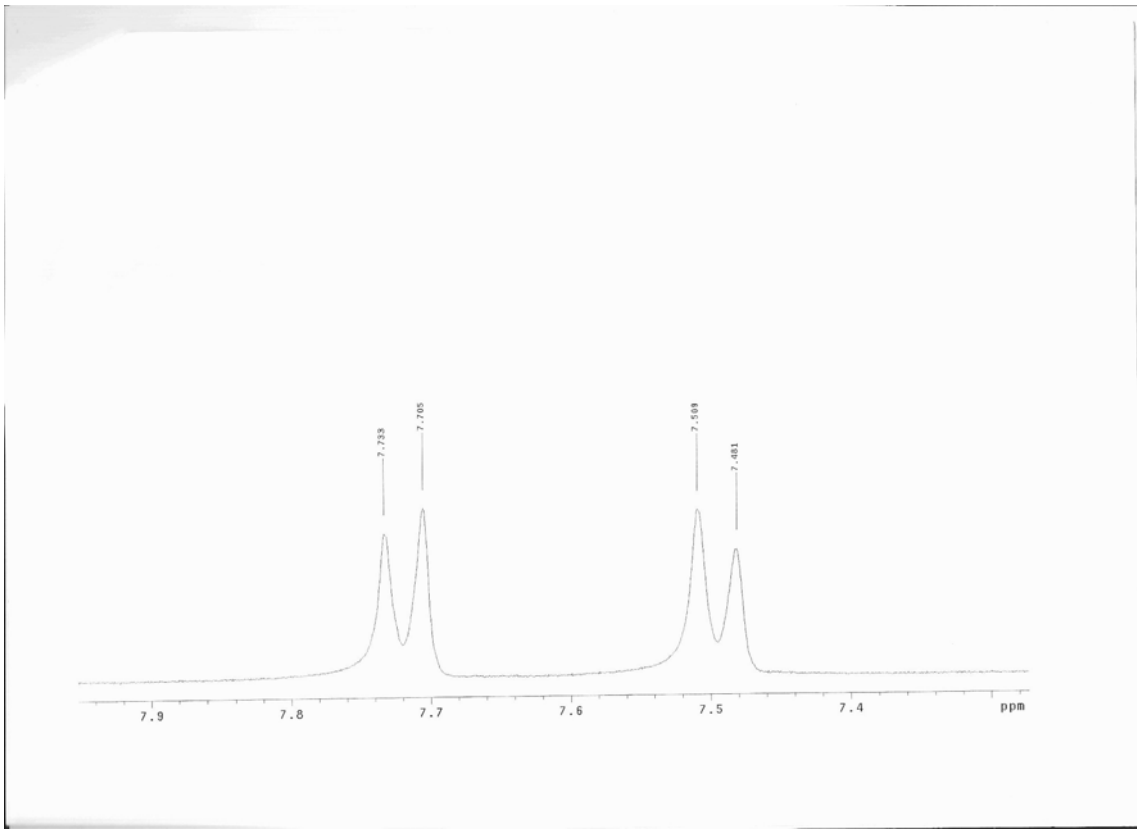

[11e] GQ-47
IV, KBr

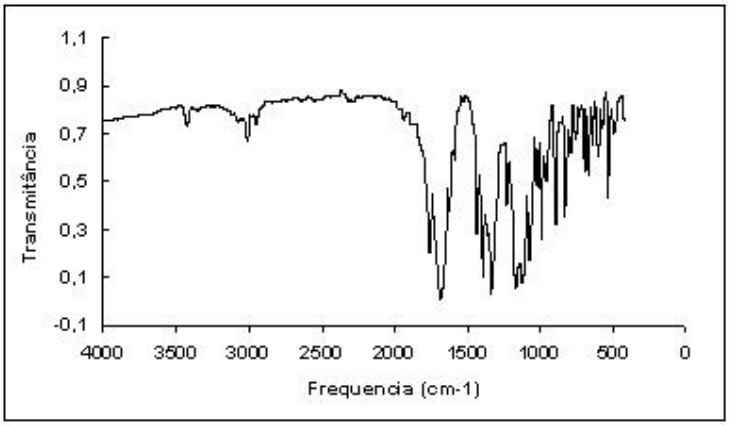

Principais Bandas:	
3417	
3007	
1753	
1671	
1385	
1326	

Espectro de Massas, ESI negativo

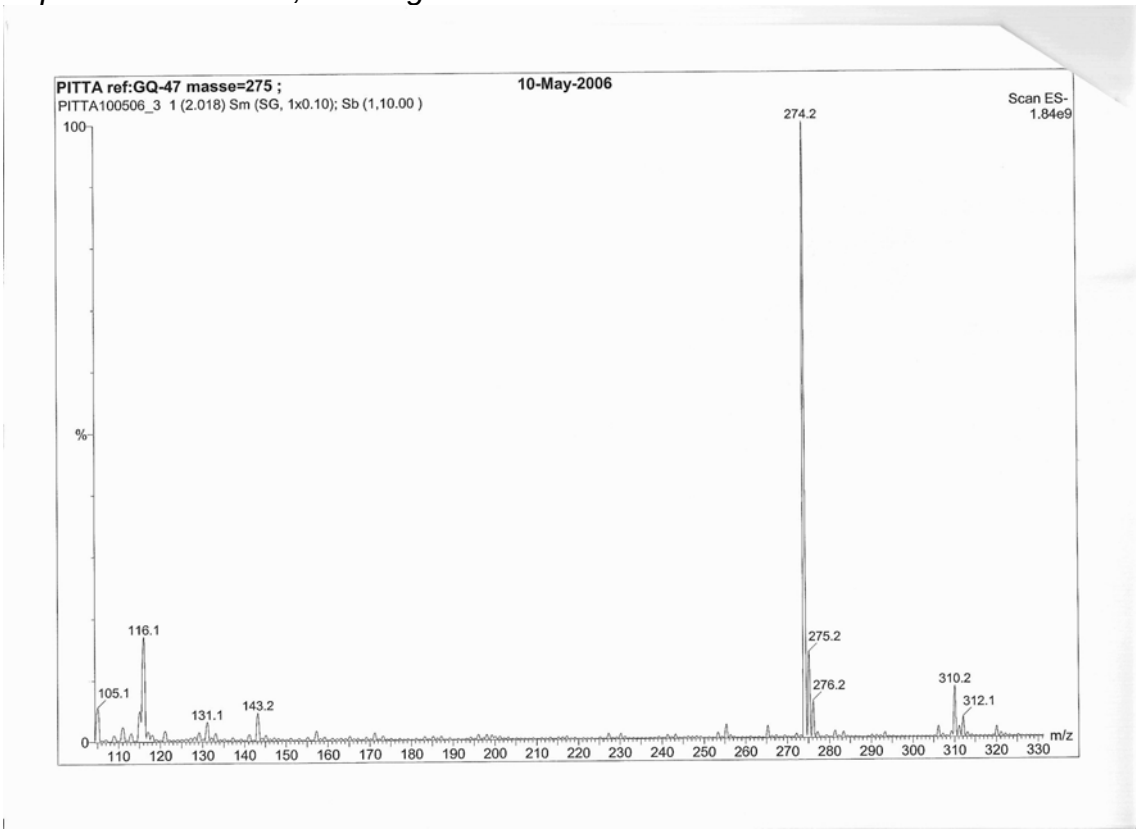

[11f] GQ-46
RMN ^{1}H, $DMSOd_6$

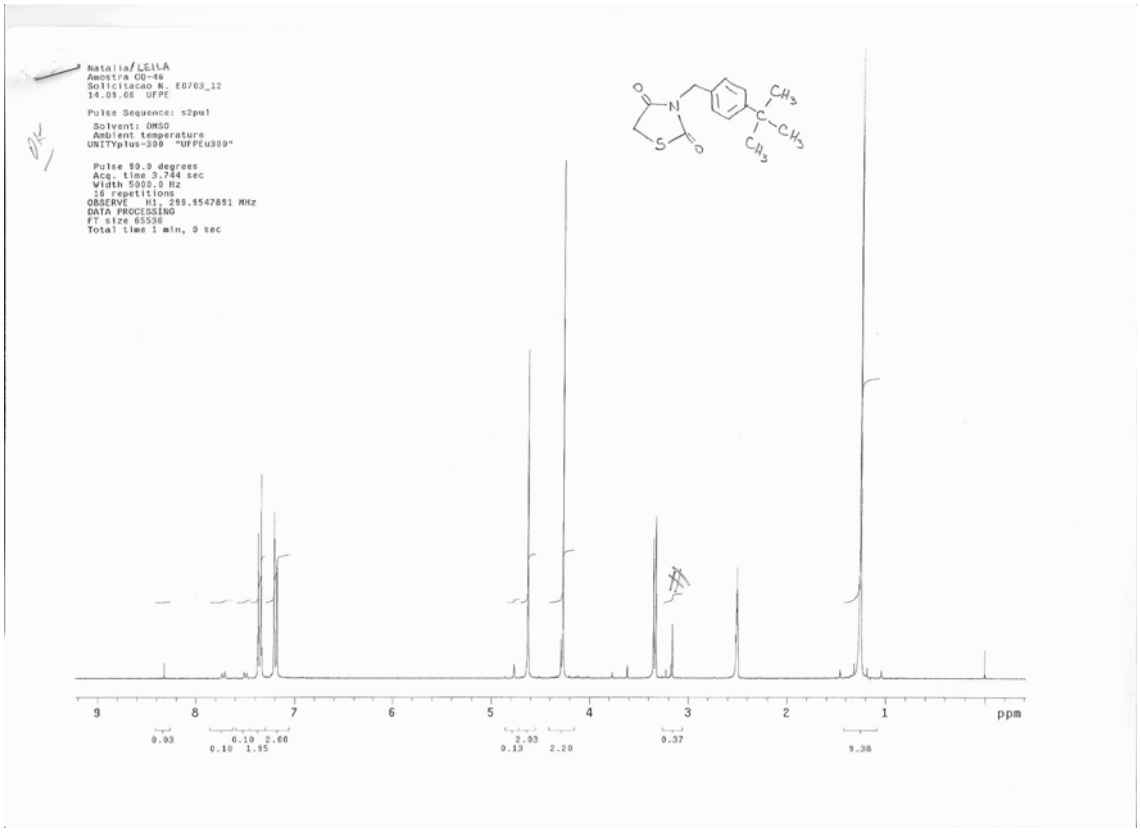

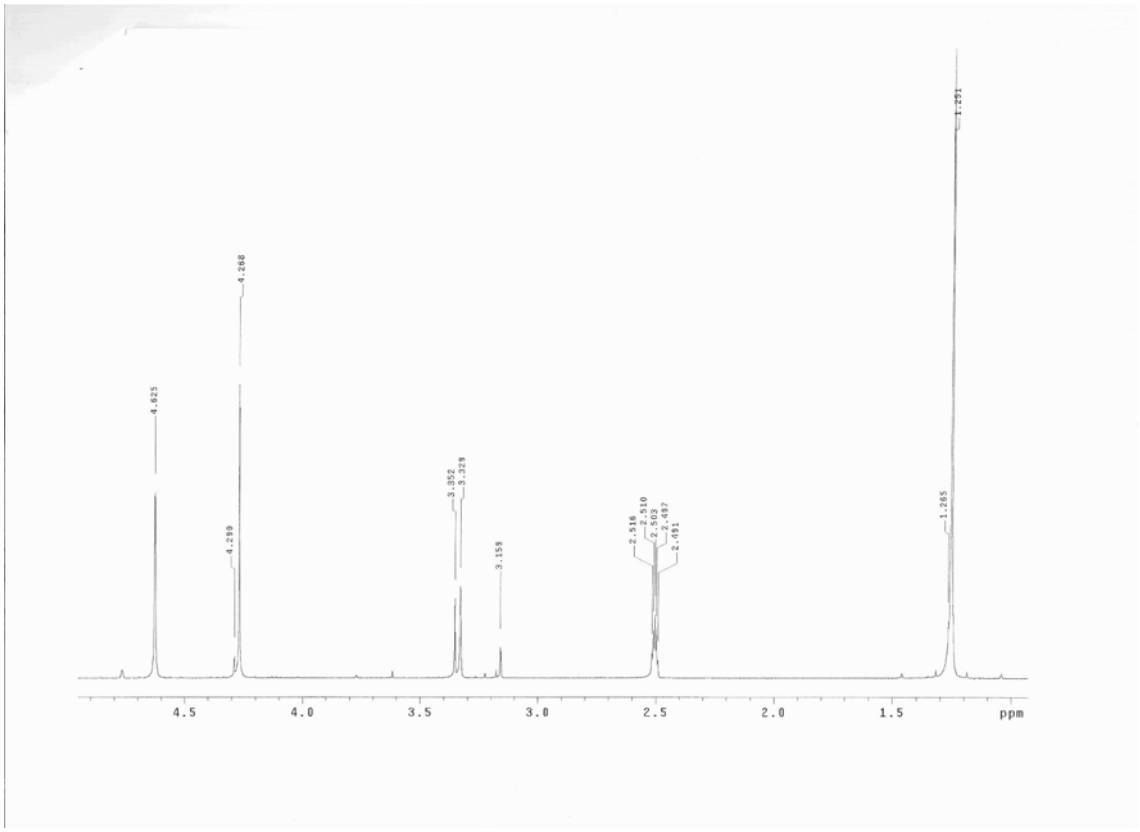

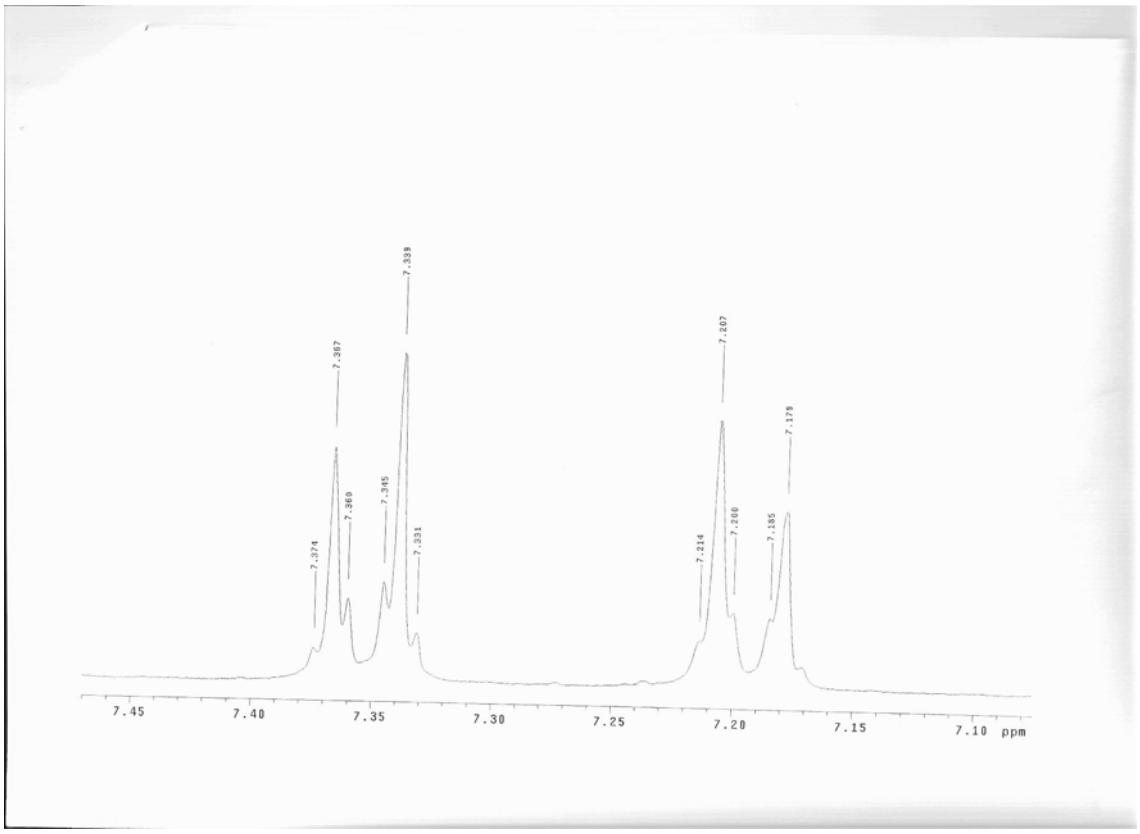

[11f] GQ-46
IV, KBr

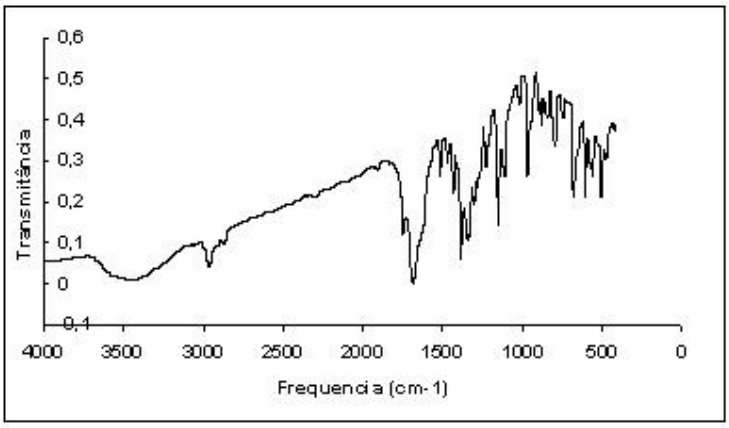

Principais Bandas:	
3395	
2951	
1713,76	
1376	
1150	

Espectro de Massas, ESI positivo

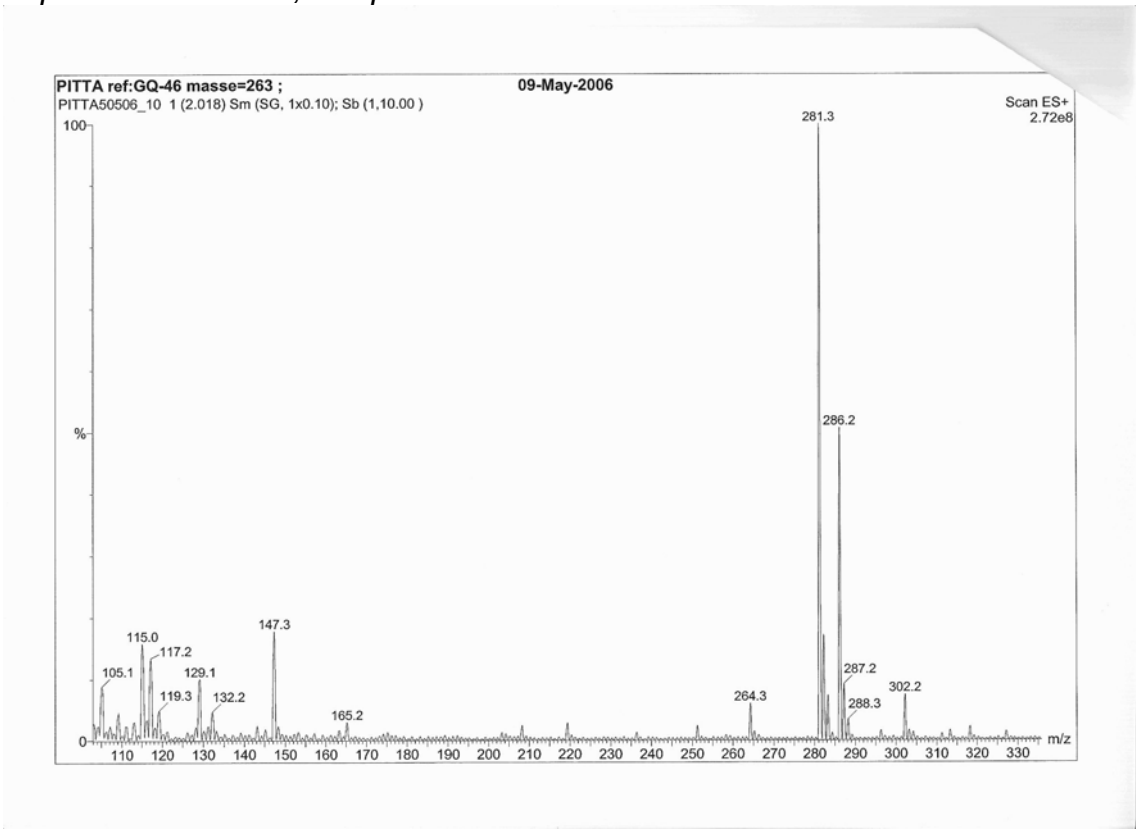

[11h] GQ-52
RMN ^{1}H, $DMSOd_6$

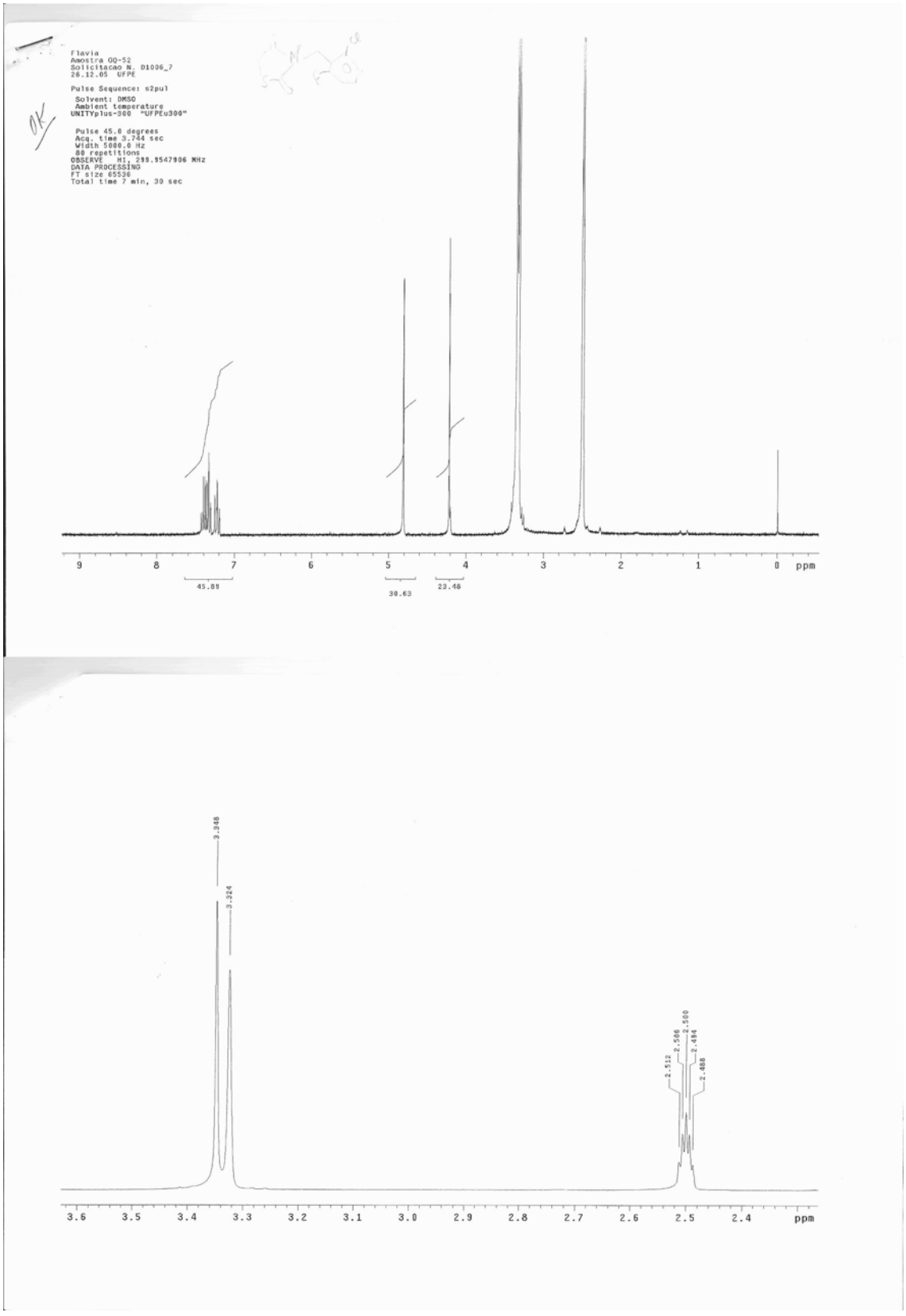

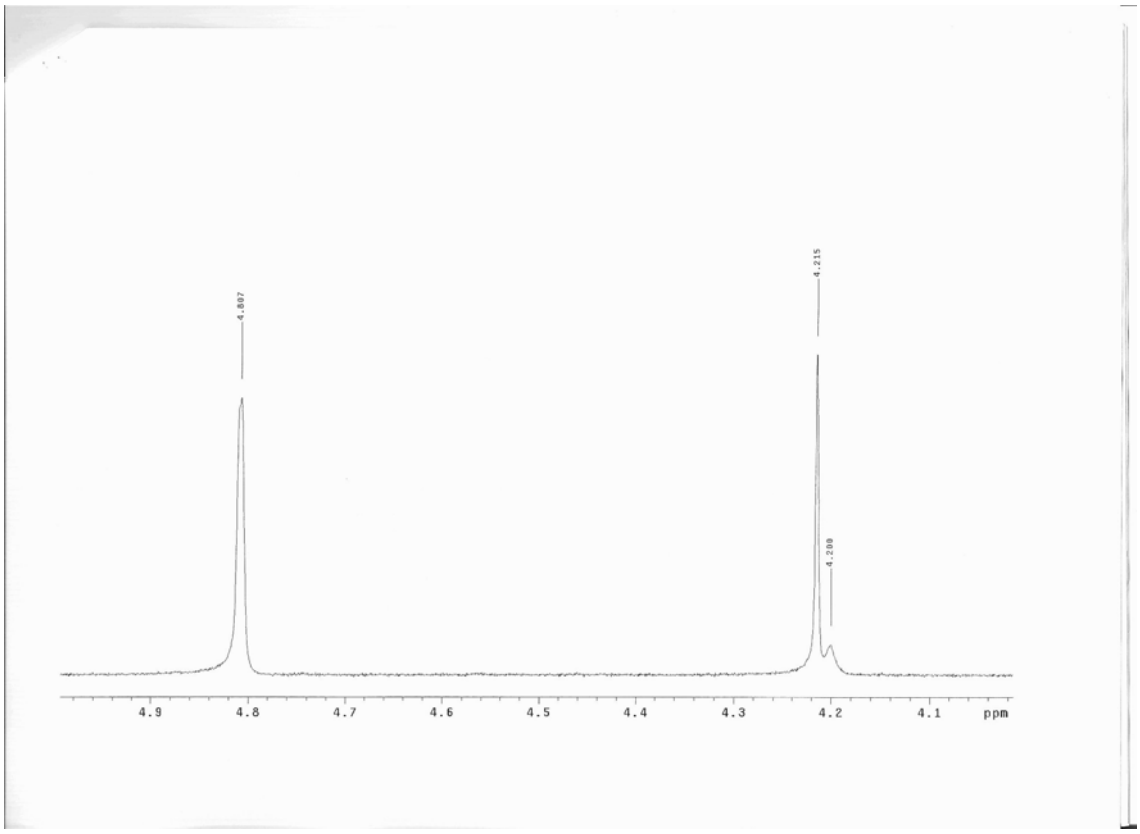
4.807
4.215
4.208
4.9
4.8
4.7
4.6
4.5
4.4
4.3
4.2
4.1
ppm

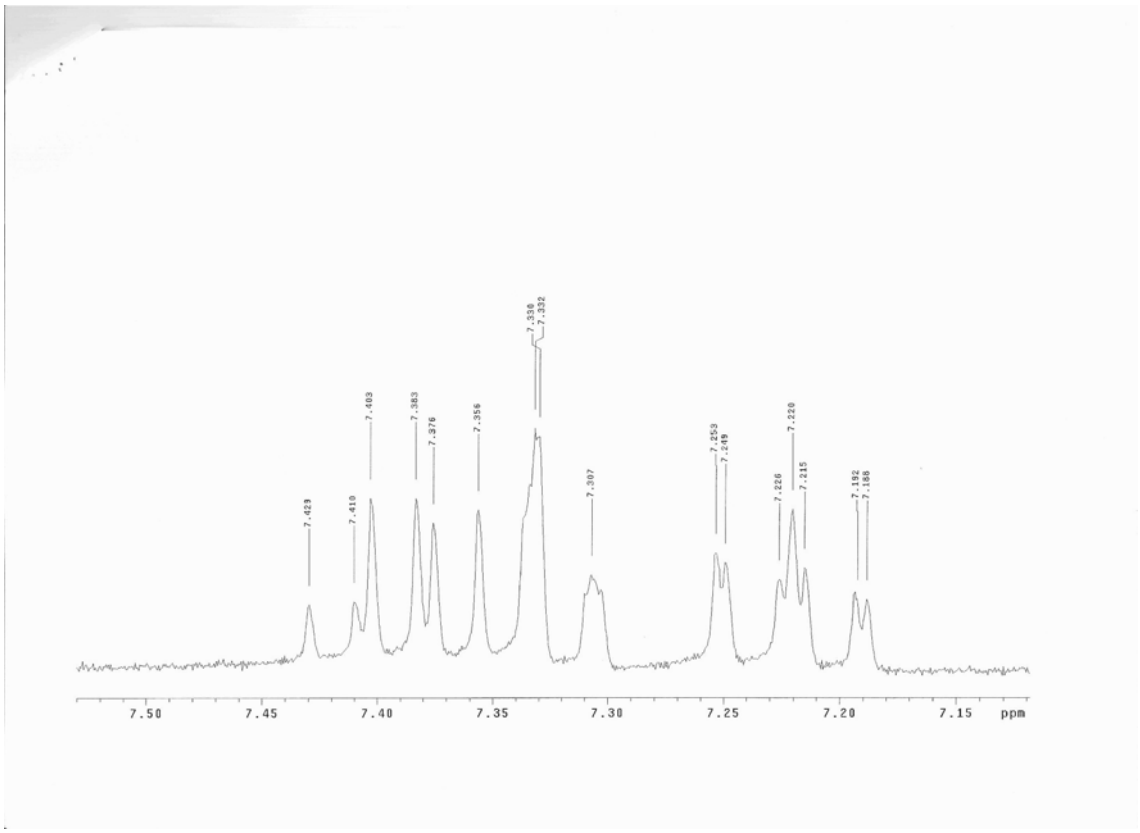
7.429
7.419
7.403
7.383
7.376
7.356
7.338
7.332
7.307
7.253
7.249
7.226
7.220
7.215
7.192
7.188
7.50
7.45
7.40
7.35
7.30
7.25
7.20
7.15
ppm

[11h] GQ-52
IV, KBr

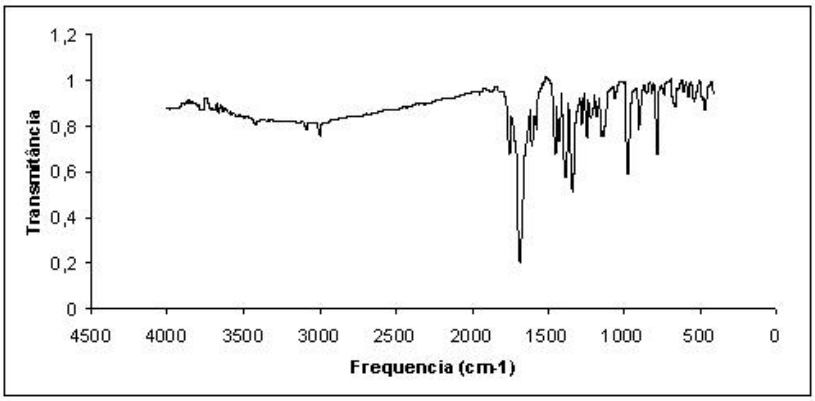

Principais bandas (cm-1)

1681,62
1380,72
1337,07
970,66
781,67

Espectro de Massas, ESI positivo

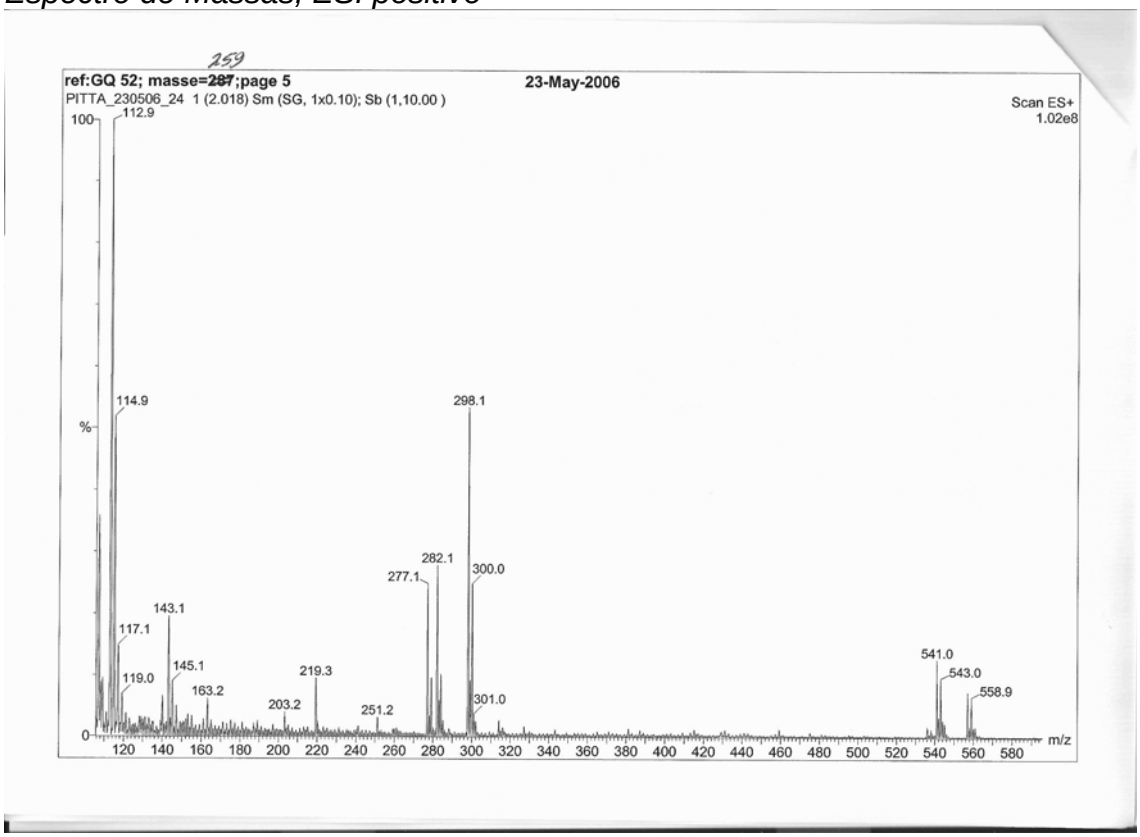

[11i] GQ-56
RMN ^{1}H, $DMSOd_6$

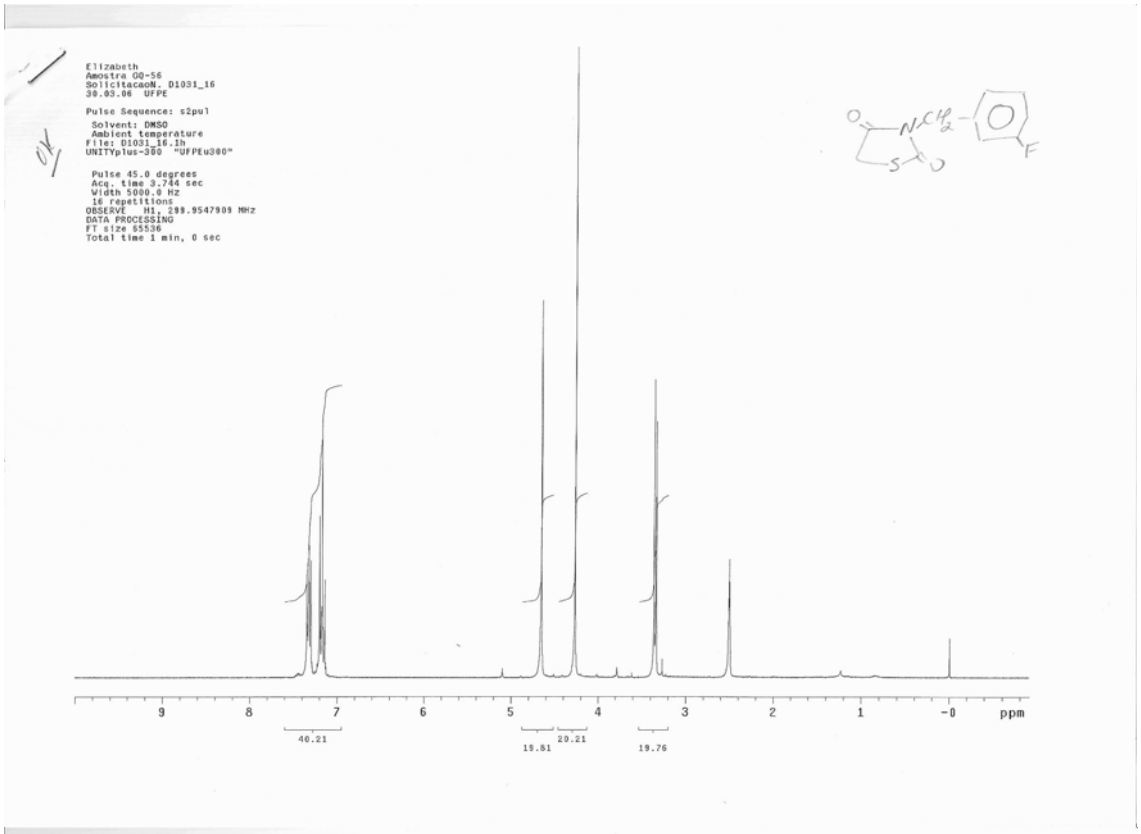

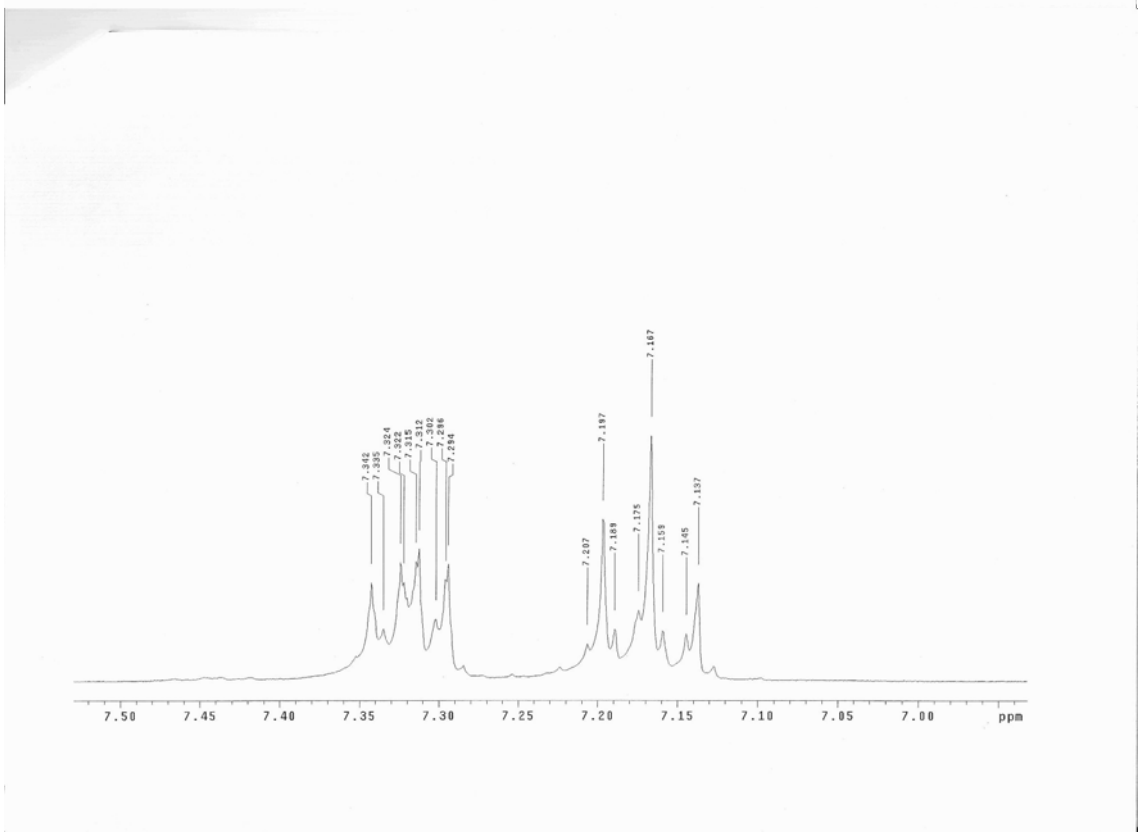

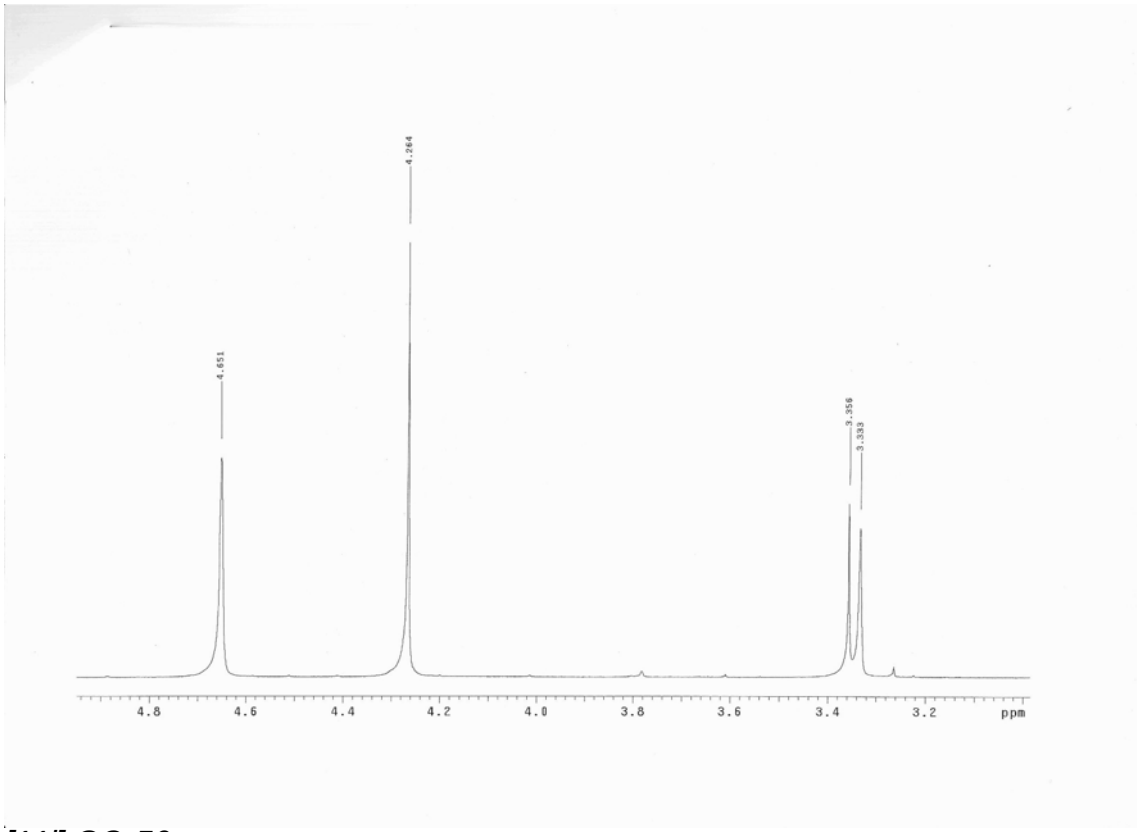

[11i] GQ-56
IV, KBr

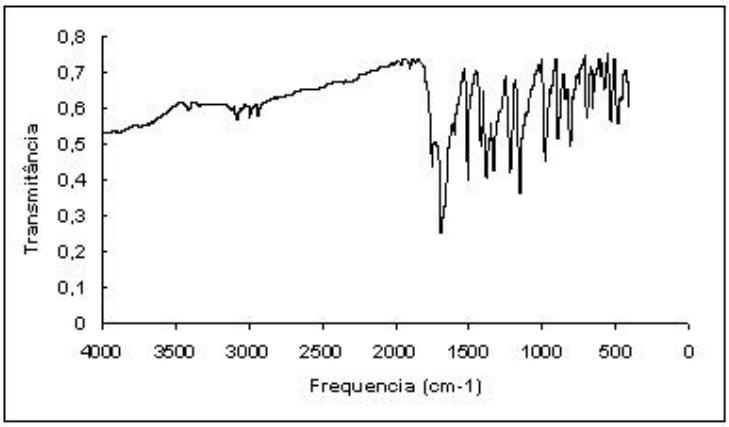

Principais bandas:

3075
2982
2924
1744
1682
1506
1379
1154

Espectro de Massas, ESI positivo

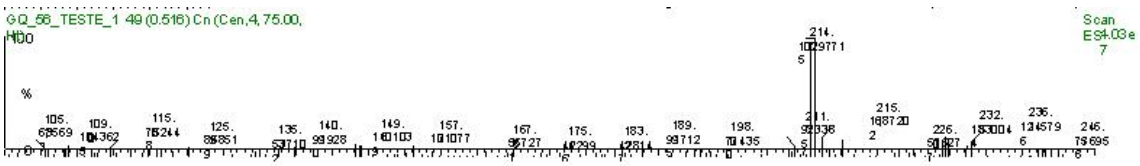

[12b] IP-59
RMN ^{1}H, $DMSOd_6$

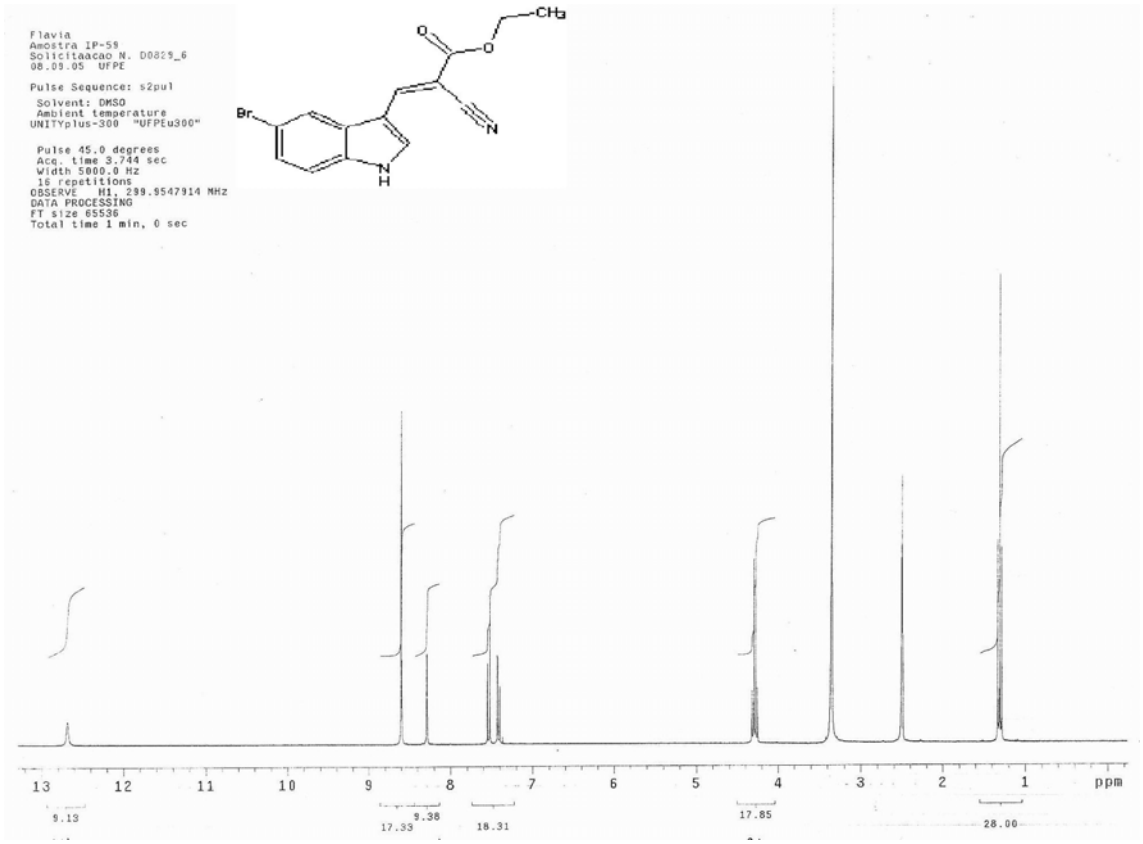

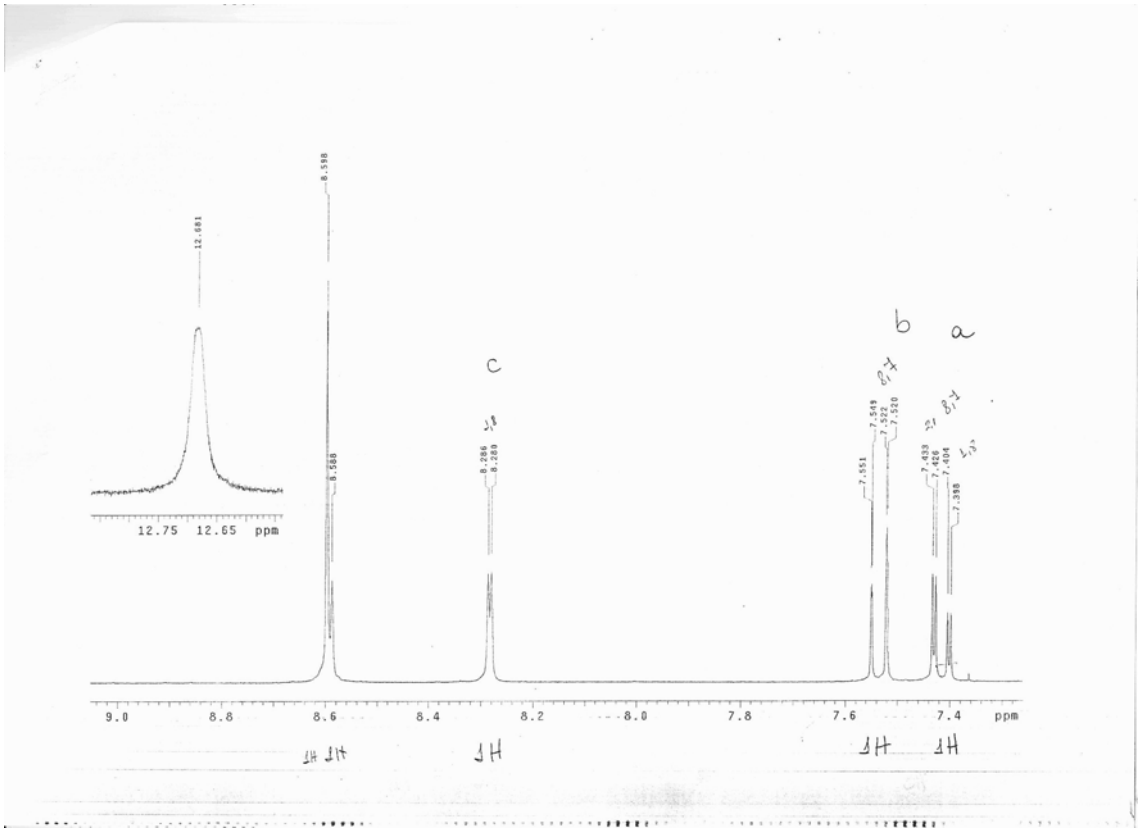

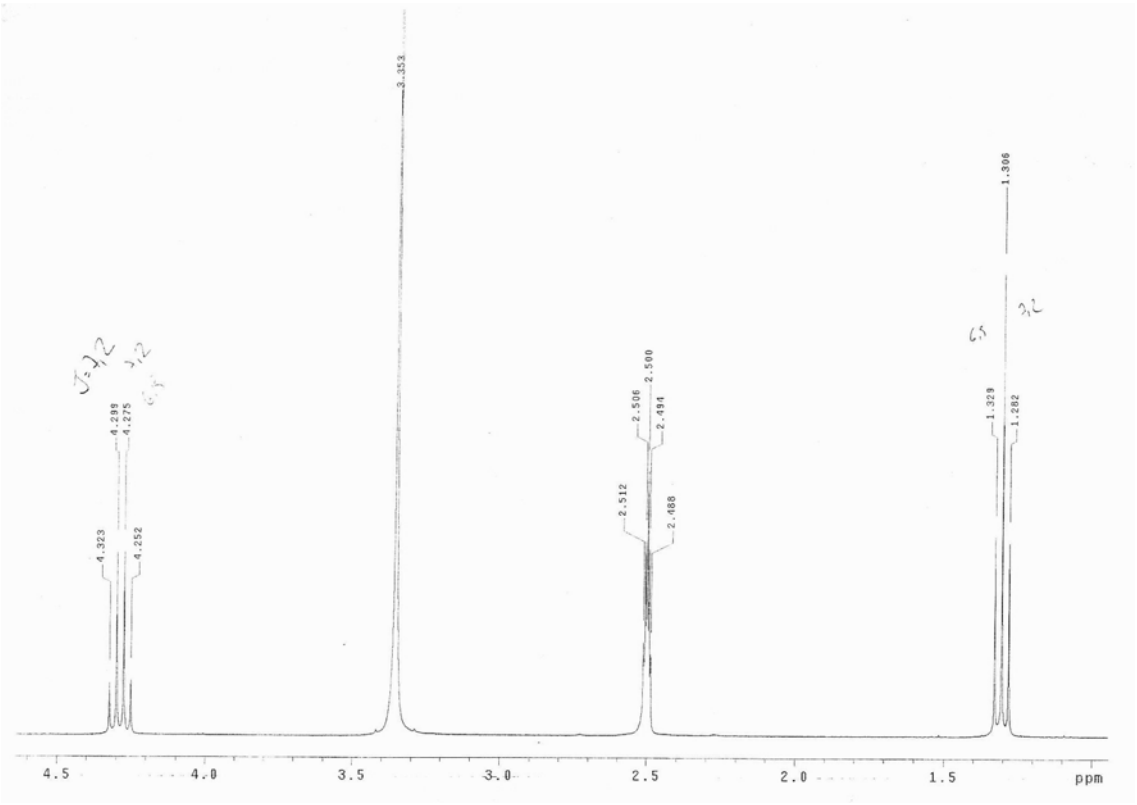
4.323
4.299
4.275
4.252
3.353
2.512
2.506
2.500
2.494
2.488
1.329
1.306
1.282
4.5
4.0
3.5
3.0
2.5
2.0
1.5
ppm

[12b] IP-59
IV, KBr

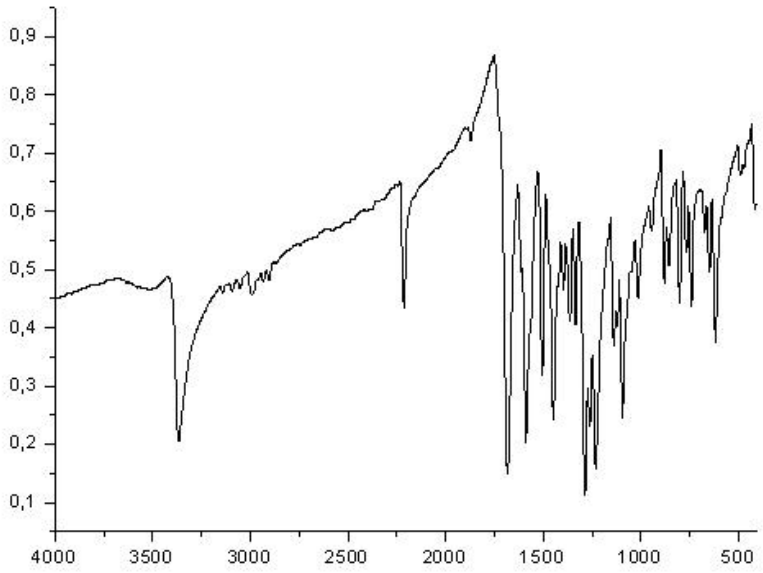

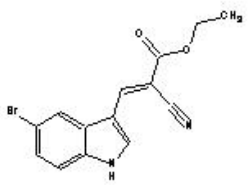

Principais Bandas (cm-1)

3366,21
2990,82
2213,35
1683,00
1588,21
1504,71
1447,91
1364,78
1333,94
1288,80
1262,48
1231,63
1093,97

Espectro de Massas, ESI negativo

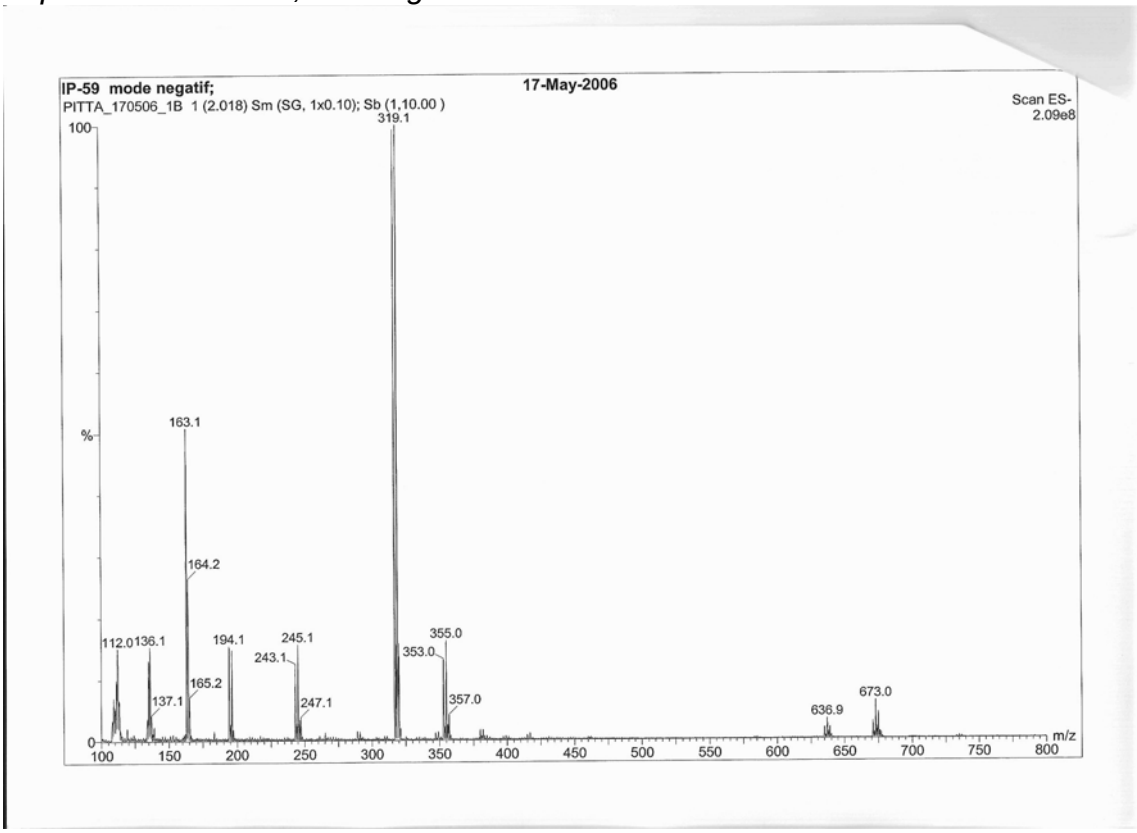

[12c] IP-60
RMN ^{1}H, $DMSOd_6$

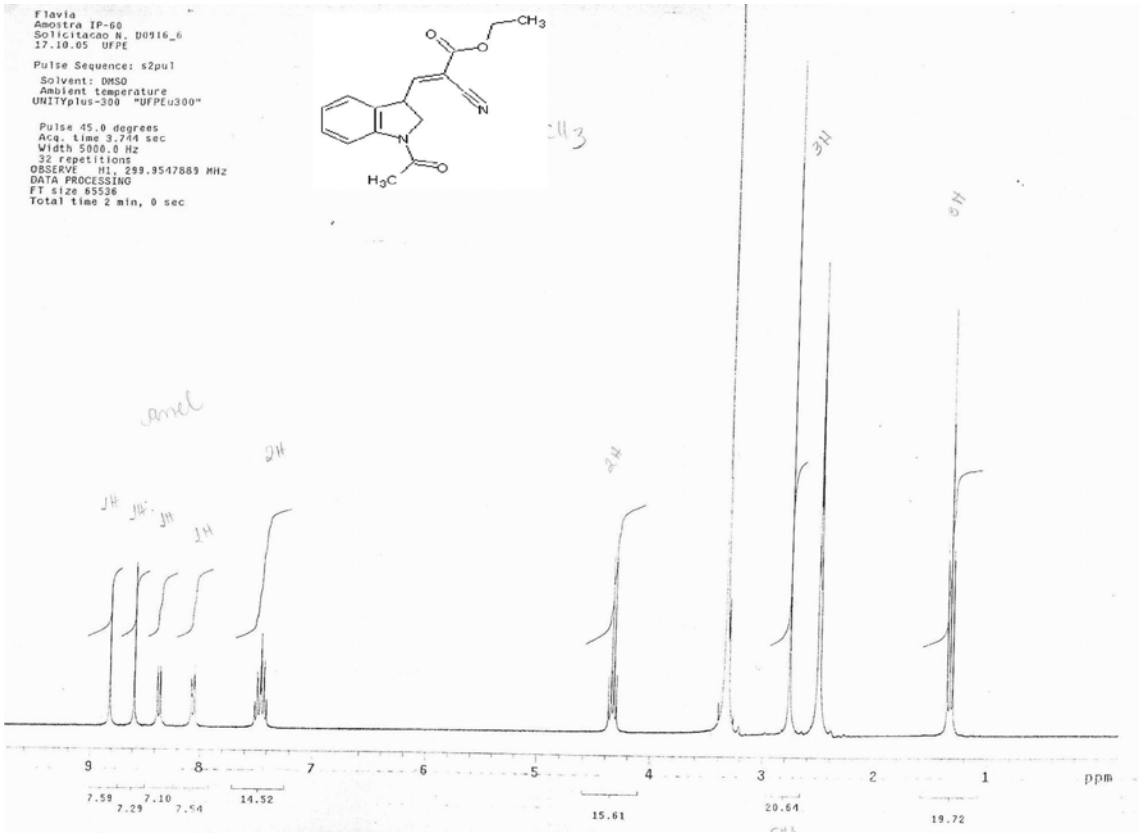

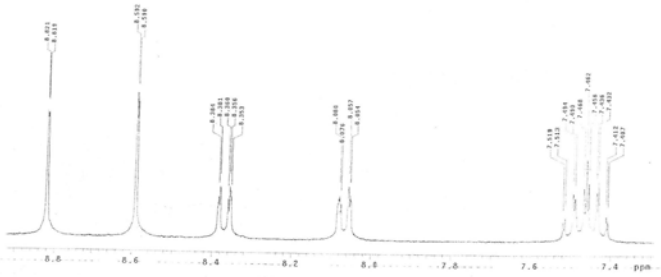

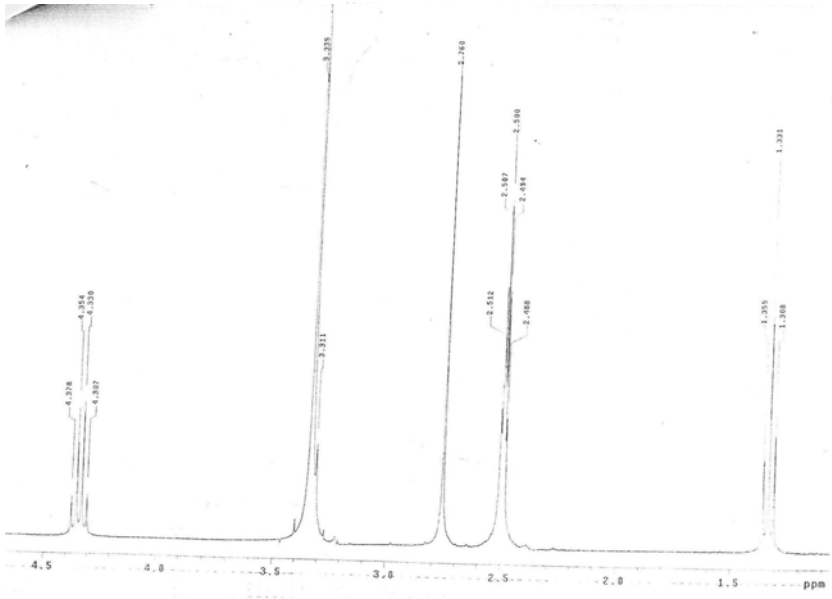

[12c] IP-60
IV, KBr

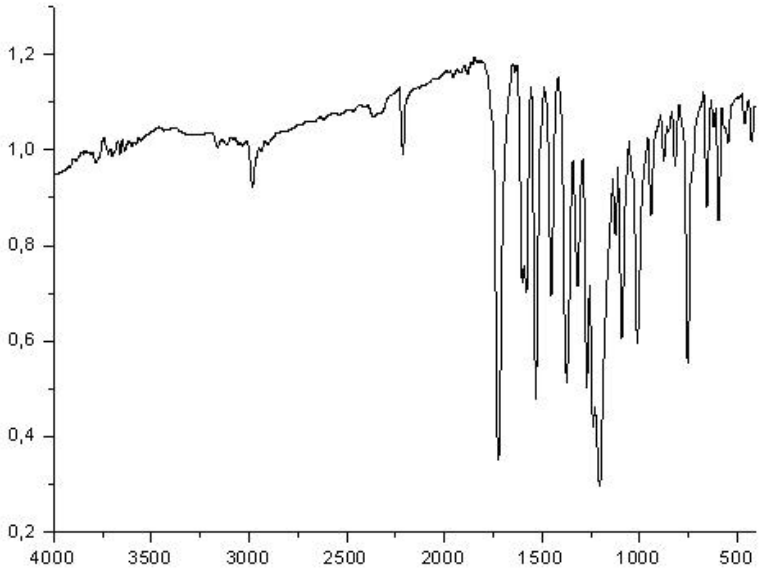

Principais Bandas (cm-1):

2983,67
2363,05
2213,35
1723,62
1602,50
1576,17
1531,04
1452,80
1374,19
1317,39
1238,78
1205,68
1090,96
1012,72
753,56

Espectro de Massas, ESI positivo

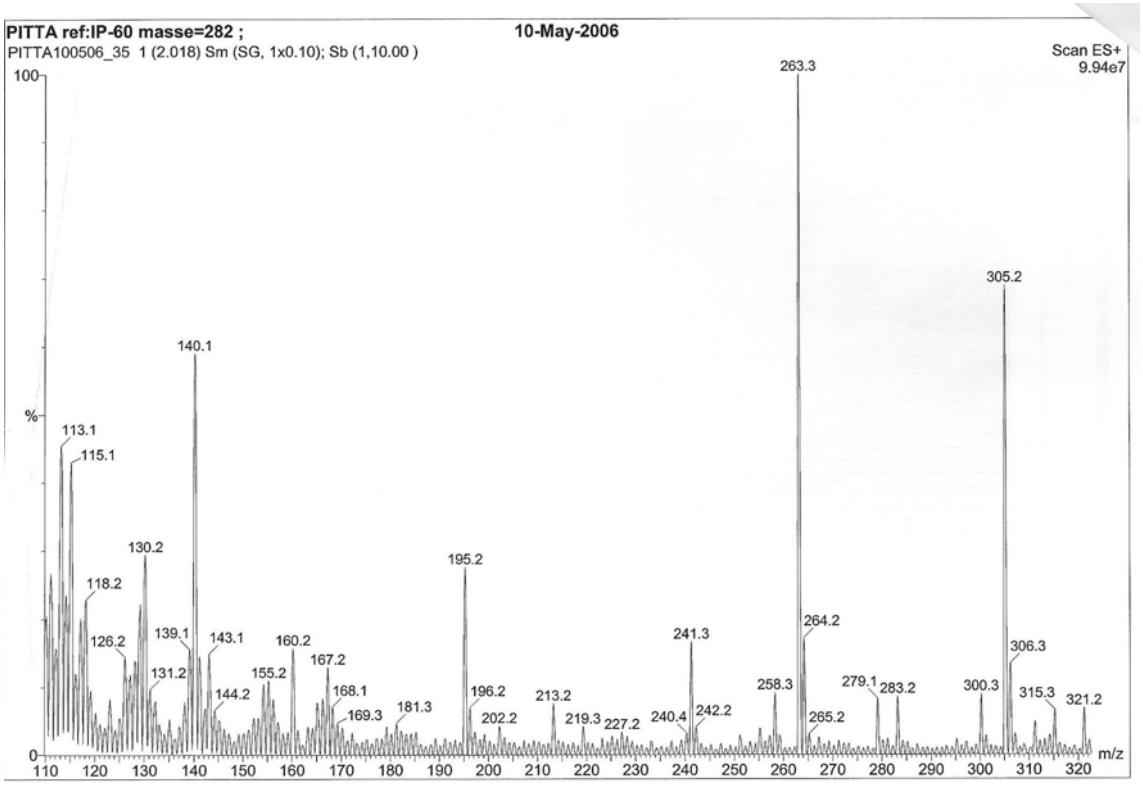

[13 a] RA-4
RMN ^{1}H, DMSOd_6

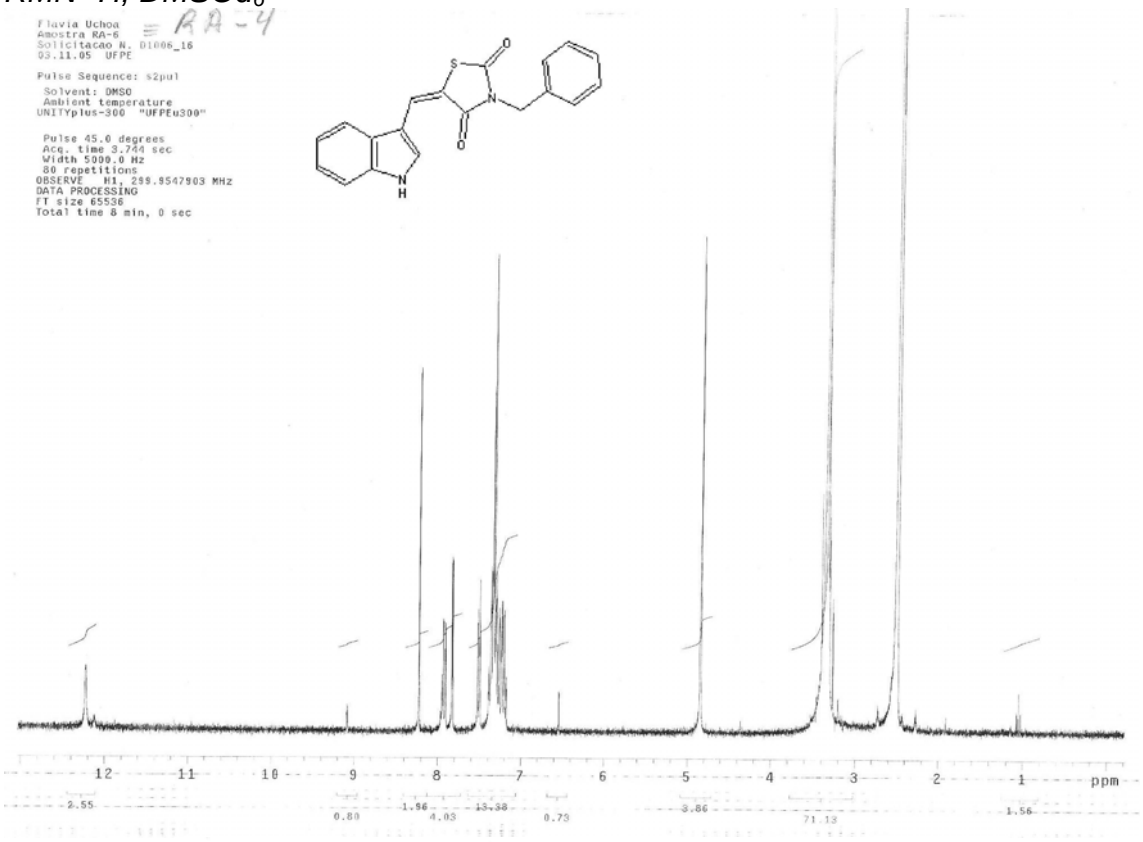

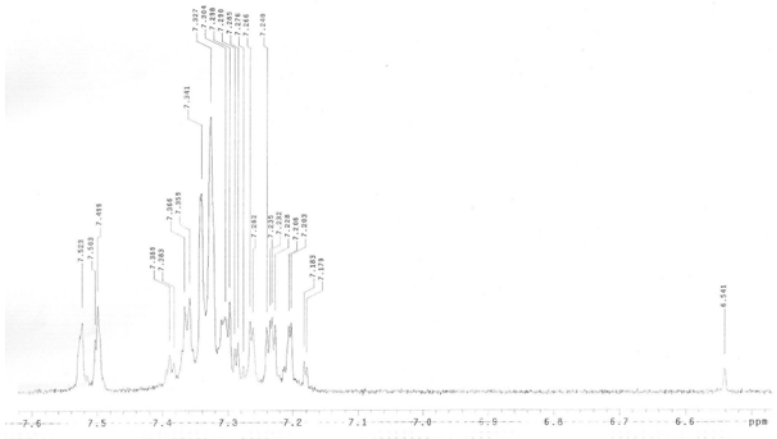

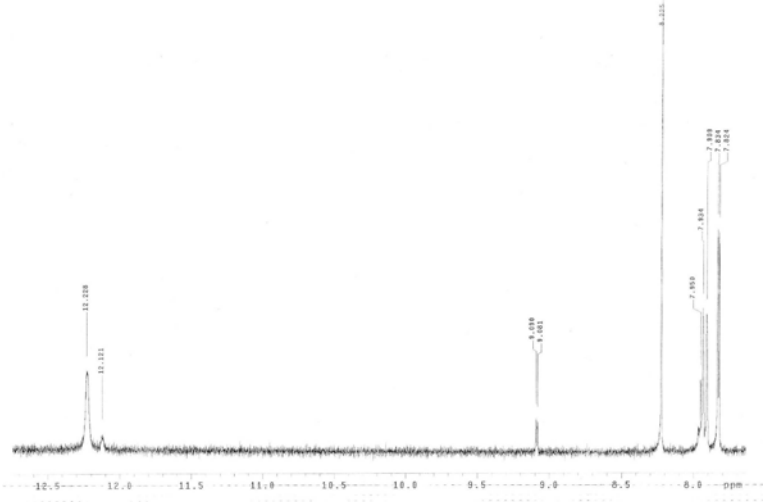

[13 a] RA-4
IV, KBr

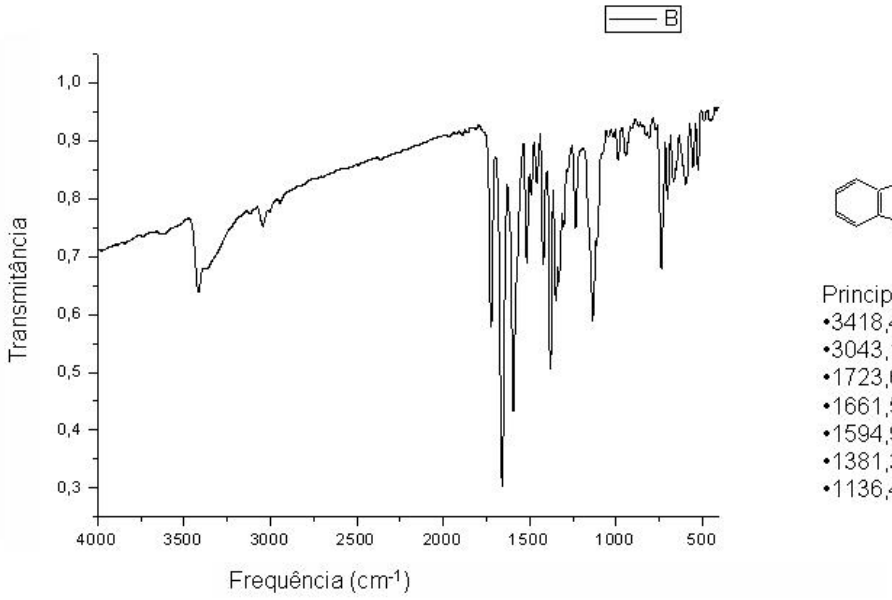

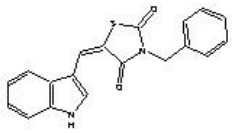

Principais bandas (cm^{-1}):
- 3418,49
- 3043,10
- 1723,62
- 1661,56
- 1594,98
- 1381,33
- 1136,47

[13 b] RA-5
RMN ^{1}H, $DMSOd_6$

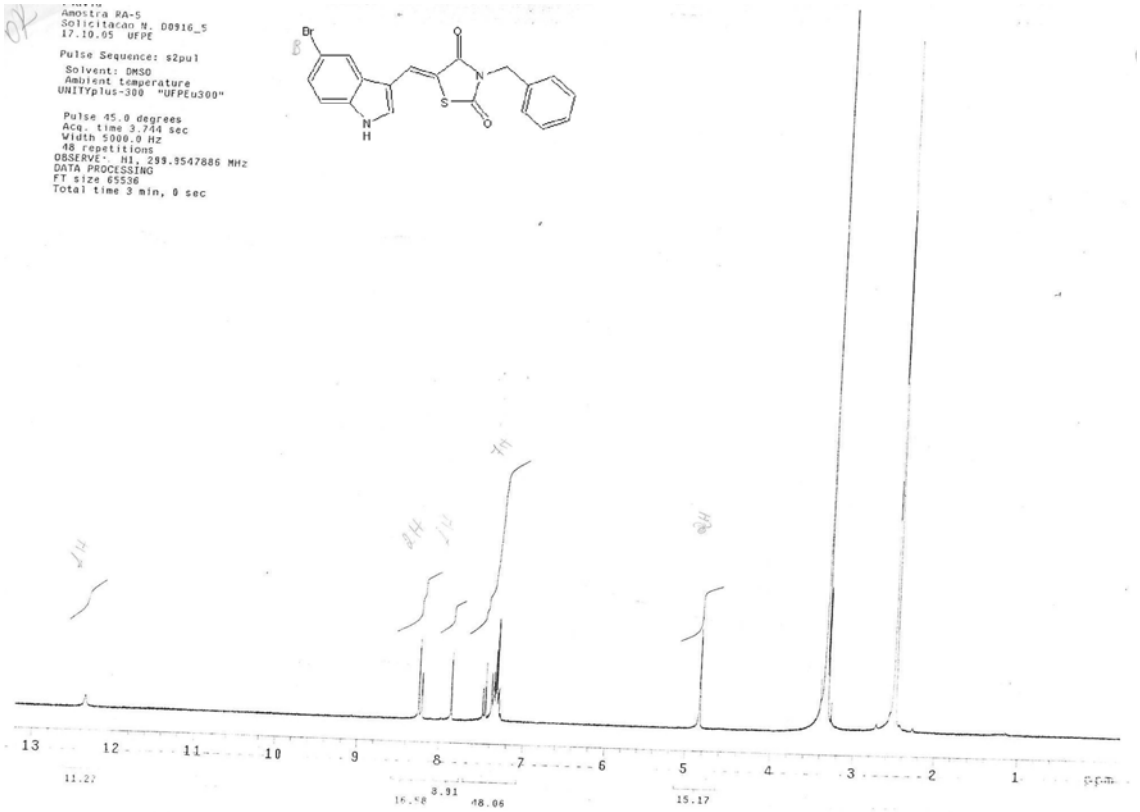

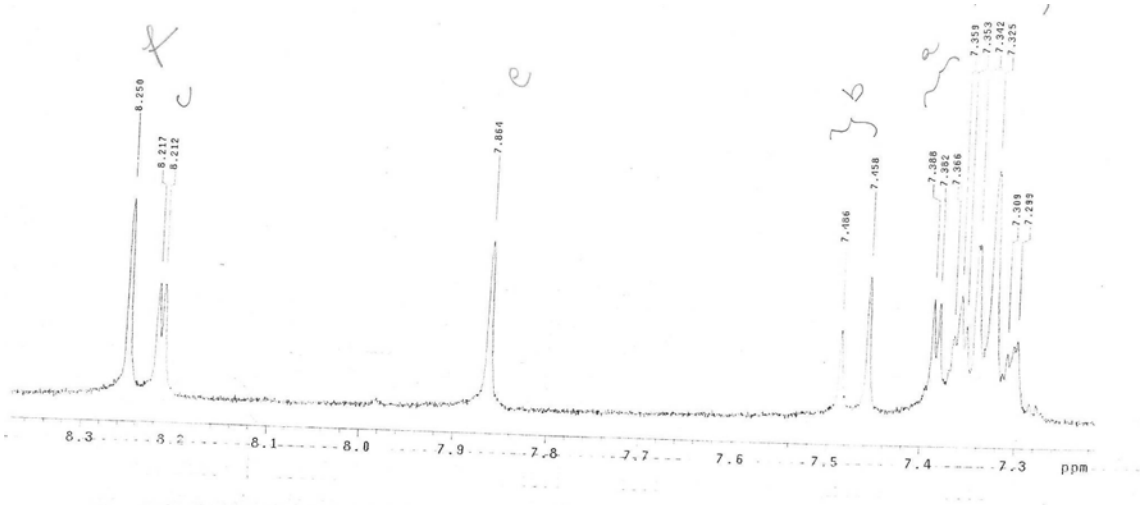

[13 a] RA-5
IV, KBr

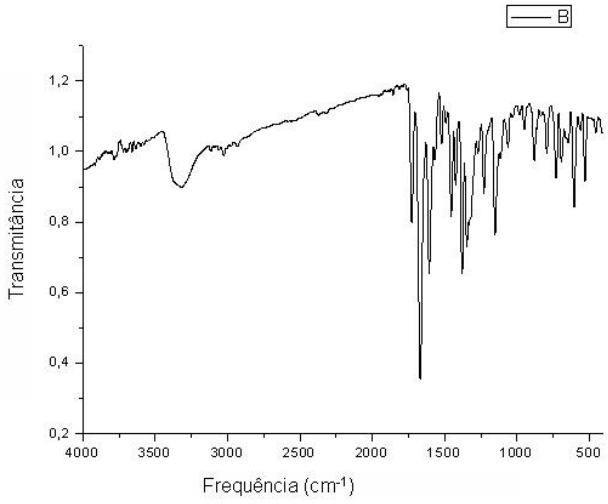

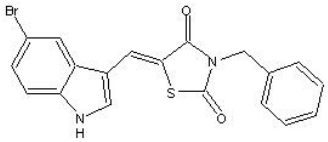

Principais Bandas (cm^{-1}):
- 3316,56
- 1728,51
- 1671,34
- 1607,02
- 1455,06
- 1378,70
- 1347,86
- 1229,38
- 1150,76
- 606,12

Espectro de Massas, ESI negativo

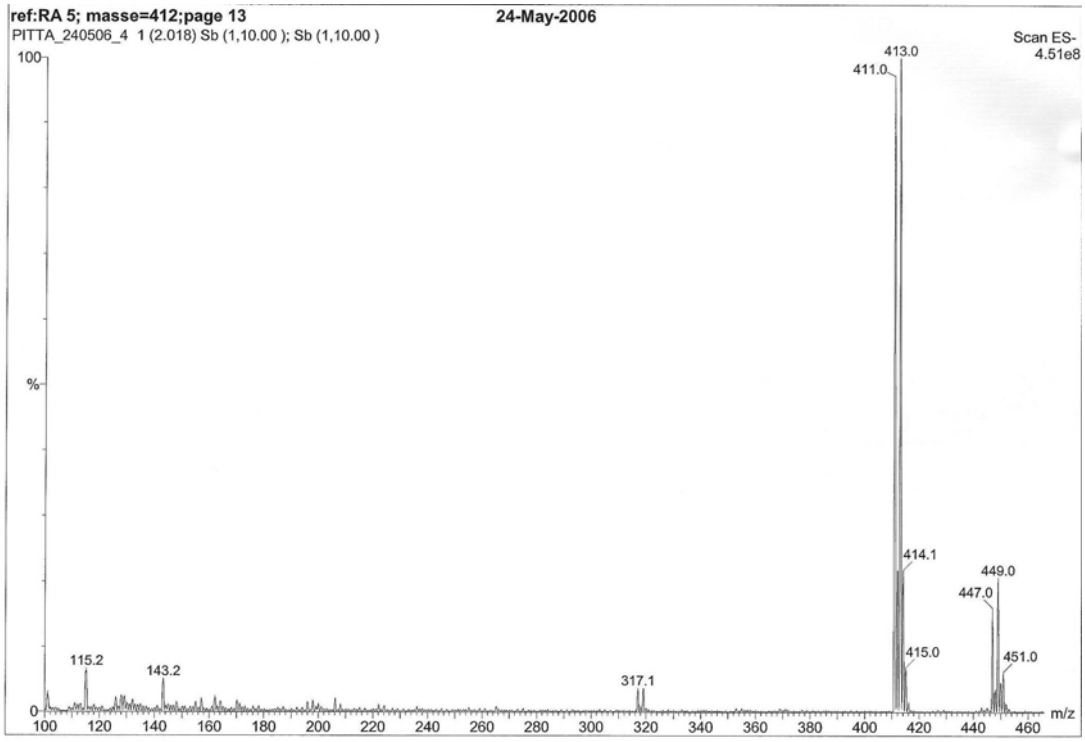

[13 c] RA-6
RMN ^{1}H, $DMSOd_6$

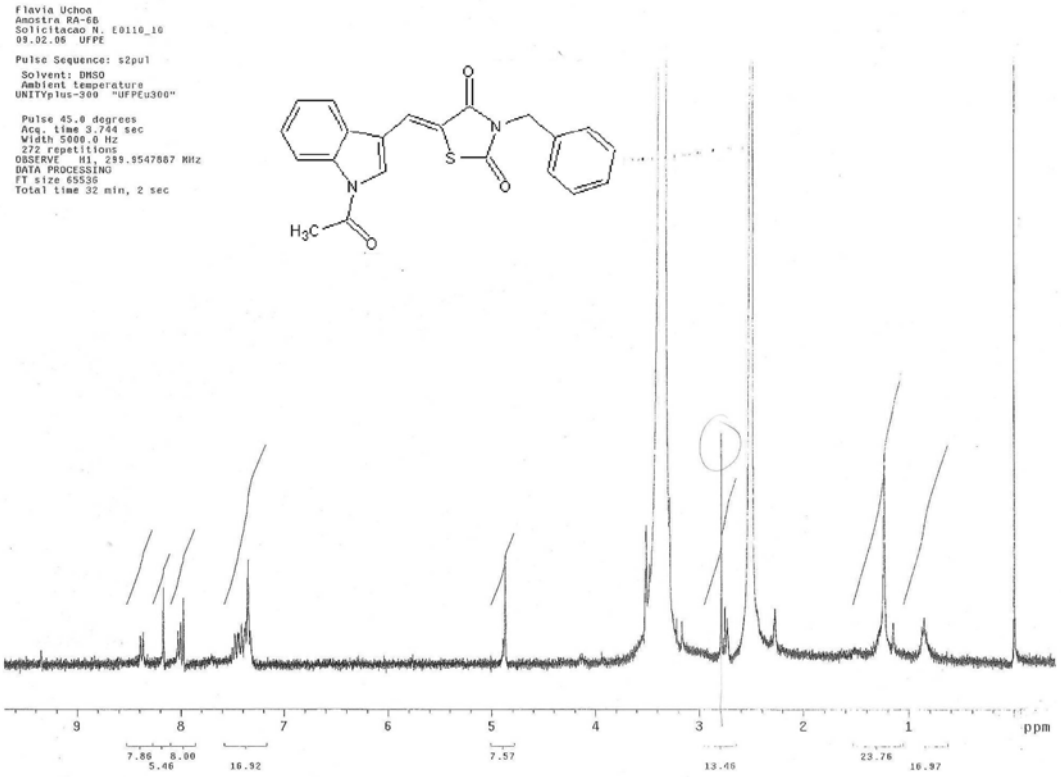

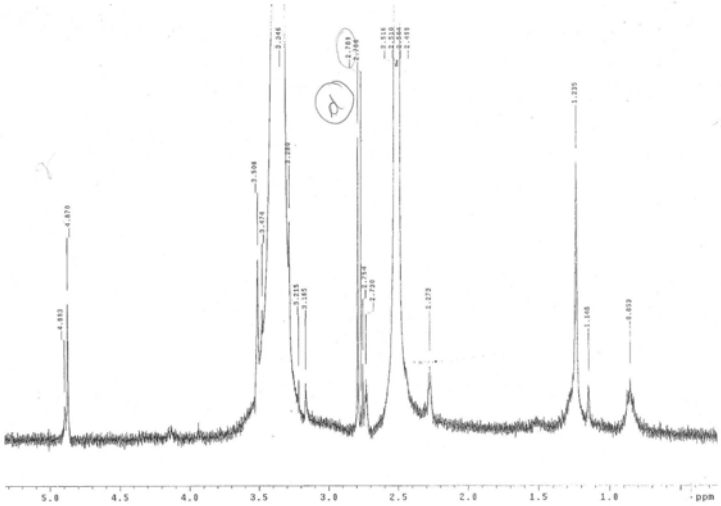

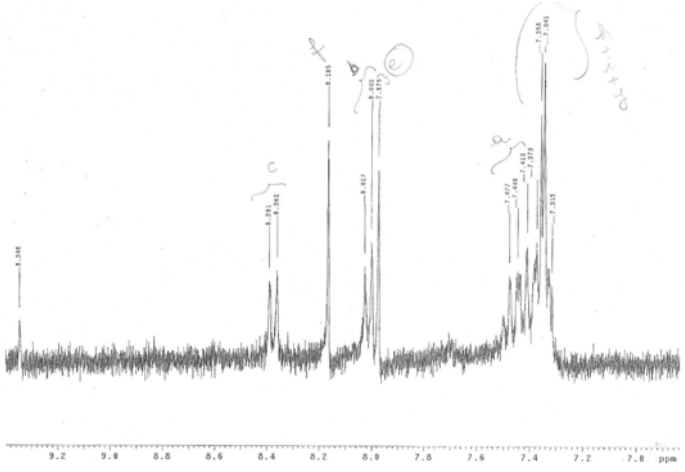

Espectro de Massas, ESI positivo

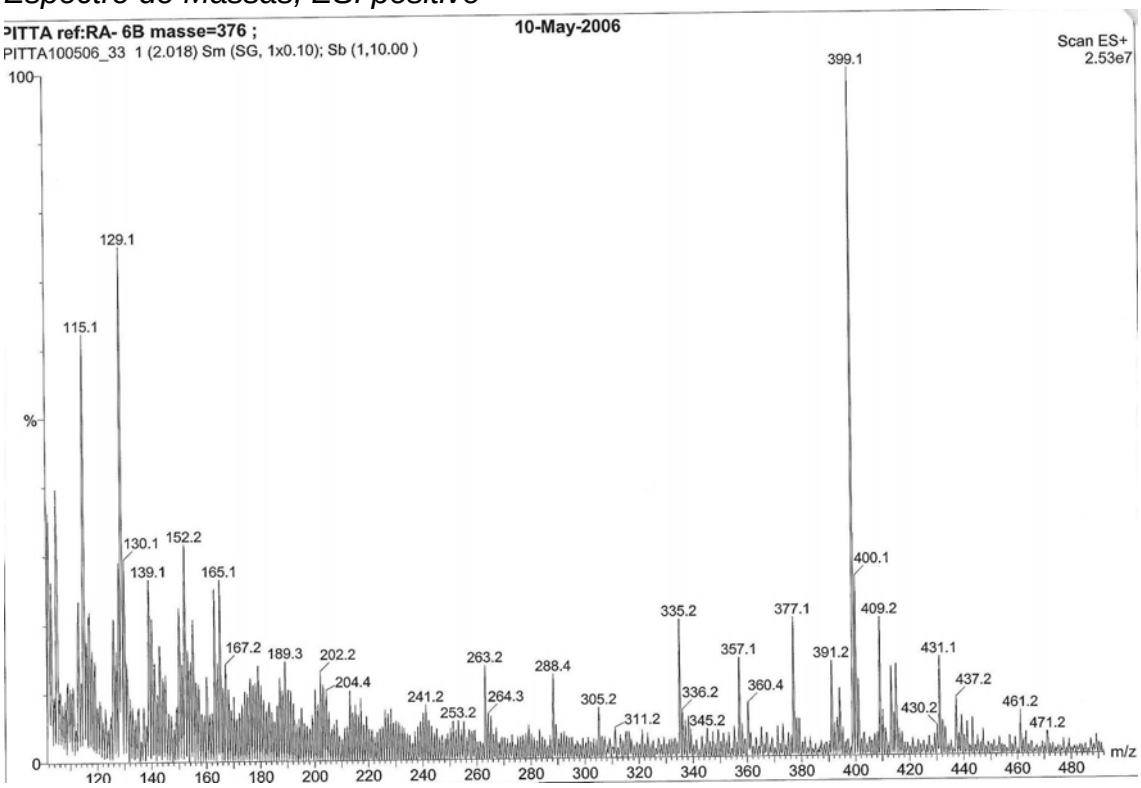

[13 d] AL-16
RMN ^{1}H, $DMSOd_6$

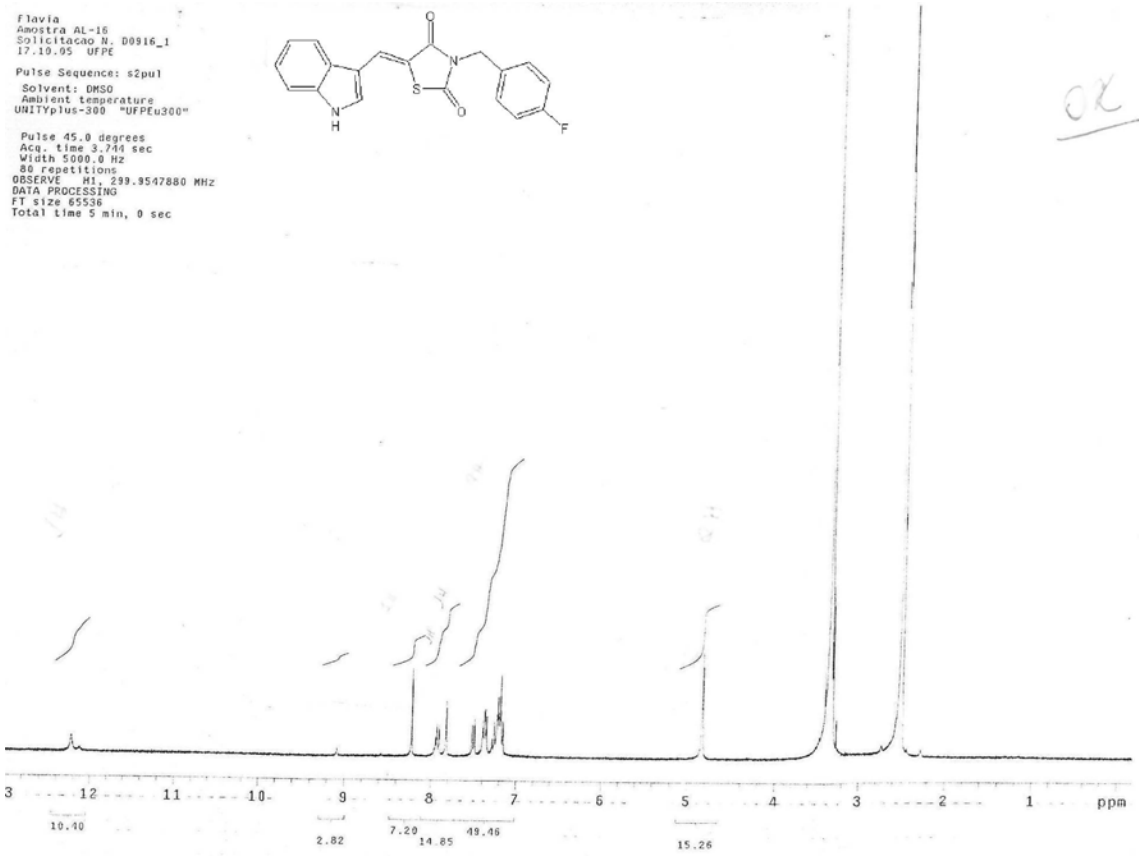

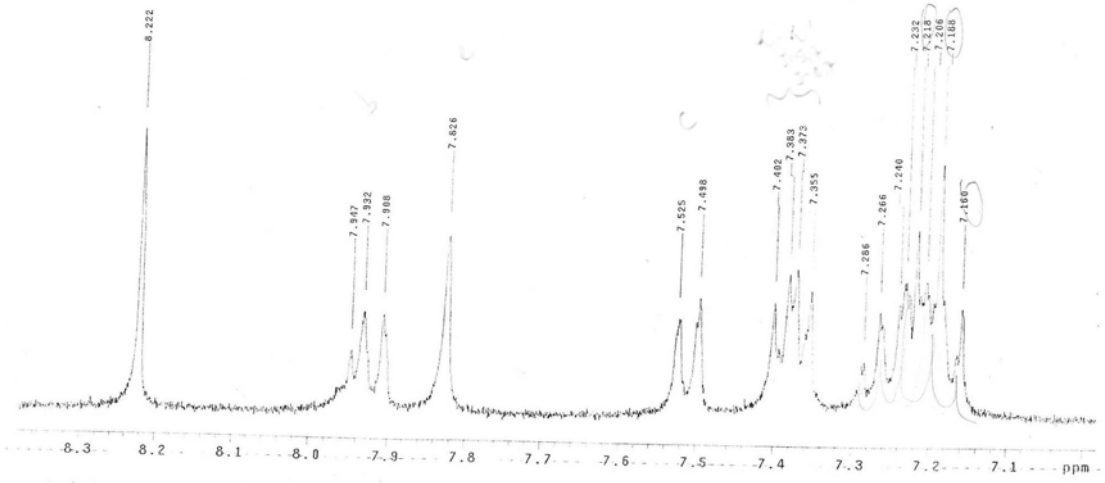

[13 d] AL-16
IV, KBr

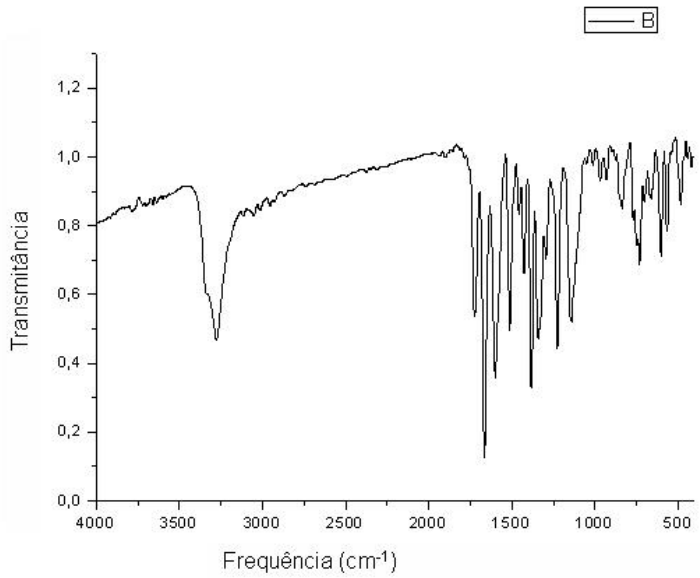

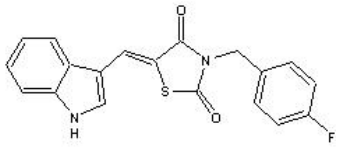

Principais bandas (cm^{-1})
- 3278,19
- 1723,62
- 1666,45
- 1599,87
- 1511,85
- 1383,59
- 1343,34
- 1224,49

Espectro de Massas, ESI negativo

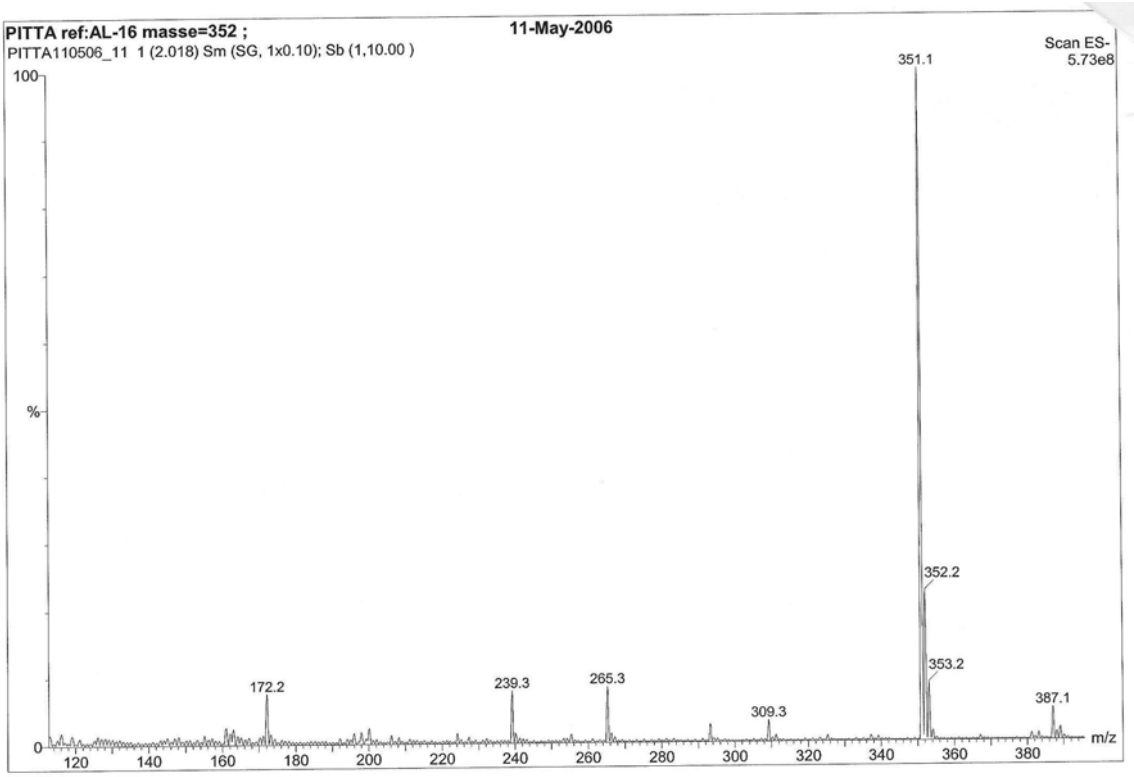

[13 e] LYSO-5
RMN ^{1}H, $DMSOd_6$

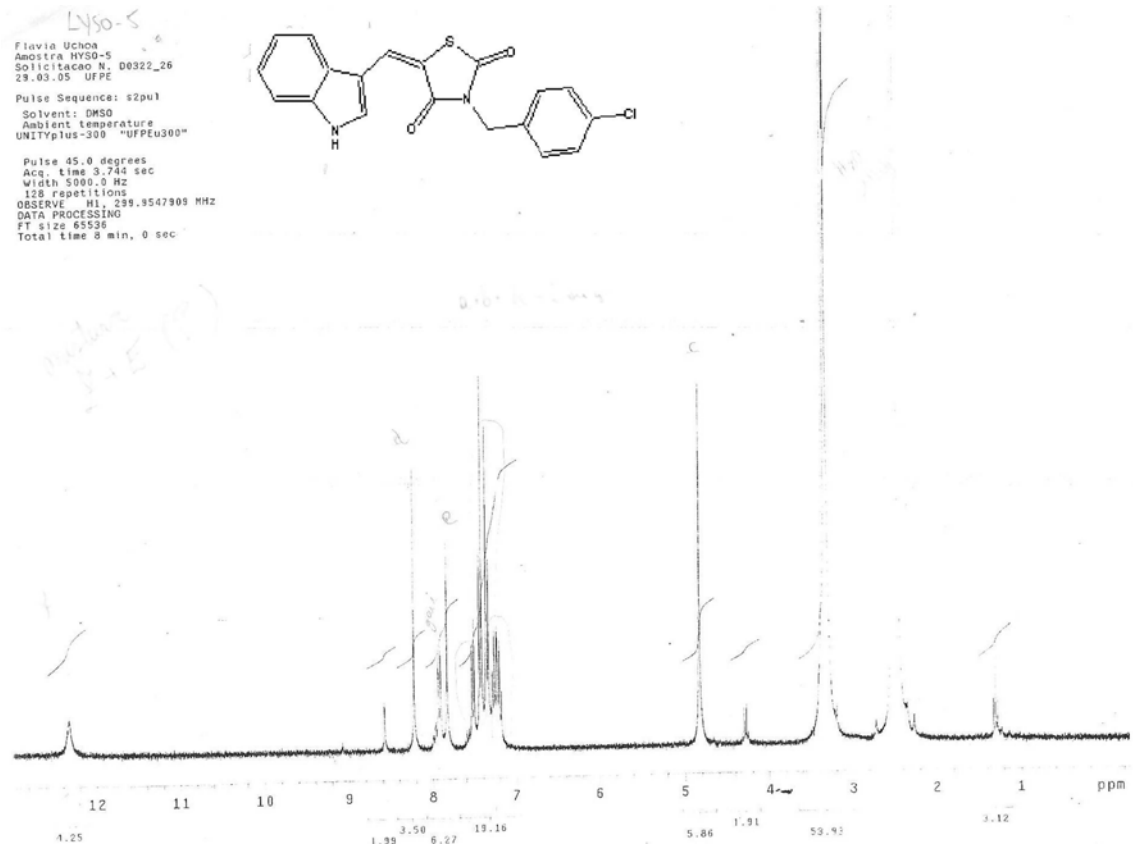

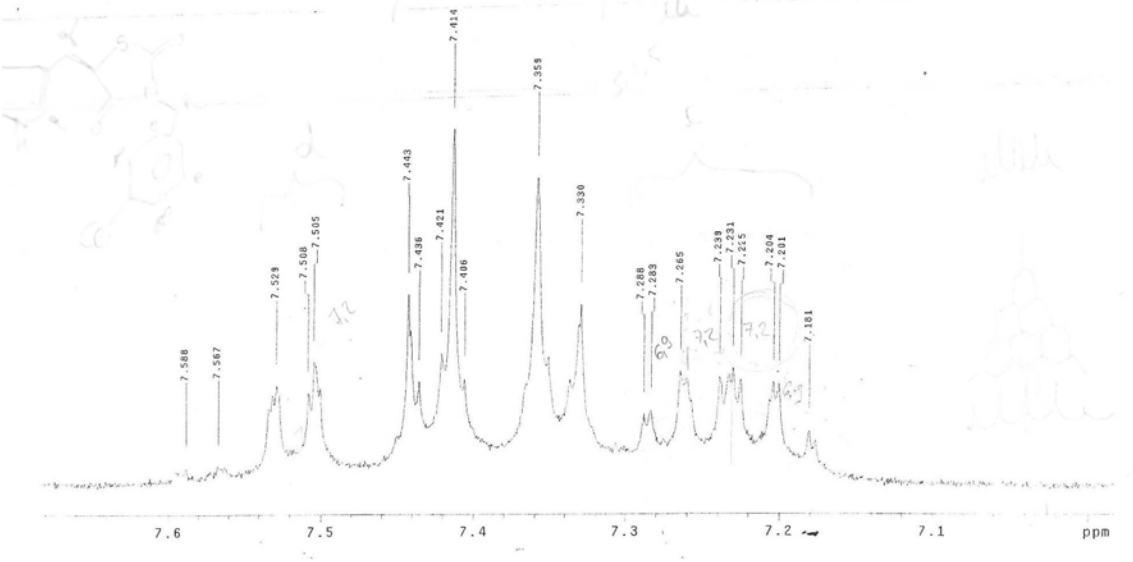

[13 e] LYSO-5
IV, KBr

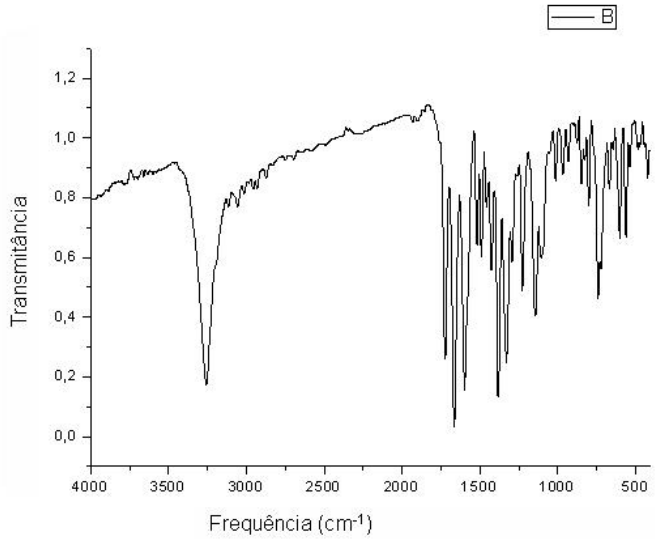

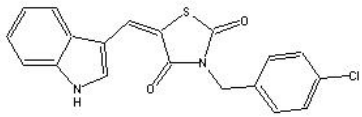

Principais bandas (cm^{-1}):
- 3259,38
- 3057,40
- 1723,62
- 1666,45
- 1599,87
- 1380,96
- 1331,31

Espectro de Massas, ESI negativo

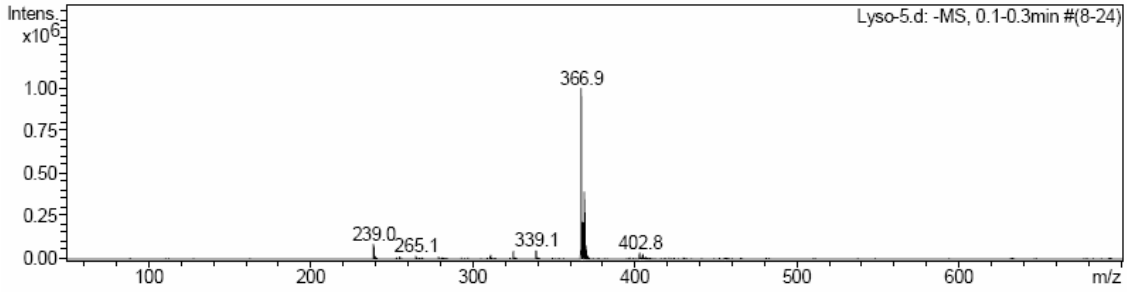

#	m/z	I	I %
1	239.0	86507	8.7
2	240.0	14084	1.4
3	255.1	11134	1.1
4	265.1	15246	1.5
5	279.1	12946	1.3
6	281.2	6726	0.7
7	311.1	21950	2.2
8	325.1	46030	4.6
9	326.1	7210	0.7
10	339.1	48697	4.9
11	340.1	7581	0.8
12	366.9	995725	100.0
13	367.9	214043	21.5
14	368.9	391720	39.3
15	369.9	77959	7.8
16	370.9	17756	1.8
17	402.8	33655	3.4
18	404.8	25608	2.6
19	405.8	7021	0.7
20	406.8	7664	0.8

[13 f] LYSO-7
RMN ^{1}H, $DMSOd_6$

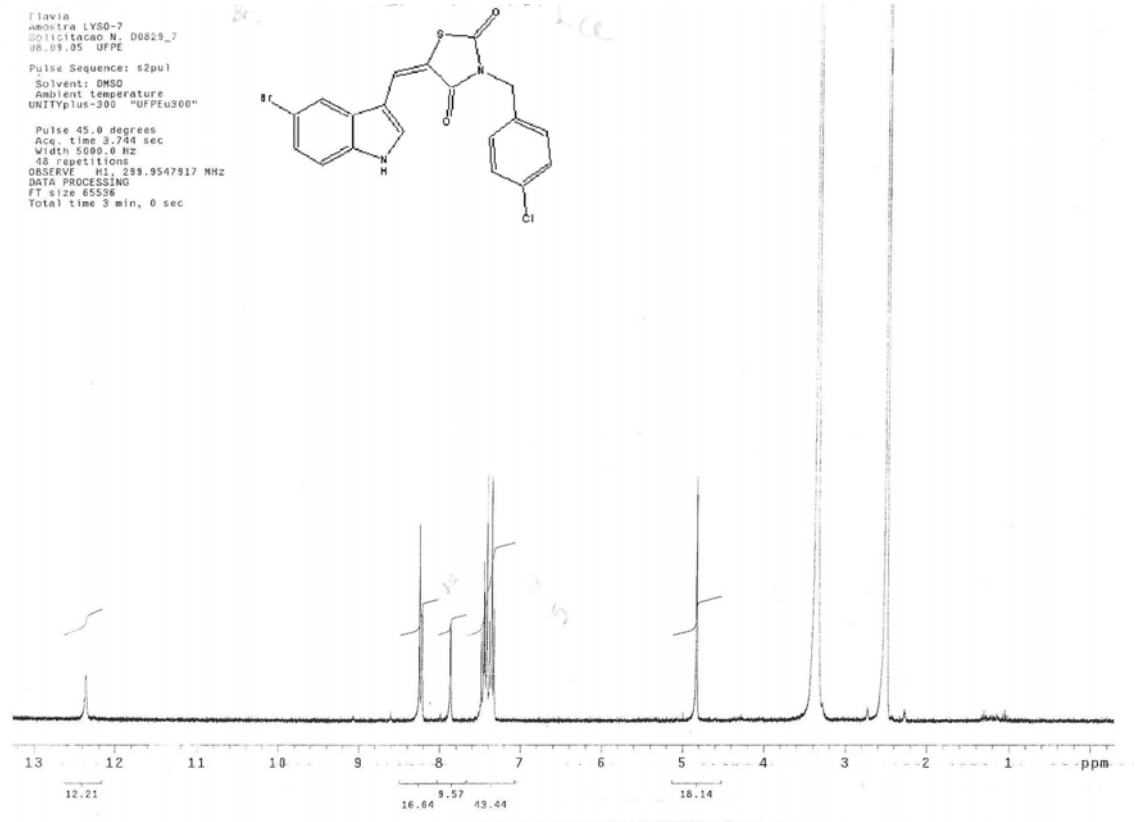

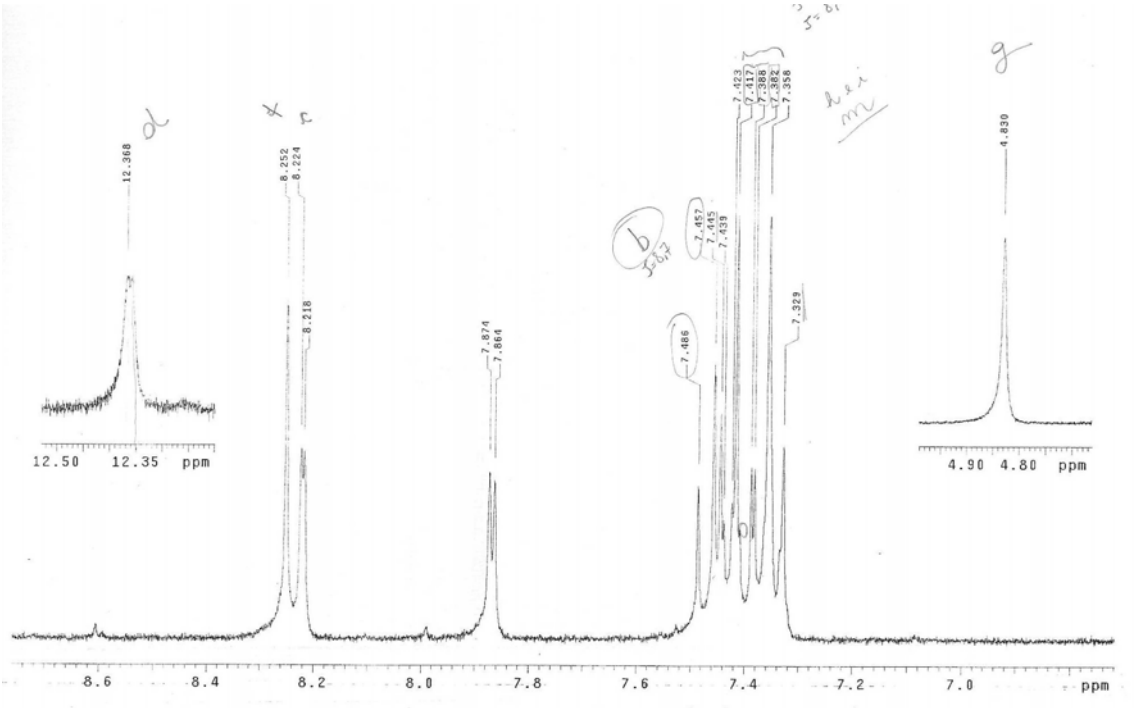

[13 f] LYSO-7
IV, KBr

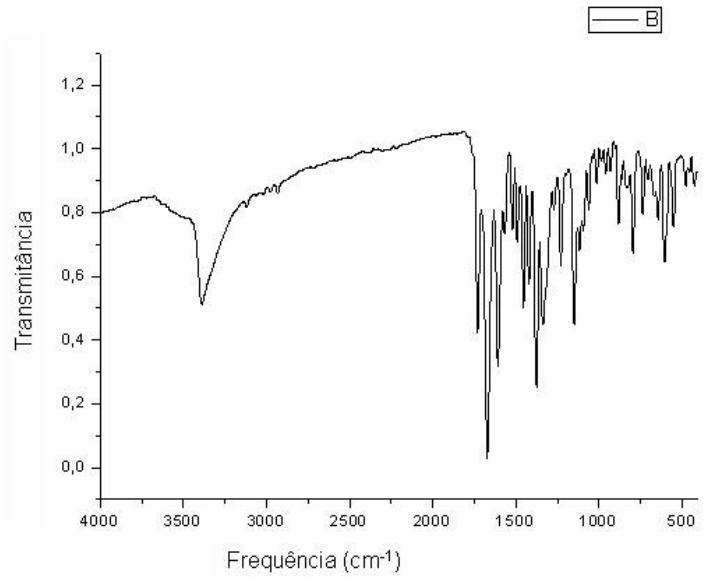

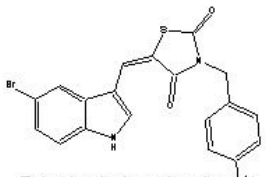

Principais bandas (cm^{-1})
- 3389,90
- 3119,08
- 2933,65
- 1730,77
- 1671,34
- 1607,02
- 1455,06
- 1419,32
- 1376,44
- 1336,20
- 1148,51

Espectro de Massas, ESI negativo

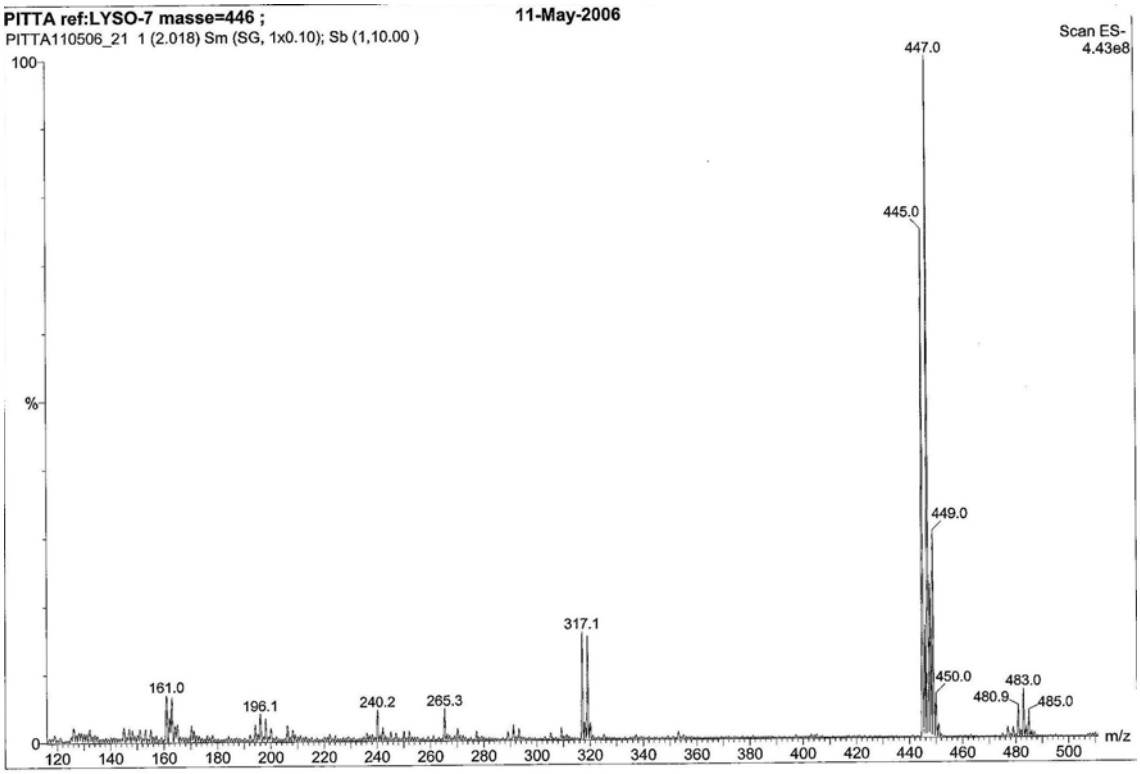

[13 g] LYSO-8
RMN ^{1}H, $DMSOd_6$

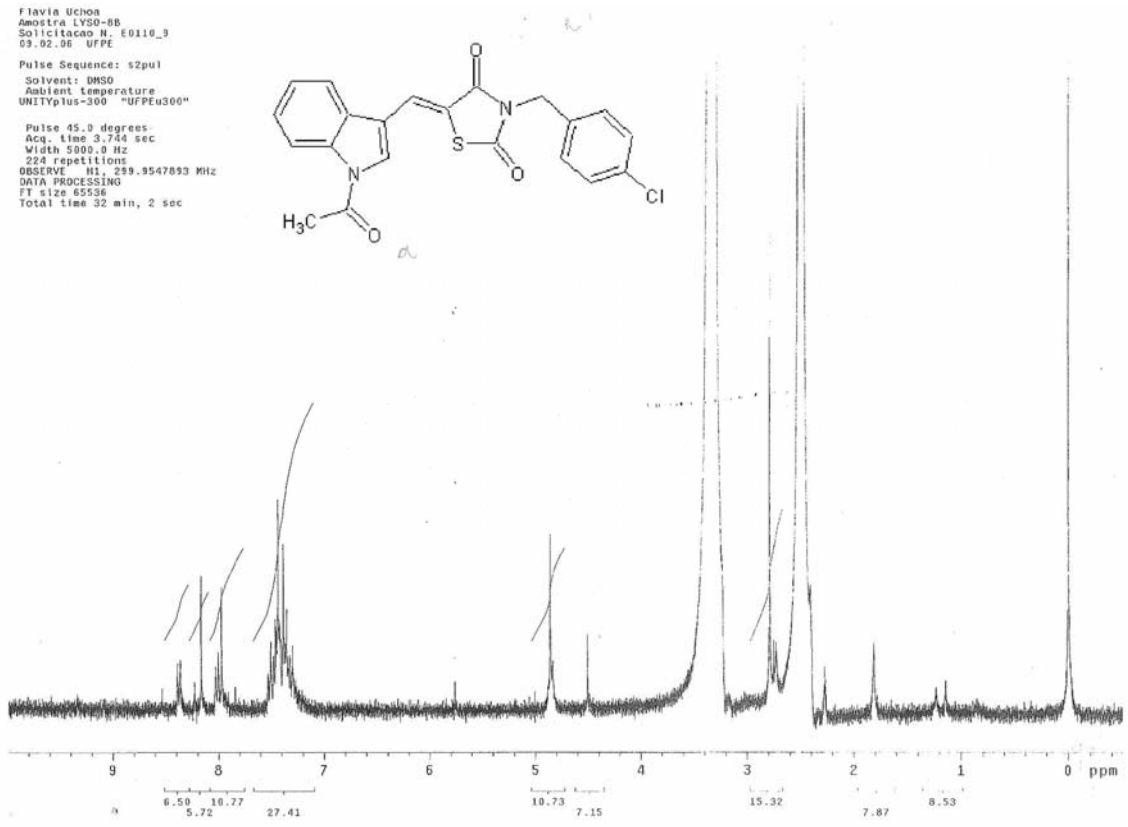

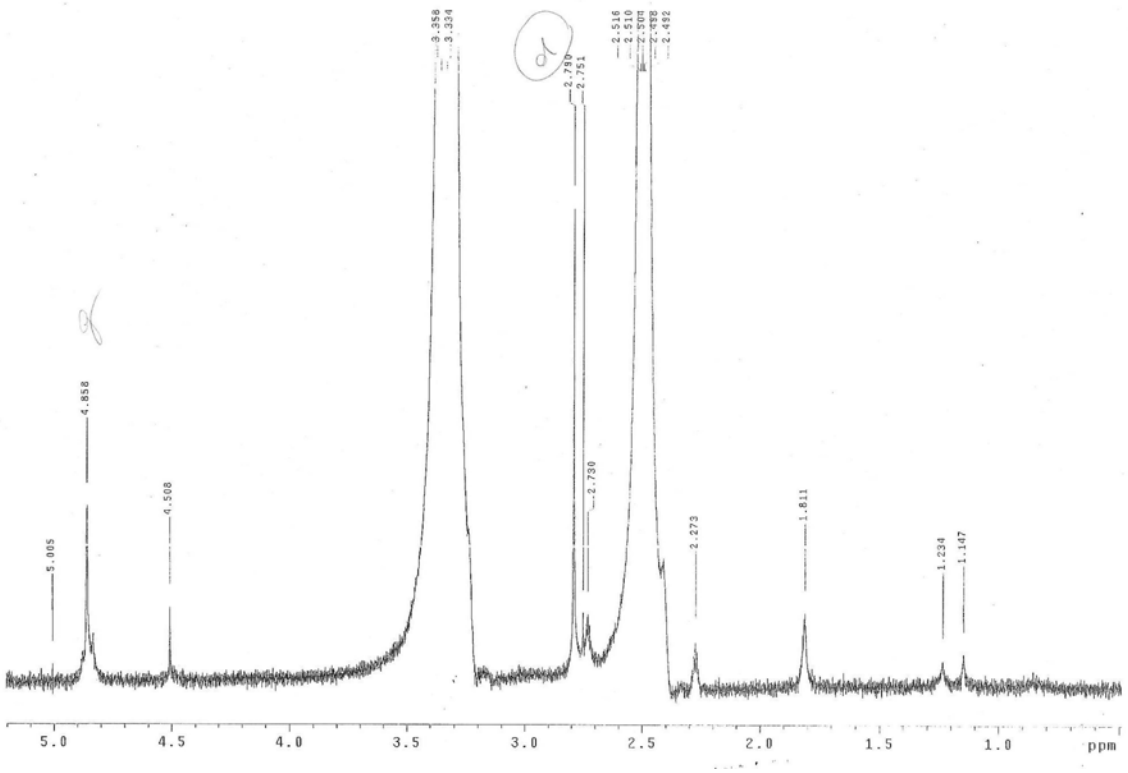

[13 g] LYSO-8

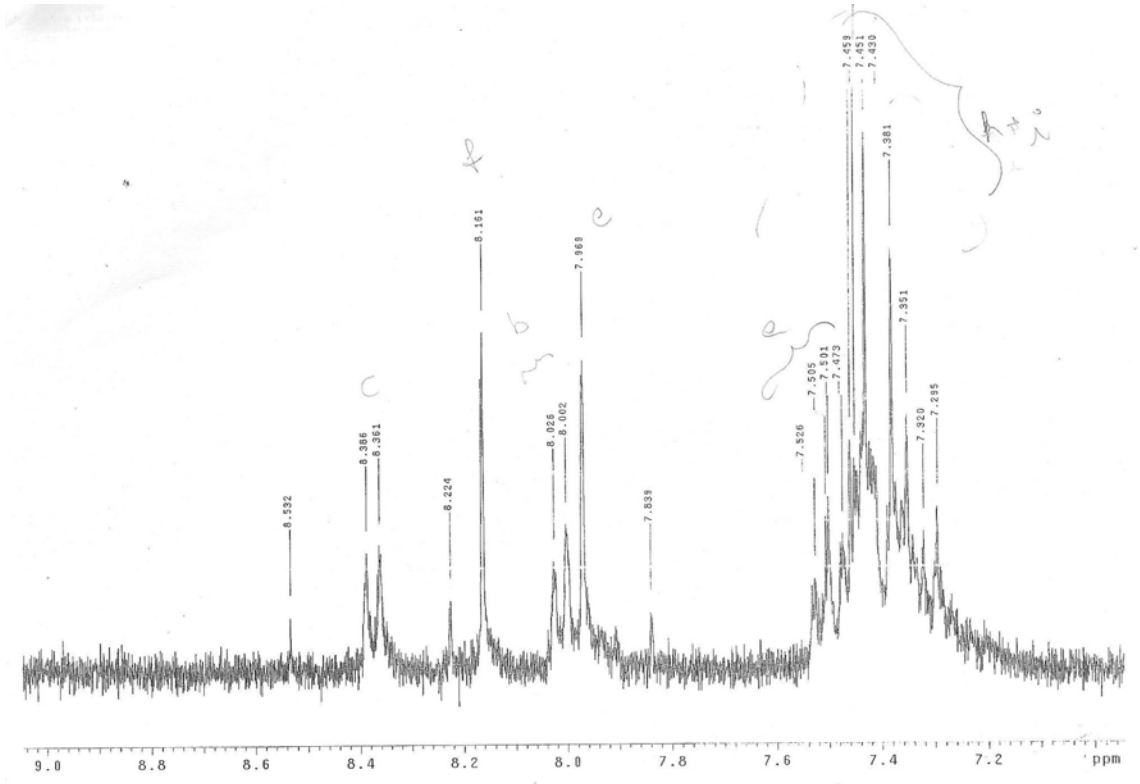

Espectro de Massas, ESI negativo

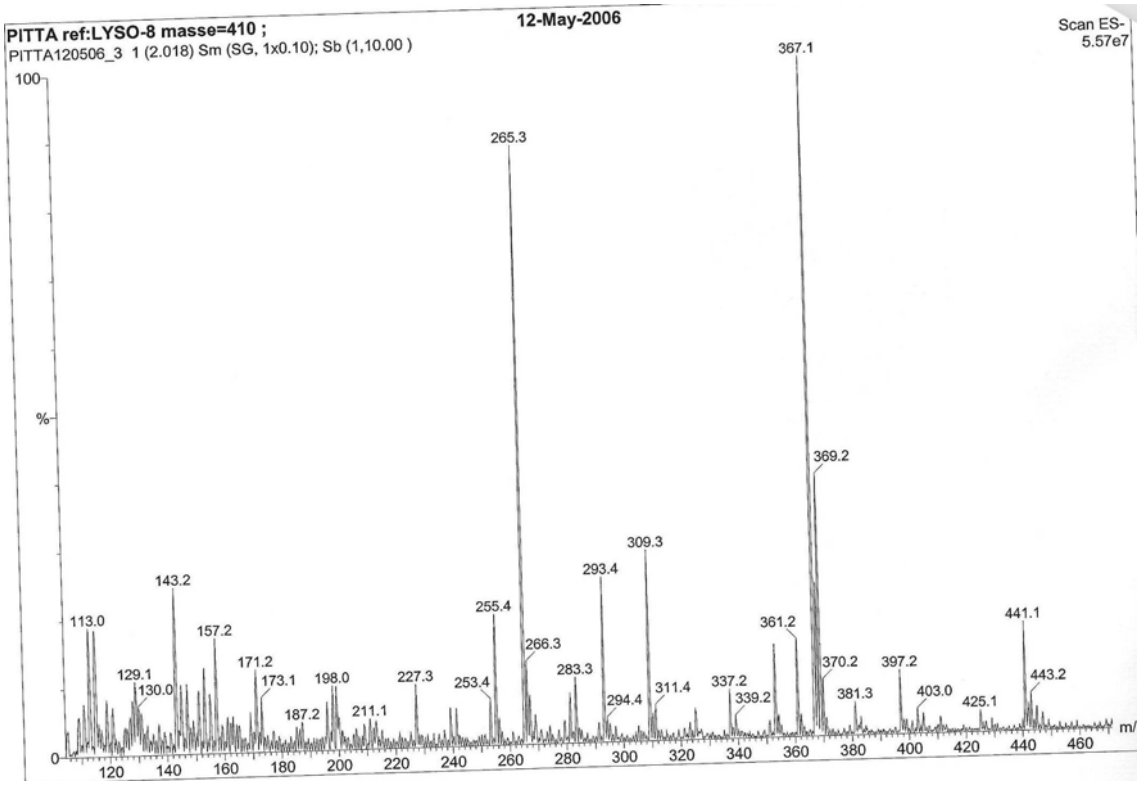

[13 h] CR-26
RMN ^{1}H, $DMSOd_6$

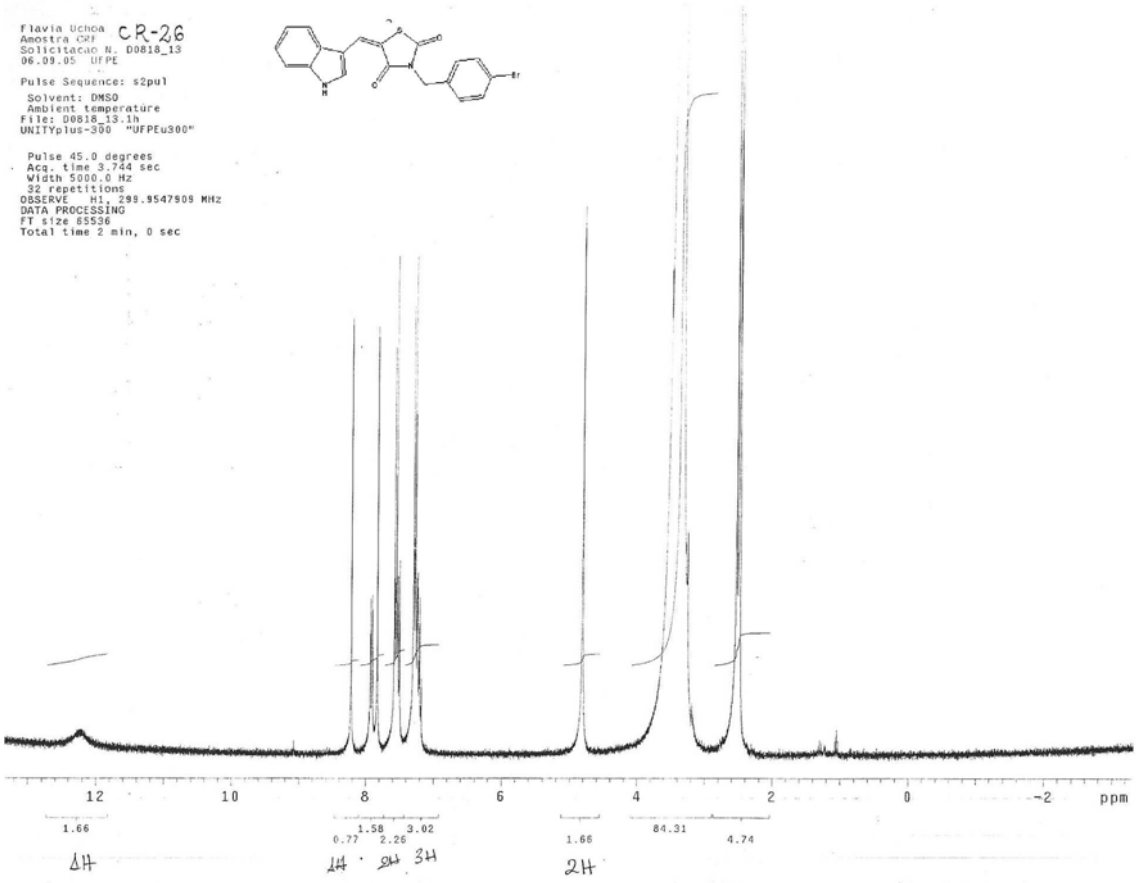

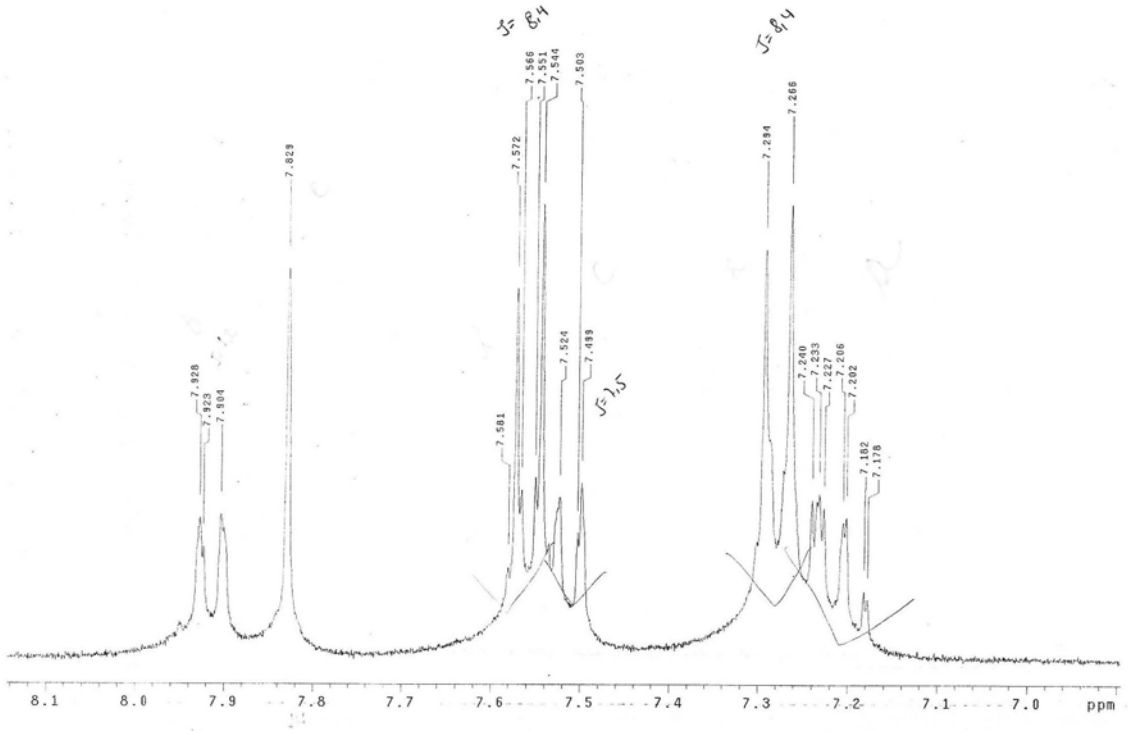

[13 h] CR-26
IV, KBr

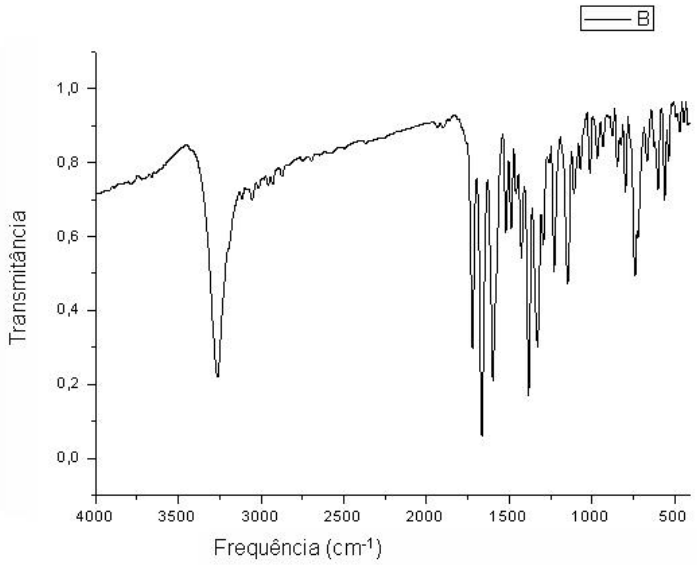

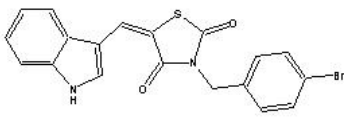

Principais bandas (cm^{-1}):
- 3264,27
- 3054,76
- 1721,36
- 1664,19
- 1599,87
- 1383,89
- 1329,05

Espectro de Massas, ESI negativo

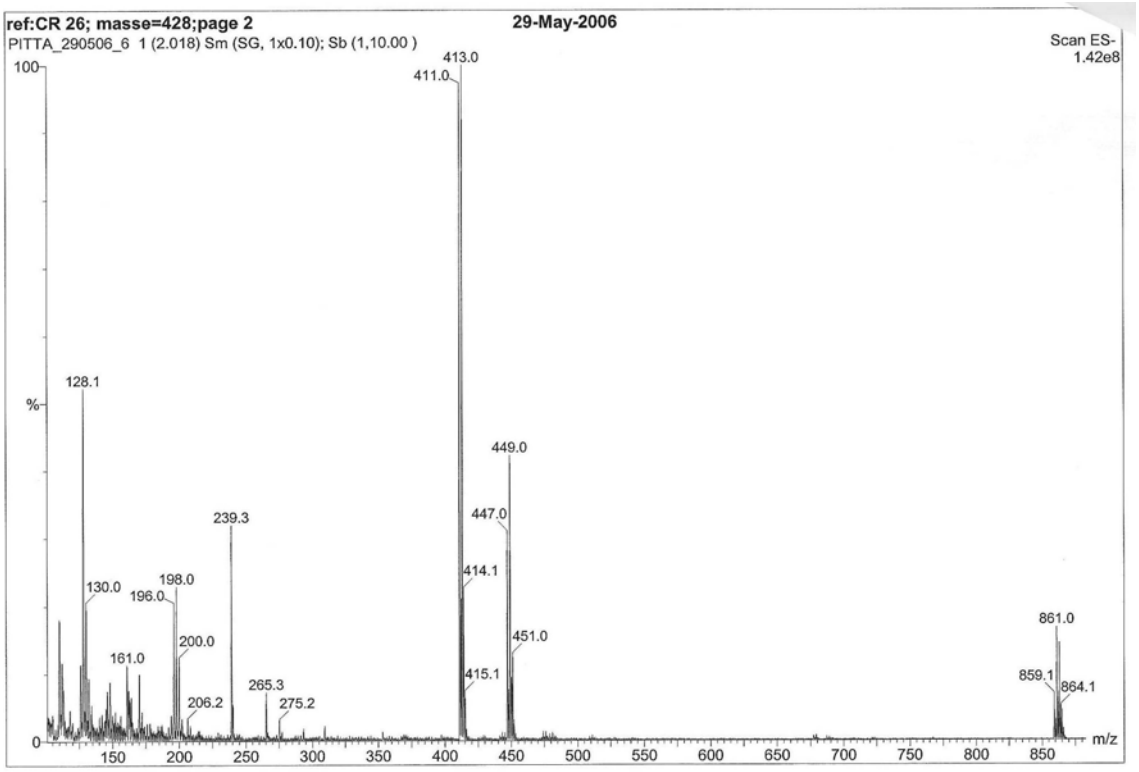

[13 i] CR-27
RMN ^{1}H, $DMSOd_6$

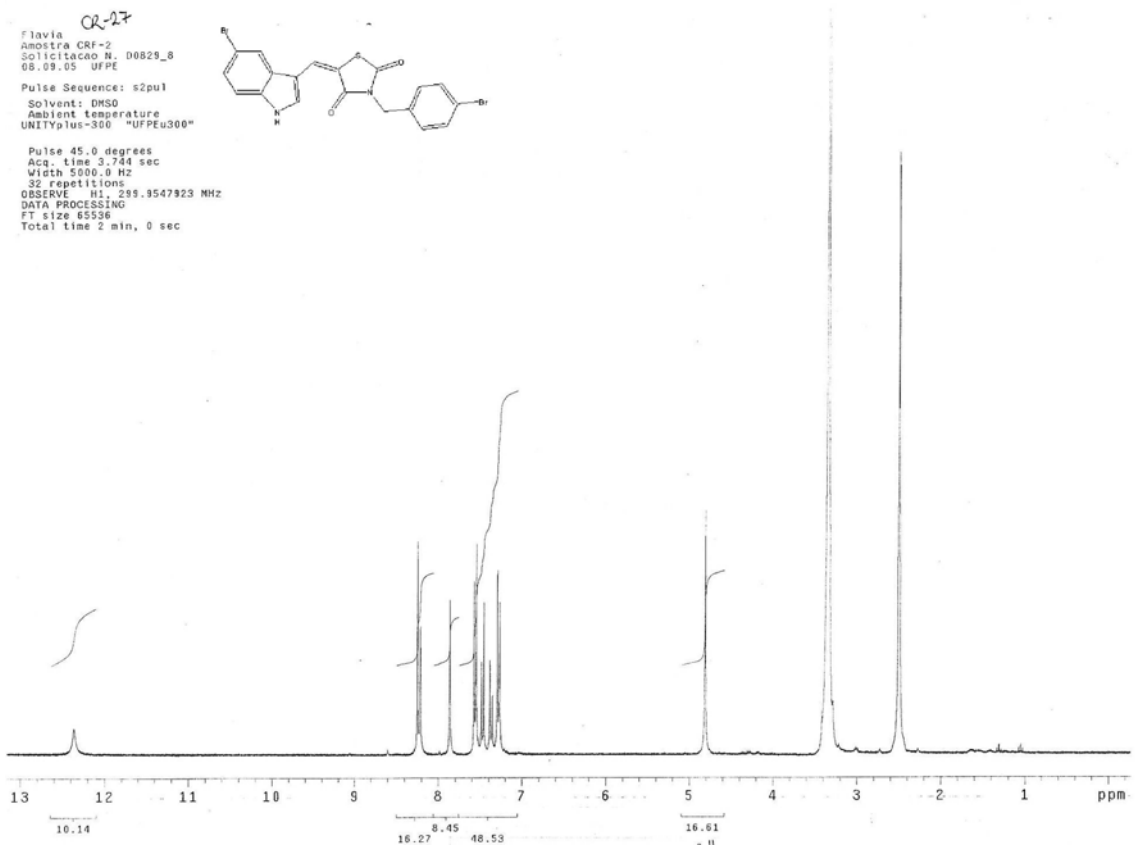

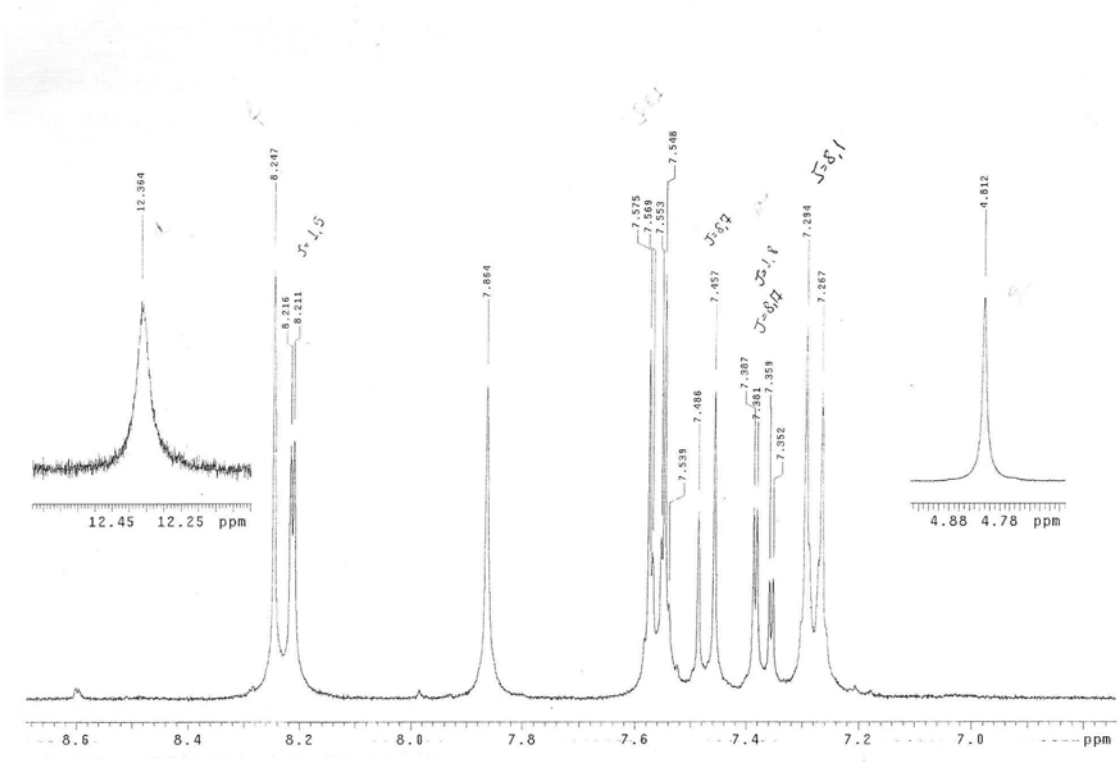

[13 i] CR-27
IV, KBr

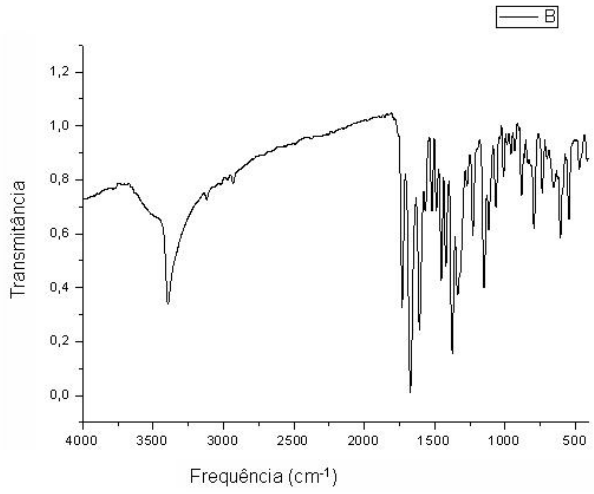

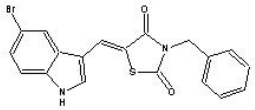

Principais bandas (cm^{-1})
- 3395,17
- 3121,72
- 2931,39
- 1730,77
- 1673,59
- 1609,65
- 1452,42
- 1419,32
- 1376,44
- 1336,20
- 1150,76

Espectro de Massas, ESI negativo

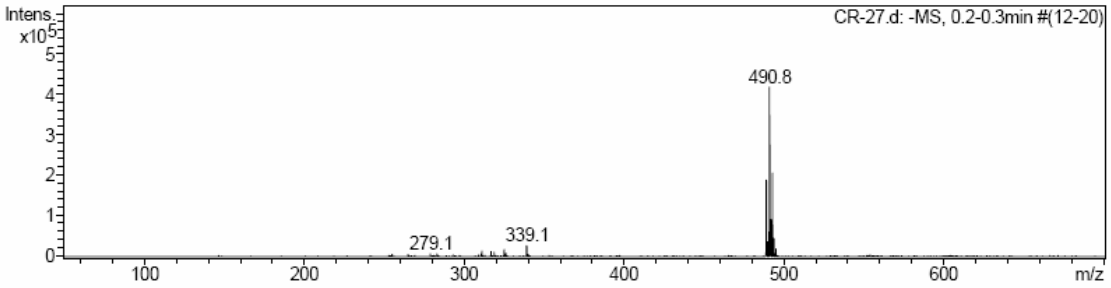

#	m/z	I	I %
1	255.1	5588	1.3
2	265.1	5668	1.4
3	279.1	6418	1.5
4	283.2	6092	1.5
5	309.1	3346	0.8
6	311.1	13148	3.2
7	316.9	12011	2.9
8	318.9	10803	2.6
9	325.1	17030	4.1
10	326.1	7982	1.9
11	339.1	26172	6.3
12	340.1	4874	1.2
13	488.8	188282	45.2
14	489.8	35393	8.5
15	490.8	416726	100.0
16	491.7	90275	21.7
17	492.7	205335	49.3
18	493.7	43695	10.5
19	494.7	18105	4.3
20	553.6	3543	0.9

[13 j] GQ-50
RMN ^{1}H, $DMSOd_6$

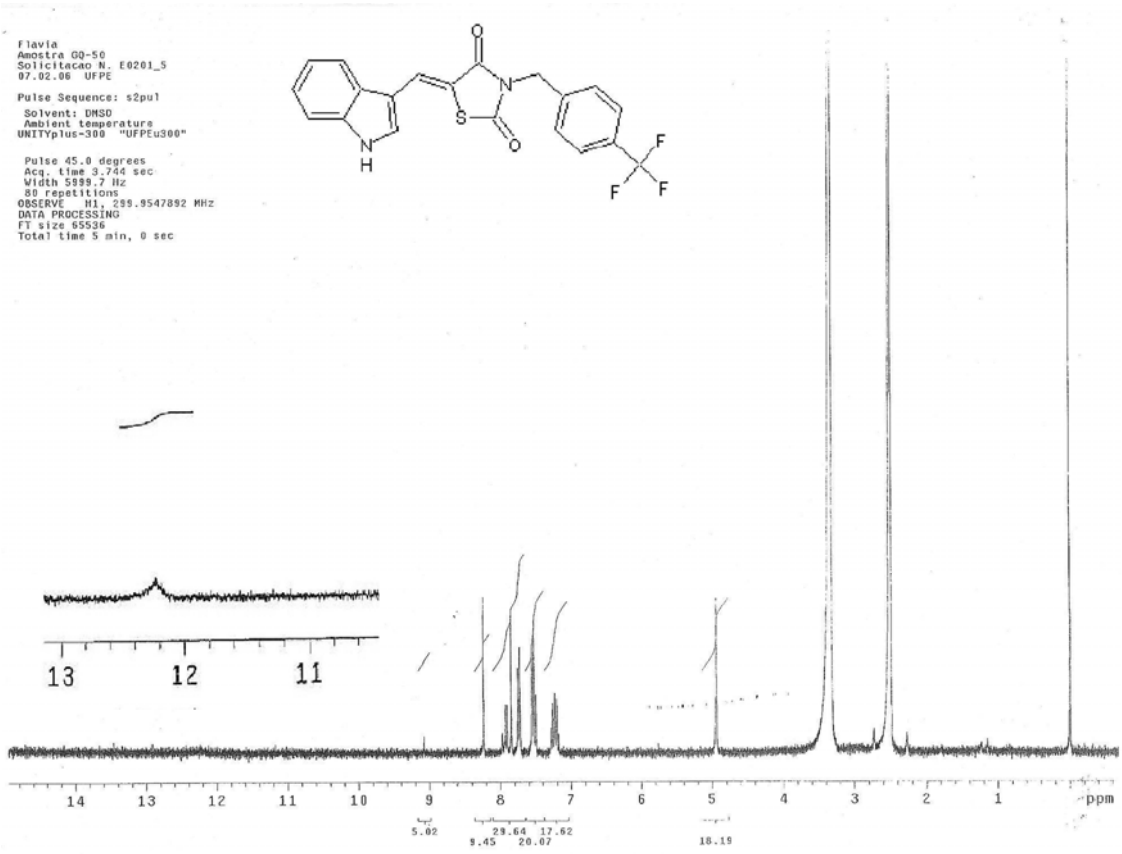

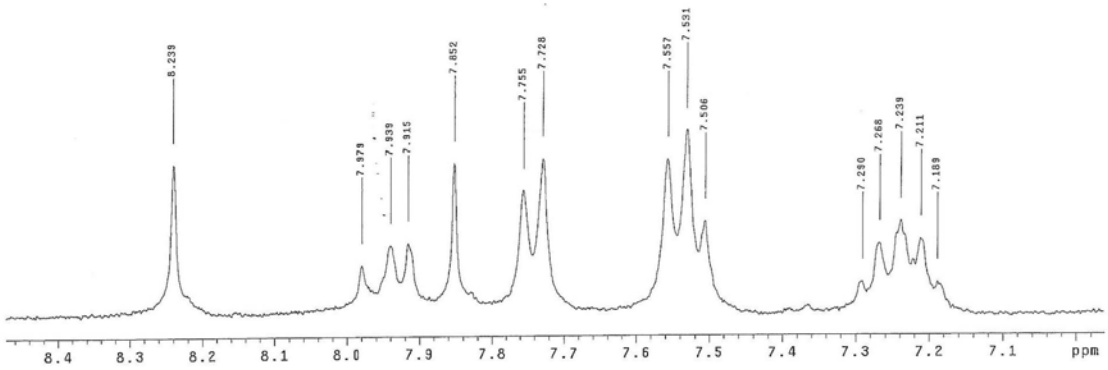

[13 j] GQ-50
IV, KBr

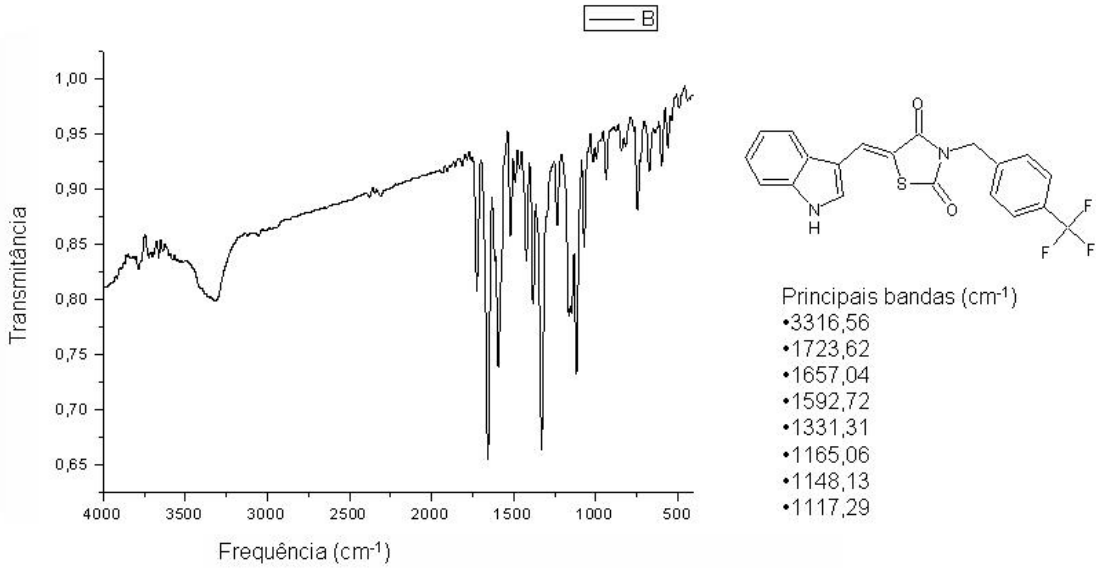

Espectro de Massas, ESI negativo

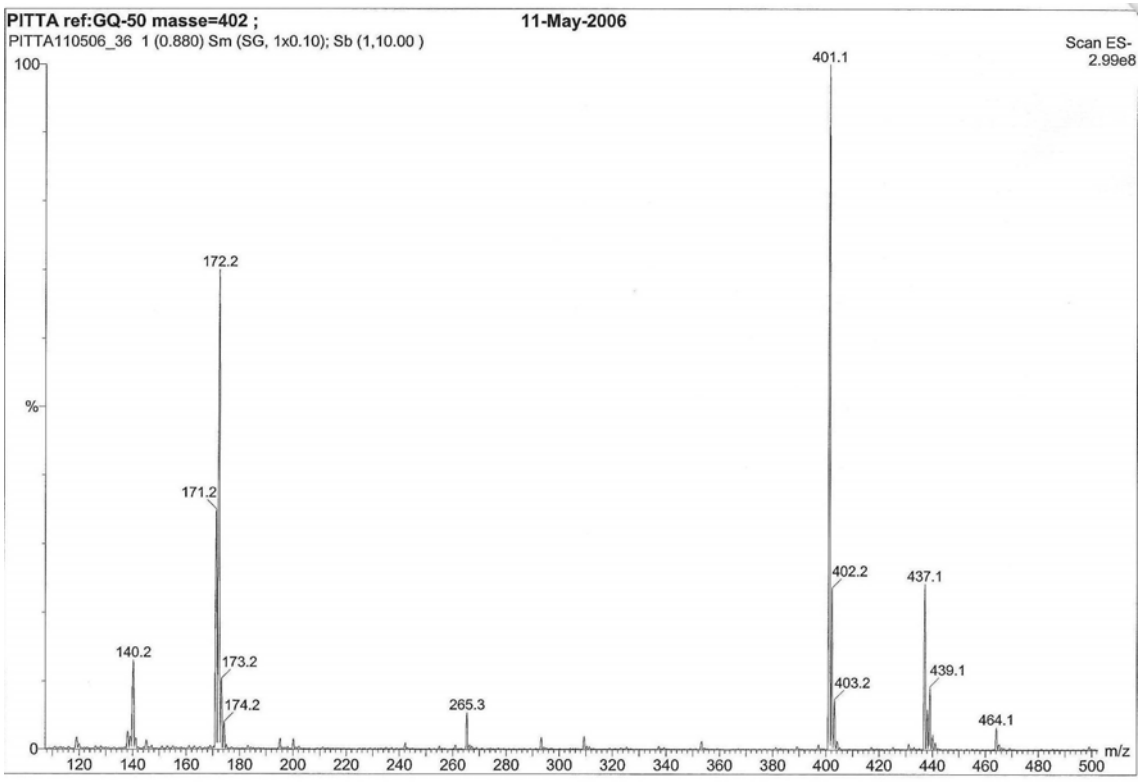

[13 k] GQ-51
RMN ^{1}H, $DMSOd_6$

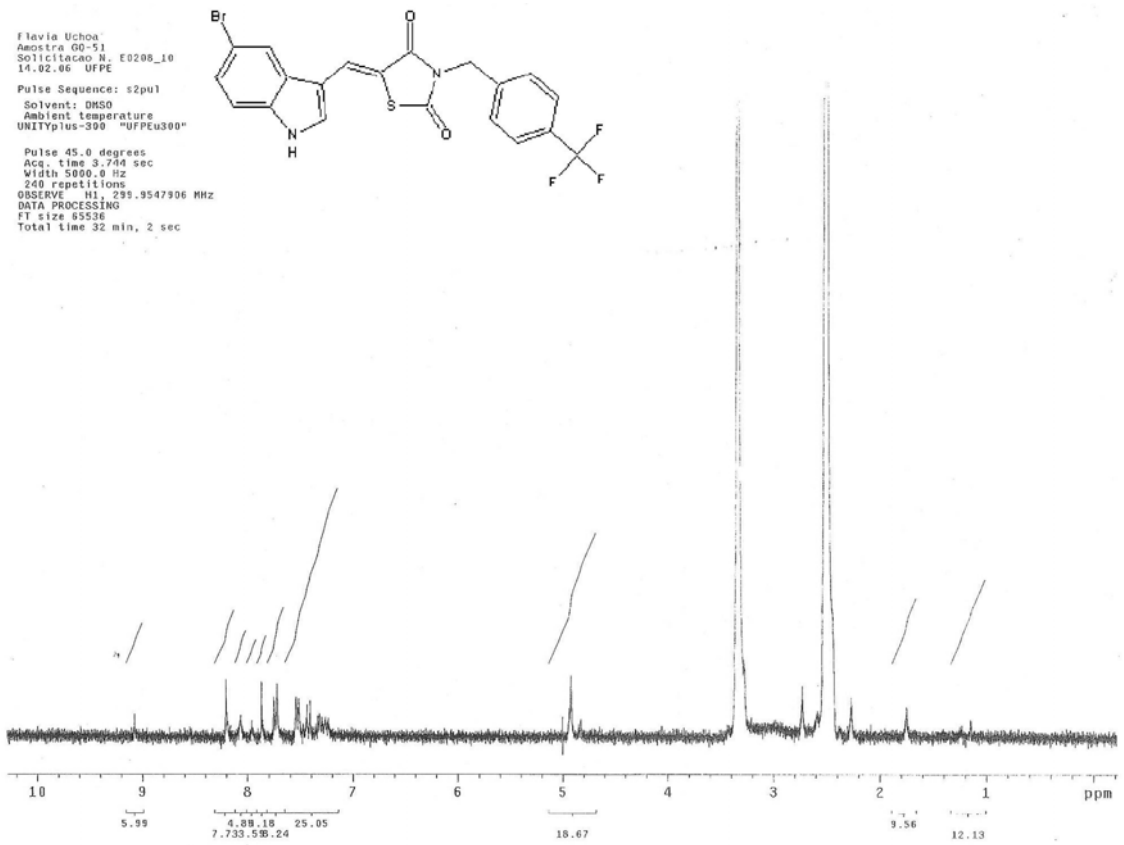

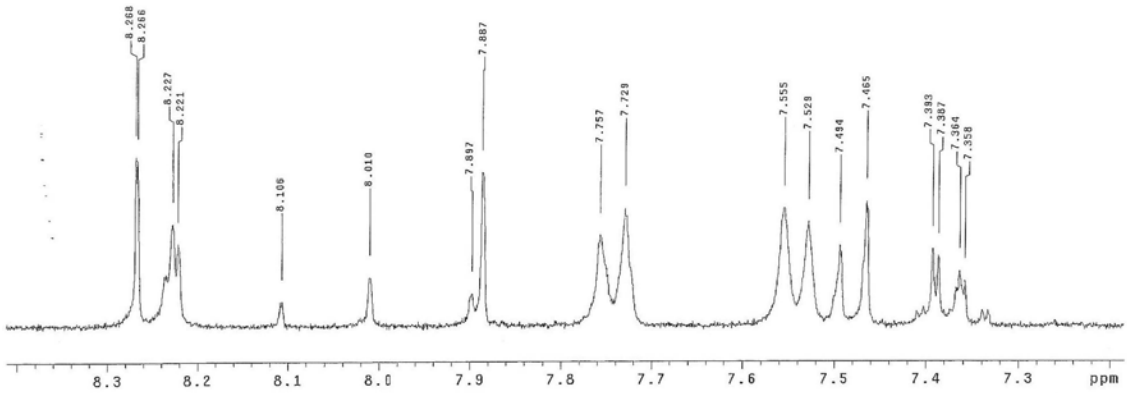

[13 k] GQ-51
IV, KBr

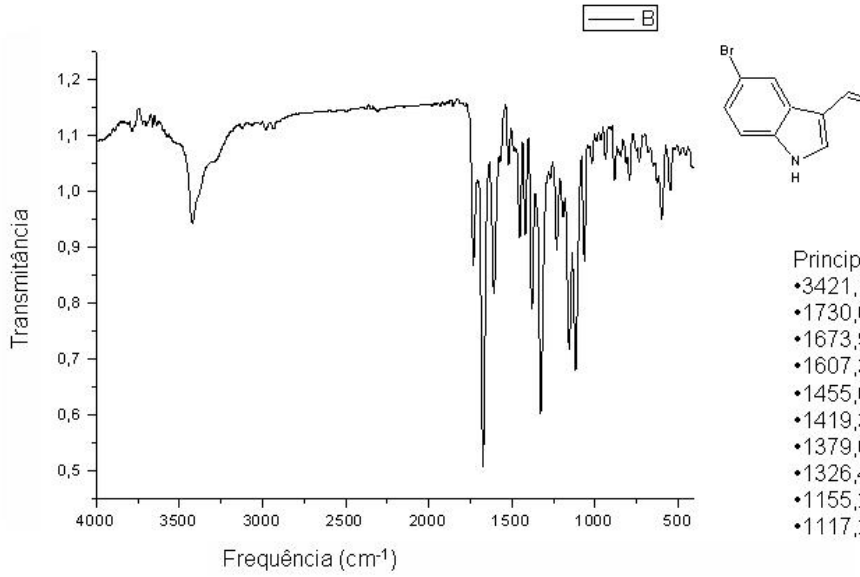

Principais bandas (cm^{-1})

- 3421,12
- 1730,67
- 1673,97
- 1607,39
- 1455,06
- 1419,32
- 1379,08
- 1326,42
- 1155,28
- 1117,29

[13 l] 137
RMN ^{1}H, $DMSOd_6$

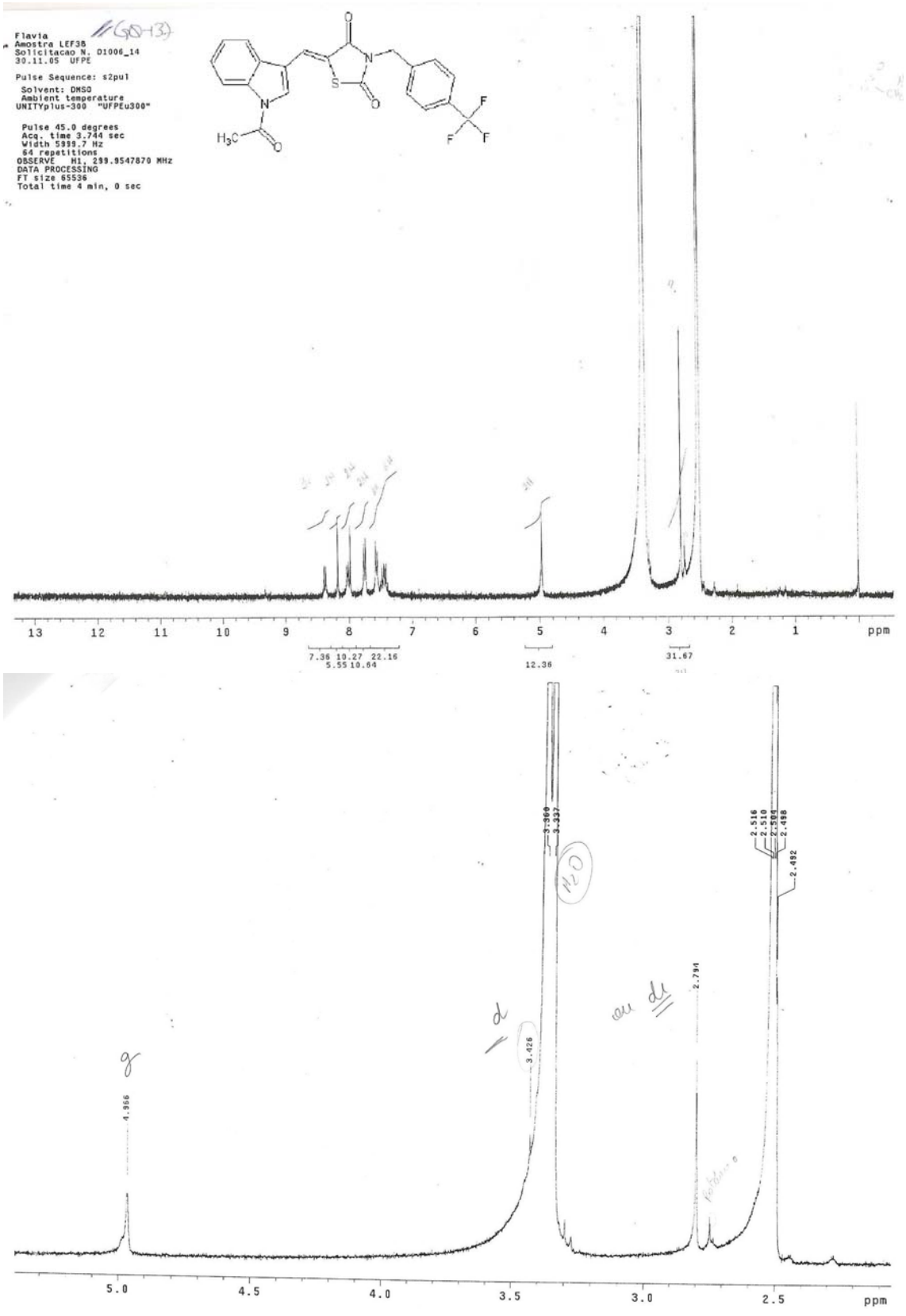

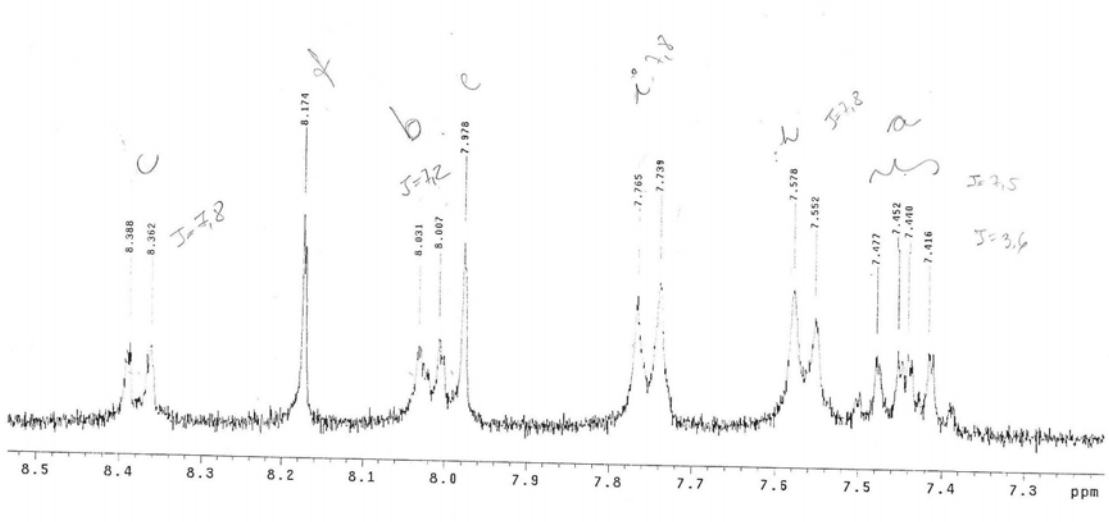

[13 l] GQ-137
IV,
KBr

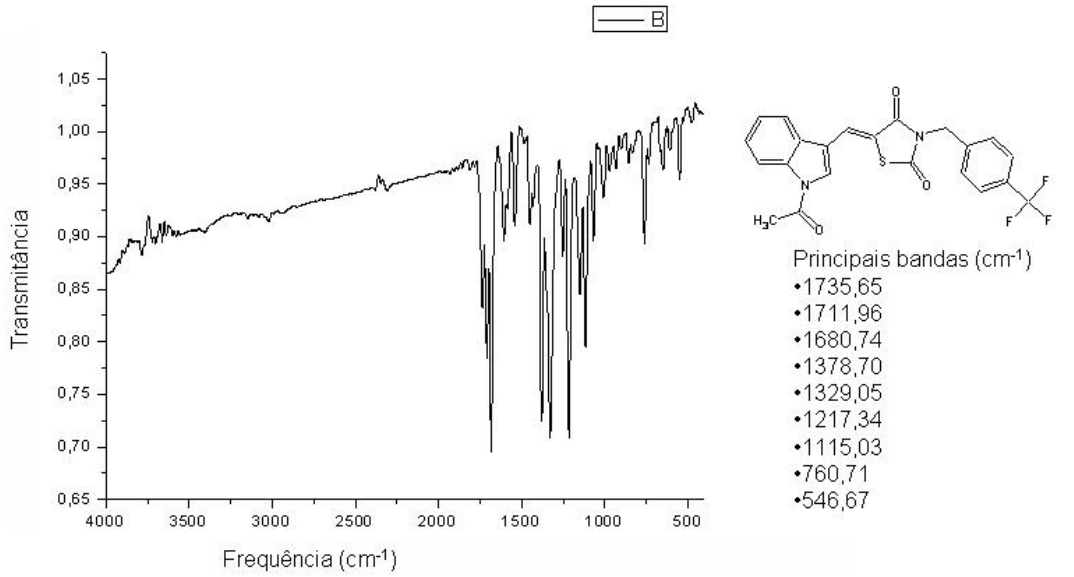

Principais bandas (cm^{-1})

- 1735,65
- 1711,96
- 1680,74
- 1378,70
- 1329,05
- 1217,34
- 1115,03
- 760,71
- 546,67

[13 l] GQ-137

Espectro de Massas, ESI negativo

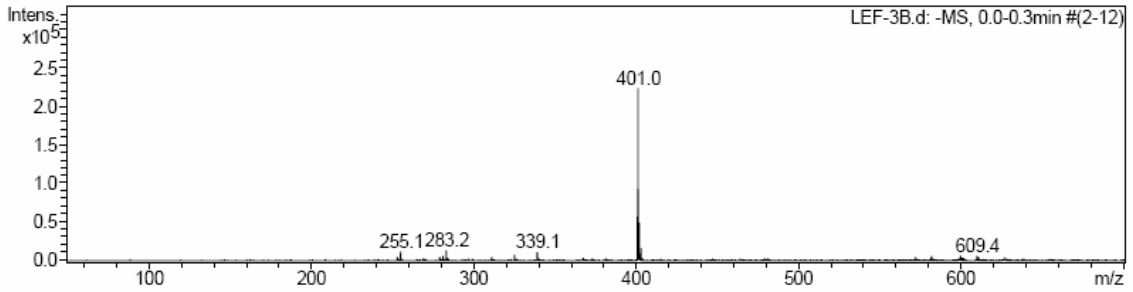

#	m/z	I	I %
1	253.1	4481	2.0
2	255.1	11280	5.1
3	279.1	4524	2.0
4	281.2	5842	2.6
5	283.2	12745	5.7
6	311.1	4089	1.8
7	325.1	7070	3.2
8	339.1	10675	4.8
9	367.3	2941	1.3
10	401.0	222525	100.0
11	401.9	48544	21.8
12	403.0	15278	6.9
13	403.9	2764	1.2
14	571.4	3932	1.8
15	581.3	5370	2.4
16	599.3	5567	2.5
17	600.4	2779	1.2
18	609.4	5763	2.6
19	610.4	3781	1.7
20	626.3	3446	1.5

[13 m] GQ-79
RMN ^{1}H, $DMSOd_6$

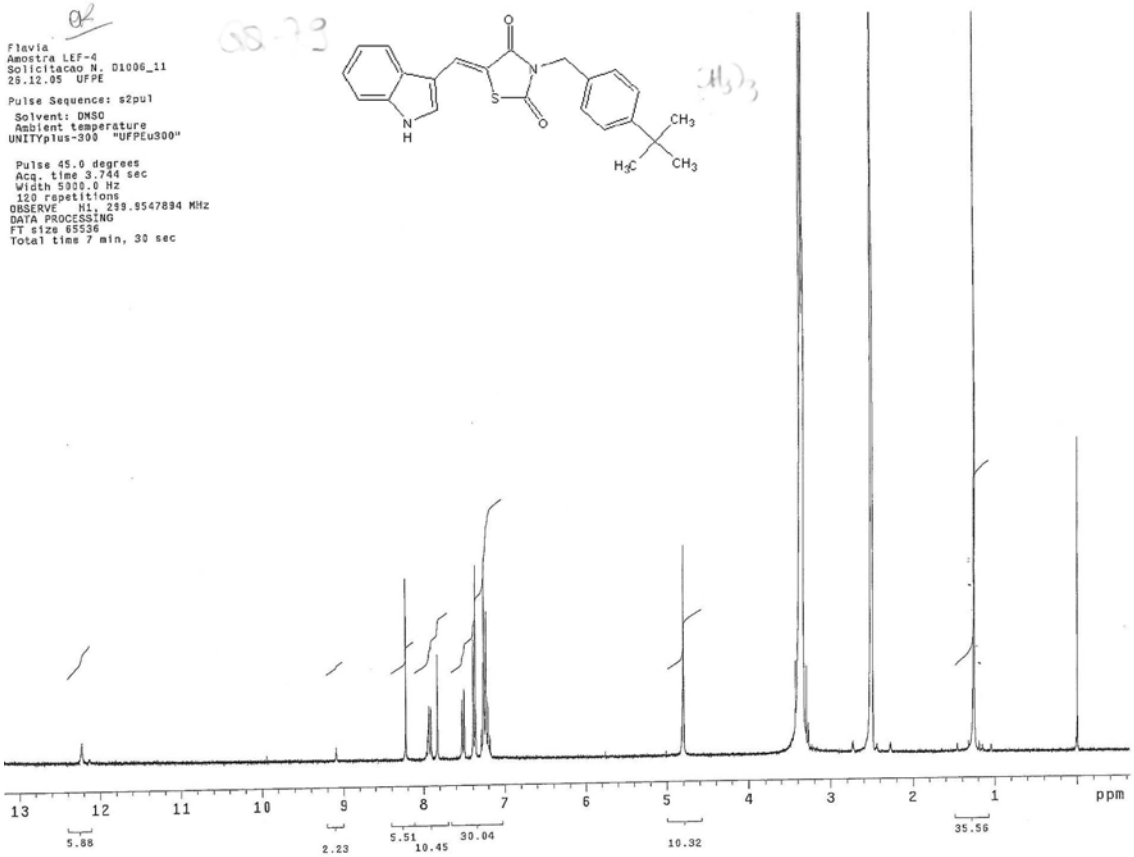

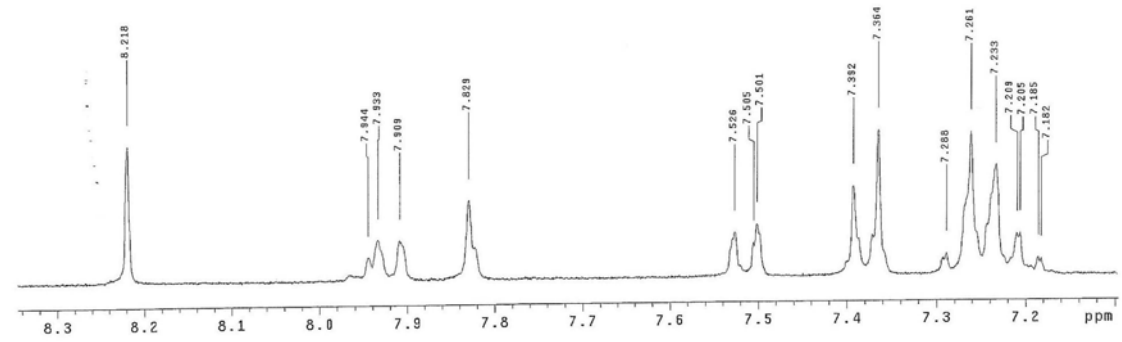

[13 m] GQ-79
IV, KBr

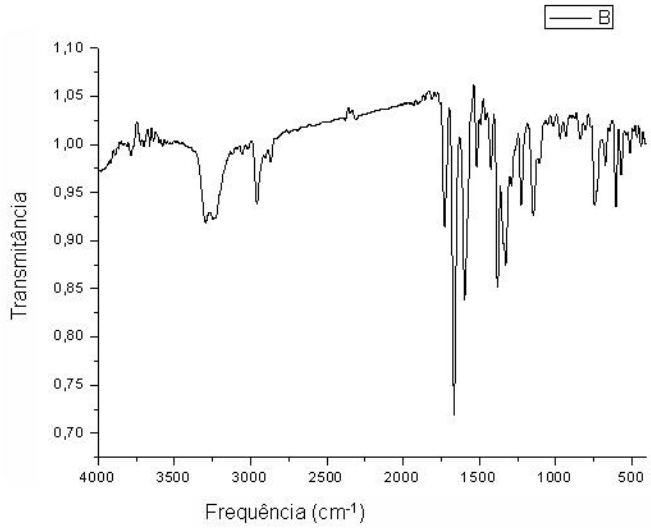

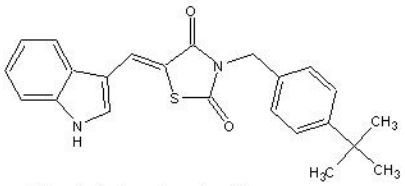

Principais bandas (cm^{-1})
- 3297,37
- 3242,46
- 2957,35
- 1728,51
- 1666,45
- 1597,61
- 1381,33
- 1326,79
- 1143,63
- 741,90
- 604,24

Espectro de Massas, ESI negativo

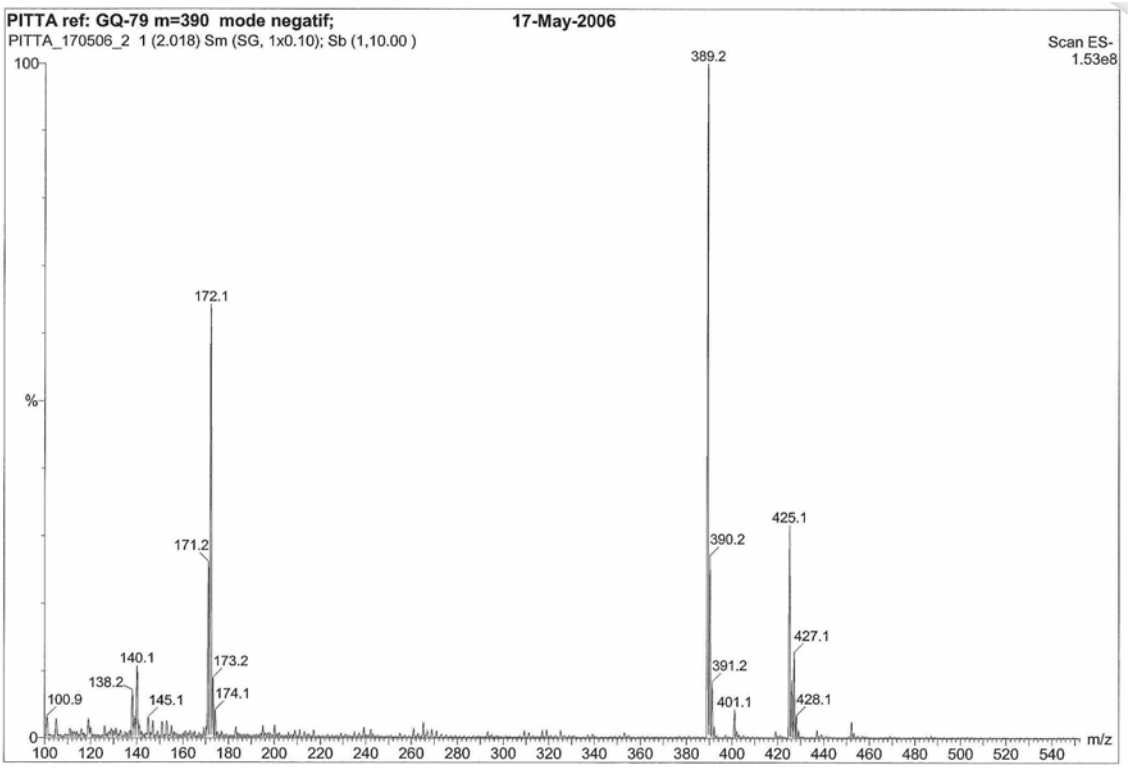

[13 n] GQ-81
RMN ^{1}H, $DMSOd_6$

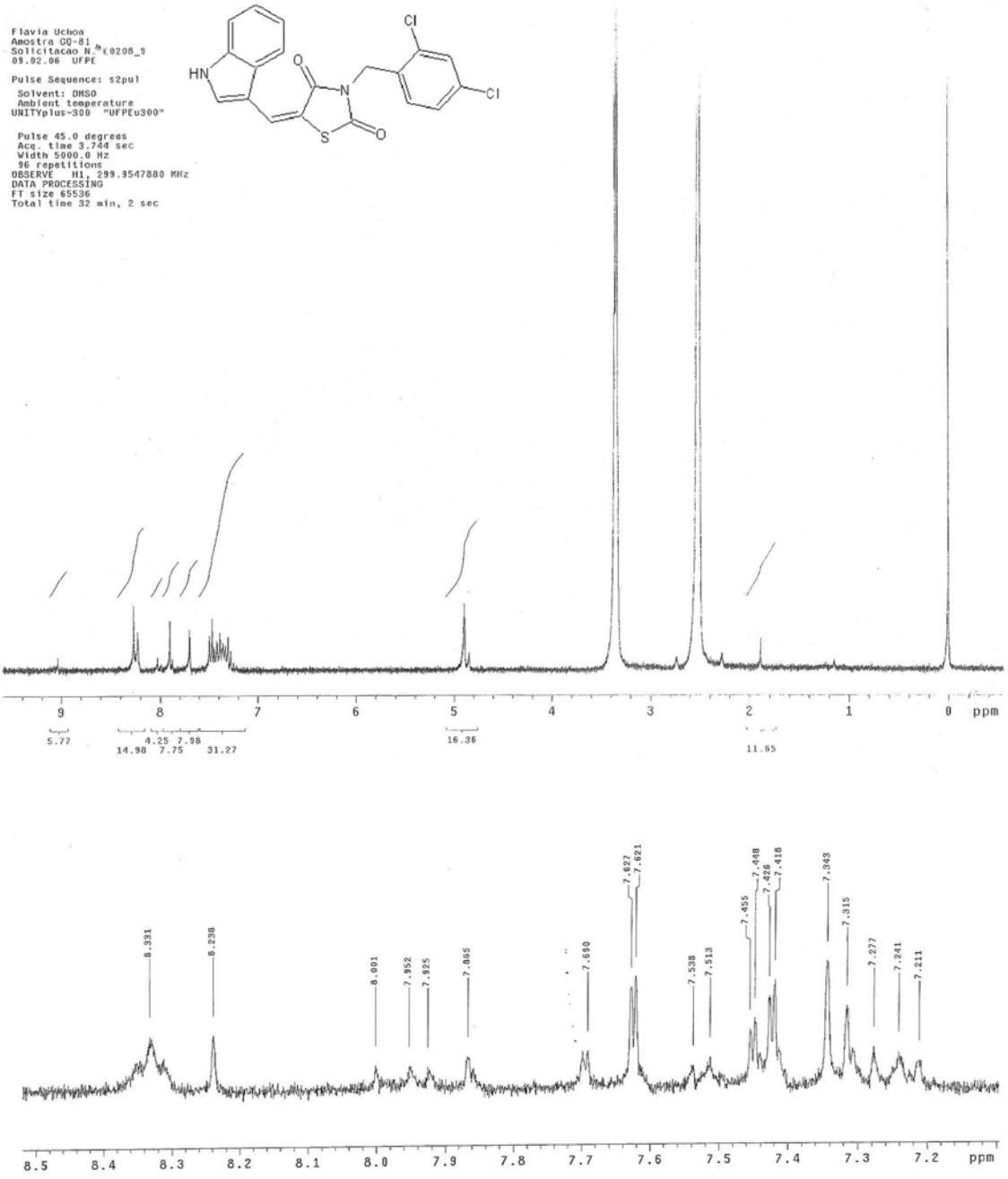

[13 n] GQ-81
IV, KBr

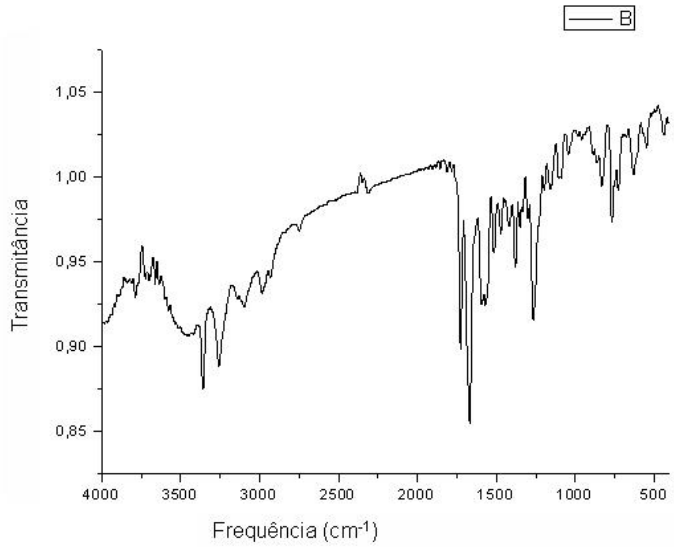

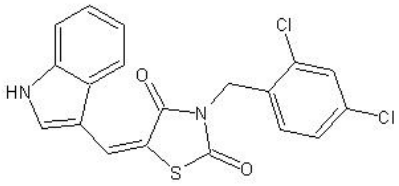

Principais bandas (cm^{-1})
- 3356,80
- 3257,13
- 3095,37
- 2285,93
- 1728,51
- 1669,08
- 1595,36
- 1569,03
- 1264,73
- 765,60

Espectro de Massas, ESI negativo

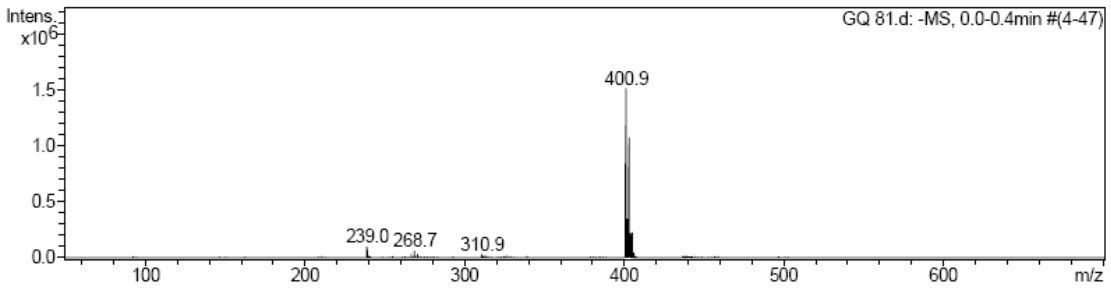

#	m/z	I	I %
1	239.0	97724	6.5
2	240.0	12223	0.8
3	266.7	27236	1.8
4	268.7	57781	3.8
5	270.7	29992	2.0
6	272.7	9912	0.7
7	310.9	29494	2.0
8	312.9	21063	1.4
9	326.7	11530	0.8
10	328.7	10694	0.7
11	400.9	1508505	100.0
12	401.9	342967	22.7
13	402.8	1072501	71.1
14	403.8	214984	14.3
15	404.8	220873	14.6
16	405.8	41490	2.8
17	406.8	8783	0.6
18	436.7	15033	1.0
19	438.8	15445	1.0
20	458.8	8546	0.6

[13 o] GQ-82
RMN ^{1}H, $DMSOd_6$

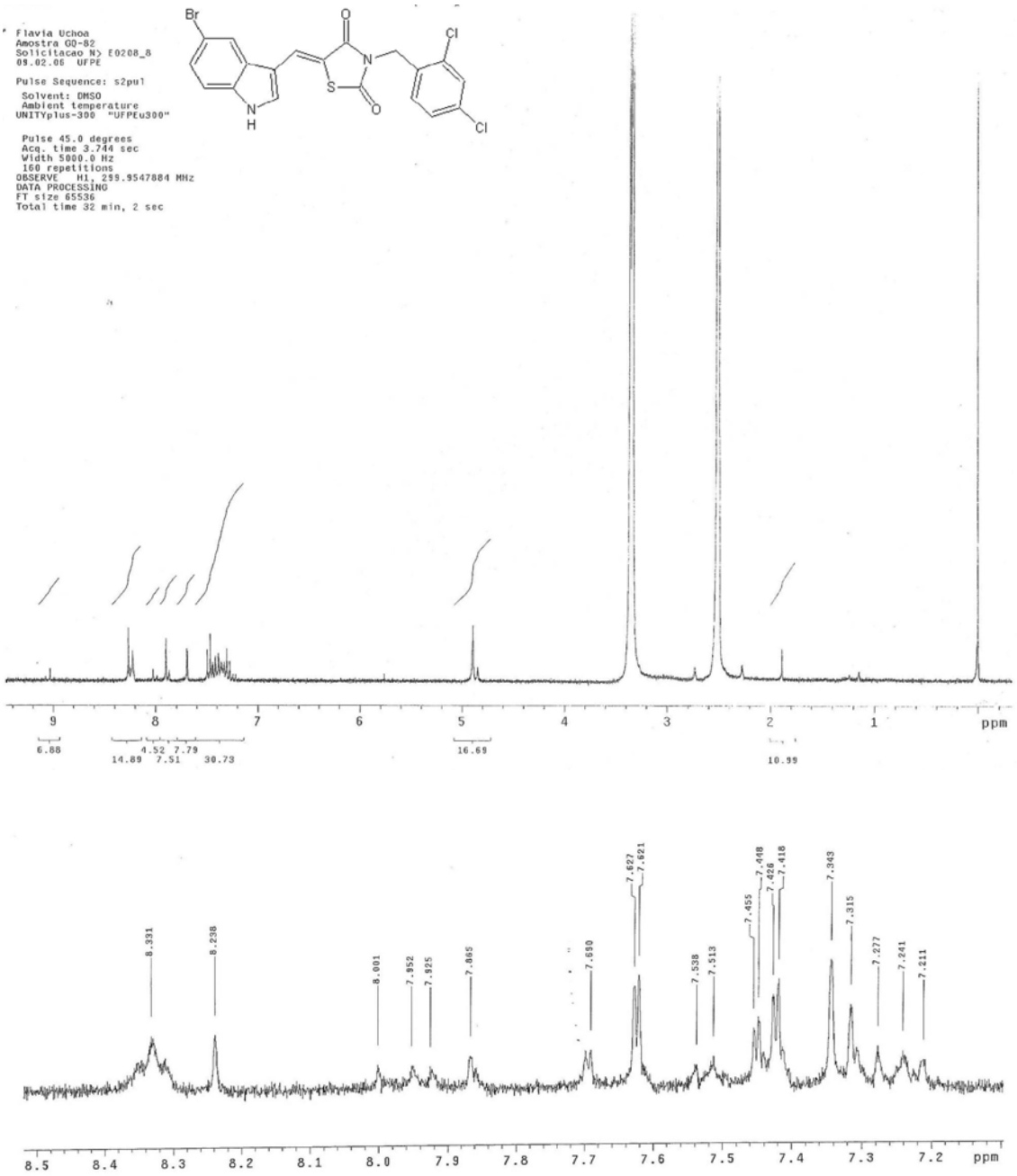

[13 o] GQ-82
IV, KBr

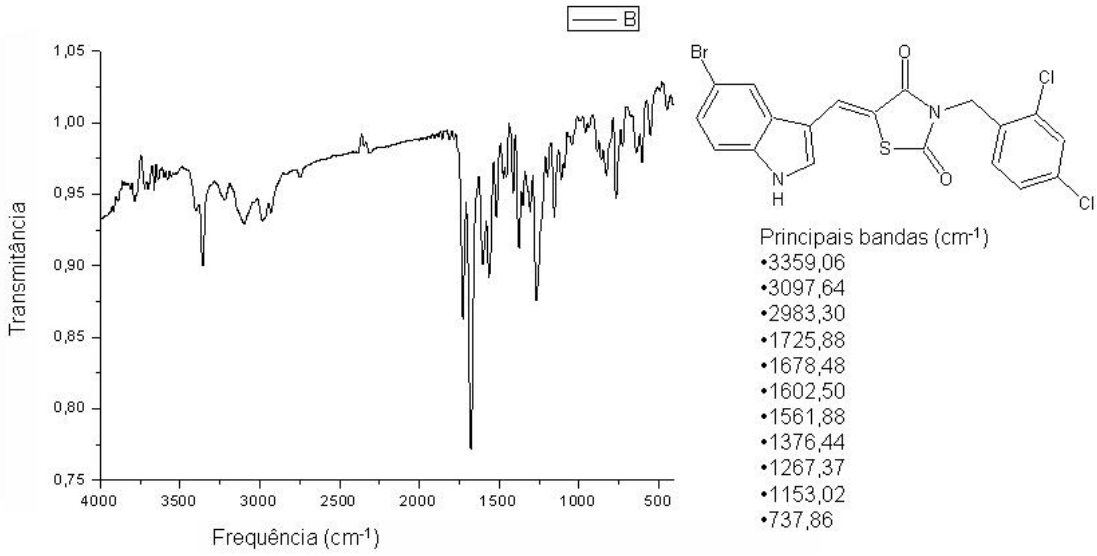

Espectro de Massas, ESI negativo

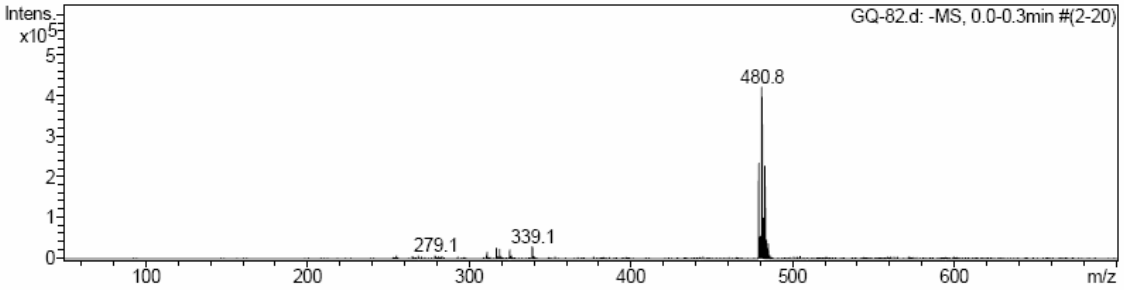

#	m/z	I	I %
1	255.2	6226	1.5
2	265.1	5452	1.3
3	268.7	6682	1.6
4	279.1	7171	1.7
5	283.2	4834	1.2
6	311.1	15681	3.7
7	316.9	25196	6.0
8	318.9	22620	5.4
9	325.2	21552	5.1
10	326.1	6371	1.5
11	339.1	28958	6.9
12	478.8	233181	55.6
13	479.9	55369	13.2
14	480.8	419506	100.0
15	481.8	98762	23.5
16	482.7	227017	54.1
17	483.7	44801	10.7
18	484.7	36686	8.7
19	485.7	7762	1.9
20	504.4	4576	1.1

[13 p] GQ-83
RMN ^{1}H, $DMSOd_6$

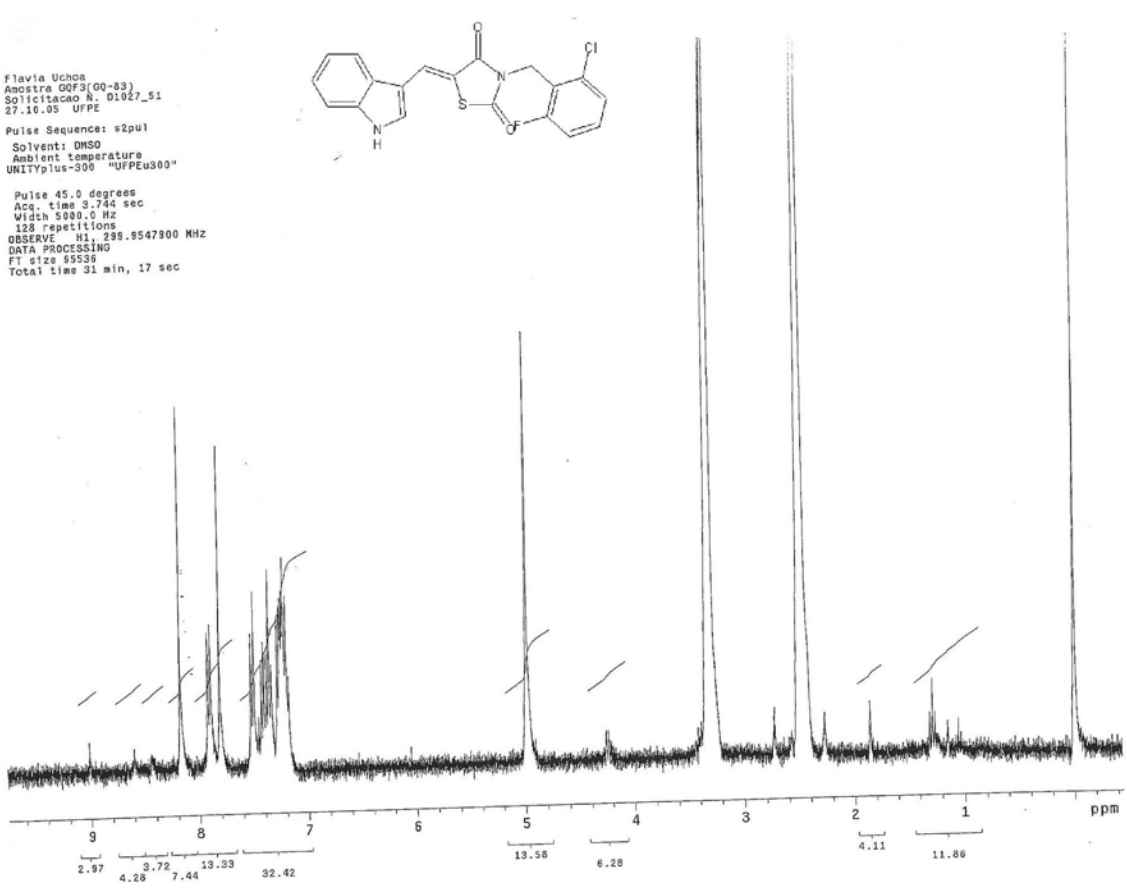

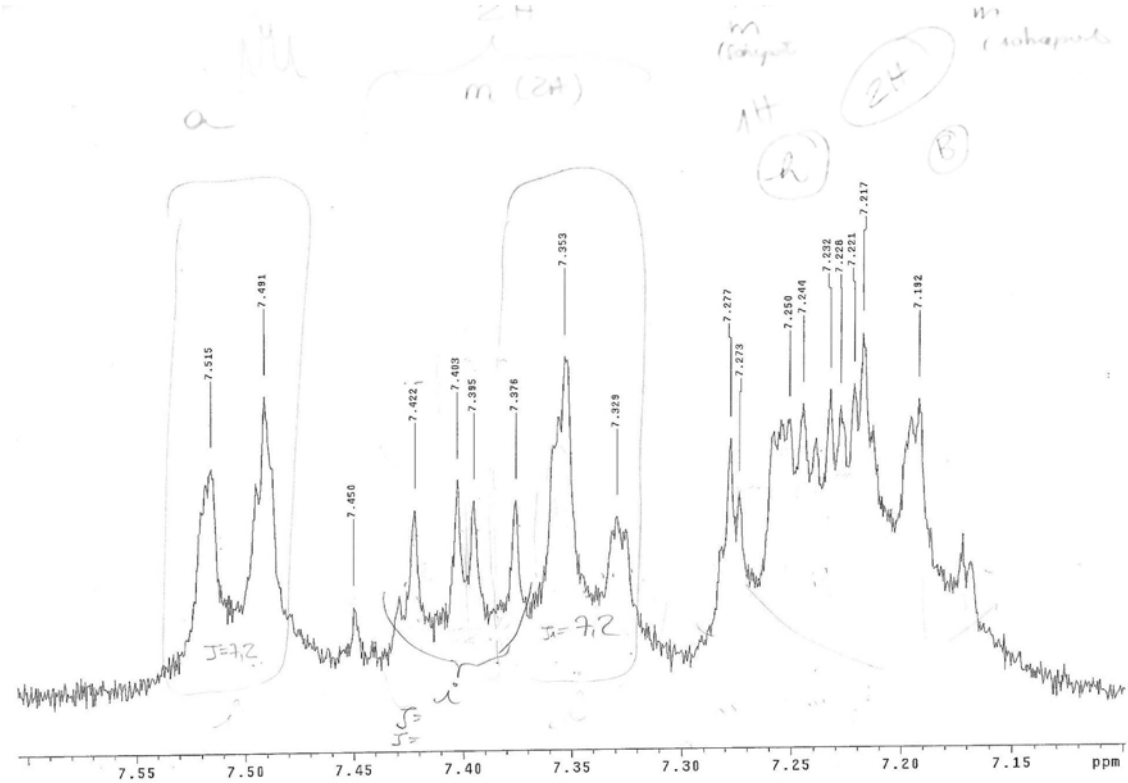

[13 p] GQ-83
IV, KBr

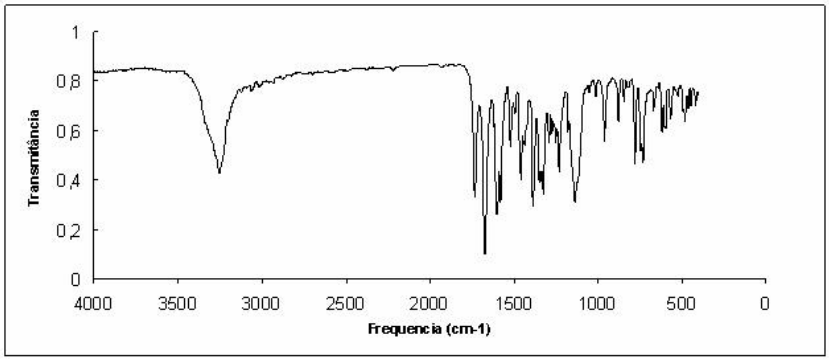

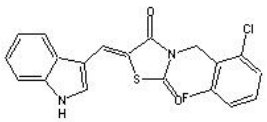

Principais bandas (cm^{-1})

- 3244
- 1729
- 1668
- 1596
- 1133

Espectro de Massas, ESI negativo

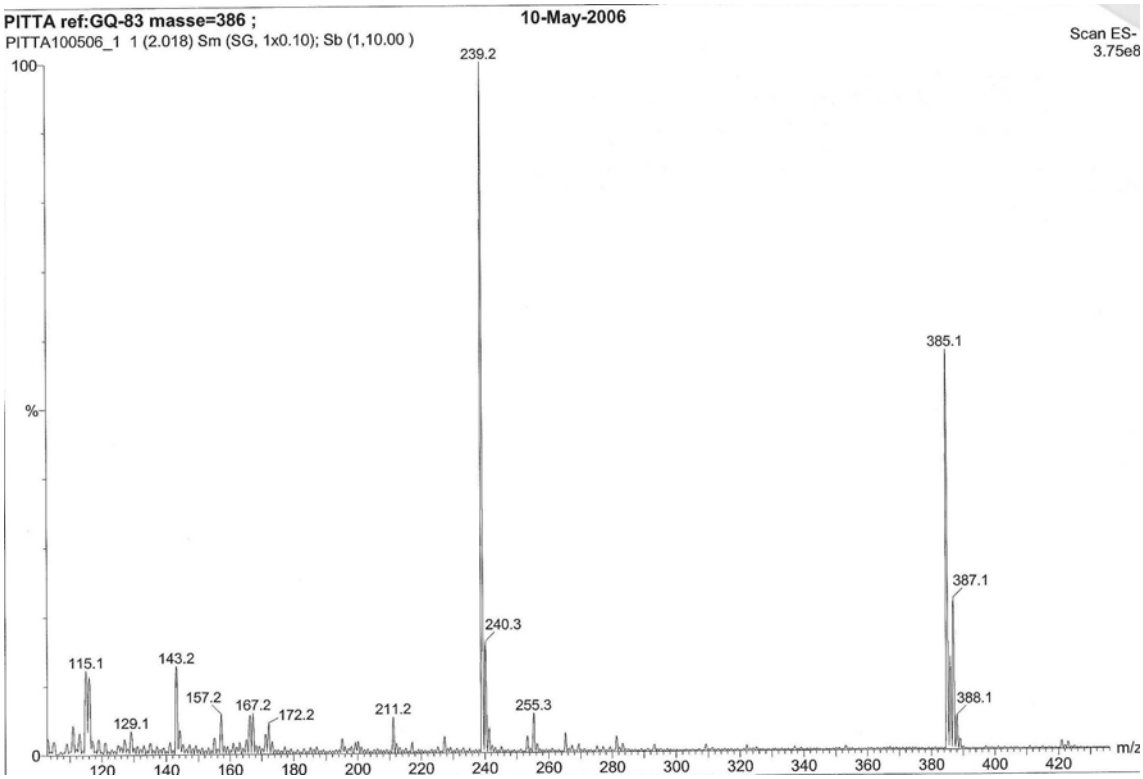

[13 q] GQ-84
RMN ^{1}H, $DMSOd_6$

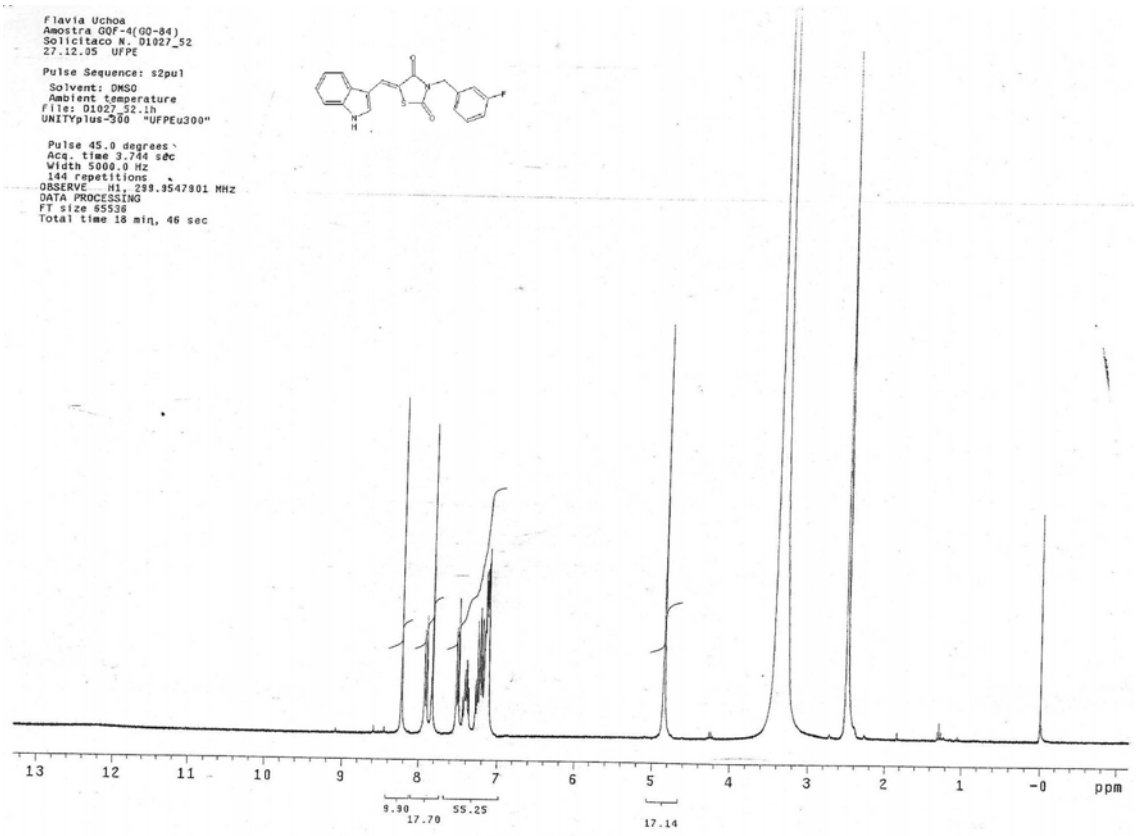

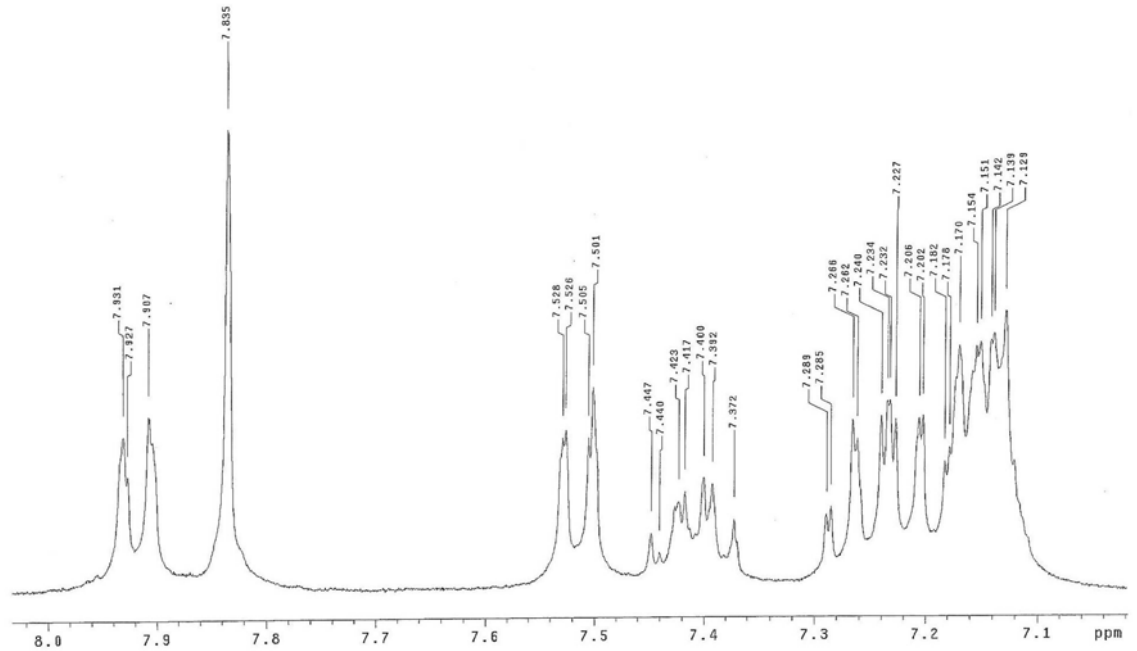

[13 q] GQ-84
IV, KBr

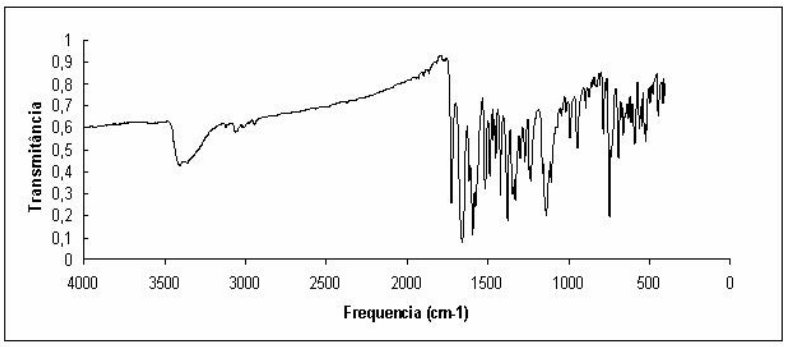

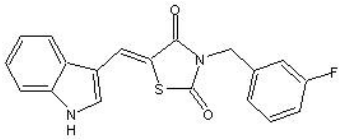

Principais bandas (cm^{-1})
- 3394
- 1721
- 1655
- 1590
- 1515
- 1419
- 1376
- 1133
- 744

Espectro de Massas, ESI negativo

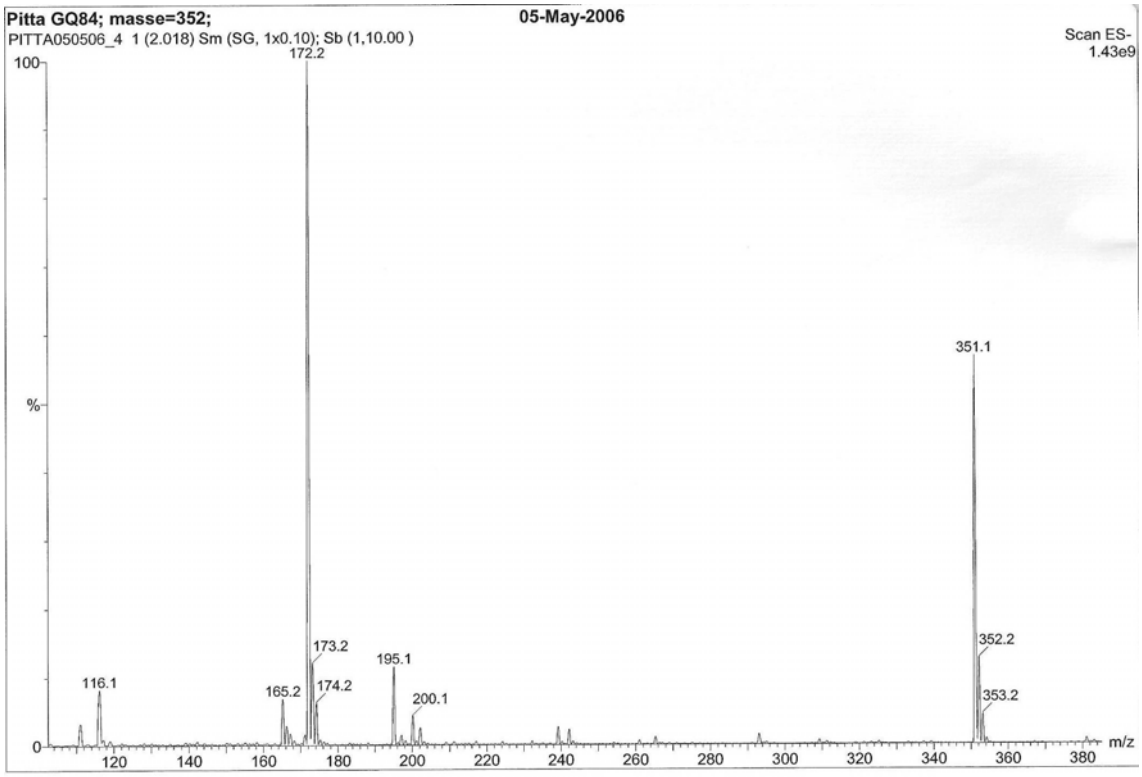

[13 r] GQ-85
RMN ^{1}H, $DMSOd_6$

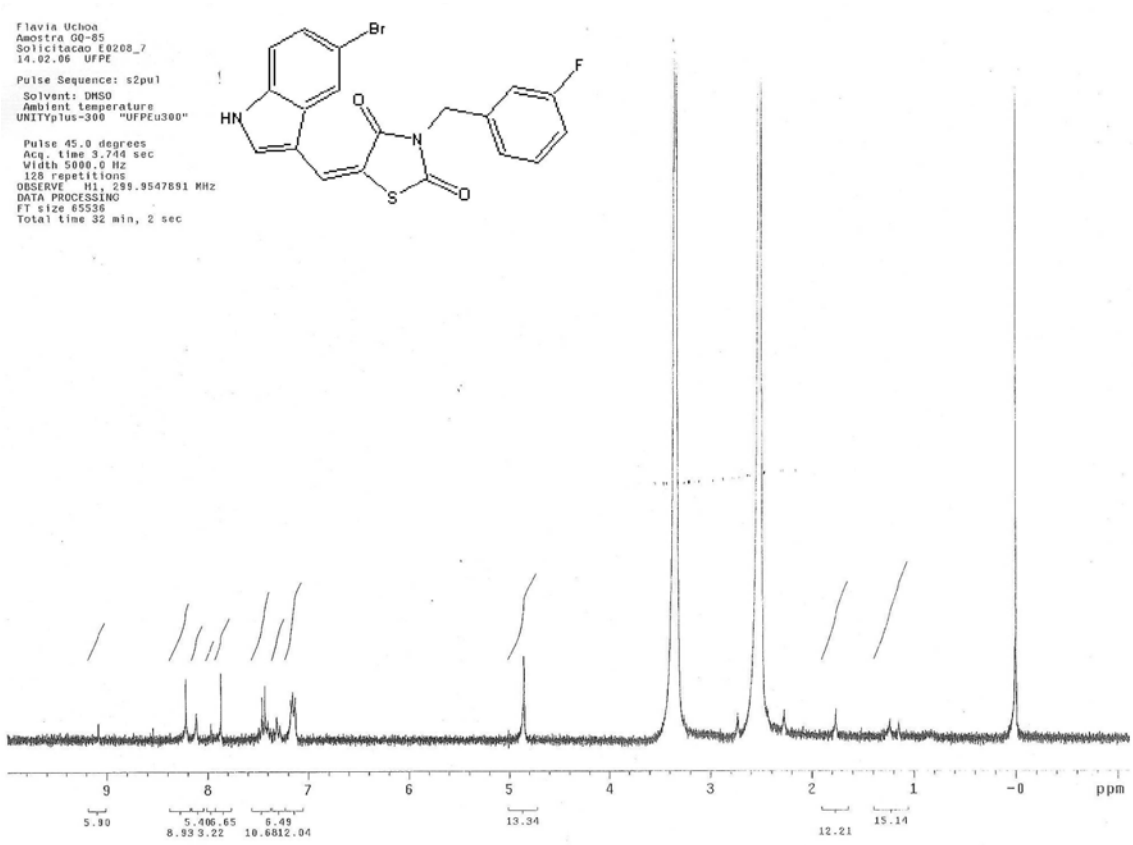

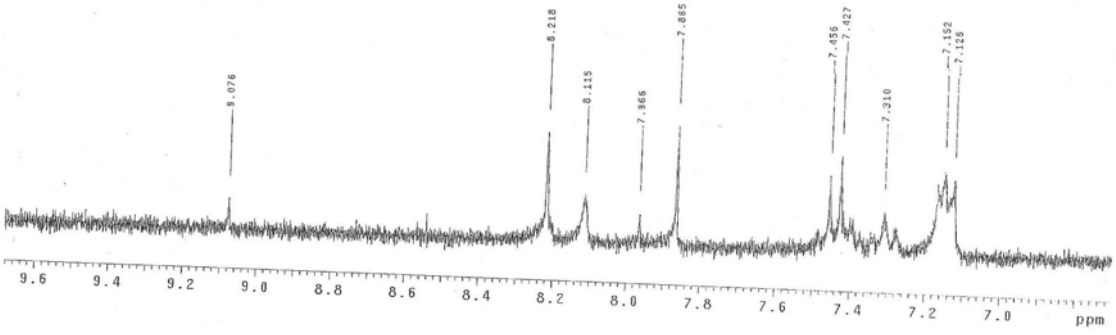

[13 r] GQ-85
IV, KBr

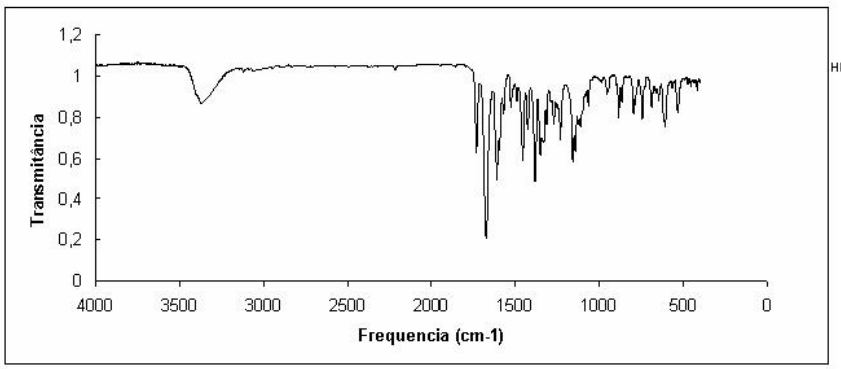

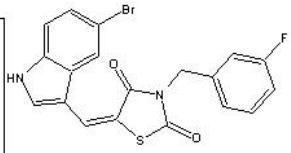

Principais bandas (cm^{-1})
- 3354
- 1729
- 1668
- 1605
- 1378
- 1154

Espectro de Massas, ESI negativo

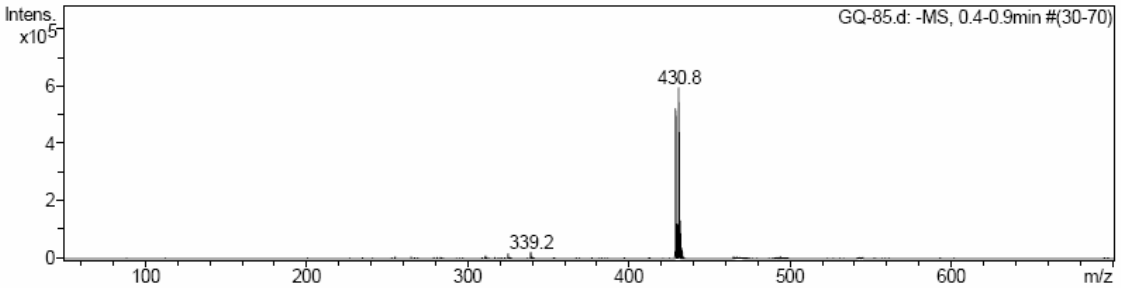

#	m/z	I	I %
1	255.2	5746	1.0
2	265.1	6230	1.1
3	279.1	4477	0.8
4	283.2	4212	0.7
5	311.1	8678	1.5
6	316.9	3991	0.7
7	325.1	17733	3.0
8	339.2	21141	3.6
9	340.1	4748	0.8
10	428.9	520878	87.9
11	429.9	118563	20.0
12	430.8	592510	100.0
13	431.8	130766	22.1
14	432.8	35311	6.0
15	433.8	4886	0.8
16	464.7	5698	1.0
17	466.7	5478	0.9
18	468.7	3744	0.6
19	493.7	6442	1.1
20	544.7	4308	0.7

[13 s] GQ-134
RMN ^{1}H, $DMSOd_6$

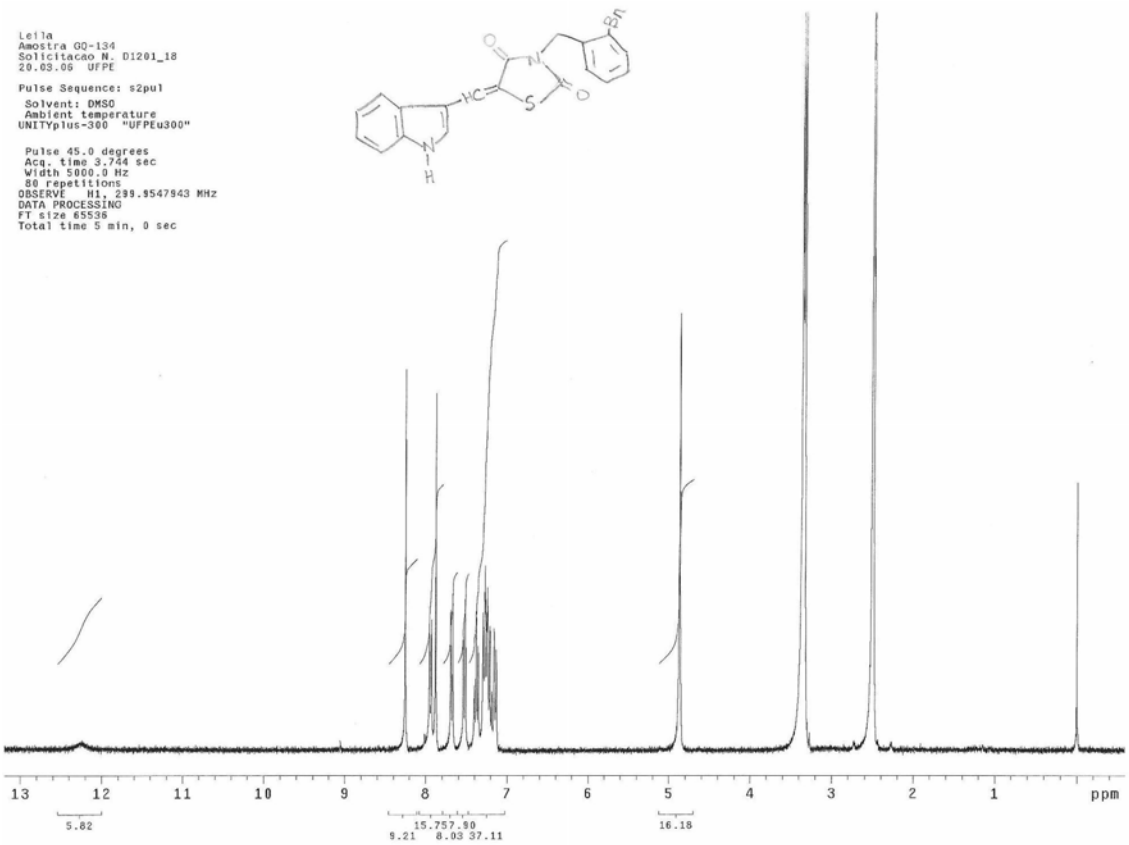

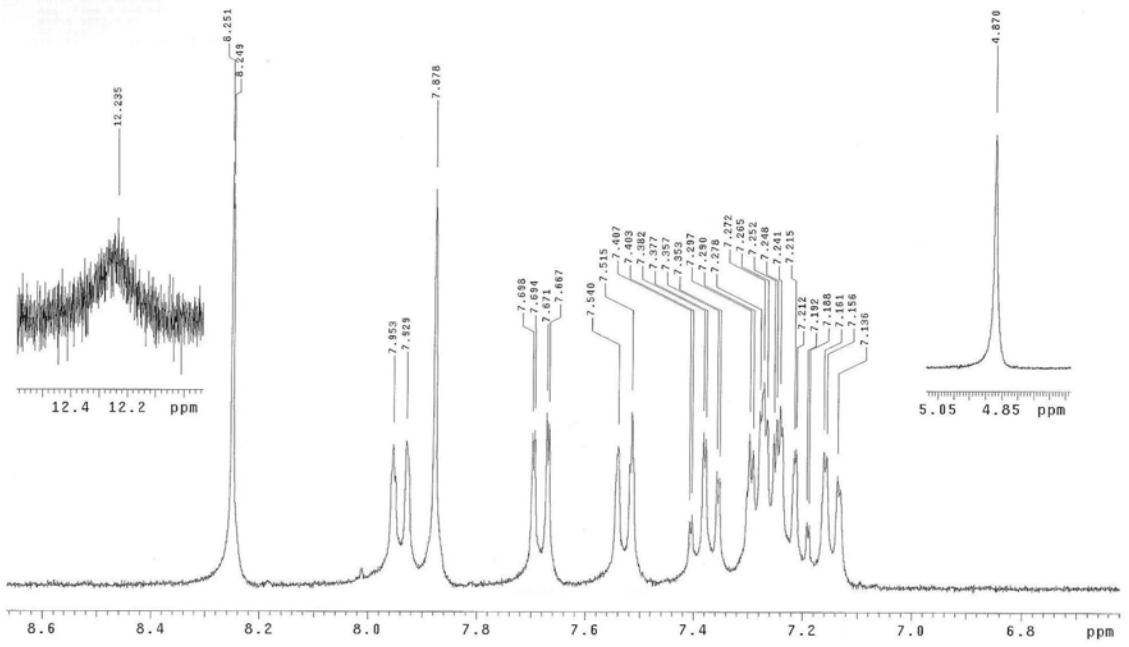

[13 s] GQ-134
IV, KBr

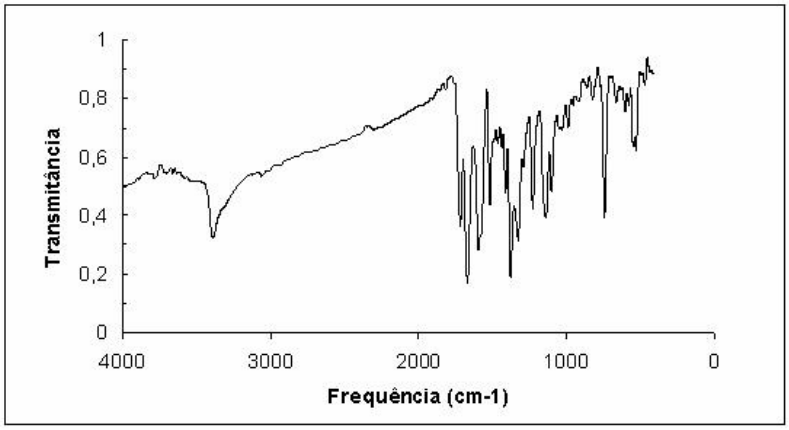

Principais bandas (cm^{-1})

- 3385
- 1712,47
- 1663
- 1587
- 1373
- 1131
- 739

[13 t] PS-34
RMN ^{1}H, $DMSOd_6$

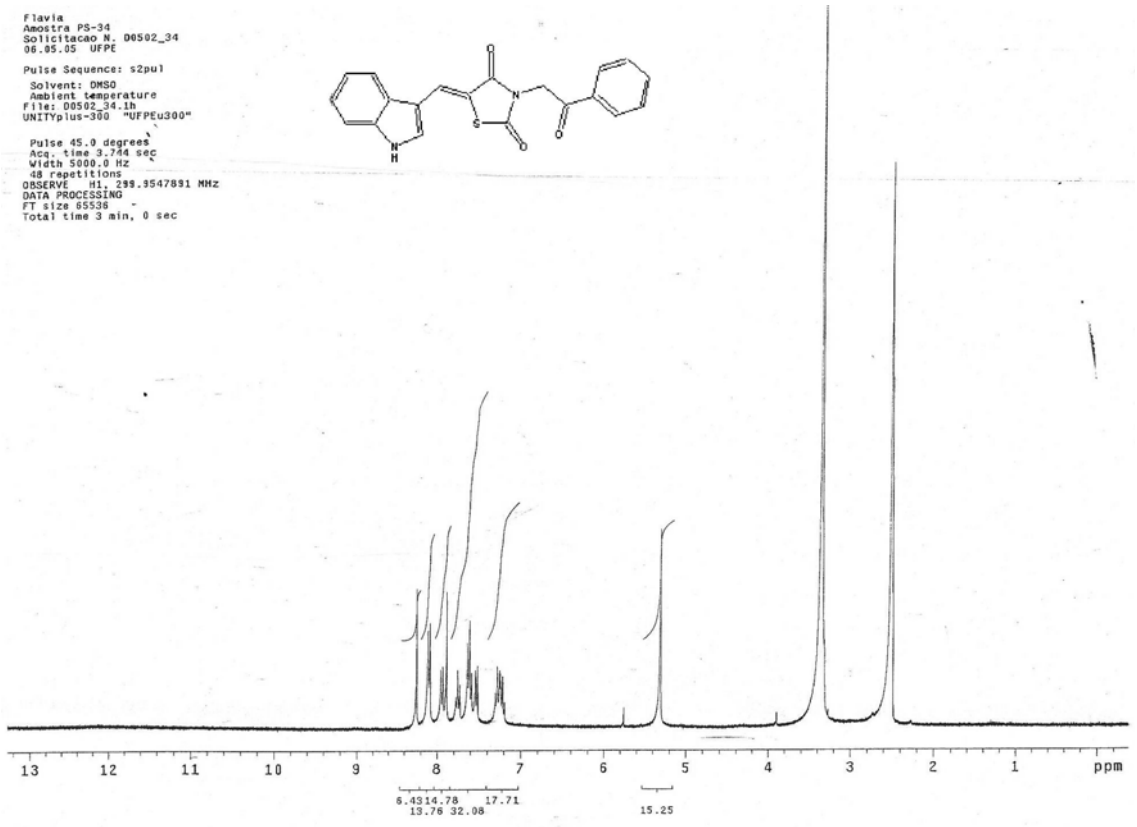

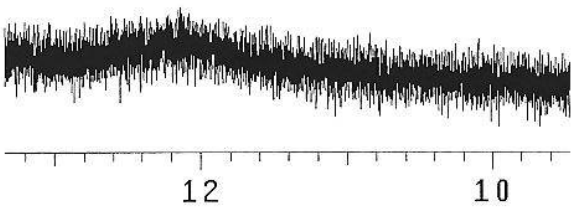

[13 t] PS-34
IV, KBr

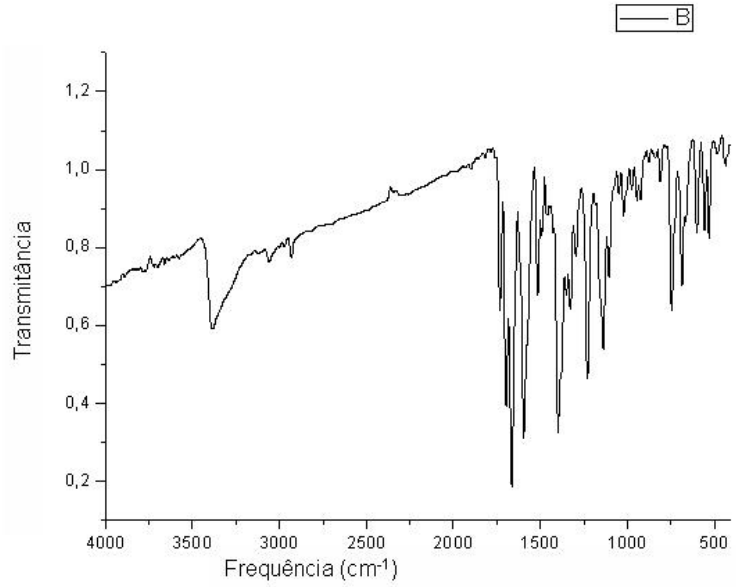

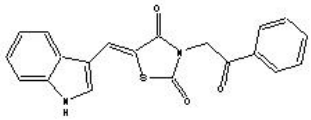

Principais bandas (cm^{-1}):
3382,76
3059,65
2933,65
1730,77
1699,92
1661,90
1595,36
1400,52
1229,38

Espectro de Massas, ESI negativo

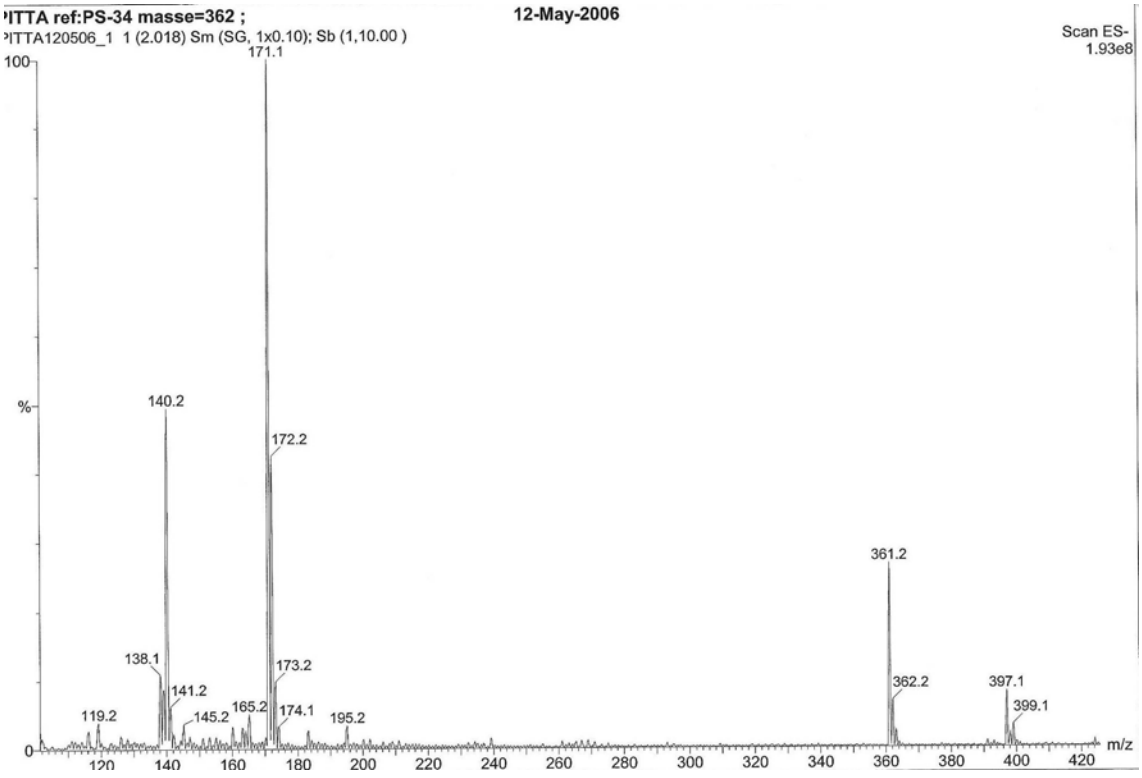

[13 u] PS-38
RMN ^{1}H, $DMSOd_6$

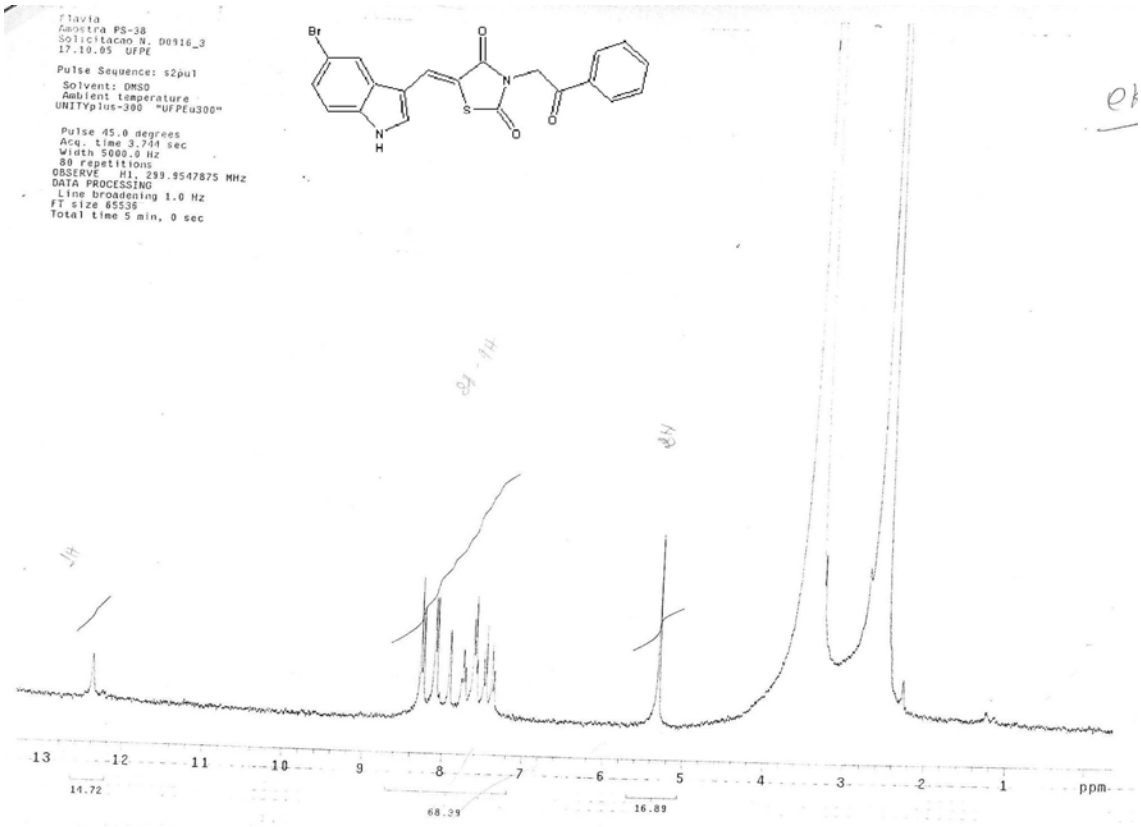

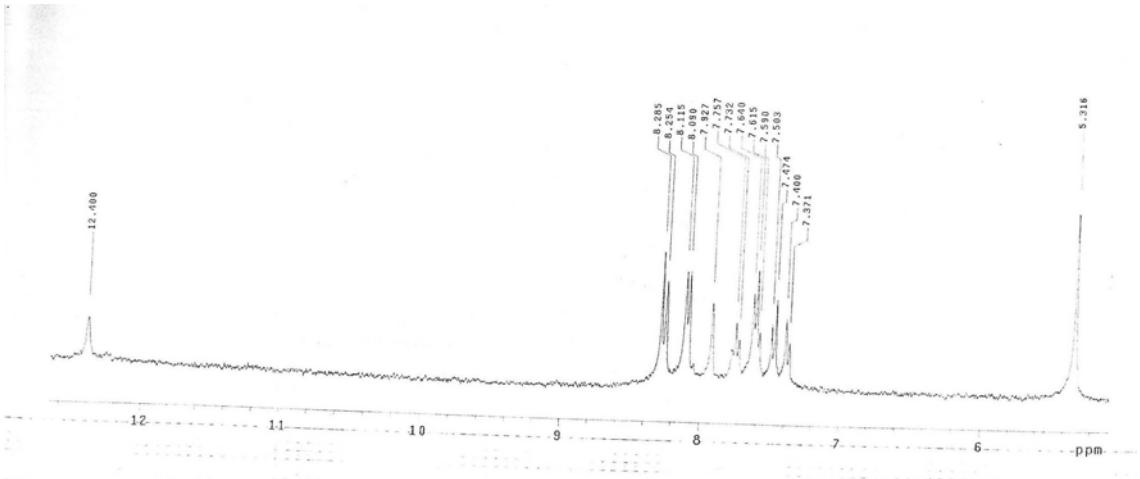

[13 u] PS-38
IV, KBr

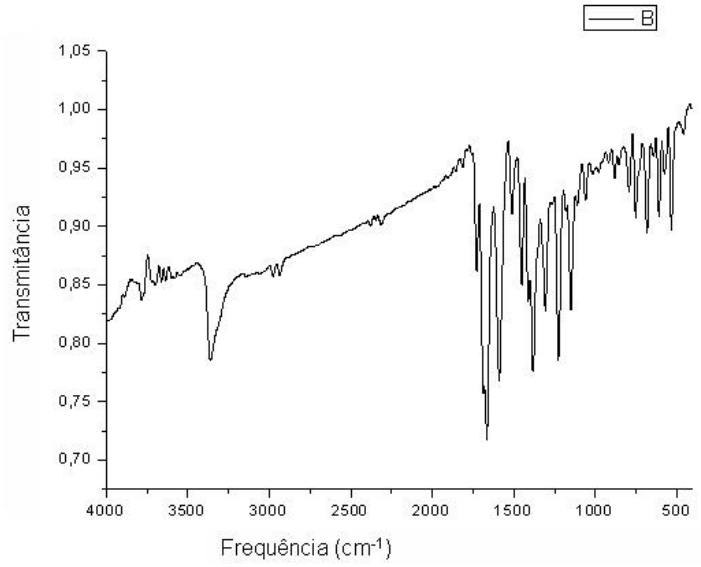

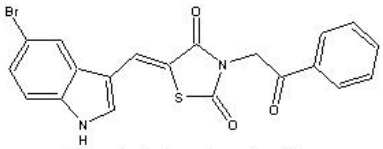

Principais bandas (cm^{-1})
- 3361,69
- 2976,53
- 1726,25
- 1692,13
- 1666,82
- 1588,21
- 1452,80
- 1381,33
- 1305,35
- 1224,49
- 1148,51
- 684,73
- 532,39

Espectro de Massas, ESI negativo

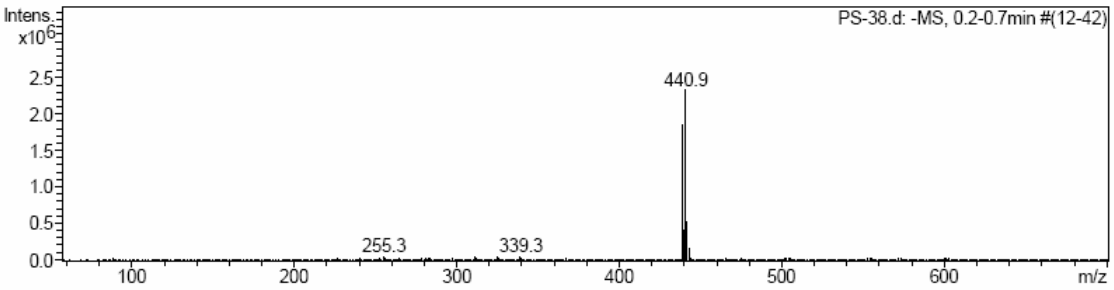

#	m/z	I	I %
1	253.2	22135	1.0
2	255.3	53803	2.3
3	281.3	27487	1.2
4	283.3	28350	1.2
5	311.2	39829	1.7
6	325.3	46687	2.0
7	326.1	20460	0.9
8	339.3	51085	2.2
9	340.1	24129	1.0
10	439.2	1842477	79.2
11	439.9	408406	17.5
12	440.9	2327473	100.0
13	441.8	517854	22.2
14	442.9	160234	6.9
15	443.9	24260	1.0
16	502.0	27936	1.2
17	503.9	27305	1.2
18	552.9	24023	1.0
19	571.6	22752	1.0
20	599.8	21552	0.9

[13 v] PS-36
RMN ^{1}H, $DMSOd_6$

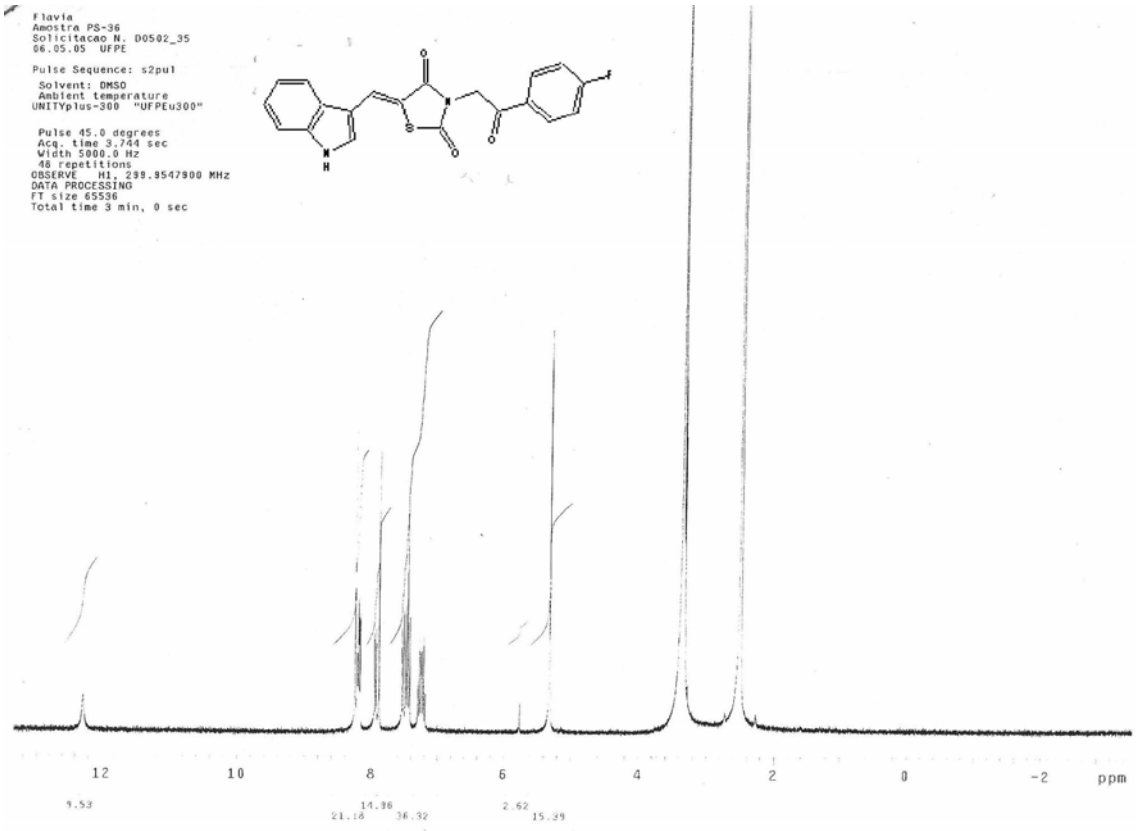

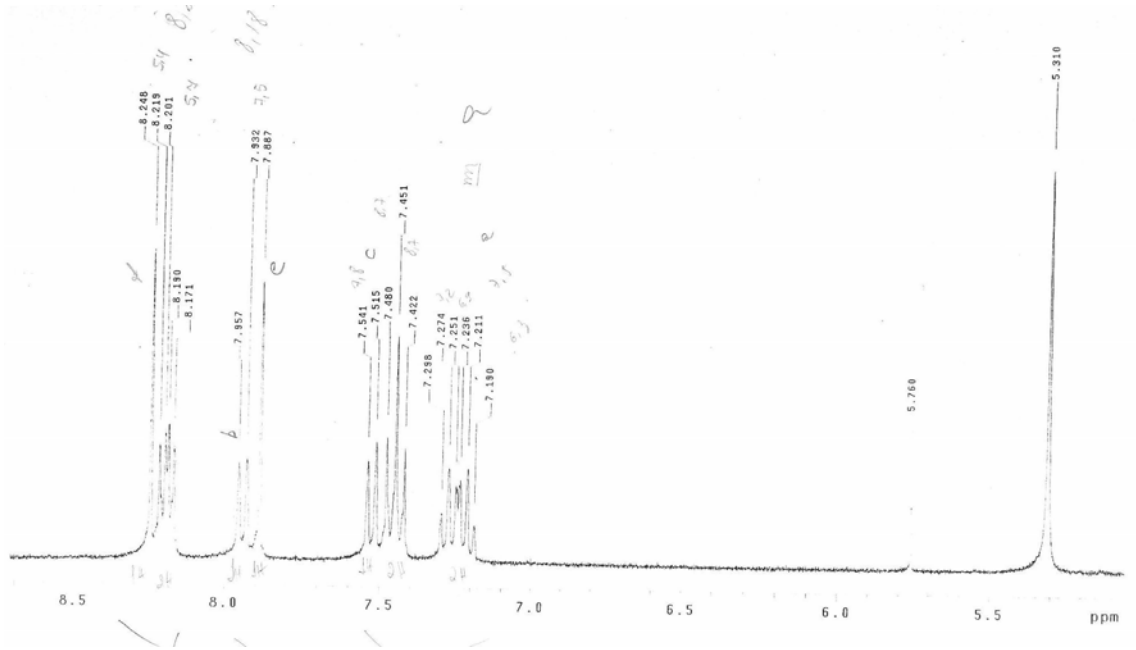

[13 v] PS-36
IV, KBr

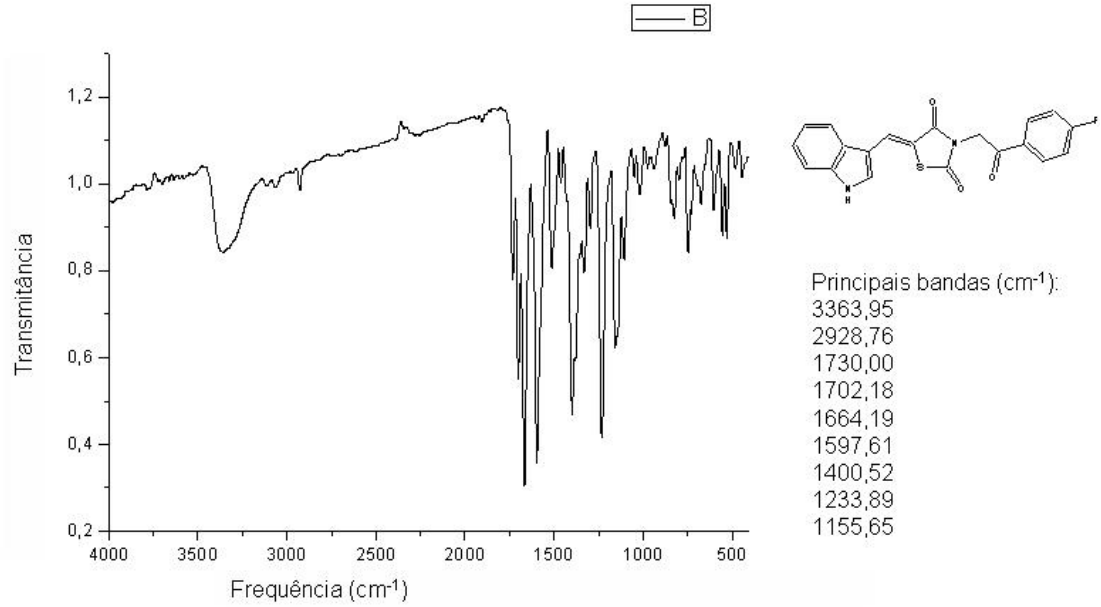

Espectro de Massas, ESI negativo

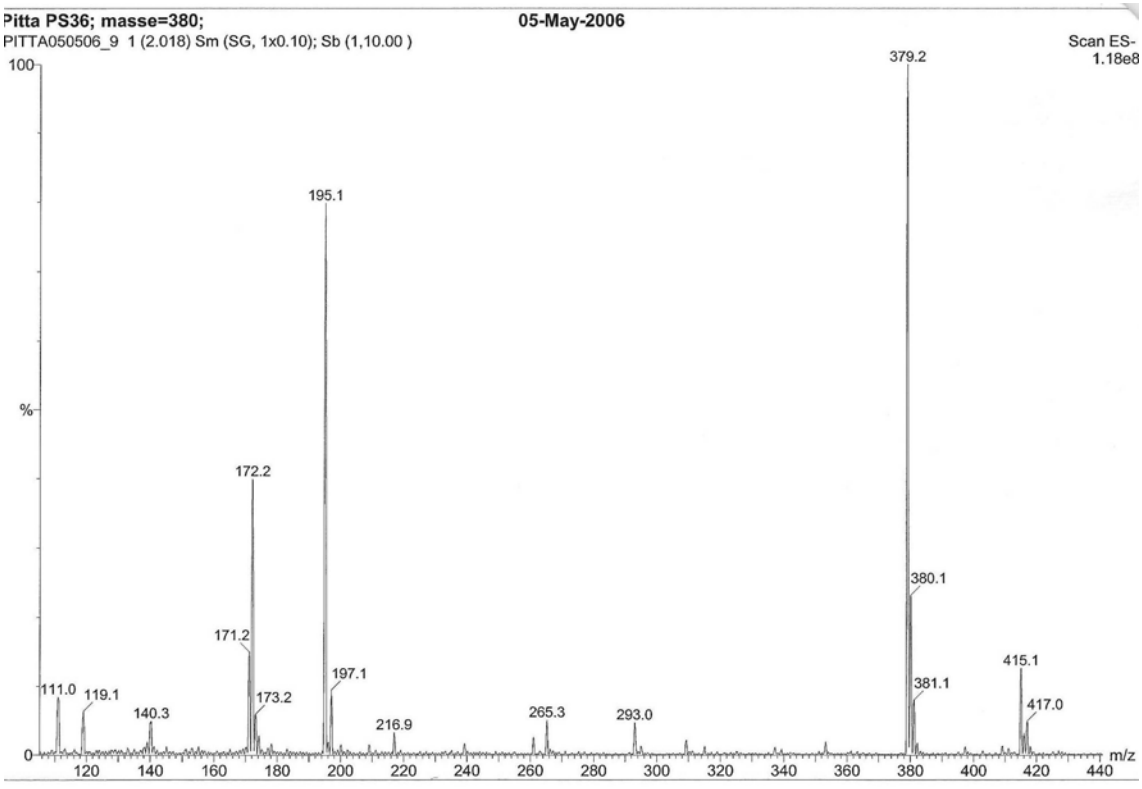

[13 w] PS-39
RMN ^{1}H, $DMSOd_6$

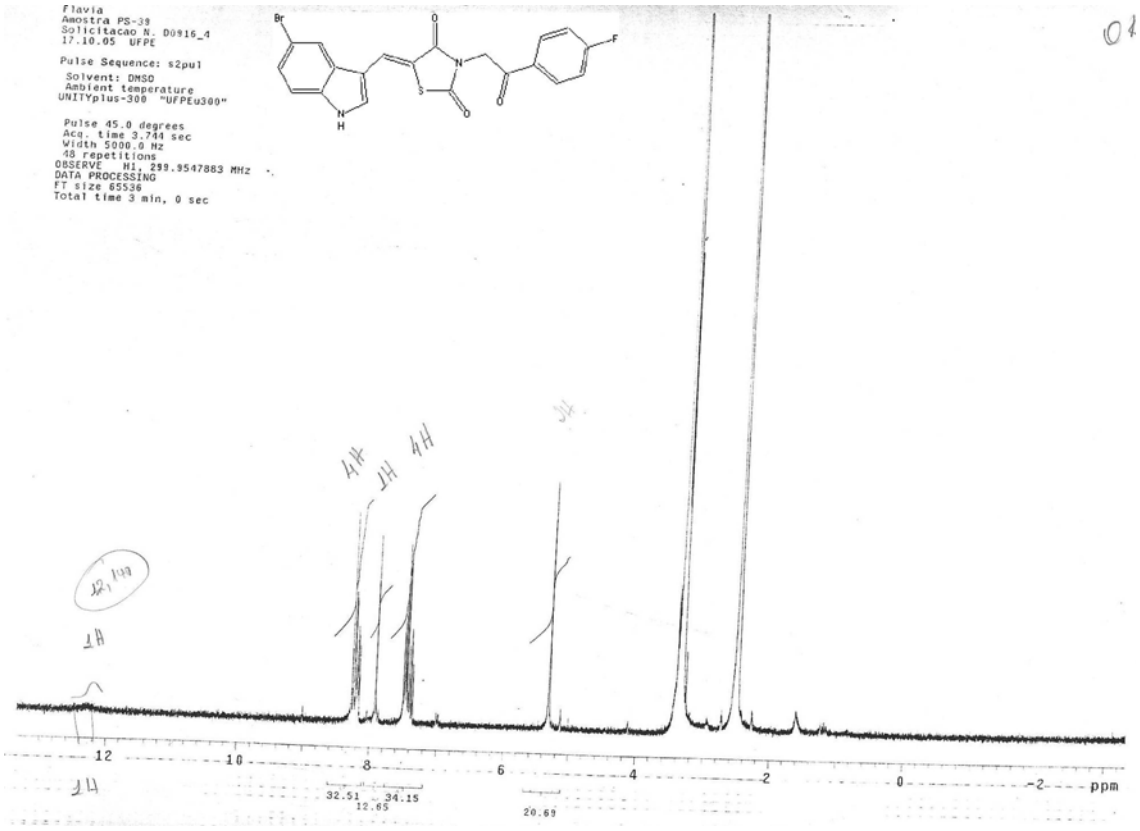

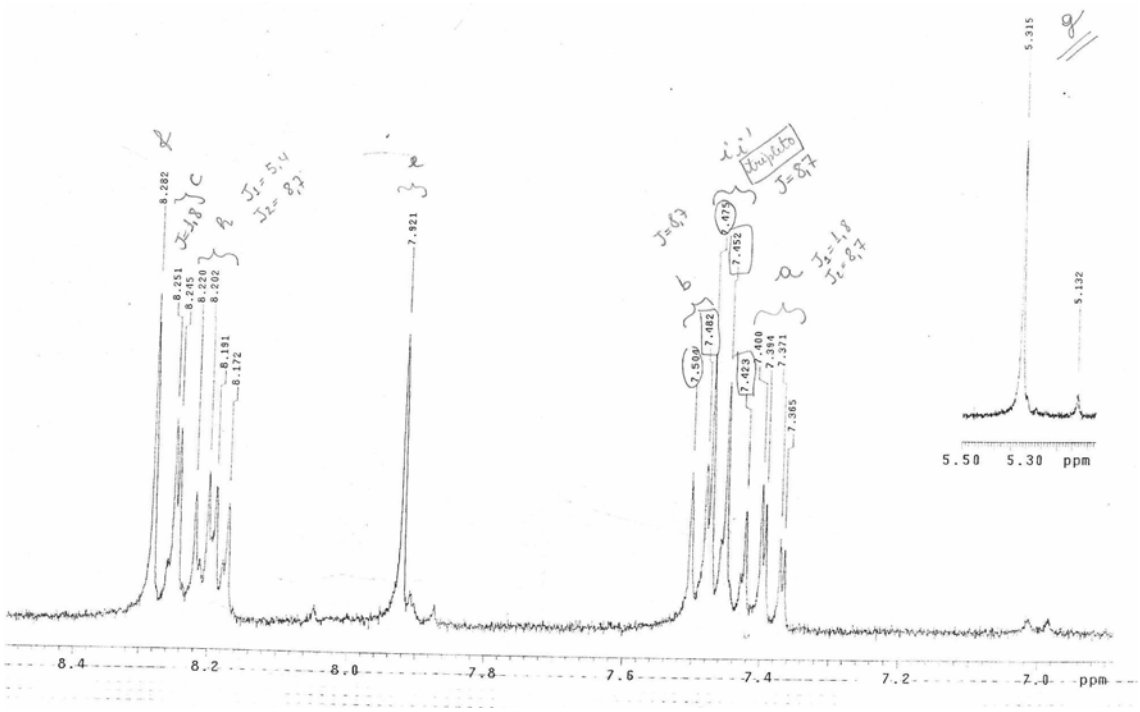

[13 w] PS-39
IV, KBr

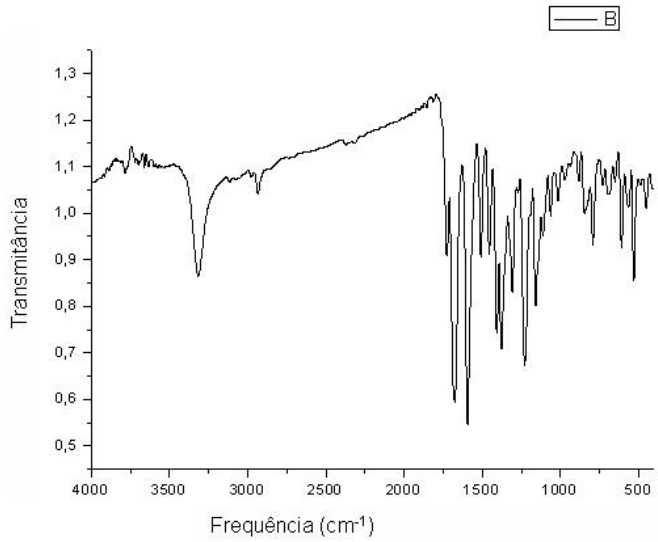

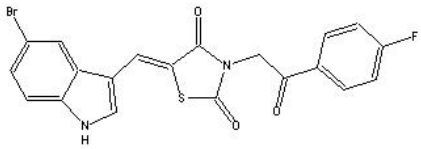

Principais bandas (cm^{-1})
- 3318,81
- 2933,65
- 1728,51
- 1676,23
- 1592,72
- 1409,92
- 1376,44
- 1307,61
- 1226,74
- 1157,91
- 530,51

Espectro de Massas, ESI negativo

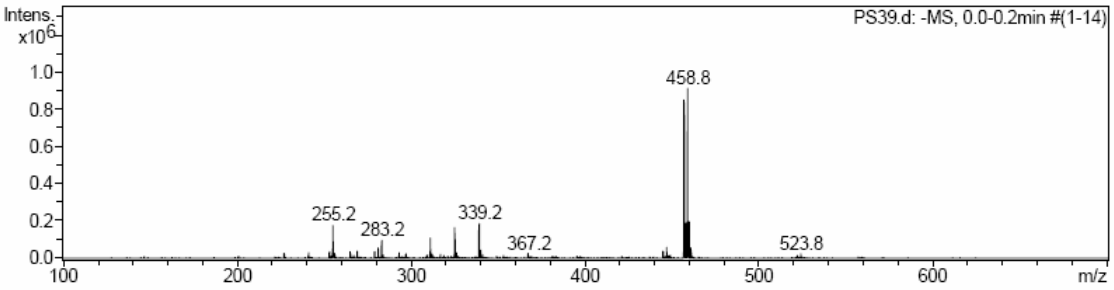

#	m/z	I	I %
1	241.2	27531	3.0
2	253.2	34698	3.8
3	255.2	175624	19.2
4	265.2	34841	3.8
5	269.2	38146	4.2
6	279.2	34788	3.8
7	281.2	54016	5.9
8	283.2	97299	10.7
9	311.1	108784	11.9
10	325.1	163031	17.9
11	326.2	28351	3.1
12	339.2	187983	20.6
13	340.1	44477	4.9
14	444.8	39000	4.3
15	446.8	57170	6.3
16	456.9	850357	93.1
17	457.9	189945	20.8
18	458.8	913022	100.0
19	459.8	196262	21.5
20	460.8	55143	6.0

[13 x] PG-15
RMN ^{1}H, $DMSOd_6$

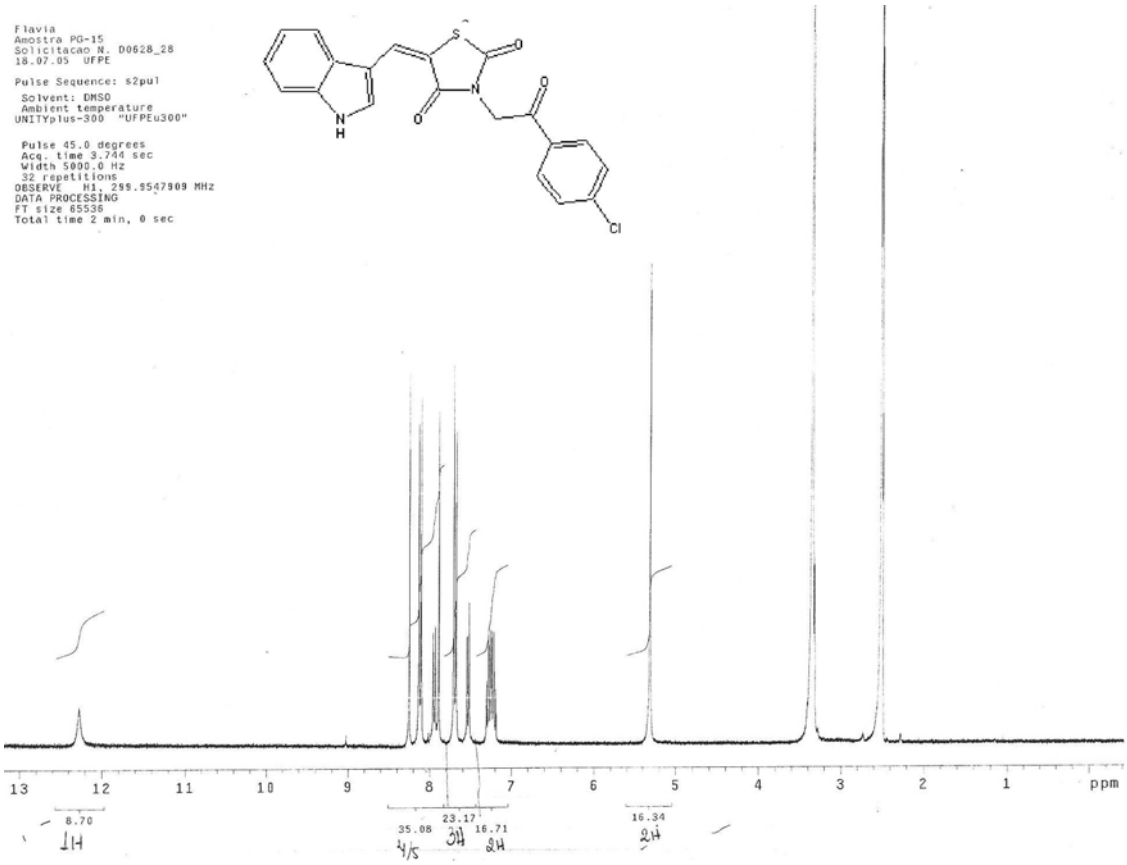

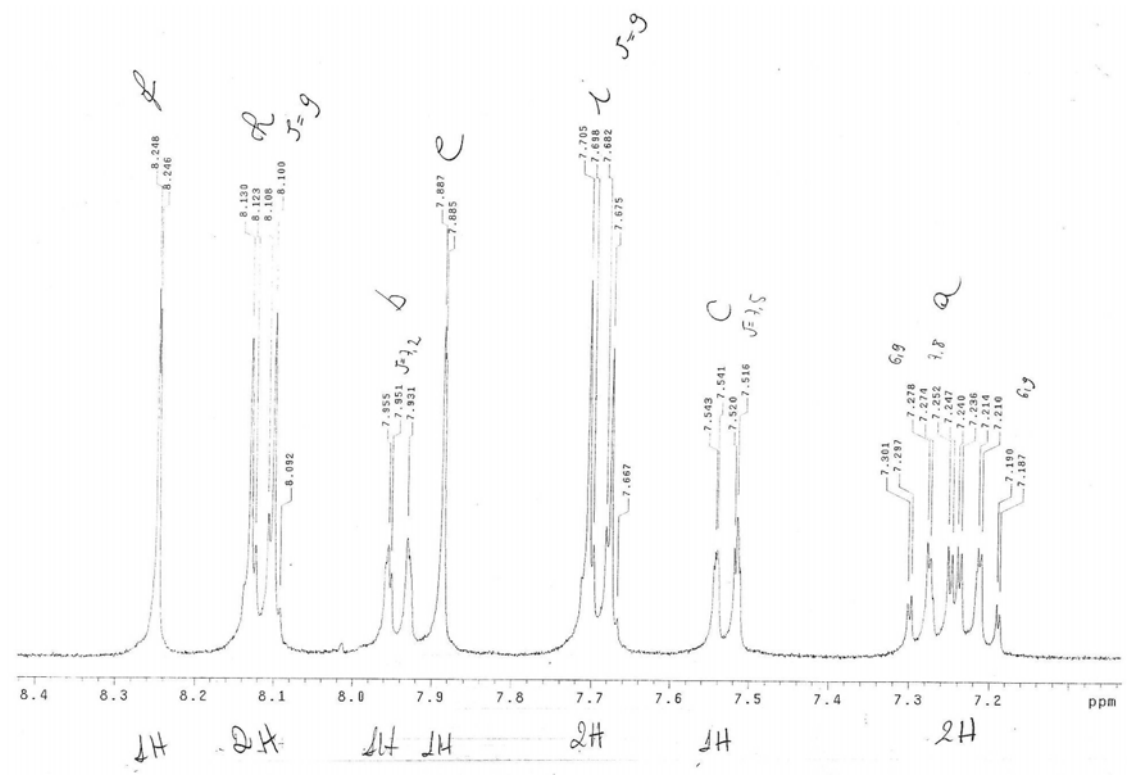

[13 x] PG-15
IV, KBr

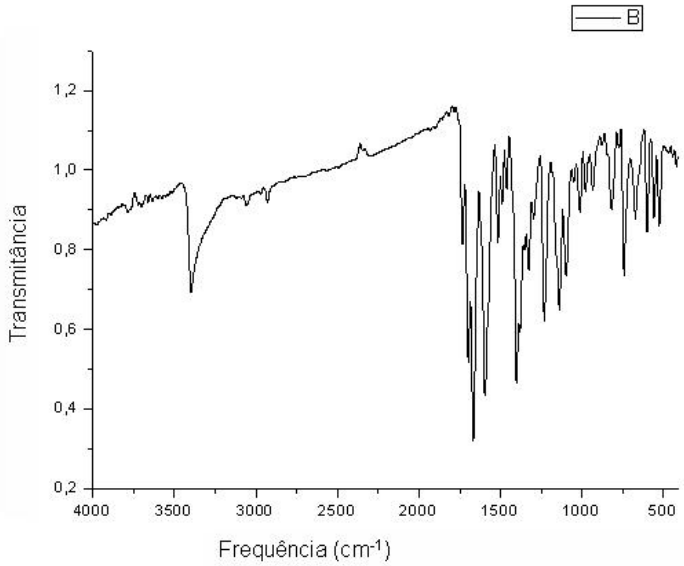

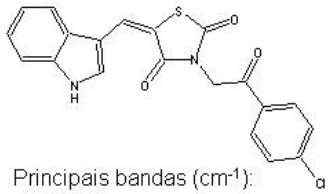

Principais bandas (cm^{-1}):
- 3397,42
- 3057,40
- 2929,14
- 1733,02
- 1697,29
- 1666,45
- 1595,36
- 1400,14
- 1231,63
- 1138,73

Espectro de Massas, ESI negativo

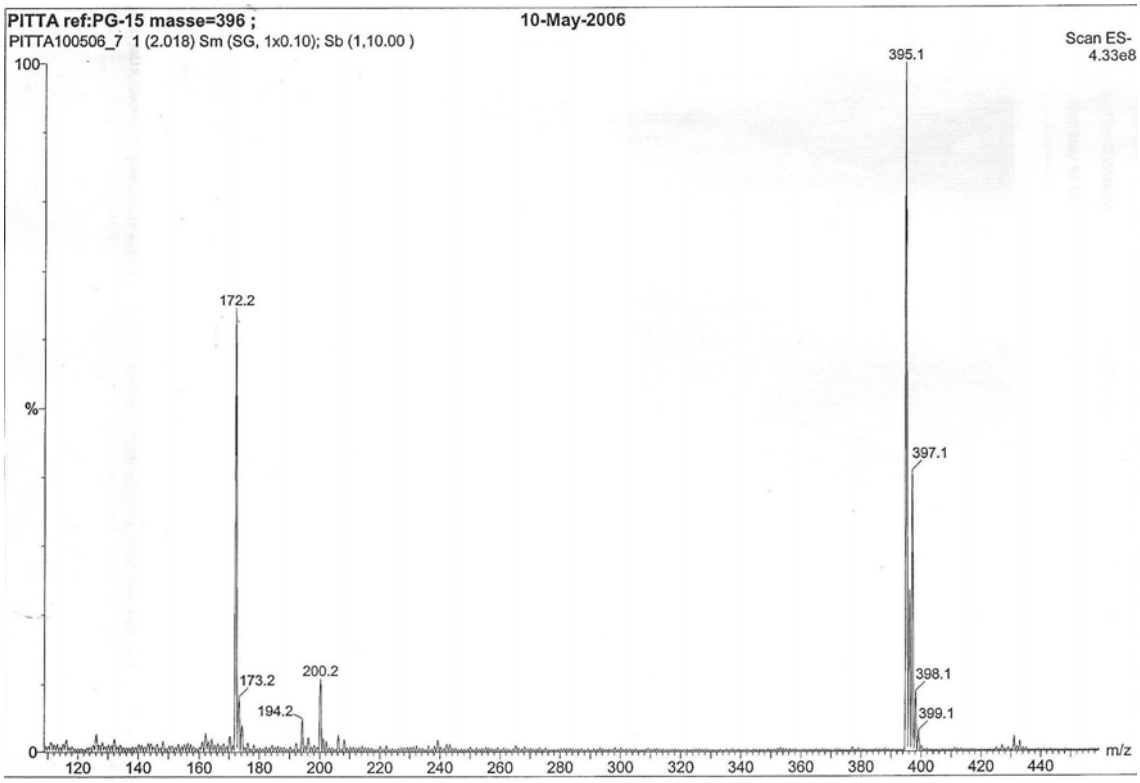

[13 y] PG-16
RMN ^{1}H, $DMSOd_6$

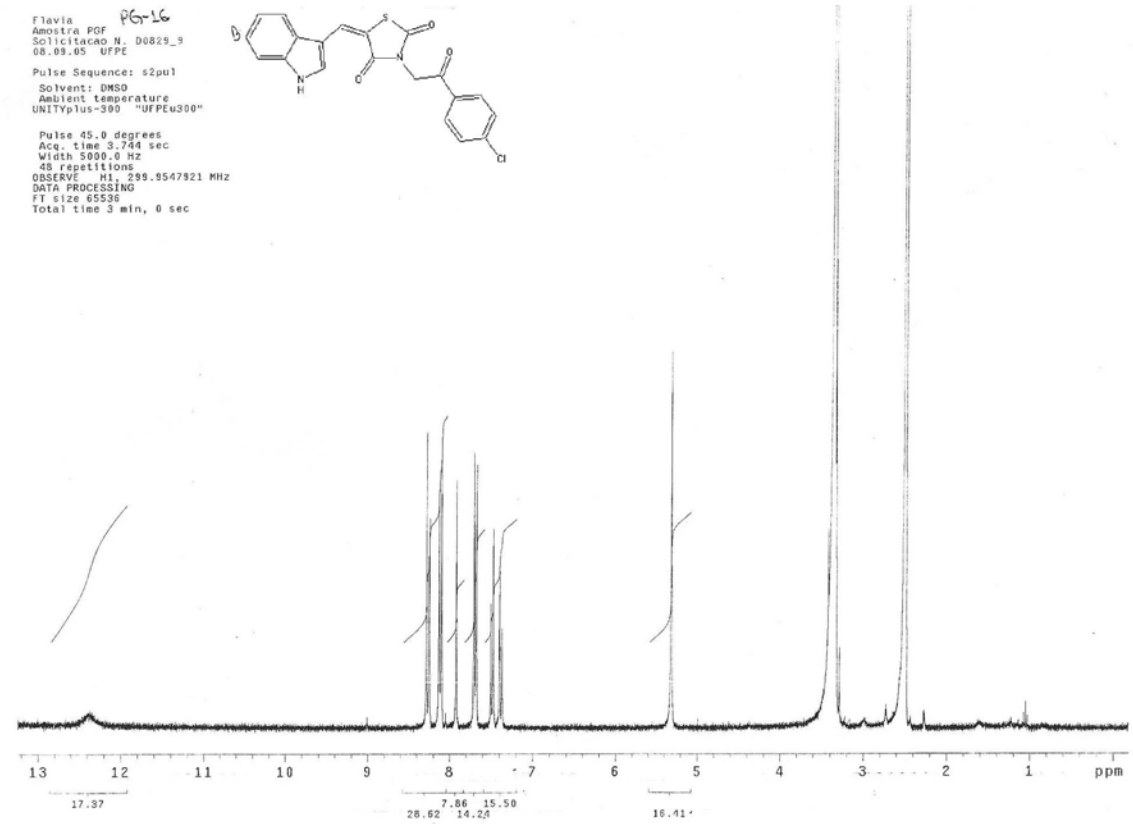

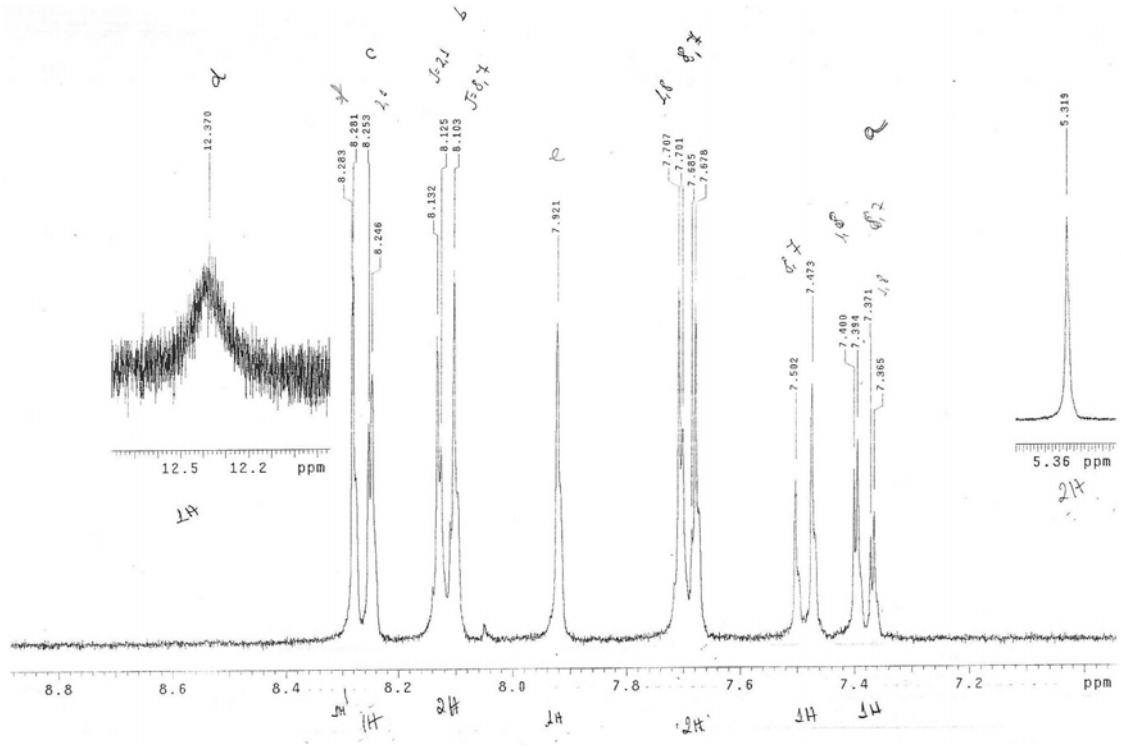

[13 y] PG-16
IV, KBr

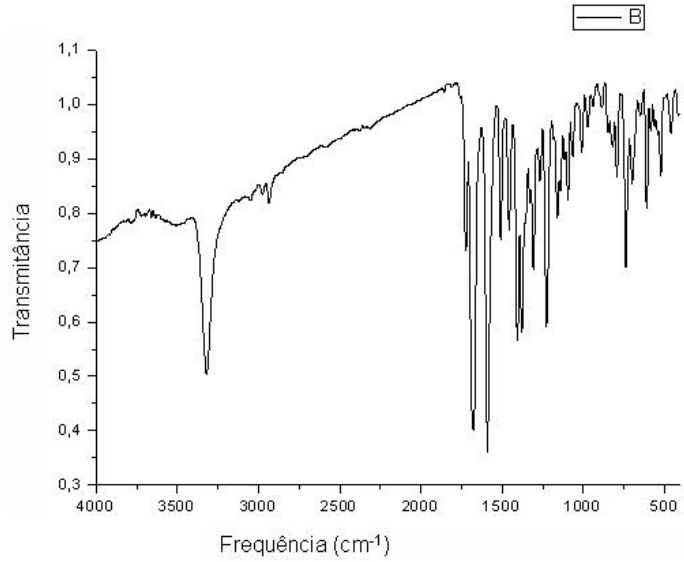

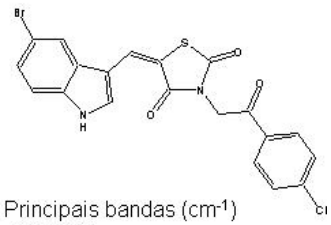

Principais bandas (cm-1)
- 3321,45
- 2933,65
- 1720,99
- 1675,85
- 1590,47
- 1509,60
- 1457,31
- 1407,66
- 1381,33
- 1307,61
- 1226,74

Espectro de Massas, ESI negativo

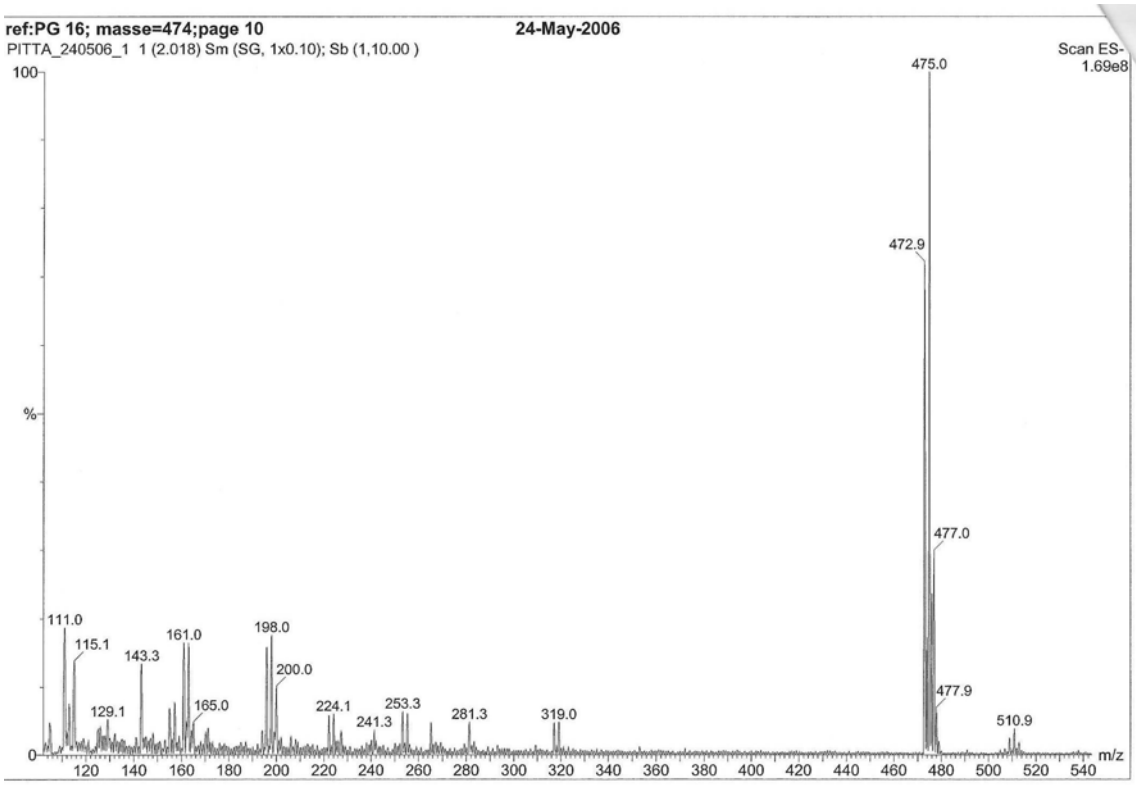

[13 z] HQ-16
RMN ^{1}H, $DMSOd_6$

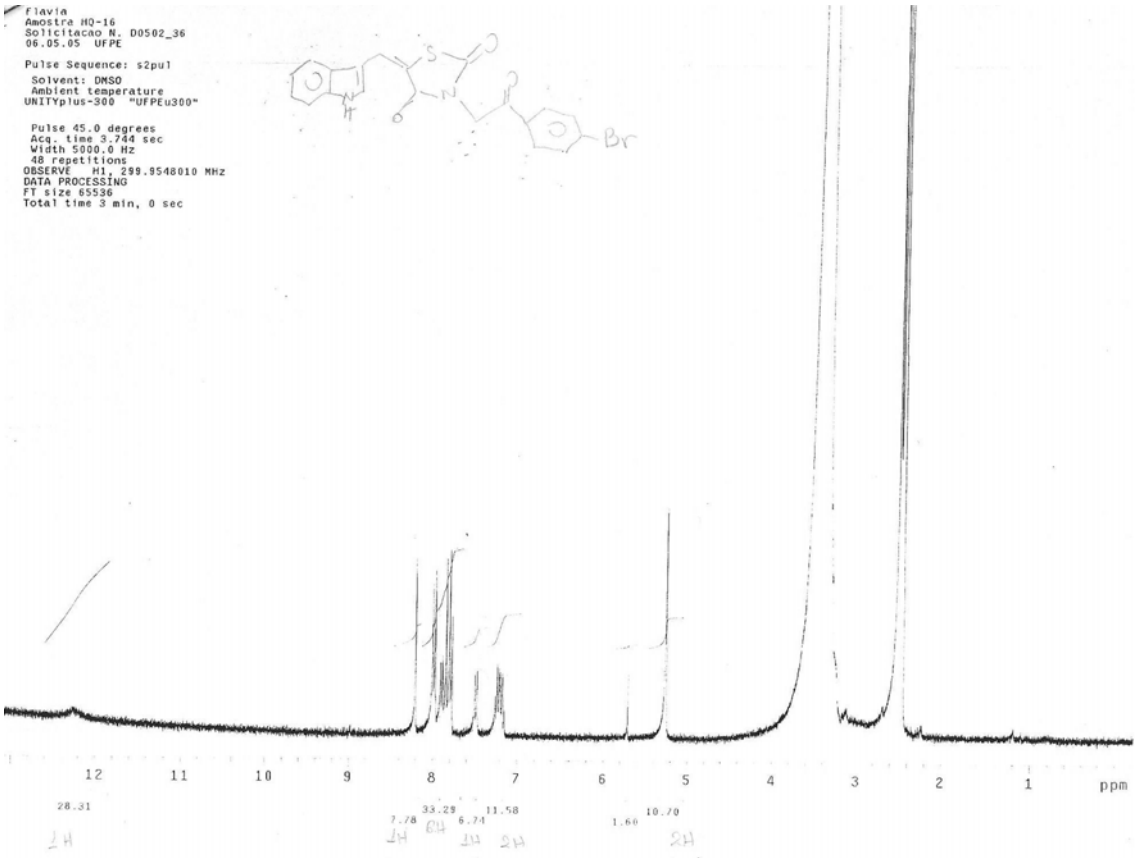

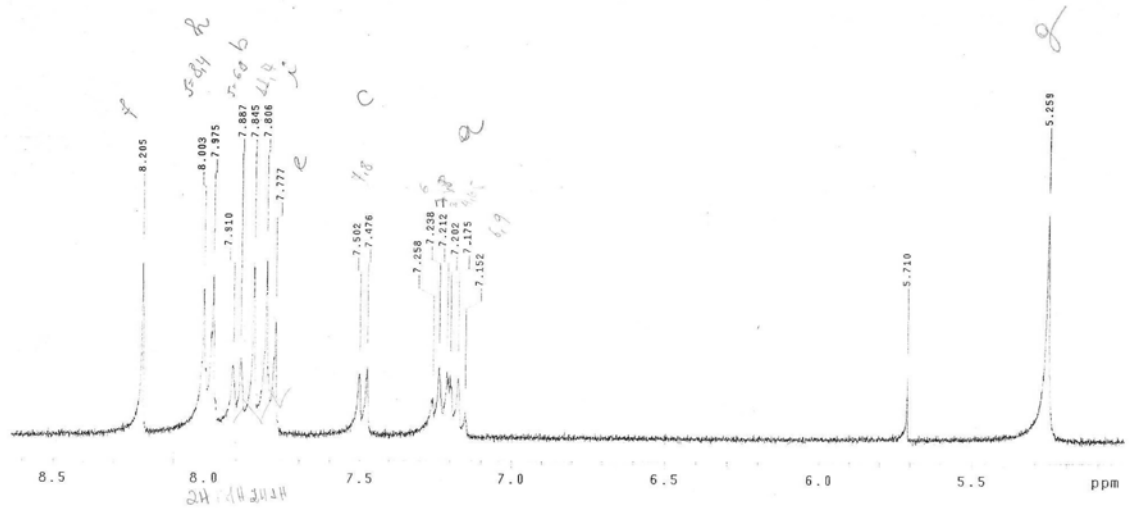

[13 z] HQ-16
IV, KBr

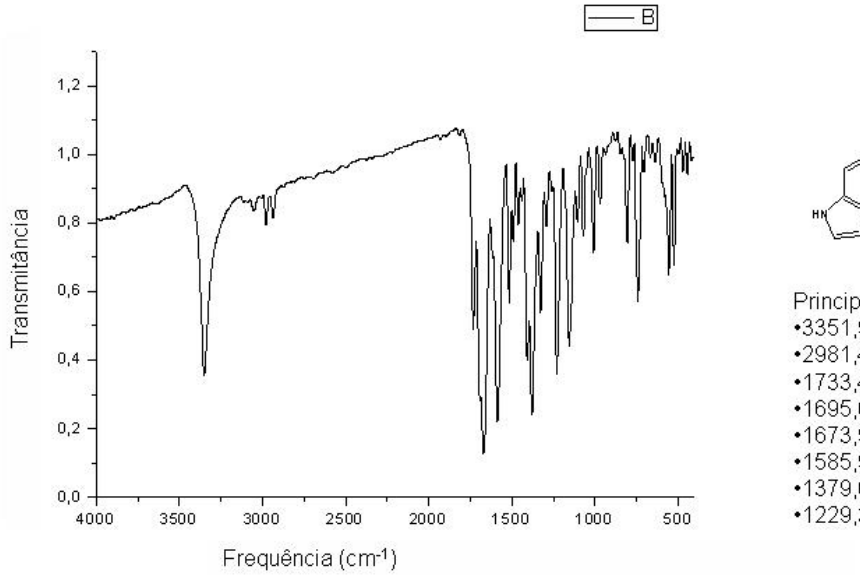

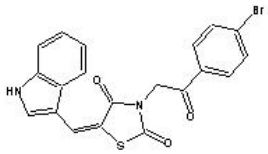

Principais bandas (cm^{-1})
- 3351,91
- 2981,42
- 1733,40
- 1695,03
- 1673,97
- 1585,95
- 1379,08
- 1229,38:

Espectro de Massas, ESI negativo

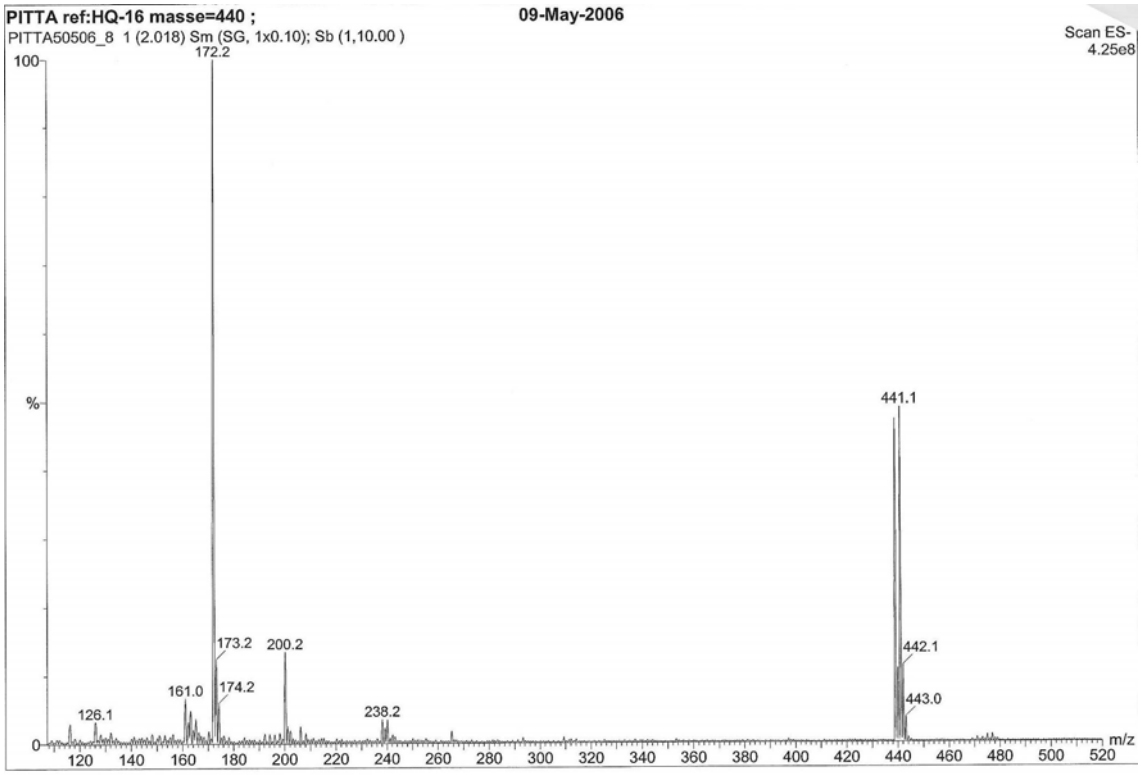

[13 z'] HQ-17
RMN ^{1}H, $DMSOd_6$

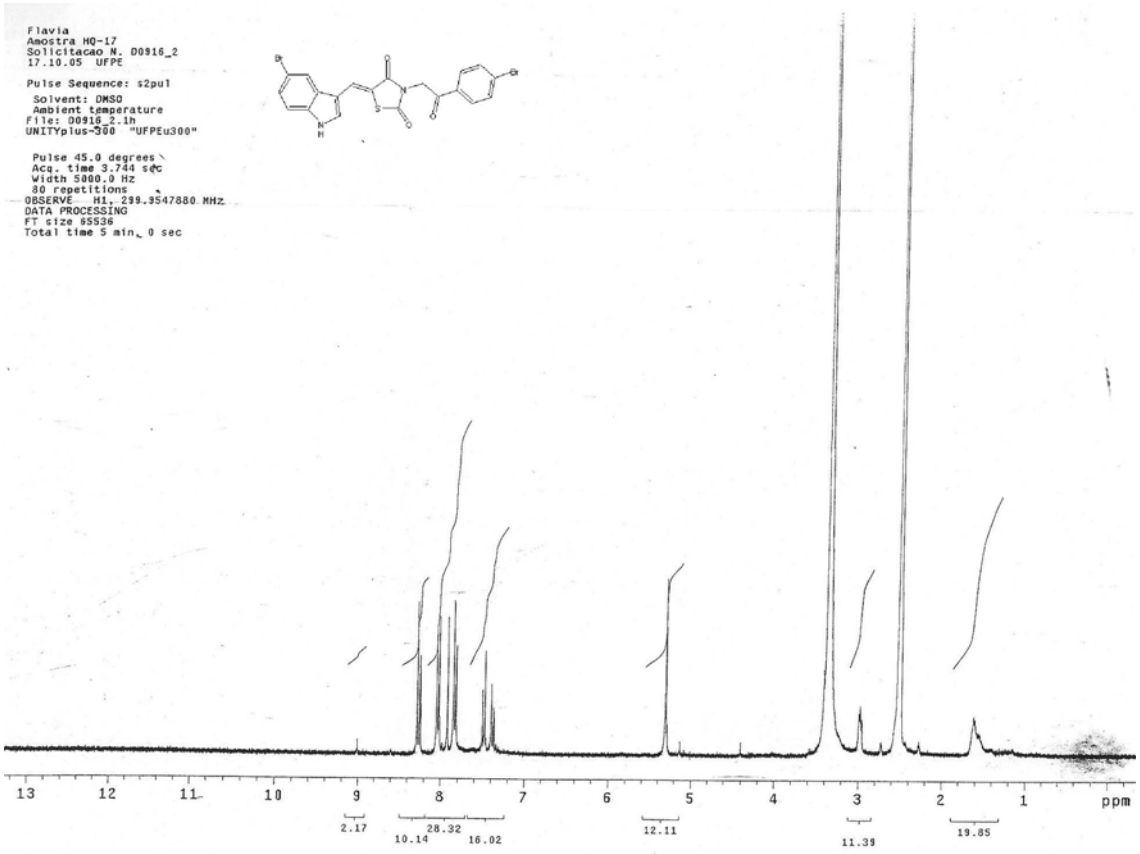

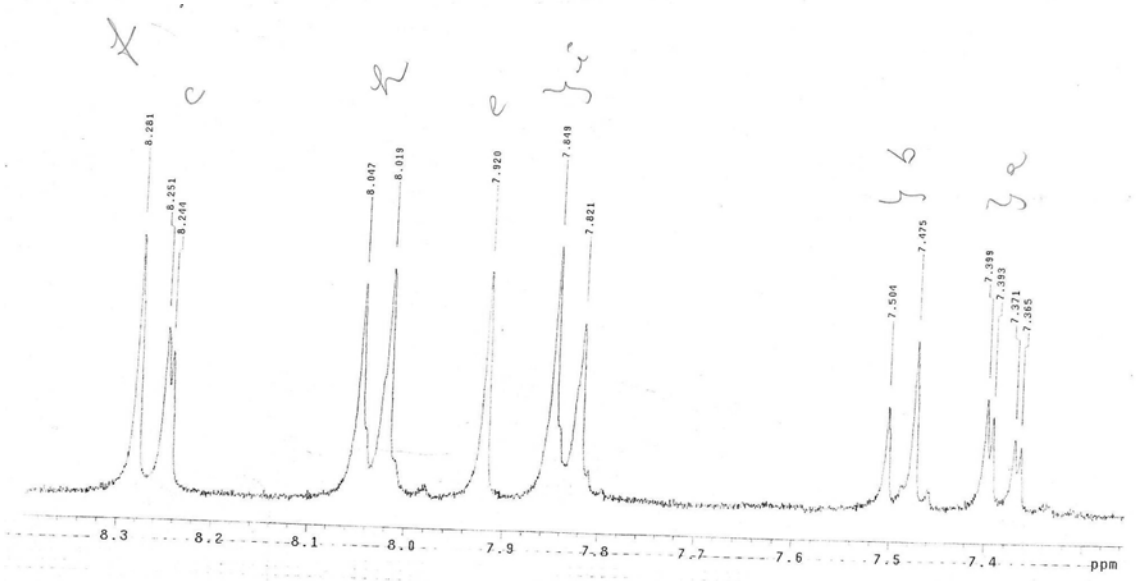

[13 z'] HQ-17
IV, KBr

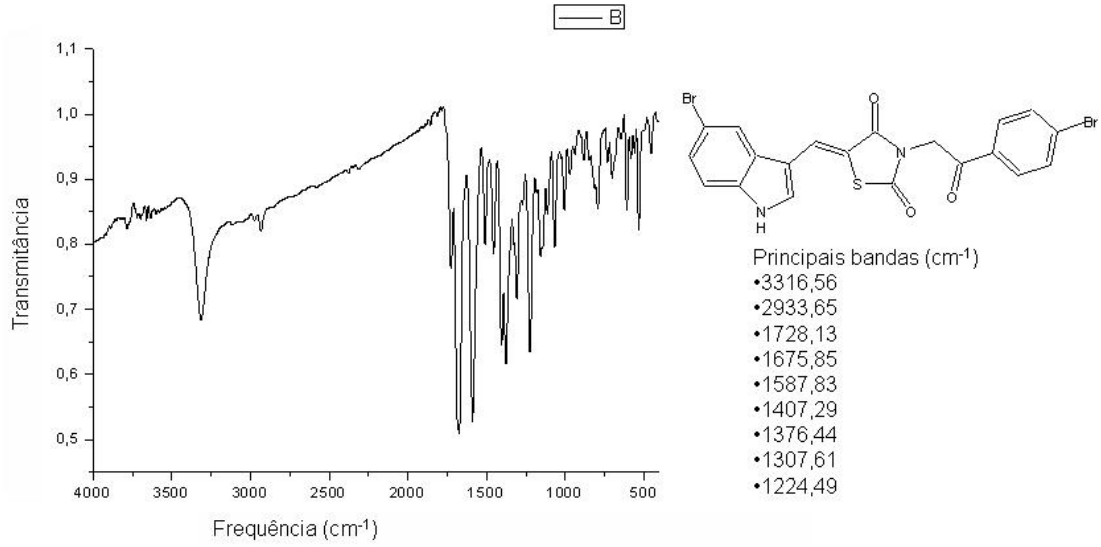

Espectro de Massas, ESI negativo